Eigenfunctions from Open Topological Strings

François, Matijn

UNIVERSITÉ DE GENÈVE

FACULTÉ DES SCIENCES

DOCTORAT ÈS SCIENCES, MENTION INTERDISCIPLINAIRE

Thèse de Monsieur Matijn FRANCOIS

intitulée :

«Eigenfunctions from Open Topological Strings»

La Faculté des sciences, sur le préavis de

Madame A. GRASSI, professeure associée et directrice de thèse
Section de mathématiques

Monsieur M. MARINO BEIRAS, professeur ordinaire
Département de physique théorique et Section de mathématiques

Monsieur F. DEL MONTE, professeur
School of Mathematics, University of Birmingham, Birmingham, United Kingdom

autorise l'impression de la présente thèse, sans exprimer d'opinion sur les propositions qui y sont énoncées.

Genève, le 9 janvier 2026

Thèse - 5971 -

La Doyenne

N.B. - La thèse doit porter la déclaration précédente et remplir les conditions énumérées dans les "Informations relatives aux thèses de doctorat à l'Université de Genève".

UNIVERSITÉ DE GENÈVE
Section de mathématiques

FACULTÉ DES SCIENCES
Professeure Alba Grassi

Eigenfunctions from Open Topological Strings

THÈSE

Présentée à la Faculté des sciences de l'Université de Genève
pour obtenir le grade de Docteur ès sciences, mention interdisciplinaire

Par

Matijn FRANÇOIS

de

Brasschaat (Belgique)

Thèse N° 5971

GENÈVE

2026-03-02

Cette thèse regroupe les travaux publiés dans [1–3].

[1] M. François and A. Grassi, *Painlevé Kernels and Surface Defects at Strong Coupling*, *Ann. Henri Poincaré* **26** (2025) 2117 [2310.09262]

[2] M. François and A. Grassi, *On the open TS/ST correspondence*, *arXiv preprints* (2025) [2503.21762]

[3] M. François, A. Grassi and T. Pedroni, *Eigenfunctions of deformed Schrödinger equations*, *arXiv preprints* (2025) [2511.10636]

Résumé en français

Bien que l'existence de solutions à de nombreux problèmes en mathématiques et en physique puisse souvent être rigoureusement démontrée, ou du moins physiquement justifiée, la construction explicite de ces solutions constitue un problème complexe, rarement réalisable concrètement. Or, la proposition de correspondance entre théorie des cordes topologiques et théorie spectrale de [4, 5] relève précisément ce défi pour deux problèmes distincts. Elle relie une description non perturbative de certaines théories des cordes topologiques aux solutions de systèmes quantiques simples, fournissant ainsi des solutions explicites pour les deux termes. Il est intéressant de noter que les problèmes quantiques concernés sont des équations aux différences finies et non des équations différentielles.

Si cette correspondance est bien comprise au niveau des cordes topologiques fermées, ou de manière équivalente au niveau du spectre du problème quantique, son application aux cordes topologiques ouvertes ou aux fonctions propres reste encore mal comprise. Des progrès importants ont été réalisés dans [6, 7] si $\hbar = 2\pi$. Nous proposons une extension de leurs résultats à tout $\hbar > 0$ pour une famille particulière de théories des cordes topologiques correspondant à la théorie de Yang-Mills supersymétrique SU(N) en cinq dimensions. Une caractéristique distinctive de cette construction est que les fonctions propres sont des fonctions entières, solutions de l'équation aux différences pertinente pour toute valeur des paramètres, et qu'elles deviennent des fonctions propres au sens de l'espace de Hilbert pour un ensemble discret de valeurs propres. Il s'agit donc d'un progrès partiel vers la correspondance entre théorie des cordes topologiques et théorie spectrale.

Nous étudions également deux limites intéressantes de notre proposition, qui établissent une relation entre la théorie de Yang-Mills $\mathcal{N} = 2$ supersymétrique en quatre dimensions et un problème spectral associé. La première limite permet de construire les fonctions propres de la courbe de Seiberg-Witten quantifiée à l'aide des fonctions de partition du défaut de la théorie de jauge dans la limite dite de Nekrasov-Shatashvili. Ces systèmes de mécanique quantique sont des analogues par différences finies de l'équation de Schrödinger à potentiel polynomial, où le terme cinétique normal p^2 est remplacé par $\cosh(p)$. De plus, pour des valeurs particulières des paramètres, ils correspondent à l'équation de Baxter du réseau de Toda.

L'autre limite possible de la correspondance entre la théorie des cordes topologiques ouvertes et la théorie spectrale donne les fonctions propres de noyaux intégraux spéciaux en fonction des fonctions de partition de défaut de la théorie de jauge dans la phase autoduale du fond Ω. Une caractéristique intéressante de cette construction est qu'elle relie la fonction de partition de défaut à un modèle matriciel admettant un développement naturel autour du point de monopole magnétique de couplage fort. De plus, grâce à la construction explicite des fonctions propres à partir de la théorie de jauge, on trouve également une relation fonctionnelle entre ce noyau intégral et la courbe de Seiberg-Witten quantifiée.

Acknowledgements

Firstly, none of this would have been possible without the careful guidance and the support of Alba. Moreover, this is a cumulative thesis that doesn't deviate from the original work in [1–3], so I want to thank in particular my collaborators on these projects, which are Alba for [1, 2] and Alba and Tommaso for [3]. This thesis is equally well their achievement as it is mine. My gratitude goes furthermore to the people in the jury, which are Alba, Marcos Mariño, and Fabrizio Del Monte, for a careful reading and evaluation of the thesis.

All the projects [1–3] grew thanks to discussions with many people. For [1] these are in particular Anton Nedelin for collaborating during the early stages of the project, and Severin Charbonnier, Shi Cheng, Qianyu Hao, Saebyeok Jeong, Rinat Kashaev, Marcos Mariño, Andy Neitzke, Nicolas Orantin, François Pagano, Sara Pasquetti, Lukas Schimmer, Yasuhiko Yamada, and Szabolcs Zakany for useful discussions and correspondence, and two anonymous referees for their comments and valuable suggestions. For [2] I want to thank Frederico Ambrosino, Giulio Bonelli, Shi Cheng, Fabrizio Del Monte, Pavlo Gavrylenko, Jie Gu, Saebyeok Jeong, Marcos Mariño, Nicolas Orantin, Maximilian Schwick, Alessandro Tanzini, and Szabolcs Zakany for interesting and valuable discussions, and in particular Fabrizio Del Monte and Marcos Mariño, as well as two anonymous referees, for a careful reading of the draft. For [3] we have to thank Giulio Bonelli, Matteo Gallone, Saebyeok Jeong, Marcos Mariño and Alessandro Tanzini for interesting discussions. Let me mention that [1–3] heavily rely on the work done in [4, 6–8] and too many others to list, so I want to thank all authors for providing the solid basis on which we could build. Also thanks to all my colleagues at the university of Geneva and CERN, for providing an inspiring scientific and social environment. Tot slot wil ik ook mijn familie en vrienden bedanken, en in het bijzonder mijn ouders, voor hun steun doorheen de jaren.

This work is partially supported by the Swiss National Science Foundation Grant No. 185723.

Contents

Chapter 1

Introduction and motivation

In this thesis, we are interested in quantizations of simple curves of the form

$$H(x,y) = \sum_{k\in\mathcal{I}}\sum_{\ell\in\mathcal{J}} c_{k,\ell}\, \mathrm{e}^{kx+\ell y} = E\,, \qquad \mathcal{I},\mathcal{J}\subseteq\mathbb{Z}\,, \qquad c_{k,\ell}\in\mathbb{R}\,, \tag{1.0.1}$$

where $\mathcal{I},\mathcal{J}$ are *finite* index sets. Let us for simplicity consider the situation in which the Riemann surface parametrized by $H(x,y)$ with $x,y\in\mathbb{C}$ has genus $g\geqslant 1$, and where level sets for fixed $E>0$ are bounded when $x,y\in\mathbb{R}$ with $H(x,y)>0$ without loss of generality. The basic motivation for the later choice is simple: a bounded phase space volume implies a discrete spectrum once we quantize the theory, so this gives an interesting setting to study a quantization of (1.0.1). Many of these conditions can nevertheless be relaxed, but this would complicate the current discussion. Let us thus promote x,y to Heisenberg operators

$$[x,y] = \mathrm{i}\hbar\,, \qquad \hbar>0\,, \tag{1.0.2}$$

and we consider (1.0.1) as an operator equation on the Hilbert space of square integrable functions $L^2(\mathbb{R})$. That is

$$H(x,y) : D(H)\to L^2(\mathbb{R}) : \psi\mapsto H(x,y)\psi \tag{1.0.3}$$

$$D(H) := \left\{\psi\in L^2(\mathbb{R}) \,\middle|\, \forall k\in\mathcal{I},\forall\ell\in\mathcal{J} : \mathrm{e}^{kx+\ell y}\psi\in L^2(\mathbb{R})\right\}\,, \tag{1.0.4}$$

Let me also mention that the constraint coming from y can be reformulated as the requirement that $\psi(x)$ should be analytic in strip parallel to the real axis, by a variation on the Paley-Wiener theorem [9, thm. IX.13]. Analyticity of eigenfunctions of $H(x,y)$ will come back in a stronger form later on. Equation (1.0.1) becomes then a finite difference equation for $\psi(x)$. Note that $D(H)$ is dense in $L^2(\mathbb{R})$ since all Hermite functions are in $D(H)$, and $H(x,y)$ is symmetric because $c_{k,\ell}\in\mathbb{R}$. Moreover, since $H(x,y)$ is a positive semi-bounded operator there exists a canonical self-adjoint extension, which is the so-called Friedrichs extension [9, p. 177] [10, p. 234].

It turns out that the spectral problem associated with this self-adjoint extension is very well-behaved. It was conjectured in [4] that the inverse ρ of this extension is a

bounded, positive-definite, self-adjoint operator on $L^2(\mathbb{R})$ which is of *trace class*. At a physics level of rigour this can be seen from Bohr-Sommerfeld estimates on the spectrum, and it was proven for many examples in [11, 12]. The fact that ρ is trace class puts tight constraints on the spectrum and the eigenfunctions. Due to the Riesz-Schauder theorem [13, th. VI.15], ρ has a discrete spectrum and every non-zero value in the spectrum is an eigenvalue with finite multiplicity, and the eigenfunctions form a basis of Hilbert space by the Hilbert-Schmidt theorem [13, th. VI.16]. These facts are true for generic compact[1], self-adjoint operators, but trace class operators also allow the construction of the spectral determinant [10, eq. (9.30)],

$$\det : \mathbb{C} \to \mathbb{C} : E \mapsto \det(1 - E\rho) := \prod_{\lambda \in \sigma(\rho)} (1 - E\lambda) \ , \tag{1.0.5}$$

where $\sigma(\rho)$ is the spectrum of ρ. This is the direct analogue of the characteristic function in finite dimensional vector spaces, and the roots of the spectral determinant coincide with the spectrum of our extended quantized curve ρ^{-1}. Moreover, the spectral determinant is an *entire* function of E which is bounded by $\exp(c\,|E|)$ with $c = \sum_{\lambda \in \sigma(\rho)} \lambda$ for all $E \in \mathbb{C}$ [10, p. 217]. Since we started from a concrete operator in (1.0.1), this raises the question of what the solutions are to this well-behaved spectral problem. In particular, what is the spectral determinant, what is the spectrum, what are the eigenfunctions? In general, this is an almost impossible problem. However, for the quantizations of (1.0.1) we can give a construction of the spectral determinant and the eigenfunctions.

The curves in (1.0.1) can be realized as the mirror curves of toric Calabi-Yau threefolds, and it was found [4, 5] that the spectral determinant can be given in terms of refined topological string partition functions on the toric Calabi-Yau threefolds in question. Let me emphasize that this not only solves the spectral problem in terms of topological string theory, but it also gives a non-perturbative completion of the topological string partition function in terms of the spectral theory. With a non-perturbative completion, we mean a well-defined function of the string coupling g_s that in the $g_s \to 0$ expansion gives the usual asymptotic genus expansion at the topological string side, and is background independent, i.e. has good analytic properties in the moduli. This connection is called the topological string/spectral theory correspondence (TS/ST). It can be considered a strong-weak type of duality. One has $g_s/2\pi = 2\pi/\hbar$, so the usual topological string in the $g_s \ll 1$ regime corresponds to the "strong coupling" regime of the spectral theory $\hbar \gg 1$, and vice versa. See [6, 7] for a pedagogical introduction. The mathematically inclined reader should note that while there are many non-trivial checks of the proposal, and even special limits that can be proven rigorously [14, 15], there is no rigorous proof of the TS/ST correspondence at the moment.

While the spectral determinant was constructed in terms of closed topological strings in [4, 5], the construction of the eigenfunctions in terms of open topological string partition

[1] Compact operators map bounded subsets of $L^2(\mathbb{R})$ to "relatively compact subsets", that is, subsets which have a compact closure. Trace class operators are a particular class of compact operators.

functions is still an open problem. This thesis contains some partial progress in that direction. Crucial steps were made in [6, 7], where it was found how to write down well-defined functions that solve the relevant difference equations. However, these functions still have poles in x, so while they are well-defined functions of $\hbar$ solving the difference equation, they are not eigenfunctions in the Hilbert space sense. This problem was overcome in [6] for local $\mathbb{F}_0$ and in [7] for local $\mathbb{P}^2$ and the $\mathbb{C}^3/\mathbb{Z}_5$ orbifold at the so-called maximally supersymmetric point $\hbar = 2\pi = g_s$. In this thesis, we want to extend the construction to generic $\hbar > 0$ and to other geometries. In particular, we will work towards the eigenfunctions for the so-called crepant resolutions of the $Y^{N,0}$ singularities, which have mirror curves

$$\Lambda^N \left(\mathrm{e}^{y} + \mathrm{e}^{-y}\right) + \sum_{\ell=0}^{N} \kappa_\ell \, \mathrm{e}^{\left(\frac{N}{2}-\ell\right)x} = 0\,, \qquad \kappa_0 = 1 = \kappa_N\,. \tag{1.0.6}$$

These are interesting examples to study since the mirror curves have genus $N-1$. Moreover, in a geometric engineering picture they correspond to five-dimensional, $\mathcal{N} = 1$, SU(N) supersymmetric Yang Mills theory on $\mathbb{R}^4 \times \mathbb{S}^1$, and they admit interesting limits to four-dimensional, $\mathcal{N} = 2$ gauge theories. While the $Y^{N,0}$ form hence an interesting and non-trivial case to study, it should be noted that writing down the eigenfunctions for generic curves of the form (1.0.1) is currently still an open problem.

Many interesting spectral problems can be obtained as special limits of (1.0.1). These include among others the spectral problems related to quantized Seiberg-Witten curves of four-dimensional, $\mathcal{N} = 2$ supersymmetric Yang-Mills theory, as well as a family of integral kernel operators that are related to Painlevé equations. While these are in many ways simpler spectral problems than the quantized mirror curves in (1.0.1), they are largely unexplored at the level of the eigenfunctions. Making progress on the open topological string/spectral theory correspondence, which gives the eigenfunctions in terms of open topological strings, should help to understand and solve many derived spectral problems, see chapter 4. Moreover, it also aids in discovering a priori unexpected functional relations between these very different operators, see subsection 3.4.3. For this purpose, it is important to construct the TS/ST eigenfunctions at any $\hbar > 0$, since the derived spectral problems are found in limits $\hbar \to 0, \infty$

The logic flow of this thesis will, however, go in the opposite direction. We will follow the chronology in which the papers [1–3] appeared. In chapter 2 we discuss the spectral problem given by an integral kernel that is related to the Painlevé III_3 equation. The eigenfunctions can be written down in terms of defect partition functions of four-dimensional, $\mathcal{N} = 2$, SU(2) Seiberg-Witten theory in the self-dual phase, following [6, 14]. In chapter 3 we use the insights of chapter 2 and [6] to make a proposal for the eigenfunctions of a finite difference analogue of the modified Mathieu equation, which is the quantized mirror curve of local $\mathbb{F}_0 = \mathbb{P}^1 \times \mathbb{P}^1$. We study two limits in some detail, and find a functional relation between the quantized Seiberg-Witten curve and the Painlevé III_3 kernel. In chapter 4 we give then the proposal for the eigenfunctions for crepant resolutions of the $Y^{N,0}$ singularities. We focus mostly on the standard four-dimensional

limit to $\mathcal{N} = 2$, SU(N) gauge theory in the Nekrasov-Shatashvili phase, and we write down the eigenfunctions of the quantized Seiberg-Witten curve in terms of the gauge theory partition functions. These operators are finite difference analogues of Schrödinger operators with arbitrary polynomial potentials. We end with a short conclusion and some open problems in chapter 5.

Chapter 2

Eigenfunctions of the Painlevé III_3 kernel

In this chapter, we build on the work of [6, 14] to construct the eigenfunctions of a specific integral kernel (2.1.1) in terms of four-dimensional, $\mathcal{N} = 2$, SU(2) supersymmetric Yang-Mill theory in the self-dual phase of the Ω-background. This chapter is essentially [1] which is joint work with Alba Grassi.

2.1 Introduction

Building upon the work of Seiberg and Witten [16, 17], important results have been obtained for $\mathcal{N} = 2$ supersymmetric gauge theories in four dimensions. One remarkable achievement is the exact evaluation of the path integral, made possible thanks to localization techniques and the introduction of the Ω-background [18–21]. This led to the discovery of a new class of special functions, the so-called Nekrasov functions [20, 21], which today have found a wide range of applications in various fields of mathematics and theoretical physics. Examples of such functions are given in (2.3.10) and (2.6.1). Despite the exceptional control Nekrasov functions grant us over the weak gauge coupling regime, a strong coupling expansion requires alternative methods. This is one of the motivations behind the present work. In addition, this simultaneously explores a particular extension of the correspondence relating $\mathcal{N} = 2$ supersymmetric gauge theories in four dimensions to the spectral theory of quantum mechanical operators on the space of square-integrable functions $L^2(\mathbb{R})$.

The first concrete example of such correspondence was obtained in [22], where the authors showed how to use $\mathcal{N} = 2$ supersymmetric gauge theories in the four-dimensional Nekrasov-Shatashvili (NS) phase of the Ω-background ($\epsilon_2 = 0$) to solve the spectral theory of a certain class of ordinary differential equations. For example, the quantization condition for the operator spectrum corresponds to the quantization of the twisted superpotential [22–26], while the eigenfunctions are computed from the surface defect partition functions [27–40]. More recently, explicit expressions for the Fredholm determinants [41, 42] and the

connection coefficients [37] of such differential equations have been derived in closed form.[1] See also [46–54] for related development in the context of WKB and four-dimensional gauge theories, and [55] for a different quantization scheme in higher-rank gauge theories. All the operators appearing in the above setup can be obtained via the canonical quantization of four-dimensional Seiberg-Witten (SW) curves [22, 23, 56], or equivalently, by considering the semiclassical limit of BPZ equations [57].

In this chapter, we explore another facet of the interplay between spectral theory and supersymmetric gauge theories. On the gauge theory side, we focus on four-dimensional $\mathcal{N} = 2$ gauge theories in the *self-dual* phase of the Ω-background ($\epsilon_1 = -\epsilon_2 = \epsilon$), while on the operator theory side we study a class of operators which do *not* correspond to canonically quantized four-dimensional SW curves. These operators originally appeared in the framework of isomonodromic deformation equations [58–62]. Their relevance in the context of four-dimensional supersymmetric gauge theories and topological string theory was pointed out in [14, 15, 63, 64], in close connection with the TS/ST duality [4, 5, 11, 65] and the isomonodromy/CFT/gauge theory correspondence [66–71]. Geometrically, we construct such operators from mirror curves to toric CY manifolds, after implementing a suitable canonical transformation combined with a special scaling limit [14, 63], see subsection 2.3.2 and subsection 2.3.4.

Here we focus on a specific example of such an operator which is associated with the Painlevé III_3 equation, and whose spectral traces compute correlation functions in the 2d Ising model [58, 61, 72]. Its integral kernel $\rho(x, y)$ on $\mathbb{R}$ reads[2]

$$\rho(x,y) = \frac{\mathrm{e}^{-4t^{1/4}\cosh x}\mathrm{e}^{-4t^{1/4}\cosh y}}{\cosh\left(\frac{x-y}{2}\right)}\,, \tag{2.1.1}$$

and the corresponding Fredholm determinant $\det(1+\kappa\rho)$ computes the tau function of Painlevé III_3 [58]. For $t > 0$, the kernel (2.1.1) is positive and of trace class on $L^2(\mathbb{R})$; hence, the corresponding operator has a discrete, positive spectrum $\{E_n\}_{n\geqslant 0}$, with real-valued, square-integrable eigenfunctions $\{\varphi_n(x,t)\}_{n\geqslant 0}$,

$$\int_{\mathbb{R}} \mathrm{d}y\ \rho(x,y)\,\varphi_n(y,t) = E_n\varphi_n(x,t)\ . \tag{2.1.2}$$

As we review in subsection 2.3.2, the spectrum is computed by the Nekrasov function of 4d, $\mathcal{N} = 2$, SU(N) super Yang-Mills (SYM) in the self-dual phase of the Ω-background [14], see (2.3.7) and (2.3.8). The purpose of this chapter is to study the eigenfunctions of (2.1.1) and relate them to surface defects in the same gauge theory. Specifically, we find that the eigenfunctions $\varphi_n(x,t)$ are the Zak transform of the sum of two partition functions of surface defects, which are simply related by a change in some parameters. See equation

[1] A rigorous derivation of some of these results can be found in [43]. A q-perturbative approach to connection coefficients is also discussed in [44, 45], see also [35].

[2] We refer to (2.1.1) as a Fermi gas operator, since it corresponds to the density matrix of an ideal Fermi gas in the external potential $8t^{1/4}\cosh(x)$.

(2.2.6) for the explicit expression. We test this proposal numerically in subsection 2.6.4. The relevance of this result is twofold. On the one hand, it provides an efficient description of eigenfunctions of (2.1.1) at small t. On the other hand, it offers a tool to resum both the instanton expansion and the ϵ expansion in the defect partition function, hence allowing to probe the gauge theory at strong coupling (large t). This is possible because, following [6, 62], we can provide an alternative matrix model description for such eigenfunctions (2.2.1), which is exact in t and hence exact in the gauge coupling.

2.2 Summary

2.2.1 Results

The chapter can be summarized as follows. Adopting the approach of [62], which is nicely summarized in [6, sec. 2.3], we construct eigenfunctions of (2.1.1) from expectation values of a determinant-like expression,

$$\Xi_{\pm}(x,t,\kappa) = \mathrm{e}^{-4t^{1/4}\cosh x}\mathrm{e}^{\pm x/2}\sum_{N\geqslant 0}(\pm\kappa)^N\Psi_N(\mathrm{e}^x,t)\,, \qquad x\in\mathbb{R}\,, \tag{2.2.1}$$

$$\Psi_N(z,t) = \frac{1}{N!}\int_{\mathbb{R}^N_{>0}}\left(\prod_{i=1}^N \frac{\mathrm{d}z_i}{z_i}\frac{z-z_i}{z+z_i}\,\exp\left(-4t^{1/4}\left(z_i+z_i^{-1}\right)\right)\prod_{j=i+1}^N\left(\frac{z_i-z_j}{z_i+z_j}\right)^2\right). \tag{2.2.2}$$

More precisely, (2.2.1) are square-integrable eigenfunctions φ_n of (2.1.1) if we set $\kappa = -E_n^{-1}$, where E_n is an eigenvalue of the operator (2.1.1),

$$\varphi_n(x,t) = \Xi_+\left(x,t,-\frac{1}{E_n}\right) = (-1)^n\,\Xi_-\left(x,t,-\frac{1}{E_n}\right). \tag{2.2.3}$$

In section 2.6, we show that (2.2.1) and (2.2.2) are explicitly related to surface defects in 4d, $\mathcal{N}=2$, SU(N) SYM in the self-dual phase ($\epsilon_1=-\epsilon_2=\epsilon$) of the Ω-background[3]. We consider the surface defect which is engineered using the open topological vertex with a D-brane on the external leg, see section A.3 for details. Using the explicit vertex expression of section A.3, one can see that this corresponds to the special case of a 2d/4d defect called a type II defect in [32, sec. 2.3.3][4]. Hence, we denote its partition function by $Z^{\mathrm{II}}_{\mathrm{tot}}(q,t,\sigma)$. The explicit expression is given in (2.6.1) and (2.6.4). In the gauge theory, we typically use

$$q = \frac{y}{2\epsilon}\,, \qquad t = \left(\frac{\Lambda}{\epsilon}\right)^4, \qquad \sigma = \mathrm{i}\frac{a}{2\epsilon}\,, \tag{2.2.4}$$

[3]This is in line with the generic expectation that matrix model averages are related to partitions functions in the presence of D-branes [56, 73–78].

[4]Following [32, sec. 2.3.3], the two-dimensional $\mathcal{N}=(2,2)$ theory here consists of 2 free chiral multiplets living on a disc. See also [79–81].

where y is the position of the defect[5], $\epsilon = \epsilon_1 = -\epsilon_2$ is the Ω-background parameter, a is the Coulomb branch parameter, and $\Lambda \sim \mathrm{e}^{-1/g_{\mathrm{YM}}^2}$ is the instanton counting parameter, with g_{YM} the gauge coupling. The relation between the determinant like expression (2.2.1) and the defect partition function $Z_{\mathrm{tot}}^{\mathrm{II}}$ is given in (2.6.7) and reads

$$\Xi_{\pm}\left(x, t, \frac{\cos(2\pi\sigma)}{2\pi}\right) = \frac{\mathrm{e}^{3\zeta'(-1)}\mathrm{e}^{4\sqrt{t}}}{2^{11/12}\pi^{3/2}t^{3/16}} \int_{\mathbb{R}} \mathrm{d}q\ \mathrm{e}^{\mathrm{i}2qx} \sum_{k\in\mathbb{Z}} \left(Z_{\mathrm{tot}}^{\mathrm{II}}\left(\pm q, t, \sigma + k\right) + Z_{\mathrm{tot}}^{\mathrm{II}}\left(\mp q - \frac{\mathrm{i}}{2}, t, \sigma + k + \frac{1}{2}\right)\right) . \tag{2.2.5}$$

The quantization condition for the energy spectrum of (2.1.1) was derived in [14], see (2.3.7) and (2.3.8). By evaluating the defect partition function on the right-hand side of (2.2.5) at the corresponding quantized values of $\sigma = 1/2 + \mathrm{i}\sigma_n$, we obtain the eigenfunctions φ_n of (2.1.1),

$$\varphi_n(x, t) = \frac{\mathrm{e}^{3\zeta'(-1)}\mathrm{e}^{4\sqrt{t}}}{2^{11/12}\pi^{3/2}t^{3/16}} \int_{\mathbb{R}} \mathrm{d}q\ \mathrm{e}^{\mathrm{i}2qx} \sum_{k\in\mathbb{Z}} \left(Z_{\mathrm{tot}}^{\mathrm{II}}\left(q, t, k + \frac{1}{2} + \mathrm{i}\sigma_n\right) + Z_{\mathrm{tot}}^{\mathrm{II}}\left(-q - \frac{\mathrm{i}}{2}, t, k + \mathrm{i}\sigma_n\right)\right) , \tag{2.2.6}$$

where $\sigma_n \in \mathbb{R}_{>0}$ are solutions to (2.3.8). The eigenfunctions φ_0 and φ_1 are shown in figure 2.1.

In section 2.6 and subsection A.1.1, we show that we can equivalently write (2.2.5) as

$$\int_{\mathbb{R}+\mathrm{i}\sigma_*} \mathrm{d}\sigma \frac{\tan\left(2\pi\sigma\right)}{\left(2\cos(2\pi\sigma)\right)^N} \left(Z_{\mathrm{tot}}^{\mathrm{II}}\left(q, t, \sigma\right) + Z_{\mathrm{tot}}^{\mathrm{II}}\left(-q - \frac{\mathrm{i}}{2}, t, \sigma + \frac{1}{2}\right)\right) = \mathrm{i}\frac{2^{11/12}\sqrt{\pi}t^{3/16}}{\mathrm{e}^{3\zeta'(-1)}\mathrm{e}^{4\sqrt{t}}\left(4\pi\right)^N} \int_{\mathbb{R}} \mathrm{d}x\ \mathrm{e}^{-\mathrm{i}2qx}\mathrm{e}^{-4t^{1/4}\cosh x}\mathrm{e}^{x/2}\Psi_N\left(\mathrm{e}^x, t\right) , \tag{2.2.7}$$

where σ_* is such that $0 < \sigma_* < |\mathrm{Re}(q)|$ if $\mathrm{Re}(q) \neq 0$, and simply $\sigma_* > 0$ if $\mathrm{Re}(q) = 0$. This choice of σ^* guarantees that the integration over σ in (2.2.7) avoids the poles of the integrand. Let us elaborate more on the meaning of (2.2.7).

- The Fourier transform on the right-hand side of (2.2.7) relates two types of defects [32, sect. 2.3.3], or more precisely, two phases of the same defect [34, sect. 4.2][6]. In

[5]The parameter y corresponds to the insertion of the defect on the Riemann sphere C in the 6d, $\mathcal{N} = (2, 0)$ theory on $\mathbb{R}^4 \times C$, and it is a position in that sense. From the perspective of the two-dimensional $\mathcal{N} = (2, 2)$ chiral multiplets, it corresponds to the twisted mass for the $U(1)$ flavour symmetry of the chirals, see e.g. [78].

[6]Both surface defects are defined by coupling the 4d theory to the same 2d gauged linear sigma model, but in different phases of the 2d theory. The transition between these phases explains the Fourier transform relation between their vacuum expectation values as explained in [34]. We thank Saebyeok Jeong for pointing that out.

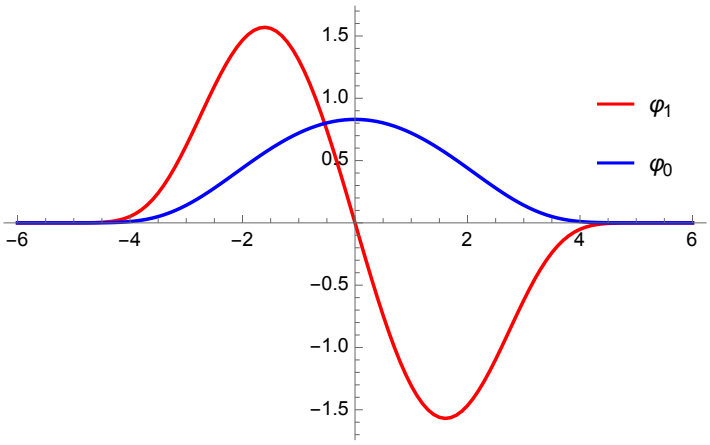

Figure 2.1. The first (blue) and second (red) eigenfunction of (2.1.1) computed using the surface defect expression in (2.2.6) for $t = 1/100\pi^8$.

particular, while $Z^{\rm II}_{\rm tot}(q,t,\sigma)$ is geometrically engineered in topological string theory by inserting a brane on the external leg of the toric diagram, its Fourier transform with respect to the defect variable q makes contact with a brane in the inner edge of the toric diagram [34], see also [56, 82–84][7]. Following [32, sect. 2.3.3], we refer to the inverse Fourier transform of a type II defect as a type I defect[8]. Via the AGT correspondence [85], the latter is realized in Liouville CFT by considering the five-point function of four primaries with one degenerate field, the so-called $\Phi_{2,1}$ field [39, 40, 77, 86–88]. One can equivalently realize this defect by coupling the four-dimensional theory to a two-dimensional theory, see, for instance, [30–35, 80, 89–91] and references therein.

This also means that we could get rid of the inverse Fourier transform on the right-hand side of (2.2.5) by replacing the partition function of the type II defect $Z^{\rm II}$ with the partition function of the type I defect $Z^{\rm I}$. The instanton counting-like expression of type I defect can be found, for instance, in [30]; however, we will not use such expression here as we will mainly focus on type II defects. The reason for this is that, in the latter case, the gauge theoretic expression is represented by a convergent series in t, whose coefficients are exact rational functions of σ and q. Conversely, for the type I defect, the gauge theoretic expression is more cumbersome, involving double series expansions in both t and in q.

- The integral over σ on the left-hand side of (2.2.7) is responsible for the change of frame: it brings us from the weakly coupled electric frame, where $Z^{\rm II}_{\rm tot}$ is defined,

[7] We would like to thank A. Neitzke for useful discussions on this point.

[8] Since we consider gauge theories of rank 1 this is equivalent to a type III defect as defined in [32, sect. 2.3.3].

to the strongly coupled magnetic frame, which is the suitable frame to describe the magnetic monopole point of SYM, see section 2.5.

In summary, (2.2.7) means that the matrix model average (2.2.2) computes the type I surface defect partition function of 4d, $\mathcal{N} = 2$, SU(N) SYM, in the *self-dual phase* of the Ω-background ($\epsilon_1 = -\epsilon_2 = \epsilon$), and in the *magnetic frame*. In this identification, $z = \exp(x)$ is related to the position of the defect and the 't Hooft parameter of the matrix model is identified with the dual period, $N\epsilon = a_D$.

Note also that (2.2.2) is exact both in Λ and in ϵ; it resums the instanton expansion of the defect partition function and provides an explicit interpolation from the weak to the strong coupling region. The $1/\Lambda$ expansion can be obtained straightforwardly from (2.2.2) since it corresponds to expanding the matrix model around its Gaussian point, see [15, sect. 5] and references therein.

2.2.2 Derivation

Let us briefly comment on the derivation of equations (2.2.5), (2.2.6), and (2.2.7). Firstly, we obtained these results by analyzing the large N expansion of the matrix models (2.2.2) and then extrapolating to finite N. Secondly, part of the idea also comes from the open version of the TS/ST correspondence [6, 7], see subsection 2.3.4 and section 2.7. By combining these two approaches we obtained (2.2.5)-(2.2.7), which we further tested numerically. However, we do not have a rigorous mathematical proof of these results.

This chapter is structured as follows. In section 2.3, we give an overview of the well-established relationship between the modified Mathieu operator and the four-dimensional, $\mathcal{N} = 2$, SU(N) SYM in the NS phase of the Ω-background. We then present the connection between the operator (2.1.1) and the same gauge theory, but in the self-dual phase of the Ω-background. In section 2.4, we compute the planar resolvent of (2.2.2) as well as the planar two-point function and show how the Seiberg-Witten geometry emerges from it. In section 2.5, we show that the 't Hooft expansion of (2.2.2) reproduces the ϵ expansion of the type I self-dual surface defect in the magnetic frame. To establish this connection, we rely on two crucial findings. Firstly, according to the results presented in [77], the ϵ expansion of the self-dual type I surface defect in the electric frame is determined by topological recursion [92]. Secondly, the self-dual surface defect (or, more generally, the open topological string partition function) behaves as a wave function under a change of frame [93]. In section 2.6, we test (2.2.7) numerically for finite N and analytically in a $1/N$ expansion, and we verify (2.2.6) numerically.

2.3 Preparation: spectral theory and 4d, $\mathcal{N} = 2$ gauge theory

2.3.1 Known: differential operators and the NS phase of the Ω-background

Let us start by reviewing the correspondence relating ordinary differential equations to four-dimensional $\mathcal{N} = 2$ gauge theories in the *NS phase* of the Ω-background, where $\epsilon_2 = 0$ and $\epsilon_1 = \epsilon \neq 0$ [22]. In this paper, we focus on SU(N) SYM.

Consider the so-called modified Mathieu operator O_{Ma} acting as

$$\mathrm{O}_{\mathrm{Ma}}\,\varphi(x,t) = \left(-\partial_x^2 + \sqrt{t}\cosh(x)\right)\varphi(x,t)\,. \tag{2.3.1}$$

If $t > 0$, the operator (2.3.1) has a positive discrete spectrum with square-integrable eigenfunctions. One can make the connection to gauge theory by noting that the modified Mathieu operator corresponds to the canonically quantized SW curve of SU(N) SYM, if we set $t = (\Lambda/\epsilon)^4$ as in (2.2.4). This relationship was exploited in [22], showing how gauge theory can be efficiently used to find the spectrum of (2.3.1). The first ingredient in this relation is the quantization condition of the twisted superpotential which reads

$$\partial_\sigma F^{\mathrm{NS}}(t,\sigma) = \mathrm{i}2\pi n\,, \qquad\qquad n \in \mathbb{N}\,, \tag{2.3.2}$$

where F^{NS} is the NS free energy and $\sigma = \mathrm{i}a/2\epsilon$ as in (2.2.4). The small t or weak coupling expansion is given by

$$\begin{aligned} F^{\mathrm{NS}}(t,\sigma) = {} & -\psi^{(-2)}(1-2\sigma) - \psi^{(-2)}(1+2\sigma) + \sigma^2\ln(t) \\ & + \frac{2t}{4\sigma^2-1} + \frac{(20\sigma^2+7)\,t^2}{(4\sigma^2-1)^3\,(4\sigma^2-4)} + \mathcal{O}\left(t^3\right)\,, \end{aligned} \tag{2.3.3}$$

where ψ is the polygamma function of order -2. Higher-order terms in t in (2.3.3) can be computed by using combinatorics of Young diagrams [20, 94, 95], see [96] for a review and further list of references. The resulting expansion in (2.3.3) is convergent[9] when $2\sigma \notin \mathbb{Z}$. Equation (2.3.2) has then a discrete set of solutions $\{\sigma_n\}_{n\geqslant 0}$ for a fixed value of $t > 0$. The quantum Matone relation [99, 100],

$$E = -t\partial_t F^{\mathrm{NS}}(t,\sigma)\,. \tag{2.3.4}$$

gives at last the connection to the spectrum $\{E_n\}_{n\geqslant 0}$ of the modified Mathieu operator (2.3.1).

There is a parallel development for the eigenfunctions, but one has to consider the four-dimensional partition function with the insertion of a type I defect[10] in the NS phase of the Ω-background, see [27–34] and references there.

[9] Beside numerical and physical evidence, we are not aware of a rigorous mathematical proof of this fact, see [97, 98] for related discussions and proofs in other phases of the Ω-background.

[10] As before, we are following the terminology of [32, sect. 2.3.3]. We also note that, since we are considering only rank 1 theories, type I and type III defects as in [32, sect. 2.3.3] are identified.

2.3.2 New: Painlevé kernels and the self-dual phase of the Ω-background

In this work, we consider a class of operators whose spectral properties are encoded in the gauge theory partition functions in the *self-dual phase* of the Ω-background, where $\epsilon_1 + \epsilon_2 = 0$. We focus on the four-dimensional, $\mathcal{N} = 2$, SU(N) SYM. In this case, the relevant operator ρ has the integral kernel $\rho(x, y)$ given by [14]

$$\rho(x,y) = \frac{\sqrt{v(x)}\sqrt{v(y)}}{\cosh\left(\frac{x-y}{2}\right)}, \qquad v(x) = \mathrm{e}^{-8t^{1/4}\cosh(x)}. \tag{2.3.5}$$

This operator ρ can be seen as the density matrix of an ideal Fermi gas in an external potential $-\ln[v(x)]$ [72]. We therefore refer to (2.3.5) as a Fermi gas operator. Unlike the example of the modified Mathieu operator, the relation of this operator to the quantization of the four-dimensional SU(N) Seiberg-Witten curves is far from obvious. This connection was originally found in [14] as a prediction of the TS/ST correspondence [4]. It can be understood as a consequence of the fact that the operator (2.3.5) can be constructed starting from the quantum mirror curve to local $\mathbb{F}_0$, and implementing a particular scaling limit, as we review in subsection 2.3.4. However, we do not yet have a direct method to derive (2.3.5) using any quantization scheme that starts from the four-dimensional SW curve. We have to rely on the TS/ST correspondence. See also the discussion at the end of subsection 2.3.4.

For $t > 0$ (2.3.5) is a trace class operator on $L^2(\mathbb{R})$ with a positive discrete spectrum $\{E_n\}_{n\geqslant 0}$,

$$\int_{\mathbb{R}} \mathrm{d}y\ \rho(x,y)\,\varphi_n(y,t) = E_n \varphi_n(x,t)\,. \tag{2.3.6}$$

It was shown in [14] that the spectrum is given by

$$E_n^{-1} = -\frac{1}{2\pi}\cos\left(2\pi\left(\frac{1}{2} + \mathrm{i}\sigma_n\right)\right), \tag{2.3.7}$$

where $\sigma_n \in \mathbb{R}_{>0}$ are solutions to

$$\sum_{k\in\mathbb{Z}} Z^{\mathrm{Nek}}\left(t, \frac{1}{2} + \mathrm{i}\sigma_n + k\right) = 0\,. \tag{2.3.8}$$

This result follows from the identity [14, eqs 3.26, 3.49, 3.55] [63, eq. 2.19]

$$\det\left(1 + \frac{\cos(2\pi\sigma)}{2\pi}\rho\right) = 2^{1/12}\mathrm{e}^{3\zeta'(-1)}t^{-1/16}\mathrm{e}^{4\sqrt{t}}\sum_{k\in\mathbb{Z}} Z^{\mathrm{Nek}}(t, \sigma + k)\,, \tag{2.3.9}$$

which was proved using the theory of Painlevé equations. The function $Z^{\mathrm{Nek}}(t,\sigma)$ in (2.3.8) and (2.3.9) is the Nekrasov partition function in the self-dual phase of the Ω-background,

$$Z^{\mathrm{Nek}}(t,\sigma) = \frac{t^{\sigma^2}}{G(1-2\sigma)G(1+2\sigma)}\left(1 + \frac{t}{2\sigma^2} + \frac{(8\sigma^2+1)\,t^2}{4\sigma^2\,(4\sigma^2-1)^2} + \mathcal{O}\left(t^3\right)\right), \tag{2.3.10}$$

with G the Barnes G-function. Higher-order terms in t are defined systematically by using combinatorics of Young diagrams, see [97, eqs. 3.4, 3.6] for the precise definition. The convergence of this series is shown in [97] for any $t > 0$ and fixed $2\sigma \notin \mathbb{Z}$. Even though $Z^{\text{Nek}}(t, \sigma)$ has poles when $2\sigma \in \mathbb{Z}$, the sum on the right-hand side of (2.3.9) removes these poles, and the resulting expression is well-defined for any complex value of σ [97, 101]. Let us also note that the Nekrasov function is often expressed using Λ, a and ϵ, which are related to t and σ via (2.2.4)

$$t = \left(\frac{\Lambda}{\epsilon}\right)^4 , \qquad \sigma = \mathrm{i}\frac{a}{2\epsilon} . \tag{2.3.11}$$

It is useful to write the Fredholm determinant on the left-hand side of (2.3.9) by using the spectral traces,

$$\det\left(1 + \kappa\rho\right) = \sum_{N \geqslant 0} \kappa^N Z(t, N) , \tag{2.3.12}$$

$$Z(t, N) = \frac{1}{N!} \sum_{s \in S_N} (-1)^{\text{sgn}(s)} \int_{\mathbb{R}} \mathrm{d}^N x \prod_{i=1}^{N} \rho(x_i, x_{s(i)}) , \tag{2.3.13}$$

where S_N is the permutation group of N elements. The Cauchy identity allows us to write (2.3.13) as [72]

$$Z(t, N) = \frac{1}{N!} \int_{\mathbb{R}^N_{>0}} \left(\prod_{i=1}^{N} \frac{\mathrm{d}z_i}{z_i} \mathrm{e}^{-4t^{1/4}\left(z_i + z_i^{-1}\right)} \prod_{j=i+1}^{N} \left(\frac{z_i - z_j}{z_i + z_j}\right)^2 \right) , \tag{2.3.14}$$

which can be analysed in the regime $t \to +\infty$, since this corresponds to expanding the potential around its Gaussian point. It was found in [14] that the matrix model (2.3.14) computes the partition function of $\mathcal{N} = 2$, SU(N) SYM in the self-dual phase of the Ω-background and in the magnetic frame[11]. The relation to the Nekrasov function (2.3.10) can be obtained from (2.3.9) and reads [63, eq. 2.28]

$$Z(t, N) = -\mathrm{i}(4\pi)^N 2^{1/12} \mathrm{e}^{3\zeta'(-1)} t^{-1/16} \mathrm{e}^{4\sqrt{t}} \int_{\mathbb{R}+\mathrm{i}\sigma_*} \mathrm{d}\sigma \frac{\tan\left(2\pi\sigma\right)}{\left(2\cos(2\pi\sigma)\right)^N} Z^{\text{Nek}}\left(t, \sigma\right) , \tag{2.3.15}$$

where[12] $\sigma_* > 0$. Therefore, the matrix model (2.3.14) provides a resummation of the instanton expansion in the Nekrasov function (2.3.10), which is an expansion around $t = 0$. In this context, we identify the 't Hooft parameter of the matrix model, $N\epsilon$, with the dual or magnetic period in SW theory[13]

$$a_D = N\epsilon . \tag{2.3.16}$$

[11] The magnetic frame can be obtained from the usual electric frame by an S-duality transformation. It allows us to study the behaviour of the gauge theory near the magnetic monopole point. See section 2.5 and [96] for more details.

[12] One can take $\sigma_* = \text{arccosh}(2\pi)/2\pi$ as in [63] or any other $\sigma^* > 0$ as long as the integral over σ in (2.3.15) does not hit the poles of the integrand.

[13] It is possible to analytically continue the results to non-integer values of N [63, 102].

The equality (2.3.15) was demonstrated in [14, 63]. Finally, we emphasise that (2.3.14) is exact both in the instanton counting parameter Λ and in the Ω-background parameter ϵ. When we expand (2.3.14) at large Λ while keeping ϵ and a_D fixed, we obtain an analogous expansion to that found when performing a large-time expansion in isomonodromic deformation equations [15, 97, 103–107]. On the matrix model side, this is an expansion around the Gaussian point. Similarly, if we expand at small ϵ while keeping Λ and a_D fixed, we recover the expansion resulting from the holomorphic anomaly algorithm [108, 109].

The goal of this work is to extend these results to the eigenfunctions of (2.3.5), which on the gauge theory side corresponds to inserting surface defects. As a first observation, we note that the kernel (2.3.5) falls in the class of operators studied in [62], and more recently in [6, sect. 2]. In particular, following [6, 62] we can construct eigenfunctions of (2.3.5) using the matrix model (2.3.14). Let us define

$$\Xi_{\pm}\left(x,t,\kappa\right)=\mathrm{e}^{-4t^{1/4}\cosh(x)}\mathrm{e}^{\pm x/2}\sum_{N\geqslant 0}(\pm\kappa)^{N}\Psi_{N}\left(\mathrm{e}^{x},t\right),\qquad x\in\mathbb{R}\,,\tag{2.3.17}$$

$$\Psi_{N}(z,t)=\frac{1}{N!}\int_{\mathbb{R}_{>0}^{N}}\left(\prod_{i=1}^{N}\frac{\mathrm{d}z_{i}}{z_{i}}\frac{z-z_{i}}{z+z_{i}}\,\exp\left(-4t^{1/4}\left(z_{i}+z_{i}^{-1}\right)\right)\prod_{j=i+1}^{N}\left(\frac{z_{i}-z_{j}}{z_{i}+z_{j}}\right)^{2}\right).\tag{2.3.18}$$

The $\Xi_{\pm}(x,t,\kappa)$ in (2.3.17) are then square-integrable eigenfunctions $\varphi_n(x,t)$ of (2.3.5) if we evaluate them at $\kappa=-E_n^{-1}$,

$$\varphi_{n}(x,t)=\Xi_{+}\left(x,t,-\frac{1}{E_{n}}\right)=(-1)^{n}\,\Xi_{-}\left(x,t,-\frac{1}{E_{n}}\right).\tag{2.3.19}$$

This can be verified by using [6, eqs. 2.46, 2.59] and $\varphi_n(x,t)=(-1)^n\varphi_n(-x,t)$. We will argue in the forthcoming sections that the matrix model with insertion $\Psi_N(z,t)$ corresponds to a surface defect in four-dimensional, $\mathcal{N}=2$, SU(N) SYM in the *self-dual phase* of the Ω-background and in the *magnetic frame*.

2.3.3 Comment on blowup equations

It was first pointed out in [110] that the five-dimensional NS and self-dual partition functions are closely connected, which was subsequently demonstrated using Nakajima–Yoshioka blowup equations in [111]. The interplay between these two phases of the Ω-background was extended to surface defects in four dimensions in [112, 113]. Applications in the context of Painlevé equations are discussed in [107, 112–116]. The relevance of blowup equations in the context of resurgence was also recently investigated in [117].

Given such results, it is natural to wonder whether blowup equations can be used to relate the spectrum and eigenfunctions of (2.3.1) and (2.3.5). Regarding the spectrum, the blowup formula presented in [115, eq. 5.7] reveals a one-to-one correspondence between the solutions $\{\sigma_n\}_{n\geqslant 0}$ of (2.3.2) and the solutions $\{\sigma_n\}_{n\geqslant 0}$ of (2.3.8). However, to obtain the spectrum we further need the quantum Matone relation (2.3.4) on the Mathieu side and the relation (2.3.7) on the Fermi gas side. These two relations are very different, and

therefore, the spectrum of (2.3.1) and (2.3.5) is related in a highly non-trivial way. It would be interesting to see if blowup equations in the presence of defects [112, 113] could be used to establish a map between the eigenfunctions of these two operators.

2.3.4 Two limits of quantum mirror curves

Both operators (2.3.1) and (2.3.5) can be obtained as different limits of the quantized mirror curve corresponding to the toric Calabi-Yau (CY) manifold known as local $\mathbb{F}_0$, which we review here briefly.

It is well known that four-dimensional $\mathcal{N}=2$ supersymmetric theories can be engineered by using topological string theory on toric CY manifolds [118–120]. The partition function of refined topological string theory is then identified with the partition function of a five-dimensional $\mathcal{N}=1$ theory on $\mathbb{R}^4\times S^1$ [121, 122]. If we shrink the S^1 circle we get the 4d theory we are interested in, we refer to [96] for a review and more references. For $\mathcal{N}=2$, SU(N) SYM the relevant setup is topological string theory on local $\mathbb{F}_0$. The mirror curve of local $\mathbb{F}_0$ is

$$\mathrm{e}^{x}+\mathrm{e}^{-x}+\frac{1}{m_{\mathbb{F}_0}}\mathrm{e}^{y}+\mathrm{e}^{-y}+\widehat{\kappa}=0\,, \tag{2.3.20}$$

where $\widehat{\kappa}$ and $m_{\mathbb{F}_0}$ are the complex moduli. The quantization of this curve [8, 56] leads to the operator

$$\mathrm{O}_{\mathbb{F}_0}=\mathrm{e}^{\mathrm{x}}+\mathrm{e}^{-\mathrm{x}}+\frac{1}{m_{\mathbb{F}_0}}\mathrm{e}^{\mathrm{y}}+\mathrm{e}^{-\mathrm{y}}\,,\qquad [\mathrm{x},\mathrm{y}]=\mathrm{i}\hbar\,. \tag{2.3.21}$$

If $\hbar, m_{\mathbb{F}_0}>0$ the inverse operator

$$\rho_{\mathbb{F}_0}=\mathrm{O}_{\mathbb{F}_0}^{-1} \tag{2.3.22}$$

is of trace class with a positive discrete spectrum[14] [4, 11, 125]. Hence, a natural object to consider is its Fredholm determinant

$$\det\left(1+\widehat{\kappa}\rho_{\mathbb{F}_0}\right)\,. \tag{2.3.23}$$

The operator (2.3.1) can be obtained from (2.3.21) by implementing the usual geometric engineering limit [118, 120] where we scale

$$m_{\mathbb{F}_0}=\frac{\beta^4 t}{4}\,,\qquad \widehat{\kappa}=-\frac{4}{\beta^2\sqrt{t}}+\frac{2E}{\sqrt{t}}\,,\qquad \hbar=\beta\,, \tag{2.3.24}$$

and take $\beta\to 0$. In this limit, we obtain the modified Mathieu operator (2.3.1),

$$\left(\mathrm{O}_{\mathbb{F}_0}+\widehat{\kappa}\right)\psi(x)=0\;\;\to\;\;\left(\mathrm{O}_{\mathrm{Ma}}+E\right)\psi(x)=0\,. \tag{2.3.25}$$

Likewise, the Fredholm determinant becomes

$$\det\left(1+\widehat{\kappa}\rho_{\mathbb{F}_0}\right)\to\det\left(1+E\,\mathrm{O}_{\mathrm{Ma}}^{-1}\right)\,, \tag{2.3.26}$$

[14] It is also possible to take $\hbar$ and $m_{\mathbb{F}_0}$ imaginary within some range. In this case, one still has the trace class property, but the spectrum may no longer be real [123, 124].

and we have an explicit expression for this determinant via the NS functions [41, sect. 5]

$$\det\left(1+E\,\mathrm{O}_{\mathrm{Ma}}^{-1}\right)=C(t)\frac{\sinh\left(\partial_\sigma F^{\mathrm{NS}}(t,\sigma)\right)}{\sin\left(2\pi\sigma\right)}\,, \tag{2.3.27}$$

where $C(t)$ is a normalization constant and the relation $\sigma\equiv\sigma(t,E)$ is obtained from (2.3.4).

On the other hand, the Fermi gas operator (2.3.5) can be obtained from $\rho_{\mathbb{F}_0}$ by implementing a rescaled limit [14],

$$\ln\left(m_{\mathbb{F}_0}\right)=4\pi\mathrm{i}\sigma-\frac{2\pi}{\beta}\ln(\beta^4 t)\,,\qquad\qquad \widehat{\kappa}=2\cos\left(2\pi\sigma\right)\,,\qquad\qquad \hbar=\frac{(2\pi)^2}{\beta}\,, \tag{2.3.28}$$

and $\beta\to 0$. This is called "the dual 4d limit" in [14]. The scaling (2.3.28) may seem strange at first sight, but it is a natural limit from the point of view of the TS/ST correspondence [4]. In the dual 4d limit, we have

$$\det\left(1+\widehat{\kappa}\rho_{\mathbb{F}_0}\right)\to\det\left(1+\left(\frac{\cos(2\pi\sigma)}{2\pi}\right)\rho\right), \tag{2.3.29}$$

where ρ is the operator (2.3.5). The determinant at the right-hand side can also be written as the Zak transform of the self-dual Nekrasov function (2.3.9).

Let us conclude this section by emphasizing that (2.3.1) has a natural interpretation directly within the four-dimensional theory, independently of the five-dimensional quantum curve. In particular, (2.3.1) is the canonical quantization of the four-dimensional SW curve of SU(N) SYM, which is related to the semiclassical limit of BPZ equations via the AGT correspondence. On the other hand, for the Fermi gas operator (2.3.5) we do not have a parallel interpretation at the moment. It may be possible to relate this operator to some other quantization scheme of the four-dimensional SW curve. Probably a scheme similar to the one used in the context of topological recursion [126–129][15].

2.4 The Seiberg-Witten geometry from the matrix model

In this section, we study the 't Hooft expansion of the matrix model (2.3.18) and show how the Seiberg-Witten geometry emerges from it. For this purpose, it is useful to parameterise $t=(\Lambda/\epsilon)^4$ as before in (2.3.11) and to introduce the potential[16] V such that

$$v\left(\ln\left(z\right)\right)=\exp\left(-\frac{V\left(z\right)}{\epsilon}\right)\,,\qquad\qquad V\left(z\right)=4\Lambda\left(z+\frac{1}{z}\right)\,, \tag{2.4.1}$$

and we take $\Lambda,\epsilon>0$ for convenience. The matrix models (2.3.14) and (2.3.18) can then be studied in a 't Hooft limit where

$$N\to+\infty\,,\qquad\qquad \epsilon\to 0\,,\qquad\qquad \lambda=N\epsilon\,, \tag{2.4.2}$$

[15] We would like to thank M. Mariño and N. Orantin for useful discussions on this point.

[16] The potential of the one-dimensional ideal Fermi gas is $-\ln\left(v\left(x\right)\right)=V\left(\mathrm{e}^x\right)/\epsilon$.

with the defect insertion parameter z, the instanton counting parameter Λ, and the 't Hooft parameter λ all kept fixed.

This limit was implemented on the matrix model without insertions (2.3.14) in [14, 72]. In particular, in this limit the eigenvalues of the matrix model distribute along

$$\left[\mathrm{g}, \mathrm{g}^{-1}\right] \subset \mathbb{R}_{>0}\,, \qquad\qquad 0 < \mathrm{g} < 1\,, \tag{2.4.3}$$

and the 't Hooft parameter λ is given by

$$\lambda = 2\Lambda \frac{\mathrm{K}\left(1-\mathrm{g}^4\right)\left[2\mathrm{E}\left(\mathrm{g}^4\right) - \left(1-\mathrm{g}^4\right)\mathrm{K}\left(\mathrm{g}^4\right)\right] - \pi}{\pi \mathrm{g} \mathrm{K}\left(\mathrm{g}^4\right)}\,, \tag{2.4.4}$$

where K and E are the complete elliptic integrals of the first (A.2.1) and second (A.2.2) kind, respectively[17]. Later we will use the inversion of this relation for small λ,

$$\mathrm{g} = 1 - \frac{\sqrt{\frac{\lambda}{\Lambda}}}{\sqrt{2}} + \frac{\lambda}{4\Lambda} - \frac{\lambda^{3/2}}{32\sqrt{2}\Lambda^{3/2}} - \frac{\lambda^2}{64\Lambda^2} + \mathcal{O}\left(\lambda^{5/2}\right)\,. \tag{2.4.5}$$

In the 't Hooft limit (2.4.2), we have the following behaviour

$$\ln Z(t, N) \simeq \sum_{g \geqslant 0} \epsilon^{2g-2} F_g\left(\Lambda, \lambda\right)\,, \tag{2.4.6}$$

where $\simeq$ stands for asymptotic equality. The first two terms read

$$\frac{\mathrm{d}^2}{\mathrm{d}\lambda^2} F_0 = -2\pi \frac{\mathrm{K}(\mathrm{g}^4)}{\mathrm{K}(1-\mathrm{g}^4)}\,, \tag{2.4.7}$$

$$F_1 = -\frac{1}{4}\ln\left(\mathrm{K}\left(1-\frac{1}{\mathrm{g}^4}\right)\mathrm{K}\left(1-\mathrm{g}^4\right)\right) - \frac{1}{6}\ln\left(\frac{1}{\mathrm{g}^2} - \mathrm{g}^2\right) + \text{constant}\,, \tag{2.4.8}$$

and higher-order terms can also be computed systematically [14].

Let us now consider the model with insertions (2.3.18). In the 't Hooft limit (2.4.2), we have the following behaviour [130–135]

$$\ln\left(\frac{\sqrt{v(z)}\Psi_N(z,t)}{Z(t,N)}\right) \simeq \sum_{n \geqslant 0} \epsilon^{n-1} \mathcal{T}_n\left(z\right)\,. \tag{2.4.9}$$

The leading-order term $\mathcal{T}_0$ is related to the even part of the planar resolvent[18] ω_+^0 [6, eq. 3.35],

$$\mathcal{T}_0\left(z\right) = -2\Lambda\left(z + \frac{1}{z}\right) + 2\lambda \int_\infty^z \mathrm{d}z_1\, \omega_+^0\left(z_1\right)\,, \tag{2.4.10}$$

and the subleading-order term $\mathcal{T}_1$ is given by [6, 134, 135]

$$\mathcal{T}_1\left(z\right) = 2\int_\infty^z \int_\infty^z \mathrm{d}z_1 \mathrm{d}z_2\, W_{++}^0\left(z_1, z_2\right)\,, \tag{2.4.11}$$

[17] See subsection A.2.1 for our conventions on elliptic integrals.

[18] The planar resolvent is defined and computed explicitly further on in subsection 2.4.1.

where W^0_{++} is the even part of the planar two-point correlator. It can be expressed explicitly in terms of g as [135], [6, eq. 3.43]

$$W^0_{++}(z_1,z_2) = \frac{\mathsf{g}^2+\mathsf{g}^{-2}-2\mathsf{g}^{-2}\frac{\mathrm{E}(1-\mathsf{g}^4)}{\mathrm{K}(1-\mathsf{g}^4)}-(z_1^2+z_2^2)\left(1-\frac{\left(\sqrt{(z_1^2-\mathsf{g}^{-2})(z_1^2-\mathsf{g}^2)}-\sqrt{(z_2^2-\mathsf{g}^{-2})(z_2^2-\mathsf{g}^2)}\right)^2}{(z_1^2-z_2^2)^2}\right)}{8\sqrt{(z_1^2-\mathsf{g}^{-2})(z_1^2-\mathsf{g}^2)}\sqrt{(z_2^2-\mathsf{g}^{-2})(z_2^2-\mathsf{g}^2)}}\,. \tag{2.4.12}$$

2.4.1 The planar resolvent

The planar resolvent is

$$\omega^0(z) = \lim_{N\to+\infty}\frac{1}{N}\left\langle\sum_{n=1}^{N}\left(\frac{1}{z-z_n}\right)\right\rangle\,, \tag{2.4.13}$$

where the normalized expectation value is with respect to the matrix model without insertions $Z(t,N)$ (2.3.14) and the z_n are the eigenvalues over which one integrates in (2.3.14). At large z, one finds

$$\omega^0(z) = \frac{1}{z}+\frac{\langle W\rangle}{z^2}+\mathcal{O}\left(\frac{1}{z^3}\right)\,, \qquad \langle W\rangle = \lim_{N\to+\infty}\frac{1}{N}\left\langle\sum_{n=1}^{N}z_n\right\rangle\,, \tag{2.4.14}$$

and we refer to $\langle W\rangle$ as a Wilson loop by analogy with [136]. It is useful to split the planar resolvent in an even and an odd part,

$$\omega^0(z) = \omega^0_+(z)+z\omega^0_-(z)\,, \tag{2.4.15}$$

where $\omega^0_\pm(z)$ are both even in z.

The even part of the planar resolvent ω^0_+ for the model (2.3.18) has the following integral form [135, eq. 4.16],

$$\lambda\omega^0_+(z) = -\frac{\mathrm{i}}{2}\oint_{\mathcal{C}}\frac{\mathrm{d}y}{2\pi\mathrm{i}}\left(\frac{V'(y)y}{z^2-y^2}\right)\frac{\sqrt{z^2-\mathsf{g}^{-2}}\sqrt{z^2-\mathsf{g}^2}}{\sqrt{\mathsf{g}^{-2}-y^2}\sqrt{y^2-\mathsf{g}^2}}\,, \tag{2.4.16}$$

where $\mathcal{C}$ is an anticlockwise contour around the branch cut from g to g^{-1}, which does not include the two poles at $y=\pm z$. In the matrix model $\Psi_N(z,t)$ (2.3.18), we naturally have $z>0$. However, it is useful to consider more generally $z\in\mathbb{C}$ from now on, and (2.4.16) makes indeed sense for complex values of z as well [135].

If $z^2\in\mathbb{C}\setminus[\mathsf{g}^2,\mathsf{g}^{-2}]$, we can write (2.4.16) as

$$\lambda\omega^0_+(z) = \left(\frac{2\Lambda}{\pi}\right)\sqrt{z^2-\mathsf{g}^{-2}}\sqrt{z^2-\mathsf{g}^2}\int_{\mathsf{g}}^{\mathsf{g}^{-1}}\mathrm{d}y\left(\frac{y-1/y}{z^2-y^2}\right)\frac{1}{\sqrt{(\mathsf{g}^{-2}-y^2)(y^2-\mathsf{g}^2)}}\,, \tag{2.4.17}$$

where we used the form of the potential given in (2.4.1). The integrand in (2.4.17) can be decomposed in partial fractions,

$$\int_b^a \mathrm{d}y \left(y-\frac{1}{y}\right)\left(\frac{1}{z^2-y^2}\right)\frac{1}{\sqrt{(a^2-y^2)\,(y^2-b^2)}} = \frac{1}{2z^2}\left[\left(1-z^2\right)\left(\mathcal{I}(z,a,b)+\mathcal{I}(-z,a,b)\right)-2\,\mathcal{I}(0,a,b)\right]\,, \tag{2.4.18}$$

where $0<b<a$ are any positive real numbers and we defined

$$\mathcal{I}\,(z,a,b) = \int_b^a \mathrm{d}y \left(\frac{1}{y-z}\right)\frac{1}{\sqrt{(a^2-y^2)\,(y^2-b^2)}}\,. \tag{2.4.19}$$

Using [137, eqs. 256.39, 257.39], one finds for $z\notin[b,a]$,

$$\begin{aligned}\mathcal{I}\,(z,a,b) &= \left(\frac{2}{a+b}\right)\left(\frac{1}{b-z}\right)\int_0^{\mathrm{K}(\mathrm{k}^2)}\mathrm{d}v\left(\frac{1-k\,\mathrm{sn}^2\,(v|k^2)}{1-k\left(\frac{z+b}{z-b}\right)\mathrm{sn}^2\,(v|k^2)}\right)\\ &= \left(\frac{2}{a+b}\right)\left(\frac{1}{a-z}\right)\int_0^{\mathrm{K}(\mathrm{k}^2)}\mathrm{d}v\left(\frac{1-(-k)\,\mathrm{sn}^2\,(v|k^2)}{1-k\left(\frac{a+z}{a-z}\right)\mathrm{sn}^2\,(v|k^2)}\right)\end{aligned} \tag{2.4.20}$$

where k is the elliptic modulus given by

$$k=\frac{a-b}{a+b}\,, \tag{2.4.21}$$

and $\mathrm{sn}\,(v|k^2)$ is the Jacobi elliptic function known as the sine amplitude (A.2.5). From [137, eq. 340.01],

$$\int \mathrm{d}v\left(\frac{1-\alpha_1^2\mathrm{sn}^2\,(v|k^2)}{1-\alpha^2\mathrm{sn}^2\,(v|k^2)}\right)=\frac{1}{\alpha^2}\left[\left(\alpha^2-\alpha_1^2\right)\Pi\left(\alpha^2,\phi\middle|k^2\right)+\alpha_1^2 v\right]\,,\qquad v=\mathrm{F}\left(\phi\middle|k^2\right)\,, \tag{2.4.22}$$

where F and Π are the incomplete elliptic integrals of the first (A.2.1) and third (A.2.3) kind, respectively. It is useful to note that $v=0$ corresponds to $\phi=0$ and $v=\mathrm{K}\,(k^2)$ corresponds to $\phi=\pi/2$. In the end, this gives

$$\begin{aligned}\mathcal{I}\,(z,a,b) &= \left(\frac{2}{a+b}\right)\left(\frac{1}{b^2-z^2}\right)\left[2b\Pi\left(\left(\frac{z+b}{z-b}\right)k\middle|k^2\right)+(z-b)\mathrm{K}\left(k^2\right)\right]\\ &= \left(\frac{2}{a+b}\right)\left(\frac{1}{a^2-z^2}\right)\left[2a\Pi\left(\left(\frac{a+z}{a-z}\right)k\middle|k^2\right)+(z-a)\mathrm{K}\left(k^2\right)\right]\end{aligned} \tag{2.4.23}$$

and hence, we have in (2.4.18) for $z^2\notin[b^2,a^2]$

$$\begin{aligned}&\mathcal{I}\,(z,a,b)+\mathcal{I}\,(-z,a,b)\\ &\quad= \left(\frac{4b}{a+b}\right)\left(\frac{1}{b^2-z^2}\right)\left[\Pi\left(\left(\frac{z+b}{z-b}\right)k\middle|k^2\right)+\Pi\left(\left(\frac{z-b}{z+b}\right)k\middle|k^2\right)-\mathrm{K}\left(k^2\right)\right]\\ &\quad= \left(\frac{4a}{a+b}\right)\left(\frac{1}{a^2-z^2}\right)\left[\Pi\left(\left(\frac{a+z}{a-z}\right)k\middle|k^2\right)+\Pi\left(\left(\frac{a-z}{a+z}\right)k\middle|k^2\right)-\mathrm{K}\left(k^2\right)\right]\end{aligned} \tag{2.4.24}$$

as well as

$$\begin{aligned}\mathcal{I}(0,a,b) &= \left(\frac{2}{a+b}\right)\left(\frac{1}{b}\right)\left[2\Pi\left(-k\middle|k^2\right)-\mathrm{K}\left(k^2\right)\right]\\ &= \left(\frac{2}{a+b}\right)\left(\frac{1}{a}\right)\left[2\Pi\left(k\middle|k^2\right)-\mathrm{K}\left(k^2\right)\right]\,.\end{aligned} \tag{2.4.25}$$

These particular combinations of elliptic integrals can be reduced to square roots by making use of the following addition formula for $0<k<1$ [137, eq. 117.02][19],

$$\Pi\left(\alpha^2\middle|k^2\right)+\Pi\left(\frac{k^2}{\alpha^2}\middle|k^2\right)-\mathrm{K}\left(k^2\right)=\frac{\pi}{2}\sqrt{\frac{\alpha^2}{(1-\alpha^2)\left(\alpha^2-k^2\right)}}\,,\qquad \alpha^2\in\mathbb{C}\setminus\mathcal{H}_{k^2}\,, \tag{2.4.26}$$

where $\mathcal{H}_{k^2}$ is

$$\mathcal{H}_{k^2}=\left[0,k^2\right]\cup[1,\infty]\,. \tag{2.4.27}$$

Combining (2.4.25) and (2.4.26) gives

$$\begin{aligned}\mathcal{I}(0,a,b) &= \left(\frac{2}{a+b}\right)\left(\frac{1}{b}\right)\left(\frac{\pi}{2}\right)\left(\frac{1}{1+k}\right)=\left(\frac{\pi}{2}\right)\left(\frac{1}{ab}\right)\\ &= \left(\frac{2}{a+b}\right)\left(\frac{1}{a}\right)\left(\frac{\pi}{2}\right)\left(\frac{1}{1-k}\right)=\left(\frac{\pi}{2}\right)\left(\frac{1}{ab}\right)\,,\end{aligned} \tag{2.4.28}$$

and the combination of (2.4.24) and (2.4.26) leads to

$$\begin{aligned}&\mathcal{I}(z,a,b)+\mathcal{I}(-z,a,b)\\ &\quad=\left(\frac{4b}{a+b}\right)\left(\frac{1}{b^2-z^2}\right)\left[\frac{\pi}{4}\left(\frac{a+b}{b}\right)\sqrt{\frac{b^2-z^2}{a^2-z^2}}\right]=-\frac{\pi}{\sqrt{z^2-a^2}\sqrt{z^2-b^2}}\\ &\quad=\left(\frac{4a}{a+b}\right)\left(\frac{1}{a^2-z^2}\right)\left[\frac{\pi}{4}\left(\frac{a+b}{a}\right)\sqrt{\frac{a^2-z^2}{b^2-z^2}}\right]=-\frac{\pi}{\sqrt{z^2-a^2}\sqrt{z^2-b^2}}\end{aligned} \tag{2.4.29}$$

where $z^2\in\mathbb{C}\setminus[b^2,a^2]$.

Taking $a^{-1}=b=\mathsf{g}$ and using everything above, we finally find for the even planar resolvent

$$\boxed{\lambda\omega_+^0(z)=\Lambda\left(\left(1-\frac{1}{z^2}\right)-\frac{\sqrt{z^2-\mathsf{g}^2}\sqrt{z^2-\mathsf{g}^{-2}}}{z^2}\right)\,.} \tag{2.4.30}$$

Even though we derive (2.4.30) for $z^2\in\mathbb{C}\setminus[\mathsf{g}^2,\mathsf{g}^{-2}]$, one can verify that (2.4.30) holds on the whole complex plane. As a consistency check, we compared the analytical result

[19] The statement in [137, eq. 117.02] is for $\alpha^2\in\mathbb{R}\setminus\mathcal{H}_{k^2}$, but when $0<k<1$, this can be extended to $\alpha^2\in\mathbb{C}\setminus\mathcal{H}_{k^2}$ by making use of the identity theorem.

(2.4.30) against the numerical evaluation of (2.4.16) and found perfect agreement. One can also see that (2.4.30) has the correct asymptotic behaviour,

$$\begin{aligned} \omega_+^0(z) &= \mathcal{O}(1)\,, && \text{for } z \to 0\,, \\ \omega_+^0(z) &= \mathcal{O}\left(z^{-2}\right)\,, && \text{for } z \to \infty\,. \end{aligned} \tag{2.4.31}$$

In addition, from the coefficient of the z^{-2}-term in the $z \to \infty$ expansion we get a closed-form expression for the Wilson loop (2.4.14),

$$\langle W \rangle = \frac{\left(\mathsf{g}^2-1\right)^2 \Lambda}{2\mathsf{g}^2\lambda}\,. \tag{2.4.32}$$

Using (2.4.5), we obtain

$$\frac{\left(\mathsf{g}^2-1\right)^2 \Lambda}{2\mathsf{g}^2\lambda} = 1 + \frac{\lambda}{16\Lambda} - \frac{\lambda^2}{256\Lambda^2} + \frac{5\lambda^3}{8192\Lambda^3} - \frac{33\lambda^4}{262144\Lambda^4} + \mathcal{O}\left(\lambda^5\right). \tag{2.4.33}$$

We cross-checked (2.4.33) by expanding the matrix model around its Gaussian point, similar to what was done in [72, app. B].

Using (2.4.30) gives for the leading-order $\mathcal{T}_0$ (2.4.10) of the matrix model (2.4.9) in the 't Hooft limit (2.4.2)

$$\partial_z \mathcal{T}_0(z) = -2\Lambda\left(1 - \frac{1}{z^2}\right) + 2\lambda\omega_+^0(z) = -2\Lambda\frac{\sqrt{z^2-\mathsf{g}^2}\sqrt{z^2-\mathsf{g}^{-2}}}{z^2}\,. \tag{2.4.34}$$

An important point of (2.4.34) is that the Seiberg-Witten curve of $\mathcal{N}=2$, SU(N) SYM,

$$y^2(z) = -4\Lambda^2\left(z^2 + z^{-2}\right) + u\,, \tag{2.4.35}$$

emerges in the planar limit, provided we identify the following quadratic differentials

$$\left[\partial_z \mathcal{T}_0(z)\,\mathrm{d}z\right]^2 = -\left[\frac{y(z)}{z}\mathrm{d}z\right]^2, \tag{2.4.36}$$

and at the same time relate g to u by

$$\mathsf{g}^2 + \mathsf{g}^{-2} = \frac{u}{4\Lambda^2}\,, \qquad \mathsf{g}^{\pm 2} = \left(\frac{u}{8\Lambda^2}\right) \mp \sqrt{\left(\frac{u}{8\Lambda^2}\right)^2 - 1}\,. \tag{2.4.37}$$

In equations (2.4.35) and (2.4.37), u denotes the vacuum expectation value of the scalar in the vector multiplet of $\mathcal{N}=2$, SU(N) SYM.

2.4.2 The planar two-point function

In the previous section, we have shown that the Seiberg-Witten curve (2.4.35) naturally emerges when considering the planar resolvent. Here we will see that the Bergman kernel emerges similarly when considering the even part of the planar two-point function. We will

see later that this characterises the annulus amplitude in the surface defect. The Bergman kernel is defined as [87]

$$B_{q_1,q_2,q_3}(z_1,z_2)=\frac{1}{2(z_1-z_2)^2}\left(\frac{2f(z_1,z_2)+G_{q_1,q_2,q_3}\left(k^2\right)(z_1-z_2)^2}{2\sqrt{\sigma(z_1)\sigma(z_2)}}+1\right)\,, \tag{2.4.38}$$

with

$$f(z_1,z_2)=\frac{u\left(z_1^2+4z_2z_1+z_2^2\right)}{24\Lambda^2}+\frac{1}{2}\left(-z_1-z_2\right)-\frac{1}{2}z_1z_2\left(z_1+z_2\right)\,, \tag{2.4.39}$$

$$G_{q_1,q_2,q_3}\left(k^2\right)=(q_1-q_3)\left[\frac{\mathrm{E}\left(k^2\right)}{\mathrm{K}\left(k^2\right)}\right]+q_3-\frac{u}{12\Lambda^2}\,,\qquad k^2=\frac{q_1-q_2}{q_1-q_3}\,, \tag{2.4.40}$$

and where q_i are the branch points of $\sigma(z)=-z\left(z^2-\left(u/4\Lambda^2\right)z+1\right)$,

$$q_i\in\left\{0,\left(\frac{u}{8\Lambda^2}\right)\mp\sqrt{\left(\frac{u}{8\Lambda^2}\right)^2-1}\right\}=\left\{0,\mathsf{g}^2,\mathsf{g}^{-2}\right\}\,. \tag{2.4.41}$$

The choice of the order fixes the choice of frame. What we find is that the relevant order here is

$$q_3=0\,,\qquad q_2=\left(\frac{u}{8\Lambda^2}\right)-\sqrt{\left(\frac{u}{8\Lambda^2}\right)^2-1}=\mathsf{g}^2\,,\qquad q_1=\left(\frac{u}{8\Lambda^2}\right)+\sqrt{\left(\frac{u}{8\Lambda^2}\right)^2-1}=\mathsf{g}^{-2}\,. \tag{2.4.42}$$

As we will discuss later, this choice makes contact with the magnetic frame. One can check that the even part of the planar two-point function (2.4.12) is related to the Bergman kernel (2.4.38) by

$$W^0_{++}\left(z_1,z_2\right)=-z_1z_2B_{q_1,q_2,q_3}\left(z_1^2,z_2^2\right)-\frac{1}{4\left(z_1+z_2\right)^2}\,, \tag{2.4.43}$$

Hence, the subleading-order $\mathcal{T}_1$ (2.4.11) of the matrix model (2.4.9) in the 't Hooft limit (2.4.2) becomes

$$\boxed{\mathcal{T}_1\left(z\right)=2\int_\infty^z\int_\infty^z\mathrm{d}z_1\mathrm{d}z_2\left(-z_1z_2B_{q_1,q_2,q_3}\left(z_1^2,z_2^2\right)-\frac{1}{4\left(z_1+z_2\right)^2}\right)}\,. \tag{2.4.44}$$

2.5 Testing the ϵ expansion for the type I defect

From the perspective of the B-model, the partition functions of open and closed topological strings can be defined as objects associated with an algebraic curve, and thus, they depend on a choice of frame, namely a choice of a symplectic basis for the homology of the algebraic curve. The transformation properties of the closed string partition function under a change of frame can be derived from the observation that such a partition function behaves like a wavefunction [138]. Consequently, the genus g free energies behave as almost modular

forms under a change of frame [139]. The wavefunction behaviour was generalized to the open topological string sector in [93].

Recall that the partition functions of the four-dimensional gauge theories under consideration are derived from the topological string partition functions via the geometric engineering construction [118–120]. As a result, the same transformation properties hold.

At the level of terminology, the large radius frame in topological string theory is mapped to the electric frame in the four-dimensional theory. In this frame, the $\mathcal{A}$ cycle and the corresponding A period on the SW curve (2.4.35) are chosen to be

$$\Pi_A = \frac{1}{2\pi \mathrm{i}} \oint_{\mathcal{A}} \frac{y(z)}{z} \mathrm{d}z = \frac{1}{\mathrm{i}\pi} \int_{-\mathrm{g}}^{\mathrm{g}} \frac{y(z)}{z} \mathrm{d}z = \frac{2\sqrt{8\Lambda^2+u}\, \mathrm{E}\left(\frac{16\Lambda^2}{8\Lambda^2+u}\right)}{\pi}, \tag{2.5.1}$$

where $y(z)$ is given in (2.4.35) and E is the complete elliptic integral of the second kind (A.2.2). We usually denote $a \equiv \Pi_A$. Likewise, $\mathcal{B}$ cycle and the corresponding period are

$$\begin{aligned} \Pi_B = \frac{1}{2\pi \mathrm{i}} \oint_{\mathcal{B}} \frac{y(z)}{z} \mathrm{d}z &= \frac{1}{\mathrm{i}\pi} \int_{\mathrm{g}}^{\mathrm{g}^{-1}} \frac{y(z)}{z} \mathrm{d}z \\ &= \frac{\sqrt{8\Lambda^2+u}}{\mathrm{i}\pi} \left(\mathrm{K}\left(\frac{2u}{8\Lambda^2+u} - 1\right) - \mathrm{E}\left(\frac{2u}{8\Lambda^2+u} - 1\right)\right) \end{aligned} \tag{2.5.2}$$

where K is the complete elliptic integral of the first kind (A.2.1). The $\mathrm{g}^{\pm 1}$ are roots of the SW curve, $y\left(\mathrm{g}^{\pm 1}\right) = 0$, and are given in (2.4.37). We usually denote $a_D \equiv \mathrm{i}\Pi_B$.

On the other hand, the conifold frame in topological strings corresponds to the magnetic frame in the four-dimensional theory. This frame is related to the electric frame by an S-duality which exchanges the $\mathcal{A}$- and $\mathcal{B}$-cycles. For the SU(N) SYM that we study in this paper, the transformation properties of the partition function under a change of frame were studied in [109]. The ϵ expansion of (2.3.15) leads exactly to such transformations, as we discuss below.

2.5.1 The electric frame

We consider a type I defect in the self-dual phase of the Ω-background ($\epsilon_1 = -\epsilon_2 = \epsilon$), and we denote the partition function of this surface defect by

$$Z^{\mathrm{I}}(z, t, \sigma) \tag{2.5.3}$$

if we are in the electric frame. As pointed out in [77], based on [140, 141], we can compute these defects via the Eynard-Orantin topological recursion [92]. More precisely, we have

$$\ln\left(Z^{\mathrm{I}}(z,t,\sigma)\right) \simeq \sum_{g\geqslant 0} \sum_{h\geqslant 1} \epsilon^{2g-2+h} \int_{\infty}^{z} \cdots \int_{\infty}^{z} W_{g,h}(z_1, \ldots, z_h)\, \mathrm{d}z_1 \cdots \mathrm{d}z_h \tag{2.5.4}$$

where $W_{g,h}(z_1, \ldots z_h)\mathrm{d}z_1 \ldots \mathrm{d}z_h$ is an infinite sequence of meromorphic differentials constructed via topological recursion [92], and whose starting point is the underlying SW

geometry (2.4.35). Note that we are implicitly using the dictionary (2.3.11) and the SW relation (2.5.1) to express $\sigma = \mathrm{i}a/2\epsilon$ as a function of the SW parameter u.

For the so-called disk amplitude $W_{0,1}$, we have[20]

$$W_{0,1}(z)\,\mathrm{d}z = -\frac{2\Lambda}{z}\sqrt{\left(z^2+\frac{1}{z^2}\right)-\frac{u}{4\Lambda^2}}\,\mathrm{d}z\,, \tag{2.5.5}$$

and we note

$$\mathcal{W}_0^{\mathrm{I}}(z,\Lambda,u) = \int_\infty^z W_{0,1}(z_1)\,\mathrm{d}z_1\,. \tag{2.5.6}$$

The annulus amplitude $W_{0,2}$ is given by

$$W_{0,2}(z_1,z_2)\,\mathrm{d}z_1\mathrm{d}z_2 = -2z_1z_2\left(B_{\widetilde{q}_1,\widetilde{q}_2,\widetilde{q}_3}(z_1^2,z_2^2)-\frac{1}{(z_1^2-z_2^2)^2}\right)\,\mathrm{d}z_1\mathrm{d}z_2\,, \tag{2.5.7}$$

where $B_{\widetilde{q}_1,\widetilde{q}_2,\widetilde{q}_3}$ is defined as in (2.4.38), but the choice of q_i's is different. Here we have

$$\widetilde{q}_1 = 0\,,\qquad \widetilde{q}_2 = \left(\frac{u}{8\Lambda^2}\right)-\sqrt{\left(\frac{u}{8\Lambda^2}\right)^2-1} = \mathfrak{g}^2\,,\qquad \widetilde{q}_3 = \left(\frac{u}{8\Lambda^2}\right)+\sqrt{\left(\frac{u}{8\Lambda^2}\right)^2-1} = \mathfrak{g}^{-2}\,, \tag{2.5.8}$$

so that $\widetilde{q}_1 = q_3$, $\widetilde{q}_2 = q_2$ and $\widetilde{q}_3 = q_1$ (2.4.42). We denote

$$\mathcal{W}_1^{\mathrm{I}}(z,\Lambda,u) = \int_\infty^z\int_\infty^z W_{0,2}(z_1,z_2)\,\mathrm{d}z_1\mathrm{d}z_2\,. \tag{2.5.9}$$

Hence, to subleading-order (2.5.4) reads

$$\ln\left(Z^{\mathrm{I}}(z,t,\sigma)\right) = \frac{1}{\epsilon}\mathcal{W}_0^{\mathrm{I}}(z,\Lambda,u)+\mathcal{W}_1^{\mathrm{I}}(z,\Lambda,u)+\mathcal{O}(\epsilon)\,. \tag{2.5.10}$$

Given the spectral curve (2.4.35) with $W_{0,1}$ and $W_{0,2}$, higher-order terms in the ϵ expansion (2.5.4) can be computed recursively by using the topological recursion [92].

2.5.2 The magnetic frame

We conjecture that the matrix model (2.3.18) computes the type I surface defect (2.5.3) in the magnetic frame. In this section, we test this proposal in the 't Hooft expansion (2.4.2).

The partition function without defects

It is useful to start by reviewing the change of frame in the partition function without defect, which follows from the ϵ expansion of (2.3.15). Using the dictionary (2.3.11), the ϵ expansion of the Nekrasov function reads

$$\ln\left(Z^{\mathrm{Nek}}(t,\sigma)\right) \simeq \sum_{g\geqslant 0}\epsilon^{2g-2}\mathcal{F}_g(\Lambda,a)\,, \tag{2.5.11}$$

[20] Here we take $z > \mathfrak{g}^{-1} > 1$ to simplify the discussion and to make contact with the standard formulas in the literature [77, 87]. Hence, we are outside the branch cut on the matrix model side.

where $\mathcal{F}_g$ are the genus g free energies of SU(N) SYM in the electric frame. Thanks to (2.3.15), we can relate (2.5.11) to the 't Hooft expansion of the matrix model (2.3.14),

$$\ln\left(Z(t,N)\right) \simeq \sum_{g\geqslant 0} \epsilon^{2g-2} F_g(\Lambda,\lambda)\,. \tag{2.5.12}$$

It was found in [14] that the F_g's in (2.5.12) are the SYM free energies in the magnetic frame. More precisely,

$$\mathrm{e}^{\sum_{g\geqslant 0}\epsilon^{2g-2}F_g(\Lambda,\lambda)} \sim \int_{\mathrm{i}\mathbb{R}} \mathrm{d}a\ \mathrm{e}^{-\pi a N/\epsilon}\ \mathrm{e}^{\sum_{g\geqslant 0}\epsilon^{2g-2}\mathcal{F}_g(\Lambda,a)}\,, \tag{2.5.13}$$

where $\sim$ indicates a proportionality between two (divergent) series[21]. The integral on the right-hand side of (2.5.13) should be understood as a saddle point expansion. This saddle point expansion characterizes the change of frame in SW theory and topological string [138], and it has a direct interpretation from the point of view of modular transformations [139]. It allows us to make the transition from the weak coupling electric frame, where the Nekrasov function (2.3.10) is defined, to the strong coupling magnetic frame, where the matrix model (2.3.14) naturally emerges.

By writing the saddle point expansion on the right-hand side of (2.5.13) explicitly, we get

$$\int_{\mathrm{i}\mathbb{R}} \mathrm{d}a\ \mathrm{e}^{-\pi a N/\epsilon}\ \mathrm{e}^{\sum_{g\geqslant 0}\epsilon^{2g-2}\mathcal{F}_g(\Lambda,a)} = \exp\left[\frac{1}{\epsilon^2}\left(\mathcal{F}_0\left(\Lambda,a(\lambda)\right) - \pi a(\lambda)\lambda\right) + \mathcal{O}(1)\right]\,, \tag{2.5.14}$$

where $\lambda = N\epsilon$ and $a(\lambda)$ is determined by the saddle point equation

$$\partial_a \mathcal{F}_0\left(\Lambda,a\right) = \pi\lambda\,. \tag{2.5.15}$$

By using (2.3.10) and the dictionary (2.3.11), we get

$$\begin{aligned}\partial_a\mathcal{F}_0(\Lambda,a) = {}& 2a(\ln(a)-\ln(\Lambda)-1)\\ &+\frac{4\Lambda^4}{a^3}+\frac{30\Lambda^8}{a^7}+\frac{480\Lambda^{12}}{a^{11}}+\frac{10283\Lambda^{16}}{a^{15}}+\frac{1287648\Lambda^{20}}{5a^{19}}+\mathcal{O}\left(\Lambda^{24}\right)\,,\end{aligned} \tag{2.5.16}$$

and if we make use of (2.4.37) together with the classical Matone relation,

$$u = -\Lambda\partial_\Lambda\mathcal{F}_0\left(\Lambda,a\right) = a^2+\frac{8\Lambda^4}{a^2}+\frac{40\Lambda^8}{a^6}+\frac{576\Lambda^{12}}{a^{10}}+\frac{11752\Lambda^{16}}{a^{14}}+\frac{286144\Lambda^{20}}{a^{18}}+\mathcal{O}\left(\Lambda^{24}\right)\,, \tag{2.5.17}$$

we find that λ in (2.5.15) agrees with (2.4.4) as it should. The matching between the two sides of (2.5.13) was discussed in [14]. We also note that the classical Matone relation (2.5.17) can be inverted and one finds the usual expression for the A-period of the SW curve (2.4.35) given in (2.5.1). Likewise $\partial_a\mathcal{F}_0$ is identified with the B-period of the SW curve[22]

$$a_D = \pi^{-1}\partial_a\mathcal{F}_0\left(\Lambda,a\right)\,, \tag{2.5.18}$$

where a_D is given in (2.5.2).

[21] For sake of notation we omitted the proportionality factor $2^{1/12}\mathrm{e}^{3\zeta'(-1)}\left(\Lambda/\epsilon\right)^{-1/4}\mathrm{e}^{4(\Lambda/\epsilon)^2}$

[22] Hence, we have $a_D = \lambda$.

The partition function with defects

We are interested in extending the analysis to the 't Hooft expansion (2.4.9) of the matrix model with insertion $\Psi_N(z,t)$ (2.3.18). More precisely, we claim that $\Psi_N(z,t)$ gives the self-dual type I surface defect (2.5.3) in the magnetic frame. As we reviewed above, the change of frame for the partition function is encoded in an integral transform (2.5.13). As first shown in [93], this is still the case if one considers the partition function in the presence of surface defects which are engineered via the open topological string partition function, see also [89].

At the level of the ϵ expansion, our conjecture reads

$$\begin{aligned}&\exp\left[\sum_{g\geqslant 0}\epsilon^{2g-2}F_g(\Lambda,\lambda)+\sum_{n\geqslant 0}\epsilon^{n-1}\mathcal{T}_n(z)\right]\\&\sim\int_{\mathrm{i}\mathbb{R}}\mathrm{d}a\;\mathrm{e}^{-\pi aN/\epsilon}\;\mathrm{e}^{\sum_{g\geqslant 0}\epsilon^{2g-2}\mathcal{F}_g(\Lambda,a)}\mathrm{e}^{\sum_{g\geqslant 0}\sum_{h\geqslant 1}\epsilon^{2g-2+h}\int_\infty^z\cdots\int_\infty^z W_{g,h}(z_1,\ldots,z_h)\mathrm{d}z_1\cdots\mathrm{d}z_h}\,,\end{aligned}\tag{2.5.19}$$

where $W_{g,h}(z_1,\ldots,z_h)\mathrm{d}z_1\cdots\mathrm{d}z_h$ are the electric differentials appearing in the topological recursion setup (2.5.4), whereas $\mathcal{T}_n$ are the magnetic matrix model coefficients appearing in (2.4.9),

$$\left(\frac{\sqrt{v(z)}\Psi_N(z,t)}{Z(t,N)}\right)\simeq\exp\left[\sum_{n\geqslant 0}\epsilon^{n-1}\mathcal{T}_n(z)\right]\,.\tag{2.5.20}$$

Parallel to (2.5.13), the integral on the right-hand side of (2.5.19) should be understood as a saddle point expansion which characterizes the change of frame. Equation (2.5.19) reads to subleading-order in ϵ

$$\epsilon^{-1}\mathcal{T}_0(z)+\mathcal{T}_1(z)+\mathcal{O}(\epsilon)=\epsilon^{-1}\mathcal{W}_0^{\mathrm{I}}(z,a(\lambda))-\frac{\left[\partial_a\mathcal{W}_0^{\mathrm{I}}(z,a(\lambda))\right]^2}{2\partial_a^2\mathcal{F}_0(a(\lambda))}+\mathcal{W}_1^{\mathrm{I}}(z,a(\lambda))+\mathcal{O}(\epsilon)\,,\tag{2.5.21}$$

where a and λ are again related by the saddle point equation (2.5.15). In (2.5.21), we already used (2.5.13) and (2.5.14) to get rid of terms involving only the free energies F_g and $\mathcal{F}_g$. We show below that the equality in (2.5.21) indeed holds, order by order in ϵ.

At the leading-order ϵ^{-1}, the matching on the two sides of (2.5.21) follows directly from (2.4.34) and (2.5.5). For the subleading-order ϵ^0, we first note that the Bergman kernel entering in $\mathcal{T}_1$ (2.4.44), can be written as

$$\begin{aligned}&B_{q_1,q_2,q_3}(z_1,z_2)=\\&B_{\widetilde{q}_1,\widetilde{q}_2,\widetilde{q}_3}(z_1,z_2)+\frac{\pi\left[z_1z_2\left(\mathsf{g}^4z_1-\mathsf{g}^2\left(z_1^2+1\right)+z_1\right)\left(\mathsf{g}^4z_2-\mathsf{g}^2\left(z_2^2+1\right)+z_2\right)\right]^{-1/2}}{8\,\mathrm{K}\left(\mathsf{g}^4\right)\mathrm{K}\left(1-\mathsf{g}^4\right)}\end{aligned}\tag{2.5.22}$$

where we used (2.4.37) and (2.5.8). Hence, we can rewrite (2.4.44),

$$\begin{aligned}\mathcal{T}_1(z) &= 2\int_\infty^z\int_\infty^z\left(-z_1z_2B_{q_1q_2q_3}\left(z_1^2,z_2^2\right)-\frac{1}{4\left(z_1+z_2\right)^2}\right)\mathrm{d}z_1\mathrm{d}z_2\\ &= \mathcal{W}_1^{\mathrm{I}}(z)-\int_\infty^z\int_\infty^z\left(\frac{\pi\mathsf{g}^4}{16\left(\mathsf{g}^4-1\right)^2\Lambda^2}\frac{\partial_{\mathsf{g}}\partial_{z_1}\mathcal{T}_0(z_1)\partial_{\mathsf{g}}\partial_{z_2}\mathcal{T}_0(z_2)}{\mathrm{K}\left(\mathsf{g}^4\right)\mathrm{K}\left(1-\mathsf{g}^4\right)}\right)\mathrm{d}z_1\mathrm{d}z_2\,,\end{aligned} \tag{2.5.23}$$

which leads then to

$$\begin{aligned}\mathcal{T}_1(z) &= \mathcal{W}_1^{\mathrm{I}}(z)-\frac{\pi\mathsf{g}^4}{16\left(\mathsf{g}^4-1\right)^2\Lambda^2}\frac{\left(\partial_{\mathsf{g}}\mathcal{T}_0(z)\right)^2}{\mathrm{K}\left(\mathsf{g}^4\right)\mathrm{K}\left(1-\mathsf{g}^4\right)}\\ &= \mathcal{W}_1^{\mathrm{I}}(z)-\left(\partial_a\mathcal{T}_0(z)\right)^2\frac{\mathrm{K}\left(\frac{4\mathsf{g}^2}{(\mathsf{g}^2+1)^2}\right)^2}{\pi\left(\mathsf{g}^2+1\right)^2\mathrm{K}\left(\mathsf{g}^4\right)\mathrm{K}\left(1-\mathsf{g}^4\right)}\,,\end{aligned} \tag{2.5.24}$$

where we used (2.5.1). From (2.5.18), we have

$$\partial_a^2\mathcal{F}_0(a)=\frac{\pi\mathrm{K}\left(\frac{2u}{8\Lambda^2+u}-1\right)}{\mathrm{K}\left(\frac{16\Lambda^2}{8\Lambda^2+u}\right)}\,, \tag{2.5.25}$$

and by combining (2.5.25) with the identity

$$\frac{\mathrm{K}\left(\frac{4\mathsf{g}^2}{(\mathsf{g}^2+1)^2}\right)}{\left(\mathsf{g}^2+1\right)^2\mathrm{K}\left(\mathsf{g}^4\right)\mathrm{K}\left(1-\mathsf{g}^4\right)}=\frac{1}{2\mathrm{K}\left(\frac{(\mathsf{g}^2-1)^2}{(\mathsf{g}^2+1)^2}\right)} \tag{2.5.26}$$

we find

$$\boxed{\mathcal{T}_1(z)=\mathcal{W}_1^{\mathrm{I}}(z)-\frac{\left(\partial_a\mathcal{T}_0(z)\right)^2}{2\partial_a^2\mathcal{F}_0}}\,, \tag{2.5.27}$$

which is precisely what we wanted to prove.

To summarize, we have tested (2.5.19) at leading and subleading-order[23] in ϵ. The matching of higher orders can be inferred from the application of topological recursion. On the canonical defect side, the fact that higher orders in (2.5.3) satisfy the topological recursion was conjectured in [77], based on [140, 141] which was recently demonstrated in [142]. On the matrix model side instead, the inclusion of topological recursion in our matrix model can be derived from [92, 143, 144]. Our computation above shows that the initial data for such recursion are the same on both sides; therefore, matching at all orders is also expected.

2.6 Matrix models, eigenfunctions and the type II defect

In this section, we consider the Fourier transform of the matrix model with insertion $\Psi_N\left(\mathrm{e}^x,t\right)$ (2.3.18). The corresponding defect in four-dimensional, $\mathcal{N}=2$, SU(N) SYM

[23] For the part involving only the free energies the all order results follows from [14, 63].

can be geometrically engineered using the open topological string partition function of local $\mathbb{F}_0$, where we insert a D-brane on the external leg, see section A.3. The partition function of the resulting type II defect in the self-dual phase of the Ω-background is

$$\begin{aligned} Z^{\mathrm{II}}(q,t,\sigma) &= \exp\left(\frac{\mathrm{i}}{2}q\ln(t)\right)\Gamma\left(-\mathrm{i}q-\sigma+\frac{1}{2}\right)\Gamma\left(-\mathrm{i}q+\sigma+\frac{1}{2}\right)Z^{\mathrm{II}}_{\mathrm{inst}}(q,t,\sigma)\,, \\ Z^{\mathrm{II}}_{\mathrm{inst}}(q,t,\sigma) &= 1-\left[\frac{\widetilde{q}}{2\sigma^2\left(\widetilde{q}^2-\sigma^2\right)}\right]t \\ &\quad+\left[\frac{\widetilde{q}\left(\widetilde{q}+1\right)^2-\widetilde{q}\left(10\widetilde{q}^2+19\widetilde{q}+10\right)\sigma^2+\left(8\widetilde{q}^2+30\widetilde{q}+9\right)\sigma^4}{4\sigma^4\left(4\sigma^2-1\right)^2\left(\widetilde{q}^2-\sigma^2\right)\left(\left(\widetilde{q}+1\right)^2-\sigma^2\right)}\right]t^2+\mathcal{O}\left(t^3\right)\,, \end{aligned} \tag{2.6.1}$$

where we defined for the sake of readability $\widetilde{q}=\mathrm{i}q+1/2$. The variables q,t,σ can be expressed in terms of y,Λ,a and ϵ as in (2.2.4). The relation between Z^{II} and the matrix model (2.3.18) reads[24]

$$\begin{aligned} &-\mathrm{i}\,2^{1/12}\mathrm{e}^{3\zeta'(-1)}t^{-1/16}\mathrm{e}^{4\sqrt{t}}\int_{\mathbb{R}+\mathrm{i}\sigma_*}\mathrm{d}\sigma\frac{\tan(2\pi\sigma)}{\left(2\cos(2\pi\sigma)\right)^N}Z^{\mathrm{Nek}}(t,\sigma)\left(\sum_s Z^{\mathrm{II}}_s(q,t,\sigma)\right) \\ &\qquad=\frac{2\sqrt{\pi}t^{1/8}}{(4\pi)^N}\int_{\mathbb{R}}\mathrm{d}x\,\mathrm{e}^{-\mathrm{i}2qx}\mathrm{e}^{-4t^{1/4}\cosh(x)+\frac{x}{2}}\Psi_N(\mathrm{e}^x,t)\,, \end{aligned} \tag{2.6.2}$$

where σ_* is chosen such that $0<\sigma_*<|\mathrm{Re}(q)|$ if $\mathrm{Re}\,(q)\neq 0$, and simply $\sigma_*>0$ if $\mathrm{Re}\,(q)=0$. This guarantees that the integral on the left-hand side does not hit the poles of the integrand. The sum over s can be seen as a sum over saddle points of the integral over x. We find that

$$\left(\sum_s Z^{\mathrm{II}}_s(q,t,\sigma)\right)=Z^{\mathrm{II}}\left(q,t,\sigma\right)+(-1)^N Z^{\mathrm{II}}\left(-q-\frac{\mathrm{i}}{2},t,\sigma\right)\,. \tag{2.6.3}$$

It is convenient to introduce the total partition function as

$$Z^{\mathrm{II}}_{\mathrm{tot}}(q,t,\sigma)=Z^{\mathrm{Nek}}(t,\sigma)Z^{\mathrm{II}}(q,t,\sigma)\,, \tag{2.6.4}$$

so that (2.6.2) can be written in a compact form as

$$\boxed{\begin{aligned} &\int_{\mathbb{R}+\mathrm{i}\sigma_*}\mathrm{d}\sigma\frac{\tan(2\pi\sigma)}{\left(2\cos(2\pi\sigma)\right)^N}\left(Z^{\mathrm{II}}_{\mathrm{tot}}(q,t,\sigma)+(-1)^N Z^{\mathrm{II}}_{\mathrm{tot}}\left(-q-\frac{\mathrm{i}}{2},t,\sigma\right)\right) \\ &\qquad=\mathrm{i}\frac{2^{11/12}\sqrt{\pi}t^{3/16}}{\mathrm{e}^{3\zeta'(-1)}\mathrm{e}^{4\sqrt{t}}(4\pi)^N}\int_{\mathbb{R}}\mathrm{d}x\,\mathrm{e}^{-\mathrm{i}2qx}\mathrm{e}^{-4t^{1/4}\cosh x+\frac{x}{2}}\Psi_N(\mathrm{e}^x,t)\,. \end{aligned}} \tag{2.6.5}$$

[24] This also suggests that the defect partition function $Z^{\mathrm{II}}(q,t,\sigma)$ for this theory has an infinite radius of convergence in t for fixed σ and q which are away from the poles. For the self-dual partition function without defect, this was rigorously proved in [97], see also [98] for more recent developments.

This can equivalently be written as

$$\sum_{k\in\mathbb{Z}}\left(Z^{\rm II}_{\rm tot}(q,t,\sigma+k)+Z^{\rm II}_{\rm tot}\left(-q-\frac{\mathrm{i}}{2},t,\sigma+k+\frac{1}{2}\right)\right)$$
$$=\frac{2^{11/12}\sqrt{\pi}t^{3/16}}{\mathrm{e}^{3\zeta'(-1)}\mathrm{e}^{4\sqrt{t}}}\int_{\mathbb{R}}\mathrm{d}x\,\mathrm{e}^{-\mathrm{i}2qx}\mathrm{e}^{-4t^{1/4}\cosh x+\frac{x}{2}}\left[\sum_{N\geqslant 0}\Psi_N(\mathrm{e}^x,t)\left(\frac{\cos(2\pi\sigma)}{2\pi}\right)^N\right]. \quad (2.6.6)$$

One can use an argument based on the Fourier series to get from (2.6.5) to (2.6.6), while the other direction uses Cauchy's residue theorem. See subsection A.1.1 for details. By inverting the Fourier transform (2.6.6), we have

$$\boxed{\begin{aligned}&\int_{\mathbb{R}}\mathrm{d}q\;\mathrm{e}^{\mathrm{i}2qx}\sum_{k\in\mathbb{Z}}\left(Z^{\rm II}_{\rm tot}\,(q,t,\sigma+k)+Z^{\rm II}_{\rm tot}\left(-q-\frac{\mathrm{i}}{2},t,\sigma+k+\frac{1}{2}\right)\right)\\&\qquad=\frac{2^{11/12}\pi^{3/2}t^{3/16}}{\mathrm{e}^{3\zeta'(-1)}\mathrm{e}^{4\sqrt{t}}}\mathrm{e}^{-4t^{1/4}\cosh x+\frac{x}{2}}\sum_{N\geqslant 0}\Psi_N(\mathrm{e}^x,t)\left(\frac{\cos(2\pi\sigma)}{2\pi}\right)^N\end{aligned}} \quad (2.6.7)$$

Following subsection 2.3.2, we get the square-integrable eigenfunctions of (2.3.5) when we evaluate (2.6.7) at the values of σ which satisfy the quantization condition (2.3.8). That is,

$$\boxed{\begin{aligned}\varphi_n(x,t)=&\frac{\mathrm{e}^{3\zeta'(-1)}\mathrm{e}^{4\sqrt{t}}}{2^{11/12}\pi^{3/2}t^{3/16}}\\&\int_{\mathbb{R}}\mathrm{d}q\,\mathrm{e}^{\mathrm{i}2qx}\sum_{k\in\mathbb{Z}}\left(Z^{\rm II}_{\rm tot}\left(q,t,k+\frac{1}{2}+\mathrm{i}\sigma_n\right)+Z^{\rm II}_{\rm tot}\left(-q-\frac{\mathrm{i}}{2},t,k+\mathrm{i}\sigma_n\right)\right)\end{aligned}} \quad (2.6.8)$$

where σ_n are solutions of (2.3.8). In figure 2.1, we plot the right-hand side of (2.6.8) for the two smallest values of σ_n that satisfy the quantization condition (2.3.8). As a cross-check, we also verified this result by a purely numerical analysis of the operator (2.3.5), see subsection 2.6.4.

Let us make a few comments on the analytic properties of the gauge theoretic functions.

- The function $Z^{\rm Nek}(t,\sigma)$ has poles when $2\sigma\in\mathbb{Z}$ and $Z^{\rm II}_{\rm tot}(q,t,\sigma)$ has additional poles when q and σ satisfy $q=\frac{\mathrm{i}}{2}\pm\mathrm{i}\sigma+\mathrm{i}\ell$ with $\ell\in\mathbb{Z}$.

- If we are strictly interested only in the spectral problem associated with the integral kernel (2.3.5), then $q\in\mathbb{R}$ and $\sigma\in\frac{1}{2}+\mathrm{i}\mathbb{R}_{>0}$. So these poles are not realized.

- However, we can go beyond this special domain. For example, if we consider the Zak transform of $Z^{\rm Nek}(t,\sigma)$ appearing on the left-hand side of (2.3.9), then this has no longer poles in σ: the summation over k in (2.3.9) removes the poles. Likewise, it seems that the summation over integers and the particular combination of defect partition functions appearing in the integrand on the left-hand side of (2.6.7) has also the effect of removing the poles.

In the forthcoming subsections, we test (2.6.5) and (2.6.8) in several ways.

2.6.1 Testing $N = 0$

As a first check of (2.6.5), we test the $N = 0$ case. From (2.3.18), one can see that $\Psi_0(\mathrm{e}^x, t) = 1$ so that the right-hand side of (2.6.5) is

$$\left(\mathrm{i}\frac{2^{11/12}\sqrt{\pi}t^{3/16}}{\mathrm{e}^{3\zeta'(-1)}\mathrm{e}^{4\sqrt{t}}}\right)\int_{\mathbb{R}}\mathrm{d}x\ \mathrm{e}^{-\mathrm{i}2qx}\mathrm{e}^{-4t^{1/4}\cosh x+\frac{x}{2}} = \left(\mathrm{i}\frac{2^{11/12}\sqrt{\pi}t^{1/16}}{\mathrm{e}^{3\zeta'(-1)}\mathrm{e}^{4\sqrt{t}}}\right)2t^{1/8}K_{\mathrm{i}2q-\frac{1}{2}}\left(4t^{1/4}\right)\,, \tag{2.6.9}$$

where K is the modified Bessel function of the second kind. By expanding at small t, we find that the Bessel function has the following structure,

$$2t^{1/8}K_{\mathrm{i}2q-\frac{1}{2}}\left(4t^{1/4}\right) = F(q,t) + F\left(-q-\frac{\mathrm{i}}{2},t\right)\,, \tag{2.6.10}$$

for some function $F(q,t)$. For instance, we have when $\mathrm{i}2q-\frac{1}{2}\notin\mathbb{Z}$

$$F(q,t) = \mathrm{e}^{\mathrm{i}\frac{q}{2}\ln(t)}\left[2^{\mathrm{i}2q-\frac{1}{2}}\Gamma\left(-\mathrm{i}2q+\frac{1}{2}\right) - 2^{\mathrm{i}2q+\frac{3}{2}}\Gamma\left(-\mathrm{i}2q-\frac{1}{2}\right)\sqrt{t}+\mathcal{O}\left(t\right)\right]\,, \tag{2.6.11}$$

Hence, we already see the structure of the left-hand side of (2.6.5) appearing. On the gauge theory side, we can perform the integral at small t by using Cauchy's residue theorem,

$$\begin{aligned}
&\int_{\mathbb{R}+\mathrm{i}\sigma_*}\mathrm{d}\sigma\tan\left(2\pi\sigma\right)Z^{\mathrm{II}}_{\mathrm{tot}}(q,t,\sigma)\\
&=\int_{\mathbb{R}+\mathrm{i}\sigma_*}\mathrm{d}\sigma\tan(2\pi\sigma)\mathrm{e}^{\mathrm{i}\frac{q}{2}\ln(t)}t^{\sigma^2}\frac{\Gamma\left(-\mathrm{i}q-\sigma+\frac{1}{2}\right)\Gamma\left(-\mathrm{i}q+\sigma+\frac{1}{2}\right)}{G(1-2\sigma)G(1+2\sigma)}\left(1+\mathcal{O}(t)\right)\\
&=\left(\mathrm{i}\frac{2^{11/12}\sqrt{\pi}t^{1/16}}{\mathrm{e}^{3\zeta'(-1)}\mathrm{e}^{4\sqrt{t}}}\right)\mathrm{e}^{\mathrm{i}\frac{q}{2}\ln(t)}\left[2^{\mathrm{i}2q-\frac{1}{2}}\Gamma\left(-\mathrm{i}2q+\frac{1}{2}\right) - 2^{\mathrm{i}2q+\frac{3}{2}}\Gamma\left(-\mathrm{i}2q-\frac{1}{2}\right)\sqrt{t}\right.\\
&\qquad\left.+2^{\mathrm{i}2q+\frac{5}{2}}\Gamma\left(-\mathrm{i}2q-\frac{3}{2}\right)t+\mathcal{O}\left(t^{3/2}\right)\right]\,.
\end{aligned} \tag{2.6.12}$$

To get the last line in (2.6.12), we have included the first instanton correction in $Z^{\mathrm{II}}_{\mathrm{tot}}$ (2.6.4), and higher instanton corrections can be treated similarly. The poles contributing to the integral in (2.6.12) are

$$\sigma = \frac{\ell}{2} \qquad \text{and} \qquad \sigma = \frac{1}{4}+\frac{\ell}{2} \qquad \text{with} \qquad \ell\in\mathbb{Z}\,. \tag{2.6.13}$$

By employing the series expansions (2.6.11) and (2.6.12), we can systematically verify (2.6.5) for $N = 0$, order by order in t.

2.6.2 Testing $N = 1$

As a second consistency check of (2.6.5), we test the $N = 1$ case. First, we note that by a change of variables, we can rewrite the double integral appearing on the right-hand side

n^{inst}	
0	2.8372834788 + 4.7204648771 i
1	2.8312289304 + 4.7137559136 i
2	2.8313227416 + 4.7137434937 i
3	2.8313226948 + 4.7137435320 i
I_1	2.8313226948 + 4.7137435320 i

n^{inst}	
0	0.050235280369 + 0.018141366757 i
1	0.050242014312 + 0.018111611547 i
2	0.050241915710 + 0.018111648299 i
3	0.050241915600 + 0.018111648316 i
I_1	0.050241915600 + 0.018111648316 i

n^{inst}	
0	0.1587865901507390 i
1	0.1587680111233355 i
2	0.1587680126408577 i
3	0.1587680126408951 i
I_1	0.1587680126408951 i

Table 2.1. Comparison between the two sides of (2.6.5) for $N = 1$, $t = 1/55\pi^4$ with $q = 1/9 + \mathrm{i}2/\sqrt{3}$ (upper left), $q = 1/\pi$ (upper right), and $q = \mathrm{i}/3$ (lower). I_1 is the integral (2.6.15) appearing on the right-hand side of (2.6.5); n^{inst} refers to the number of instantons we include in the defect partition function appearing on the left-hand side of (2.6.5).

of (2.6.5) as a one-dimensional integral. Let us define

$$I_1(q,t) = \left(\mathrm{i}\frac{2^{11/12}\sqrt{\pi}'t^{3/16}}{\mathrm{e}^{3\zeta'(-1)}\mathrm{e}^{4\sqrt{t}}\,(4\pi)}\right)\int_{\mathbb{R}}\mathrm{d}x\,\mathrm{e}^{-\mathrm{i}2qx}\mathrm{e}^{-4t^{1/4}\cosh x+\frac{x}{2}}\Psi_1(\mathrm{e}^x,t)\,. \tag{2.6.14}$$

After some algebra, we get

$$I_1(q,t) = \left(\mathrm{i}\frac{2^{11/12}t^{3/16}}{\sqrt{\pi}\mathrm{e}^{3\zeta'(-1)}\mathrm{e}^{4\sqrt{t}}}\right)\times\int_3^{+\infty}\mathrm{d}U \\ \frac{\left(\left(\frac{U^2+\sqrt{U^4-10U^2+9}-3}{2U}\right)^{-\mathrm{i}2q+\frac{1}{2}}-\left(\frac{U^2+\sqrt{U^4-10U^2+9}-3}{2U}\right)^{\mathrm{i}2q-\frac{1}{2}}\right)K_{\mathrm{i}2q-\frac{1}{2}}\left(4\sqrt[4]{t}U\right)}{U-U^{-1}}\,. \tag{2.6.15}$$

One useful observation is that the above integral vanishes when $q = -\mathrm{i}/4$, which is in perfect agreement with the left-hand side of (2.6.5). Unfortunately, we cannot compute the integral (2.6.15) analytically. Hence, for $N = 1$, the test of (2.6.5) is done numerically and we find perfect agreement. One such test is given in table 2.1.

2.6.3 Testing large N with a 't Hooft limit

Another analytical test of the identity (2.6.5) consists of comparing both sides in the 't Hooft limit, where just as in (2.4.2)

$$N \to +\infty\,, \qquad \epsilon \to 0\,, \qquad \lambda = N\epsilon > 0\,, \tag{2.6.16}$$

and with the 't Hooft coupling λ fixed. We will need to use that q and t scale as in (2.2.4),

$$q = \frac{y}{2\epsilon}\,, \qquad\qquad t = \left(\frac{\Lambda}{\epsilon}\right)^4\,, \tag{2.6.17}$$

with both the position of the defect $y \in \mathbb{C}$ and the instanton counting parameter $\Lambda > 0$ kept fixed.

The computation of the 't Hooft limit of (2.6.5) is simplified by using the corresponding statement for the theory without defects, which is given in (2.3.15) and was obtained in [14, 63]. In particular, one can divide both sides of (2.6.5) by (2.3.15) to get

$$\begin{aligned}
&\frac{\int_{\mathbb{R}+\mathrm{i}\sigma_*} \mathrm{d}\sigma \frac{\tan(2\pi\sigma)}{[2\cos(2\pi\sigma)]^N} Z^{\mathrm{Nek}}\left(\left(\frac{\Lambda}{\epsilon}\right)^4, \sigma\right)\left[Z^{\mathrm{II}}\left(\frac{y}{2\epsilon}, \left(\frac{\Lambda}{\epsilon}\right)^4, \sigma\right) + (-1)^N Z^{\mathrm{II}}\left(\frac{-y-\mathrm{i}\epsilon}{2\epsilon}, \left(\frac{\Lambda}{\epsilon}\right)^4, \sigma\right)\right]}{(2\pi)\int_{\mathbb{R}+\mathrm{i}\sigma_*} \mathrm{d}\sigma \frac{\tan(2\pi\sigma)}{[2\cos(2\pi\sigma)]^N} Z^{\mathrm{Nek}}\left(\left(\frac{\Lambda}{\epsilon}\right)^4, \sigma\right)} \\
&\quad = \frac{\sqrt{\Lambda}}{\sqrt{\pi\epsilon}} \int_{\mathbb{R}} \mathrm{d}x \, \exp\left(-\frac{\mathrm{i}}{\epsilon} xy\right) \frac{\exp\left(-4\left(\frac{\Lambda}{\epsilon}\right)\cosh(x) + \frac{x}{2}\right) \Psi_N\left(\mathrm{e}^x, \left(\frac{\Lambda}{\epsilon}\right)^4\right)}{Z\left(\left(\frac{\Lambda}{\epsilon}\right)^4, N\right)}\,.
\end{aligned} \tag{2.6.18}$$

Note that (2.6.18) is by (2.3.15) equivalent to (2.6.5), but rewritten in a form suitable and convenient for the 't Hooft limit (2.6.16).

The 't Hooft limit on the gauge theory side

The general pattern of the 't Hooft expansion of the left-hand side in (2.6.18) is the same as in subsection 2.5.2. Using that the integration variable σ can be related to the Coulomb branch parameter a by (2.3.11),

$$\sigma = \mathrm{i}\frac{a}{2\epsilon}\,, \tag{2.6.19}$$

one expands the logarithm of the Nekrasov partition function Z^{Nek} in even powers of ϵ with the leading-order being ϵ^{-2}. On the other hand, the expansion of the logarithm of the defect partition function Z^{II} contains all integer powers of ϵ starting from ϵ^{-1},

$$(2\pi)^{-1} Z^{\mathrm{II}}\left(\frac{y}{2\epsilon}, \left(\frac{\Lambda}{\epsilon}\right)^4, \mathrm{i}\frac{a}{2\epsilon}\right) \simeq \exp\left(\sum_{n\geqslant 0} \mathcal{W}_n^{\mathrm{II}}(y)\epsilon^{n-1}\right)\,. \tag{2.6.20}$$

Hence, the saddles of both integrals on the left-hand side of (2.6.18) are determined by the same equation (2.5.15). This gives the functional relation $a(\Lambda, \lambda)$, but for us it will be convenient to rather invert this to $\lambda(\Lambda, a)$ and keep a explicitly. Keeping this in mind, the 't Hooft limit of the left-hand side of (2.6.18) leads eventually to

$$\begin{aligned}
&\exp\left\{\frac{1}{\epsilon}\mathcal{W}_0^{\mathrm{II}}(y) + \left[-\frac{\left(\partial_a \mathcal{W}_0^{\mathrm{II}}(y)\right)^2}{2\partial_a^2 \mathcal{F}_0} + \mathcal{W}_1^{\mathrm{II}}(y)\right] + \mathcal{O}(\epsilon)\right\} + \\
&\quad \exp\left\{\frac{1}{\epsilon}\left[\mathrm{i}\pi\lambda + \mathcal{W}_0^{\mathrm{II}}(-y)\right] + \left[\mathrm{i}\partial_y \mathcal{W}_0^{\mathrm{II}}(-y) - \frac{\left(\partial_a \mathcal{W}_0^{\mathrm{II}}(-y)\right)^2}{2\partial_a^2 \mathcal{F}_0} + \mathcal{W}_1^{\mathrm{II}}(-y)\right] + \mathcal{O}(\epsilon)\right\}\,,
\end{aligned} \tag{2.6.21}$$

where we suppressed the functional dependence on Λ and a in the notation.

The 't Hooft limit on the matrix model side

Consider the Fourier transform on the right-hand side in (2.6.18),

$$\frac{\sqrt{2\Lambda}}{\sqrt{2\pi\epsilon}}\int_{\mathbb{R}}\mathrm{d}x\,\exp\left(-\frac{\mathrm{i}}{\epsilon}xy\right)\frac{\exp\left(-4\left(\frac{\Lambda}{\epsilon}\right)\cosh\left(x\right)+\frac{x}{2}\right)\Psi_N\left(\mathrm{e}^x,\left(\frac{\Lambda}{\epsilon}\right)^4\right)}{Z\left(t,N\right)}, \tag{2.6.22}$$

where the 't Hooft expansion of the integrand is

$$\frac{\exp\left(-4\left(\frac{\Lambda}{\epsilon}\right)\cosh\left(x\right)+\frac{x}{2}\right)\Psi_N\left(\mathrm{e}^x,\left(\frac{\Lambda}{\epsilon}\right)^4\right)}{Z\left(t,N\right)}=\exp\left[\frac{1}{\epsilon}\mathcal{T}_0\left(\mathrm{e}^x\right)+\frac{x}{2}+\mathcal{T}_1\left(\mathrm{e}^x\right)+\mathcal{O}\left(\epsilon\right)\right], \tag{2.6.23}$$

by using (2.4.9) and again suppressing the functional dependence on the other variables. In the limit $\epsilon\to 0$, the Fourier transform in (2.6.22) is dominated by its saddles and becomes

$$\begin{aligned}\sum_s\exp\left\{\frac{1}{\epsilon}\widehat{\mathcal{T}_{s,0}}\left(y\right)+\widehat{\mathcal{T}_{s,1}}\left(y\right)+\mathcal{O}\left(\epsilon\right)\right\}=\sum_s\exp\Bigg\{&\frac{1}{\epsilon}\left[-\mathrm{i}x_sy+\mathcal{T}_0\left(\mathrm{e}^{x_s}\right)\right]\\&+\left[\frac{\ln\left(2\Lambda\right)}{2}-\frac{\ln\left(-\partial_x^2\mathcal{T}_0\left(\mathrm{e}^{x_s}\right)\right)}{2}+\frac{x_s}{2}+\mathcal{T}_1\left(\mathrm{e}^{x_s}\right)\right]+\mathcal{O}\left(\epsilon\right)\Bigg\}.\end{aligned} \tag{2.6.24}$$

The sum over s is a sum over the saddles and $x_s=x_s\left(y\right)$ is determined by the saddle point equation,

$$y+\mathrm{i}\partial_x\mathcal{T}_0\left(\mathrm{e}^x\right)=y-\mathrm{i}2\Lambda\frac{\sqrt{\mathrm{e}^{2x}-\mathsf{g}^2}\sqrt{\mathrm{e}^{2x}-\mathsf{g}^{-2}}}{\mathrm{e}^x}=0\,, \tag{2.6.25}$$

where we used (2.4.34) and $z=\exp\left(x\right)$. Taking the square of this equation gives the Seiberg-Witten curve (2.4.35) if we take as before (2.4.37),

$$\mathsf{g}^2+\mathsf{g}^{-2}=\frac{u4\Lambda^2}{},\qquad\qquad \mathsf{g}^{\pm 2}=\left(\frac{u}{8\Lambda^2}\right)\mp\sqrt{\left(\frac{u}{8\Lambda^2}\right)^2-1}\,. \tag{2.6.26}$$

This leads to the following two solutions,

$$\mathrm{e}^{2x_\pm(y)}=z_\pm^2\left(y\right)=-\left[\frac{\left(y^2-u\right)\pm\sqrt{\left(y^2-u\right)^2-64\Lambda^4}}{8\Lambda^2}\right]. \tag{2.6.27}$$

Let us take a moment to consider the behaviour of $z_\pm\left(y\right)$ as a function of y. One can check that $z_\pm\left(y\right)$ is real and outside the branch cut region of the matrix model if and only if $\mathrm{i}y\in\mathbb{R}\setminus\{0\}$. It is important to note that with this choice of $\mathrm{i}y\in\mathbb{R}\setminus\{0\}$ one has $z_-^2\left(y\right)>1/\mathsf{g}^2$ and $0\leqslant z_+^2\left(y\right)<\mathsf{g}^2$. Moreover, there are no possible choices of $y\in\mathbb{C}$ such that $0\leqslant z_-^2\left(y\right)<\mathsf{g}^2$ or $z_+^2\left(y\right)>1/\mathsf{g}^2$. One finds on the other hand that $z_\pm\left(y\right)$ is real and inside the branch cut region if and only if $0\leqslant y^2\leqslant u-8\Lambda^2$, and also that $z_\pm\left(y\right)$ is purely imaginary if and only if $y^2\geqslant u+8\Lambda^2$. For all other choices of $y\in\mathbb{C}$, one will find generic complex $z_\pm\left(y\right)$.

Comparing the gauge theory and the matrix model

To analyze the leading-order of the 't Hooft expansion in (2.6.24) with the saddles (2.6.27), it is convenient to separately look at the case $y = 0$ and the derivative with respect to y. The reason is that the latter simplifies considerably as a consequence of the saddle point equation (2.6.25). Setting $y = 0$ serves then as a check of the constant term.

Let us first look at the y derivative of the leading-order part. At the matrix model side (2.6.24), one gets by making use of the saddle point equation (2.6.25) and its solutions

$$\frac{\mathrm{d}}{\mathrm{d}y}\widehat{\mathcal{T}_{\pm,0}}\left(y\right) = -\mathrm{i}x_{\pm}\left(y\right) . \tag{2.6.28}$$

Comparing this to the leading-order of the gauge theory (2.6.20), we can check that[25]

$$\frac{\mathrm{d}}{\mathrm{d}y}\left[\mathcal{W}_0^{\mathrm{II}}\left(\pm y\right) - \widehat{\mathcal{T}_{\pm S,0}}\left(y\right)\right] = 0\,, \tag{2.6.29}$$

where $S = \mathrm{sgn}\left[\arg\left(\mathrm{i}\left(y^2 - a^2\right)\right)\right]$ with the convention that $\mathrm{sgn}\left(0\right) = -1$.

Let us then look at the constant term for $y = 0$. At the gauge theory side, we have for the leading-order (2.6.20)

$$\mathcal{W}_0^{\mathrm{II}}\left(0\right) = -\frac{\pi}{2}\left|a\right|. \tag{2.6.30}$$

From (2.6.27), one can see that $z_{\pm}\left(0\right) = \mathsf{g}^{\pm} > 0$, with $\mathsf{g}^{\pm}$ as in (2.6.26). Using (2.4.10) gives for the leading-order of the matrix model (2.6.24)

$$\widehat{\mathcal{T}_{\pm,0}}\left(0\right) = \mathcal{T}_0\left(z_{\pm}\left(0\right)\right) = -2\Lambda\left(\mathsf{g} + \mathsf{g}^{-1}\right) + 2\int_{+\infty}^{\mathsf{g}^{\pm 1}} \mathrm{d}z\, \lambda\omega_+^0\left(z\right) , \tag{2.6.31}$$

where the even planar resolvent $\omega_+^0\left(z\right)$ is given in (2.4.30). Note that the difference between the leading terms of the two saddles is

$$\left[\widehat{\mathcal{T}_{+,0}}\left(0\right) - \widehat{\mathcal{T}_{-,0}}\left(0\right)\right] = -2\int_{\mathsf{g}}^{\mathsf{g}^{-1}} \mathrm{d}z\, \lambda\omega_+^0\left(z\right) = \mathrm{i}\pi\lambda\,. \tag{2.6.32}$$

The last equality can be obtained in an $\Lambda \to 0$ expansion or exactly using [135, eq. 4.18], which shows that this relation does not depend on the particular form of the potential. We have furthermore that

$$\begin{aligned}\widehat{\mathcal{T}_{-,0}}\left(0\right) &= -2\Lambda\left(\mathsf{g} + \mathsf{g}^{-1}\right) + 2\int_{+\infty}^{\mathsf{g}^{-1}} \mathrm{d}z\ \lambda\omega_+^0\left(z\right) \\ &= -2\Lambda\left[\frac{2\mathrm{E}\left(\mathsf{g}^4\right) + \left(\mathsf{g}^{-2} - \mathsf{g}^2\right)\left[-2\mathsf{g}^2\mathrm{K}\left(\mathsf{g}^4\right) + \mathrm{K}\left(\mathsf{g}^{-4}\right) + \mathrm{i}\mathrm{K}\left(1 - \mathsf{g}^{-4}\right)\right]}{\mathsf{g}}\right] = -\frac{\pi}{2}\left|a\right| ,\end{aligned} \tag{2.6.33}$$

[25] Upon using the Matone relation (2.5.17) and careful treatment of the branches.

with K and E the complete elliptic integrals of the first (A.2.1) and second (A.2.2) kind, respectively. The last equality was found in an $\Lambda \to 0$ or equivalently $\mathfrak{g} \to 0$ expansion using (2.6.26) and the Matone relation (2.5.17). Hence, from (2.6.30), (2.6.32), and (2.6.33)

$$\begin{aligned} \mathcal{W}_0^{\mathrm{II}}(0) - \widehat{\mathcal{T}_{-,0}}(0) &= 0\,, \\ \mathrm{i}\pi\lambda + \mathcal{W}_0^{\mathrm{II}}(0) - \widehat{\mathcal{T}_{+,0}}(0) &= 0\,. \end{aligned} \tag{2.6.34}$$

So the constant parts of the leading-order terms agree, and together with (2.6.29) this proves the equality in (2.6.18) and hence (2.6.5) to leading-order in the 't Hooft limit (2.6.16).

The subleading-order can be checked in analogy with section 2.5. Matching at higher order in ϵ can then be inferred from topological recursion, as we discussed near the end of section 2.5.

2.6.4 Numerical eigenfunctions

The numerical analysis of the spectrum and the eigenfunctions for the integral kernel ρ (2.3.5) is done exactly as in [145, sec. 2.2]. To make the presentation self-contained, let us review the strategy of [145, sec. 2.2]. We are interested in studying numerically the eigenvalue equation

$$\int_{\mathbb{R}} \mathrm{d}y\, \rho(x,y)\varphi_n(y,t) = E_n\varphi_n(x,t)\,, \tag{2.6.35}$$

where the kernel $\rho(x,y)$ is defined in (2.3.5). It is convenient to decompose $\rho(x,y)$ as

$$\rho(x,y) = \sum_{k\geqslant 0} \rho_k(x)\rho_k(y)\,, \qquad \rho_k(x) = \frac{\tanh^k\left(\frac{x}{2}\right)\exp\left(-4t^{1/4}\cosh(x)\right)}{\cosh\left(\frac{x}{2}\right)}\,, \tag{2.6.36}$$

and to define

$$v_k^{(n)}(t) = \int_{\mathbb{R}} \mathrm{d}y\, \rho_k(y)\varphi_n(y,t)\,. \tag{2.6.37}$$

Then, (2.6.35) reads

$$\sum_{k\geqslant 0} \rho_k(x) v_k^{(n)}(t) = E_n\varphi_n(x,t)\,, \tag{2.6.38}$$

which we can also write as

$$\sum_{k\geqslant 0} H_{\ell,k} v_k^{(n)}(t) = E_n v_\ell^{(n)}(t)\,, \tag{2.6.39}$$

with H the infinite-dimensional Hankel matrix defined by

$$H_{k,\ell} = \int_{\mathbb{R}} \mathrm{d}x \frac{\tanh^{k+\ell}\left(\frac{x}{2}\right)\exp\left(-8t^{1/4}\cosh(x)\right)}{\cosh^2\left(\frac{x}{2}\right)}\,, \qquad k,\ell \geqslant 0\,. \tag{2.6.40}$$

This means that the eigenvalues of H coincide with those of $\rho(x,y)$ and the eigenvectors of H give the eigenfunctions of $\rho(x,y)$ via (2.6.38). The advantage of working with H is that

we can numerically compute its eigenvalues and eigenfunctions by truncating the matrix to a finite size while maintaining control over the numerical error due to the truncation. Let $v^{(n,M)}(t)$ be the n^{th} eigenvector of the Hankel matrix H (2.6.40) truncated at size M. Defining $\varphi_n^{(M)}(x,t)$ by

$$\varphi_n^{(M)}(x,t) = \sum_{k=0}^{M} \rho_k(x) v_k^{(n,M)}\,, \qquad v^{(n,M)} = \begin{pmatrix} v_0^{(n,M)} \\ \vdots \\ v_M^{(n,M)} \end{pmatrix}\,, \tag{2.6.41}$$

we recover the true eigenfunctions of the kernel ρ in the $M \to +\infty$ limit,

$$\lim_{M\to+\infty} \varphi_n^{(M)}(x,t) \propto \varphi_n(x,t)\,, \tag{2.6.42}$$

where the proportionality factor is a numerical constant and φ_n is the n^{th} eigenfunction of (2.6.35) in the normalization of (2.6.8). We computed the left-hand side of (2.6.42) numerically and checked that this numerical expression agrees with the eigenfunctions computed by using the defect expression on the right-hand side of (2.6.8) with high precision. For instance, for $t = 1/(100\pi^8)$, by including 0 instantons in (2.6.8) we get a pointwise agreement of the order 10^{-6}. Likewise, by including 1, 2 and 3 instantons we get a pointwise agreement of the order 10^{-11}, 10^{-16}, and 10^{-22}, respectively[26].

2.7 Outlook and open problems

Several interesting open problems deserve our attention. We highlight a few of them:

- In this work, we focused on the specific example of 4d, $\mathcal{N} = 2$, SU(N) SYM and the operator (2.1.1). It would be interesting to extend our results in a systematic way to all 4d $\mathcal{N} = 2$ theories. For example, in the case of $\mathcal{N} = 2$, SU(N) SYM we have $N-1$ non-commuting Fermi gas operators as discussed in [15, 63]. We expect their eigenfunctions to be computed by surface defects in SU(N) SYM in the self-dual phase of the Ω background. The proposal in chapter 4 and section 4.4 in particular are an important step in this direction.

- The Fredholm determinant of (2.1.1) computes the tau function of the Painlevé III_3 equation at specific initial conditions. It would be interesting to understand the role of the eigenfunctions of (2.1.1) in the context of Painlevé equations. In particular, the relation to the solution of the linear system associated with Painlevé equations [33, 69] as well as with [146].

- The Fredholm determinant and the spectral traces of (2.1.1) can also be expressed via a pair of coupled TBA equations closely related to *two-dimensional* theories [61, 147]. It would be interesting to understand this better, since this may reveal an interesting 4d-2d interplay characterizing directly the self-dual phase of the Ω-background.

[26] One can reach this precision with Hankel matrices of size $M = 2^9 = 512$.

- The operator (2.1.1) is a particular example of a Painlevé kernel whose Fredholm determinant computes the tau function. A more general class of Fredholm determinants was constructed in [148–151]. It would be interesting to see if also in this case the corresponding (formal) eigenfunctions are related to surface defects.

- It is well known that the canonical quantization of the SW curve for SU(N) SYM leads to the modified Mathieu operator (2.3.1). We expect a different quantization scheme to produce the operator (2.1.1). It is important to understand what this other quantization scheme is. Since the spectral analysis of (2.1.1) is encoded in the self-dual phase of the Ω-background, a natural quantization scheme to investigate would be the one arising in the context of the topological recursion [126–129]. See also subsection 3.4.3 for a functional relation between (2.1.1) and the modified Mathieu equation, which gives (2.1.1) indirectly in terms of the usual canonical quantization of the SW curve.

See also the conclusion and outlook in chapter 5.

Chapter 3

Eigenfunctions of the finite difference modified Mathieu equation

Building on the previous chapter and [6, 7], we propose a construction for the eigenfunctions of the quantized mirror curve of local $\mathbb{F}_0$. This chapter bundles the work that originally appeared in [2], which is joint work with Alba Grassi.

3.1 Introduction

The topological string/spectral theory (TS/ST) correspondence [4–7] establishes a precise non-perturbative relation between the partition functions of topological string theory on local Calabi-Yau (CY) threefolds and the spectral properties of certain quantum mechanical operators on the real line. These quantum operators are obtained through the quantization of mirror curves [8, 56] and correspond to Baxter equations for a class of relativistic integrable systems, such as cluster integrable systems [152, 153] or elliptic Ruijsenaars-Schneider (RS) systems [154].

The TS/ST correspondence itself is structured in two parts: one relating closed strings to the spectrum, and the other relating open strings to the eigenfunctions. A central feature of this duality is the relationship between the string coupling constant g_s and the reduced Planck constant $\hbar$ given by

$$g_s = \frac{4\pi^2}{\hbar}\,. \tag{3.1.1}$$

This implies that string perturbation theory naturally encodes non-perturbative effects on the spectral theory side. Conversely, the usual WKB expansion in spectral theory gives us the non-perturbative effects on the topological string side. Thus, the TS/ST correspondence bridges perturbative expansions in one theory with non-perturbative phenomena in its dual counterpart. This allows for the derivation of exact, closed-form expressions for many quantities on both sides of the correspondence. Another important consequence of (3.1.1) is the existence of the so-called self-dual, or maximally symmetric point [102], given

by

$$\hbar = 2\pi = g_s \,. \tag{3.1.2}$$

At this special point, the TS/ST correspondence predicts remarkable simplifications, not only on the string theory side but also in operator theory, see e.g. [4–7, 155, 156].

We focus on the example where the underlying CY geometry is local $\mathbb{F}_0$. In the closed string sector, one important statement of the TS/ST correspondence is [4]

$$\det\left(1+\kappa\rho\right) = \sum_{k\in\mathbb{Z}} \mathrm{e}^{\mathrm{J}(\mu+\mathrm{i}2\pi k,\xi,\hbar)} \,, \qquad\qquad \kappa = \mathrm{e}^{\mu} \,, \tag{3.1.3}$$

where the operator $\rho : \ L^2(\mathbb{R}) \ \to \ L^2(\mathbb{R})$ is the inverse of the quantum mirror curve to local $\mathbb{F}_0$, that is $\rho = \mathrm{O}^{-1}$ with

$$\mathrm{O} = \mathrm{e}^{\hat{y}} + \mathrm{e}^{-\hat{y}} + \mathrm{e}^{2\xi}\left(\mathrm{e}^{\hat{x}} + \mathrm{e}^{-\hat{x}}\right) \,, \qquad\qquad [\hat{x},\hat{y}] = \mathrm{i}\hbar \,, \qquad\qquad \xi \in \mathbb{R} \,,\, \hbar \in \mathbb{R}_{>0} \,. \tag{3.1.4}$$

On the right-hand side of (3.1.3), κ parametrizes the closed string moduli space, while ξ is the so-called "mass" parameter, associated with the residue of the CY one-form at infinity. The function $\mathrm{J}(\mu,\xi,\hbar)$ represents the topological string grand potential, incorporating both perturbative and non-perturbative contributions in $g_s = 4\pi^2/\hbar$, see (3.3.9). From the perspective of the moduli space, $\mathrm{J}(\mu,\xi,\hbar)$ is defined around the large radius point, and its perturbative part in g_s is given by the standard Gopakumar-Vafa (GV) free energy, see (3.3.17) and (3.3.19). The summation over k in (3.1.3) effectively smooths all the singularities across the closed string moduli space, parametrized by κ, allowing one to move away from the large radius point. Indeed, we can prove that ρ is a trace class operator on $L^2(\mathbb{R})$ [11, 125], and therefore its spectral determinant on the left-hand side of (3.1.3) is an entire function of κ. We can expand it around $\kappa \to \infty$, the large radius point, or around $\kappa = 0$, the orbifold point [4, 5, 157]. Let us also note that the summation over k in (3.1.3) is also essential for ensuring good modular properties of the determinant [102, 158] and for connecting it with q-isomonodromic τ-functions [14, 15, 64, 68, 159–165].

The main motivation of this work is to extend the relation in (3.1.3) to the open string sector. To this end, the first step is to define the open string grand potential $\mathrm{J}(x,\mu,\xi,\hbar)$, where x is the open string modulus. This was done in [6, 7] by focusing on the case where the brane is inserted in the outer leg of the toric diagram, the explicit form is given in (3.3.22), (3.3.31). Analogous to the closed string sector, $\mathrm{J}(x,\mu,\xi,\hbar)$ incorporates both perturbative and non-perturbative contributions in $g_s = 4\pi^2/\hbar$ and is defined in the large radius frame. However, one limitation of $\mathrm{J}(x,\mu,\xi,\hbar)$ is that it is not an entire function of the open string modulus x, which is a desirable property for a background-independent, non-perturbative formulation of open strings [75]. It was further suggested in [6, 7] that this requires a combination of the form

$$\psi(x,\kappa) = \sum_{k\in\mathbb{Z}} \sum_{\sigma} \mathrm{e}^{\mathrm{J}_\sigma(x,\mu+\mathrm{i}2\pi k,\xi,\hbar)} \,, \qquad\qquad \kappa = \mathrm{e}^{\mu} \,, \tag{3.1.5}$$

where the summation over σ is expected to play a role analogous to the sum over k in (3.1.3), but for the open string modulus x. In particular, just as the sum over k smooths out all singularities in the closed string moduli, the sum over σ should similarly ensure that (3.1.5) becomes an entire function of x.

In this chapter, building on insights from [1, 6, 7], we make this expectation precise by providing an explicit form for this summation over σ in the case of local $\mathbb{F}_0$, at generic values of $\hbar$ and the complex moduli μ and ξ. Specifically, we find that the precise combination to consider is

$$\psi(x,\kappa) = \sum_{k\in\mathbb{Z}} \left(\mathrm{e}^{\mathrm{J}(x,\mu+\mathrm{i}2\pi k,\xi,\hbar)} + \mathrm{e}^{\frac{\mathrm{i}}{\hbar}\frac{\pi^2}{2}+\frac{\pi x}{\hbar}+\mathrm{J}(-x-\mathrm{i}\pi,\mu+\mathrm{i}\pi+\mathrm{i}2\pi k,\xi,\hbar)} \right) . \tag{3.1.6}$$

From the perspective of spectral theory, the combination (3.1.6) is a solution of the functional difference equation corresponding to the quantized mirror curve (3.1.4),

$$\psi(x+\mathrm{i}\hbar,\kappa) + \psi(x-\mathrm{i}\hbar,\kappa) + 2\mathrm{e}^{2\xi}\cosh(x)\psi(x,\kappa) + \kappa\psi(x,\kappa) = 0\,. \tag{3.1.7}$$

Difference equations of the type (3.1.7) admit many solutions. The proposal (3.1.6) stands out in three ways. Firstly, (3.1.6) is always a well-defined function of x, κ, ξ and $\hbar$ solving (3.1.7), and not just a formal solution.[1] Secondly, (3.1.6) becomes a proper eigenfunction of the operator (3.1.4) when κ is a root of the spectral determinant (3.1.3). Thirdly, the eigenfunctions (3.1.6) are entire in x for all $\kappa \in \mathbb{C}$. We do not have a complete, mathematical proof for these statements, but we performed many analytic and numerical tests that support them.

One can further express such eigenfunctions in terms of O (2) matrix models by performing a canonical transformation [6]. More specifically we have

$$\psi(x,\kappa) = \int_{\mathbb{R}} \mathrm{d}q\, U(x,q)\, \Xi(q,\kappa)\,, \tag{3.1.8}$$

where $U(x,q)$ is the kernel of a unitary transformation, see (3.2.41), and we have

$$\Xi(q,\kappa) = \exp\left(\frac{\pi}{\sqrt{2}}\frac{q}{\hbar}\right) \mathtt{f}(q) \sum_{N=0}^{\infty} \kappa^N \Psi_N(q)\,, \tag{3.1.9}$$

where $\mathtt{f}(q)$ is given in (3.2.11) and $\Psi_N(q)$ is defined by the following unnormalized expectation value within the O (2) matrix model (3.2.19)

$$\Psi_N(q) = \left\langle \prod_{k=1}^{N} \tanh\left(\frac{\pi}{\sqrt{2}}\frac{q-q_k}{\hbar}\right) \right\rangle . \tag{3.1.10}$$

[1] By "formal solution", we mean an object that solves (3.1.7) but that is not a well-defined function. For example, objects defined via divergent series expansions or those with a dense set of poles in their domain of definitions (e.g. when $\hbar \in \mathbb{R}_{>0}$).

The expression (3.1.9) is particularly interesting because it allows one to easily connect with the conifold frame as we discuss later.

This chapter is organized as follows. In section 3.2, we analyse the matrix model (3.1.10) in some detail and show how its canonical transformation (3.1.8) naturally leads to the symmetric structure of the two contributions in (3.1.6). In section 3.3, we translate this into a conjecture for the eigenfunctions in terms of open topological strings, as given in (3.1.6), and we perform several detailed tests of the proposal. In section 3.4, we examine two specific limits of our construction: the standard four-dimensional limit [118, 120], defined in (3.4.1), and the dual four-dimensional limit [14, 63], defined in (3.4.33). In the standard four-dimensional limit, the difference equation (3.1.7) reduces to the Fourier-transformed Mathieu operator whose eigenvalue equation reads

$$\sqrt{t}\,(\phi(x+\mathrm{i}\epsilon,E)+\phi(x-\mathrm{i}\epsilon,E))+x^2\phi(x,E)-E\phi(x,E)=0\,, \tag{3.1.11}$$

where t, E and ϵ correspond to the four-dimensional limits of ξ, κ and $\hbar$ in (3.1.7), respectively. As with (3.1.7), this equation has many formal solutions. However, our construction identifies a special class of eigenfunctions that are entire, even off-shell. These are given by

$$\phi(x,E)=\phi_1\left(\frac{x}{\epsilon},\frac{\sigma}{\epsilon},\frac{t}{\epsilon^4}\right)+\phi_2\left(\frac{x}{\epsilon},\frac{\sigma}{\epsilon},\frac{t}{\epsilon^4}\right) \tag{3.1.12}$$

with

$$\phi_2(x,\sigma,t)=\phi_1(-x,\sigma,t)\left[\frac{\mathrm{e}^{-\frac{\mathrm{i}}{2}\partial_\sigma F^{4\mathrm{d}}_{\mathrm{NS}}(\sigma,t)}\left(\mathrm{e}^{2\pi x}-\mathrm{e}^{2\pi\sigma}\right)-\mathrm{e}^{\frac{\mathrm{i}}{2}\partial_\sigma F^{4\mathrm{d}}_{\mathrm{NS}}(\sigma,t)}\left(\mathrm{e}^{2\pi x}-\mathrm{e}^{-2\pi\sigma}\right)}{\mathrm{e}^{2\pi\sigma}-\mathrm{e}^{-2\pi\sigma}}\right], \tag{3.1.13}$$

where $\phi_1(x,\sigma,t)$ is defined in (3.4.13) with σ and E being related by (3.4.10). The factor in square brackets in (3.1.13) is crucial to ensuring that the off-shell function (3.1.12) is entire. When evaluated on-shell, this factor is ±1 depending on the parity of the eigenfunction, and our result reproduces the well-known expression for the on-shell eigenfunction in terms of 2d/4d surface defects in the Nekrasov–Shatashvili (NS) phase of the Ω-background [27, 28, 30, 32, 33, 35, 36, 39, 40]. On the other hand, in the dual four-dimensional limit (3.4.33), the operator (3.1.4) leads to the McCoy-Tracy-Wu operator [14]

$$\mathrm{e}^{4t^{1/4}\cosh\hat{x}}\cosh\left(\frac{\hat{y}}{2}\right)\mathrm{e}^{4t^{1/4}\cosh\hat{x}}\,, \tag{3.1.14}$$

whose eigenfunctions are computed by 2d/4d surface defects in the GV (or self-dual) phase of the Ω-background [1]. Even though the off-shell eigenfunctions of (3.1.11) and (3.1.14) are quite different, when evaluated on-shell, they are related in a remarkably simple way. This in turn provides a clear functional relation between the modified Mathieu (3.1.11) and McCoy-Tracy-Wu (3.1.14) operators, see subsection 3.4.3 and equation (3.4.50). In section 3.5, we conclude and outline some open problems. We also have four appendices that provide technical details and definitions necessary for understanding the results in the main text.

3.2 Eigenfunctions and matrix models

3.2.1 The spectral problem

The mirror curve to local $\mathbb{F}_0$ reads [118, 166]

$$e^{y} + e^{-y} + e^{2\xi}\left(e^{x} + e^{-x}\right) + \kappa = 0\,, \tag{3.2.1}$$

where κ, ξ are the complex structure moduli of local $\mathbb{F}_0$. The eigenvalue equation corresponding to the quantization of the mirror curve (3.2.1) is [8, 56]

$$\left(e^{\hat{y}} + e^{-\hat{y}} + e^{2\xi}\left(e^{\hat{x}} + e^{-\hat{x}}\right)\right)\psi(x,\kappa) + \kappa\psi(x,\kappa) = 0\,, \qquad [\hat{x},\hat{y}] = i\hbar\,, \tag{3.2.2}$$

leading to the following difference equation

$$\psi(x + i\hbar,\kappa) + \psi(x - i\hbar,\kappa) + 2e^{2\xi}\cosh(x)\,\psi(x,\kappa) + \kappa\psi(x,\kappa) = 0\,, \tag{3.2.3}$$

which also corresponds to the Baxter equation for the two-particle, relativistic, quantum Toda lattice [167]. In this chapter, we always take

$$\xi \in \mathbb{R}\,, \qquad \hbar \in \mathbb{R}_{>0}\,. \tag{3.2.4}$$

Let us now look at the domain of the operators involved, acting as self-adjoint operators on the Hilbert space of square-integrable functions $L^2(\mathbb{R})$. The domain of the multiplication operator $\left(e^{\hat{x}} + e^{-\hat{x}}\right)$ contains then all functions $\psi \in L^2(\mathbb{R})$ for which $e^{\pm x}\psi(x) \in L^2(\mathbb{R})$, and the difference operator $\left(e^{\hat{y}} + e^{-\hat{y}}\right)$ acts similarly on the functions $\psi \in L^2(\mathbb{R})$ for which $e^{\pm y}\widehat{\psi}(y) \in L^2(\mathbb{R})$, with $\widehat{\psi}$ the Fourier transform of ψ. This condition on the Fourier transform $\widehat{\psi}$ is equivalent to the statement that ψ admits an analytic continuation in the strip

$$\{x \in \mathbb{C} \mid |\mathrm{Im}(x)| < \hbar\}\,, \tag{3.2.5}$$

such that $\psi(x)$ is square-integrable for all constant $|\mathrm{Im}(x)| < \hbar$. In addition, one also requires that the limits

$$\lim_{\epsilon\to 0^+} \psi(x - i\hbar + i\epsilon,\kappa)\,, \qquad \lim_{\epsilon\to 0^+} \psi(x + i\hbar - i\epsilon,\kappa)\,, \tag{3.2.6}$$

exist in the sense of convergence in $L^2(\mathbb{R})$. The quantized mirror curve (3.2.2) is then a symmetric, strictly positive operator, defined on the intersection of the domains of the multiplication and difference operators. Hence, one can define its Friedrichs extension, see [125]. It is this self-adjoint extension we will consider in everything that follows, and we refer to it as the quantum mirror curve. This leads to a purely discrete spectrum $\{E_n\}_{n\in\mathbb{N}}$ for the quantum mirror curve, see [4, 11, 125]. Our conventions for the spectrum are

$$\left(e^{\hat{y}} + e^{-\hat{y}} + e^{2\xi}\left(e^{\hat{x}} + e^{-\hat{x}}\right)\right)\psi(x, -e^{E_n}) = e^{E_n}\psi(x, -e^{E_n})\,. \tag{3.2.7}$$

We refer to the variables x, y, and the corresponding operators $\hat{x}, \hat{y}$ in (3.2.1) as outer topological string coordinates for reasons that will become clear later.

Following [11, 65] we introduce the matrix model coordinates q, p,

$$\begin{aligned} x &= \frac{1}{\sqrt{2}}(q+p) + \xi\,, \\ y &= \frac{1}{\sqrt{2}}(-q+p) + \xi\,. \end{aligned} \tag{3.2.8}$$

After some creative algebra, one can show that the eigenvalue equation in the q, p coordinates can be written as [65, sec. 2.1]

$$\mathrm{O}\,\Xi(q,\kappa) = -\kappa\,\Xi(q,\kappa)\,, \tag{3.2.9}$$

$$\mathrm{O} = \frac{\sqrt{2}}{\hbar}(\mathtt{f}^*(\hat{q}))^{-1}\cosh\left(\frac{\hat{p}}{\sqrt{2}}\right)(\mathtt{f}(\hat{q}))^{-1}\,, \qquad [\hat{q},\hat{p}] = \mathrm{i}\hbar\,, \tag{3.2.10}$$

where we used

$$\begin{aligned} \mathtt{f}(q) &= \frac{2^{1/4}}{\sqrt{2\pi b^2}}\exp\left(-\frac{\xi}{2}\right)\exp\left(\frac{q}{2\sqrt{2}}\right)\frac{\Phi_b\left(\frac{q}{\sqrt{2}\pi b} - \frac{\xi}{\pi b} + \mathrm{i}\frac{b}{4}\right)}{\Phi_b\left(\frac{q}{\sqrt{2}\pi b} + \frac{\xi}{\pi b} - \mathrm{i}\frac{b}{4}\right)}\,, \qquad \hbar = \pi b^2\,, \\ \mathtt{f}^*(q) &= \frac{2^{1/4}}{\sqrt{2\pi b^2}}\exp\left(-\frac{\xi}{2}\right)\exp\left(\frac{q}{2\sqrt{2}}\right)\frac{\Phi_b\left(\frac{q}{\sqrt{2}\pi b} + \frac{\xi}{\pi b} + \mathrm{i}\frac{b}{4}\right)}{\Phi_b\left(\frac{q}{\sqrt{2}\pi b} - \frac{\xi}{\pi b} - \mathrm{i}\frac{b}{4}\right)}\,, \qquad \hbar = \pi b^2\,, \end{aligned} \tag{3.2.11}$$

with Φ_b Faddeev's non-compact quantum dilogarithm, see subsection A.2.2. Note that $\mathtt{f}^*(q) = \overline{\mathtt{f}(q)}$ only if $q, \xi, b \in \mathbb{R}$. It is convenient to introduce the inverse operator $\rho = \mathrm{O}^{-1}$ whose integral kernel is

$$\rho(q_1, q_2) = \frac{\mathtt{f}(q_1)\mathtt{f}^*(q_2)}{2\cosh\left(\frac{q_1-q_2}{\sqrt{2}b^2}\right)}\,. \tag{3.2.12}$$

One important property is that ρ is of trace class and its Fredholm determinant admits an expansion in terms of an $\mathrm{O}(2)$ matrix model. More precisely

$$\det(1+\kappa\rho) = \prod_{n=0}^{\infty}(1+\kappa \mathrm{e}^{-E_n}) = \sum_{N=0}^{\infty}\kappa^N Z(N,\hbar) \tag{3.2.13}$$

where E_n is determined as discussed around (3.2.7) and

$$Z(N,\hbar) = \frac{1}{N!}\sum_{s\in S_N}(-1)^{\mathrm{sgn}(s)}\int_{\mathbb{R}}\mathrm{d}^N x\prod_{k=1}^{N}\rho\left(x_k, x_{s(k)}\right)\,, \tag{3.2.14}$$

where S_N is the permutation group of N elements. By applying the Cauchy identity, one can further write $Z(N,\hbar)$ as [65]

$$Z(N,\hbar) = \frac{1}{2^N N!}\int_{\mathbb{R}^N}\mathrm{d}^N q\prod_{k=1}^{N}\mathtt{v}(q_k)\prod_{\ell=k+1}^{N}\tanh^2\left(\frac{q_k-q_\ell}{\sqrt{2}b^2}\right)\,, \tag{3.2.15}$$

$$\mathtt{v}\,(q) = \mathtt{f}(q)\mathtt{f}^*(q) = \frac{\mathrm{e}^{-\xi}}{\sqrt{2}\pi b^2} \exp\left(\frac{q}{\sqrt{2}}\right) \frac{\Phi_b\left(\frac{q}{\sqrt{2}\pi b} - \frac{\xi}{\pi b} + \mathrm{i}\frac{b}{4}\right)\Phi_b\left(\frac{q}{\sqrt{2}\pi b} + \frac{\xi}{\pi b} + \mathrm{i}\frac{b}{4}\right)}{\Phi_b\left(\frac{q}{\sqrt{2}\pi b} + \frac{\xi}{\pi b} - \mathrm{i}\frac{b}{4}\right)\Phi_b\left(\frac{q}{\sqrt{2}\pi b} - \frac{\xi}{\pi b} - \mathrm{i}\frac{b}{4}\right)}\,, \tag{3.2.16}$$

where again $\hbar = \pi b^2$. It is important to stress that (3.2.13) in entire in κ, in particular, the sum on the right-hand side has an infinite radius of convergence. This is a standard result in Fredholm theory and follows from the trace class property of ρ, see [4, 11, 125].

3.2.2 Integrating quasi-periodic functions

In the following sections, we frequently encounter integrals involving Faddeev's quantum dilogarithm Φ_b. To compute these integrals, we will make extensive use of Lemma 2.1 from [168], which we briefly review for future reference. Let $f : \mathcal{U} \to \mathbb{C}$ be an analytic function with $\mathcal{U} \subseteq \mathbb{C}$ open, $\mathcal{C} \subseteq \mathcal{U}$ an oriented path, and $a \in \mathbb{C} \setminus \{0\}$ a constant such that the following properties hold:

1. $\mathcal{U} = a + \mathcal{U}$,
2. $f(z)\,(f(z+a) - f(z)) \neq 0$ for all $z \in \mathcal{C}$,
3. $f(z+a)f(z-a) = f^2(z)$ for all $z \in \mathcal{U}$,

then the following equality holds

$$\int_{\mathcal{C}} f(z)\mathrm{d}z = \left(\int_{\mathcal{C}} - \int_{a+\mathcal{C}}\right) \frac{f(z)}{1 - f(z+a)/f(z)}\mathrm{d}z\,. \tag{3.2.17}$$

If we can close the contour on the right-hand side, then the integral reduces to a sum over residues. This will be the case for the integrals of interest to us.

3.2.3 The eigenfunctions in matrix models coordinates

The general construction

Off-shell eigenfunctions in the matrix model coordinates q, p were found in [6, sec. 2], following [62]. Let us define

$$\Xi^{\pm}(q;\kappa) = E^{\pm}(q) \sum_{N=0}^{\infty} (\pm\kappa)^N\, \Psi_N(q)\,, \qquad E^{\pm}(q) = \exp\left(\pm\frac{q}{\sqrt{2}b^2}\right)\mathtt{f}(q)\,, \tag{3.2.18}$$

with $\mathtt{f}$ given in (3.2.11) and $\Psi_N(q)$ is defined by the following unnormalized expectation value

$$\Psi_N(q) = \frac{1}{2^N N!}\int_{\mathbb{R}^N} \mathrm{d}^N q \prod_{k=1}^{N} \tanh\left(\frac{q-q_k}{\sqrt{2}b^2}\right) \mathtt{v}\,(q_k) \prod_{\ell=k+1}^{N} \tanh^2\left(\frac{q_k - q_\ell}{\sqrt{2}b^2}\right)\,, \tag{3.2.19}$$

where $\mathtt{v}$ is defined in (3.2.16). Note that also (3.2.18) is entire in κ, in parallel with (3.2.13). This follows again from the trace class property of ρ.

Using (3.2.18), we can write the eigenvalue equation (3.2.9) as

$$\Omega^{\pm}\left(q+\mathrm{i}\frac{\pi b^2}{\sqrt{2}}\right)+\Omega^{\pm}\left(q-\mathrm{i}\frac{\pi b^2}{\sqrt{2}}\right)=-\sqrt{2}\pi b^2\kappa\mathtt{v}(q)\Omega^{\pm}(q,\kappa)\,, \tag{3.2.20}$$

where

$$\Omega^{\pm}(q,\kappa)=\exp\left(\pm\frac{q}{\sqrt{2}b^2}\right)\sum_{N=0}^{+\infty}\Psi_N(q)\,(\pm\kappa)^N\ . \tag{3.2.21}$$

At the level of the Ψ_N, equation (3.2.20) reads

$$\Psi_N\left(q+\mathrm{i}\frac{\pi b^2}{\sqrt{2}}\right)-\Psi_N\left(q-\mathrm{i}\frac{\pi b^2}{\sqrt{2}}\right)=\mathrm{i}\sqrt{2}\pi b^2\mathtt{v}(q)\Psi_{N-1}(q)\,. \tag{3.2.22}$$

Therefore, the spectral problem in the matrix model coordinates q,p can be formulated as follows. We look for solutions of (3.2.20) which are analytic in the strip $|\mathrm{Im}(q)|<\pi b^2/\sqrt{2}$ and which belong to $L^2(\mathbb{R})$. In the off-shell eigenfunctions (3.2.21), the first requirement is already implemented because of the specific form of $\Psi_N(q)$ given in (3.2.19), as we will verify in the case $N=1$ below. As for the $L^2(\mathbb{R})$ requirement, we have

$$\Omega^{\pm}(q,\kappa)\simeq\begin{cases}\det(1\pm\kappa\rho)\exp\left(\pm\frac{q}{\sqrt{2}b^2}\right) & q\to+\infty\\ \det(1\mp\kappa\rho)\exp\left(\pm\frac{q}{\sqrt{2}b^2}\right) & q\to-\infty\end{cases} \tag{3.2.23}$$

leading to the quantization condition $\det(1+\kappa\rho)=0$ as expected and in agreement with the discussion in subsection 3.2.1. Hence, we can regard $\Xi_{\pm}$ as an analogue of the Jost functions in one-dimensional scattering theory [6, 62]: the functions $\Xi_{\pm}(q;\kappa)$ become genuine, square-integrable eigenfunctions of (3.2.9) when $\kappa=-\exp(E_n)<0$ is on-shell,

$$\Xi_{+}\left(q;-\mathrm{e}^{E_n}\right)=(-1)^n\,\Xi_{-}\left(q;-\mathrm{e}^{E_n}\right)\in L^2\left(\mathbb{R}\right)\ . \tag{3.2.24}$$

Their canonical transformation then yields the eigenfunctions $\psi(x;-\mathrm{e}^{E_n})$ of (3.2.7) in the topological string (x,y)-coordinates, as discussed in subsection 3.2.4.

The case $N=1$ and $\hbar\in\pi\mathbb{Q}_{>0}$

In this section, we make use of subsection 3.2.2 to compute $\Psi_1(q)$ explicitly, and to test its analytic properties. We have from (3.2.19)

$$\Psi_1(q)=\frac{1}{2}\int_{\mathbb{R}}\mathrm{d}p\,\tanh\left(\frac{q-p}{\sqrt{2}b^2}\right)\mathtt{v}(p)\,,\qquad\qquad\hbar=\pi b^2\,, \tag{3.2.25}$$

where $\mathtt{v}$ is given in (3.2.16). The function $\mathtt{v}$ inherits some quasi-periodicity from the quantum dilogarithms (A.2.11), namely

$$\begin{aligned}\frac{\mathtt{v}\left(p+\mathrm{i}\sqrt{2}\pi b^2k\right)}{\mathtt{v}(p)}&=\mathrm{e}^{\mathrm{i}\pi b^2k}\\ &\prod_{n=0}^{|k|-1}\left\{\frac{\left(1+\mathrm{e}^{s_k\mathrm{i}\pi b^2\left(2n+\frac{1}{2}\right)}\mathrm{e}^{\sqrt{2}p-2\xi}\right)\left(1+\mathrm{e}^{s_k\mathrm{i}\pi b^2\left(2n+\frac{1}{2}\right)}\mathrm{e}^{\sqrt{2}p+2\xi}\right)}{\left(1+\mathrm{e}^{s_k\mathrm{i}\pi b^2}\mathrm{e}^{s_k\mathrm{i}\pi b^2\left(2n+\frac{1}{2}\right)}\mathrm{e}^{\sqrt{2}p-2\xi}\right)\left(1+\mathrm{e}^{s_k\mathrm{i}\pi b^2}\mathrm{e}^{s_k\mathrm{i}\pi b^2\left(2n+\frac{1}{2}\right)}\mathrm{e}^{\sqrt{2}p+2\xi}\right)}\right\}\end{aligned} \tag{3.2.26}$$

for $k \in \mathbb{Z}$ and $s_k = \mathrm{sgn}(k)$. One can then see that the integrand of (3.2.25) is quasi-periodic in the sense of the lemma in subsection 3.2.2 when $b^2 \in \mathbb{Q}_{>0}$: we have quasi-periodicity under shifts by $\mathrm{i}\sqrt{2}\pi b^2 m = \mathrm{i}\sqrt{2}\pi n$ when $b^2 = n/m$ with n, m positive coprime integers. However, the quasi-periodic shift is trivial when $n \in 2\mathbb{N}_{>0}$, so we can only use the lemma for $b^2 = (2n+1)/m$. In that case, one gets

$$\Psi_1(q) = \frac{1}{2}\left(\int_{\mathbb{R}+\mathrm{i}0} - \int_{\mathbb{R}+\mathrm{i}\sqrt{2}\pi(2n+1)+\mathrm{i}0}\right) \mathrm{d}p \, \tanh\left(\frac{q-p}{\sqrt{2}b^2}\right) \frac{\mathtt{v}(p)}{1 - \frac{\mathtt{v}\left(p+\mathrm{i}\sqrt{2}\pi(2n+1)\right)}{\mathtt{v}(p)}}\,, \tag{3.2.27}$$

$$\frac{1}{1 - \frac{\mathtt{v}\left(p+\mathrm{i}\sqrt{2}\pi(2n+1)\right)}{\mathtt{v}(p)}} = -\,\mathrm{i}\frac{\left(1 - \mathrm{i}\,(-1)^{n+m}\,\mathrm{e}^{-m\left(\sqrt{2}p-2\xi\right)}\right)\left(1 + \mathrm{i}\,(-1)^{n+m}\,\mathrm{e}^{m\left(\sqrt{2}p+2\xi\right)}\right)}{(-1)^{n+m}\,4\mathrm{e}^{2m\xi}\sinh\left(\sqrt{2}mp\right)}\,. \tag{3.2.28}$$

The integrand has an essential singularity at complex infinity, but it doesn't contribute to the integral since $\mathtt{v}(p) \propto \exp\left(\mp p/\sqrt{2}\right)$ when $\mathrm{Re}(p) \to \pm\infty$ with $\mathrm{Im}(p)$ constant. Hence, the integration over p reduces to a sum over the residues of the integrand in (3.2.27) with $\mathrm{Im}(p) \in \left]0, \sqrt{2}\pi\,(2n+1)\right]$.

Note that $\mathtt{v}(p)$ has poles at

$$\mathtt{v}(p): \qquad \frac{p}{\sqrt{2}} = s\xi \pm \mathrm{i}\pi\left[b^2\left(k+\frac{1}{4}\right) + \left(\ell+\frac{1}{2}\right)\right] \qquad \text{poles} \qquad k, \ell \in \mathbb{N}\,, \tag{3.2.29}$$

where $s \in \{\pm 1\}$, and the upper sign is coming from the numerator and the lower sign from the denominator of $\mathtt{v}$. Note that all the poles inside the integration contour are simple, due to the observation made around equation (A.2.15). Likewise, one finds

$$\frac{1}{1 - \frac{\mathtt{v}\left(p+\mathrm{i}\sqrt{2}\pi(2n+1)\right)}{\mathtt{v}(p)}}: \qquad \begin{cases} \frac{p}{\sqrt{2}} = \pm\xi + \mathrm{i}\frac{\pi}{m}\left[k + (-1)^{n+m}\,\frac{1}{4}\right] & \text{roots} \\ \frac{p}{\sqrt{2}} = \mathrm{i}\frac{\pi}{2}\frac{k}{m} & \text{poles} \end{cases} \qquad k \in \mathbb{Z}\,. \tag{3.2.30}$$

One can check that all the poles of $\mathtt{v}$ with positive imaginary part coincide with roots of the denominator, and hence are not realized as poles of the integrand when they are inside the integration contour, where they are simple. However, we do have m poles from the hyperbolic tangent and $2\,(2n+1)\,m$ poles from the denominator at

$$p = q + \mathrm{i}\frac{\pi}{\sqrt{2}}b^2\,(2k+1)\,, \qquad k \in \{0, \cdots, m-1\}\,, \tag{3.2.31}$$

$$p = \mathrm{i}\frac{\pi}{\sqrt{2}}\frac{\ell}{m}\,, \qquad \ell \in \{1, \cdots, 2\,(2n+1)\,m\}\,, \tag{3.2.32}$$

respectively, which have residues

$$-\sqrt{2}b^2\,, \qquad \text{and} \qquad -\,\mathrm{i}\,(-1)^{n+m+\ell}\,\frac{\cosh\,(2m\xi)}{2\sqrt{2}m}\,. \tag{3.2.33}$$

This gives finally the following expression for Ψ_1

$$\boxed{\Psi_1(q) = \Psi_1^{(1)}(q) + \Psi_1^{(2)}(q)} \tag{3.2.34}$$

$$\begin{aligned}
\Psi_1^{(1)}(q) &= -\mathrm{i}\frac{\pi}{\sqrt{2}}b^2\left[1+\mathrm{i}\,(-1)^{n+m}\cosh(2m\xi)\,\mathrm{csch}\left(\sqrt{2}mq\right)\right] \\
&\qquad \sum_{k=0}^{m-1}\mathtt{v}\left(q+\mathrm{i}\frac{\pi}{\sqrt{2}}b^2\,(2k+1)\right)\,. \\
\Psi_1^{(2)}(q) &= (-1)^{n+m+1}\,\frac{\sqrt{2}\pi}{4m}\cosh(2m\xi)\sum_{\ell=-2n}^{2n+1}(-1)^{\ell}\coth\left(\frac{q}{\sqrt{2}b^2}-\mathrm{i}\frac{\pi}{2}\frac{\ell}{2n+1}\right) \\
&\qquad \sum_{k=0}^{m-1}\mathtt{v}\left(\mathrm{i}\frac{\pi}{\sqrt{2}}\left(\frac{\ell}{m}+b^2(2k+1)\right)\right)\,.
\end{aligned} \tag{3.2.35}$$

and we remind the reader that we took $\hbar/\pi = b^2 = (2n+1)/m$ with $2n+1$ and m coprime. Furthermore, it is noteworthy that these functions are real along the real line.

Let us look at the analytic properties of Ψ_1. We can then make the following considerations.

1. Let us consider $\Psi_1^{(1)}(q)$. The simple poles of $\mathtt{v}\left(q+\mathrm{i}\pi b^2\,(2k+1)\,/\sqrt{2}\right)$ with $|\mathrm{Im}(q)| \leqslant \pi b^2/\sqrt{2}$ coincide with the simple roots of the factor in square brackets, and are hence not realized.

2. There are true simple poles for $\Psi_1^{(1)}(q)$ originating from $\mathrm{csch}\left(\sqrt{2}mq\right)$ at

$$q = \mathrm{i}\frac{\pi}{\sqrt{2}}\frac{r}{m} \qquad\qquad r \in \{-(2n+1),\cdots,+(2n+1)\}\,, \tag{3.2.36}$$

   where the upper and lower bound on r come from the requirement of being inside the strip $|\mathrm{Im}(q)| \leqslant \pi b^2/\sqrt{2}$. The residue of $\Psi_1^{(1)}(q)$ at these poles is

$$(-1)^{r+n+m}\,\frac{\pi}{2}\frac{b^2}{m}\cosh(2m\xi)\sum_{\ell=0}^{m-1}\mathtt{v}\left(\mathrm{i}\frac{\pi}{\sqrt{2}}\left(\frac{r}{m}+b^2\,(2k+1)\right)\right)\,. \tag{3.2.37}$$

3. One can see that also $\Psi_1^{(2)}(q)$ has simple poles at (3.2.36), originating from the term $\ell = r$ in (3.2.35). Moreover, $\Psi_1^{(2)}(q)$ has the same residue (3.2.37) with the opposite overall sign.

Hence, we can conclude that $\Psi_1(q)$ is analytic on the strip $-\pi b^2/\sqrt{2} \leqslant \mathrm{Im}(q) \leqslant \pi b^2/\sqrt{2}$ as expected. Note however that outside the strip there are higher order poles in $\Psi_1^{(1)}$, coming from $\mathtt{v}$, which do not get cancelled by the simple roots of the factor in square brackets or

by any poles coming from the periodic part. Hence, Ψ_1 is analytic on the strip, but not entire. One can also check that our solution (3.2.34) satisfies

$$\Psi_1\left(q+\mathrm{i}\frac{\pi b^2}{\sqrt{2}}\right)-\Psi_1\left(q-\mathrm{i}\frac{\pi b^2}{\sqrt{2}}\right)=\mathrm{i}\sqrt{2}\pi b^2\mathtt{v}\left(q\right)\,, \tag{3.2.38}$$

which is the difference equation we expect for Ψ_1 from (3.2.22).

Since $\Psi_1(q)$ reduces to the first spectral trace $Z(1,\hbar)$ in the $q\to+\infty$ limit, one gets from (3.2.34)

$$\boxed{Z\left(1,\left(\frac{2n+1}{m}\right)\pi\right)=(-1)^{n+m}\,\frac{\sqrt{2}\pi}{4m}\cosh\left(2m\xi\right)\sum_{\ell=1}^{2(2n+1)m}(-1)^{\ell}\,\mathtt{v}\left(\mathrm{i}\frac{\pi}{\sqrt{2}}\frac{\ell}{m}\right)} \tag{3.2.39}$$

where $\mathtt{v}$ is defined in (3.2.16) and $2n+1$, m are coprime. This is also the result one gets when applying the residue technique above directly to the integral defining $Z(1,\hbar)$ in (3.2.15). The expression (3.2.39) is, in some sense, complementary to that of [169, eq. (3.55)], which holds for $\mathrm{Im}(b^2)>0$.

3.2.4 The eigenfunctions in outer topological string coordinates

The general construction and symmetric structures

One motivation for considering the outer topological string (x,y)-coordinates is that they establish a direct connection with the open topological string in the presence of a D-brane on the external leg of the toric diagram, as we will discuss in section 3.3. Consequently, in these coordinates, we obtain a particularly explicit framework for computing these eigenfunctions using topological string partition functions.[2]

The eigenfunctions $\psi(x,\kappa)$ in the topological string (x,y)-coordinates and the eigenfunctions $\Xi(q,\kappa)$ in the matrix model (q,p)-coordinates are then related by a canonical transformation. More precisely,

$$\psi^{\pm}(x,\kappa)=\int_{\mathbb{R}}\mathrm{d}q\,U\left(x,q\right)\Xi^{\pm}(q,\kappa)\,, \tag{3.2.40}$$

where from [6]

$$U\left(x,q\right)=\frac{2^{1/4}}{\sqrt{2\pi\hbar}}\exp\left(\frac{\mathrm{i}}{\hbar}\left(\frac{x^2}{2}-\sqrt{2}\left(x-\xi\right)q+\frac{q^2}{2}\right)\right)\,. \tag{3.2.41}$$

Hence, if we take the eigenfunctions (3.2.18), the corresponding eigenfunctions in topological string coordinates are

$$\psi^{\pm}(x,\kappa)=\sum_{N\geqslant 0}(\pm\kappa)^N\psi_N^{\pm}(x)\,,\qquad\qquad \psi_N^{\pm}(x)=\int_{\mathbb{R}}\mathrm{d}q\,U\left(x,q\right)E^{\pm}(q)\Psi_N(q)\,. \tag{3.2.42}$$

[2]The matrix model coordinates seem more natural to describe a brane on the internal leg of the toric diagram [82, 83].

Note that this integral is only well-defined when $E^{\pm}(q)\Psi_N(q)$ is integrable. However, we have

$$E^{+}(q)\Psi_N(q) \simeq \begin{cases} \exp\left[\left(\frac{b^2-2}{2\sqrt{2}b^2}\right)(-q)\right]\exp\left(-\mathrm{i}\frac{2\sqrt{2}}{\pi}\frac{\xi q}{b^2}\right) & q\to+\infty \\ \exp\left[\left(\frac{b^2+2}{2\sqrt{2}b^2}\right)q\right] & q\to-\infty \end{cases}$$
$$E^{-}(q)\Psi_N(q) \simeq \begin{cases} \exp\left[\left(\frac{b^2+2}{2\sqrt{2}b^2}\right)(-q)\right]\exp\left(-\mathrm{i}\frac{2\sqrt{2}}{\pi}\frac{\xi q}{b^2}\right) & q\to+\infty \\ \exp\left[\left(\frac{b^2-2}{2\sqrt{2}b^2}\right)q\right] & q\to-\infty \end{cases} . \tag{3.2.43}$$

Hence, the unitary transformation (3.2.40) is well-defined only when $b^2 > 2$, as also noted in [6]. This raises the question of how to make sense of the canonical transformation (3.2.42) when $\hbar = b^2\pi \leqslant 2\pi$.[3] Our strategy to address this issue is the following. In this region, we will momentarily set aside convergence issues and directly apply the Lemma from subsection 3.2.2. This approach gives a finite result for any value of b^2, even if the starting point was problematic for $b^2 \leqslant 2$. The case $\xi = 0$, $b^2 = 2$ was analysed in [6, p. 15] using the same strategy.

Let us first make some simple observation regarding the relation between ψ^{+} and ψ^{-}. Using the parity properties of the quantum dilogarithm (A.2.10) and the expression (3.2.19), we have

$$\begin{aligned} E^{\pm}(-q)\Psi_N(-q) &= \exp\left(\mp\frac{\sqrt{2}\pi}{\hbar}q\right)\exp\left(\frac{\mathrm{i}}{\hbar}2\sqrt{2}\xi q\right)E^{\pm}(q)\,(-1)^N\,\Psi_N(q) \\ &= \exp\left(\frac{\mathrm{i}}{\hbar}2\sqrt{2}\xi q\right)E^{\mp}(q)\,(-1)^N\,\Psi_N(q)\,, \\ \psi_N^{\pm}(-x) &= \exp\left(\frac{\mathrm{i}}{\hbar}\frac{\pi^2}{2}\right)\exp\left(\mp\frac{\pi x}{\hbar}\right)(-1)^N\,\psi_N^{\pm}(x\mp\mathrm{i}\pi)\,, \\ &= (-1)^N\,\psi_N^{\mp}(x)\,. \end{aligned} \tag{3.2.44}$$

The eigenfunctions behave then as

$$\begin{aligned} \Xi^{\pm}(-q,\kappa) &= \exp\left(\mp\frac{\sqrt{2}\pi q}{\hbar}\right)\exp\left(\mathrm{i}\frac{2\sqrt{2}}{\hbar}\xi q\right)\Xi^{\pm}(q,-\kappa) \\ &= \exp\left(\mathrm{i}\frac{2\sqrt{2}}{\hbar}\xi q\right)\Xi^{\mp}(q,\kappa) \\ \psi^{\pm}(-x,\kappa) &= \exp\left(\frac{\mathrm{i}}{\hbar}\frac{\pi^2}{2}\right)\exp\left(\mp\frac{\pi x}{\hbar}\right)\psi^{\pm}(x\mp\mathrm{i}\pi,-\kappa) \\ &= \psi^{\mp}(x,\kappa)\,, \end{aligned} \tag{3.2.45}$$

[3] Curiously, if it were not for the q^2 term in the canonical transformation, the $N = 0$ version of this transform would be very close to the "integral analogue of the ${}_1\psi_1$-summation formula of Ramanujan" as given in [170, eq. (51)], which can be explicitly computed in closed form using the method of residues.

and we see in particular that the on-shell eigenfunctions in the (x, y)-coordinates have a well-defined parity while there is a local phase for generic ξ in the (q, p)-coordinates. Because of the simple relation between the two eigenfunctions, we will often work with

$$\psi_N(x) \equiv \psi_N^+(x)\,, \qquad\qquad \psi(x) \equiv \psi^+(x)\,, \tag{3.2.46}$$

and $\psi_N^-(x)$ and $\psi^-(x)$ can then simply be found from (3.2.44) and (3.2.45) respectively.

We are now going to study (3.2.40) and (3.2.42) in detail. First, it was conjectured in [6, 7] that this integral can be written as the sum of two contributions, which are in a one-to-one correspondence with the two saddles of the integrand on the right-hand side of (3.2.42). Second, in [1], a special scaling limit of (3.2.42) was analysed in detail, and it was found that the two saddles are related in a simple way. By combining these two observations, we can propose the following ansatz for the expression of the eigenfunctions in the topological string coordinates:

$$\psi^\pm(x,\kappa) = \omega^\pm(x,\kappa) + \exp\left(\frac{\mathrm{i}}{\hbar}\frac{\pi^2}{2} \pm \frac{\pi x}{\hbar}\right)\omega^\pm(-x \mp \mathrm{i}\pi, -\kappa)\,, \tag{3.2.47}$$

for some functions $\omega^\pm(x,\kappa)$. Our result reads then

$$\boxed{\psi(x,\kappa) = \omega(x,\kappa) + \exp\left(\frac{\mathrm{i}}{\hbar}\frac{\pi^2}{2} + \frac{\pi x}{\hbar}\right)\omega(-x - \mathrm{i}\pi, -\kappa)\,,} \tag{3.2.48}$$

for some function $\omega(x,\kappa)$. It is important to note that the parity relation for $\psi^\pm(x,\kappa)$ in (3.2.45) is the same as the one relating the two terms in (3.2.48), ensuring the self-consistency of our proposal (3.2.48). At the level of components in the κ expansion (3.2.18), equation (3.2.47) becomes

$$\psi_N^\pm(x) = \omega_N^\pm(x) + (-1)^N \exp\left(\frac{\mathrm{i}}{\hbar}\frac{\pi^2}{2} \pm \frac{\pi x}{\hbar}\right)\omega_N^\pm(-x \mp \mathrm{i}\pi)\,, \tag{3.2.49}$$

for some functions $\omega_N^\pm(x)$ where $\omega_N^-(x) = (-1)^N\omega_N^+(-x)$. Equation (3.2.49) reads equivalently

$$\boxed{\psi_N(x) = \omega_N(x) + (-1)^N \exp\left(\frac{\mathrm{i}}{\hbar}\frac{\pi^2}{2} + \frac{\pi x}{\hbar}\right)\omega_N(-x - \mathrm{i}\pi)\,,} \tag{3.2.50}$$

for some function $\omega_N(x)$.

We will test this proposal in several ways and, we also give explicit expressions for ω by using topological string theory, see subsection 3.3.3. As we discuss in subsection A.1.2, the case $\xi = 0$, $\hbar = 2\pi$ analysed in [6, 7] is special and the above structure is hidden.

The case $N = 0$ and $\hbar \in \pi\mathbb{Q}_{>0}$

In this subsection, we compute $\psi_N = \psi_N^+$ for $N = 0$ and $\hbar \in \pi\mathbb{Q}_{>0}$,[4] which serves two goals. Firstly, it will provide some evidence that we can expect the off-shell eigenfunctions

[4]The result for ψ_N^- follows immediately from (3.2.44). Hence, we adopt the notation (3.2.46).

of the quantum mirror curve to be entire in x,[5] and secondly, we will use it as an analytical check of our conjecture (3.2.50). We are interested in

$$\psi_0(x) = \int_{\mathbb{R}} \mathrm{d}q\, U(x,q)\, E(q)\,, \qquad\qquad E(q) = E^+(q)\,. \tag{3.2.51}$$

It is important to note that the integrand in (3.2.51) is a meromorphic function of q, which inherits some quasi-periodicity from the quantum dilogarithms (A.2.12),

$$\begin{aligned}\frac{U\big(x,q+\mathrm{i}\sqrt{2}\pi k b^2\big)E\big(q+\mathrm{i}\sqrt{2}\pi k b^2\big)}{U(x,q)E(q)} &= \mathrm{e}^{-\mathrm{i}\pi k^2 b^2}\mathrm{e}^{-2k\xi}\mathrm{e}^{2kx}\mathrm{e}^{-\sqrt{2}kq}\mathrm{e}^{\mathrm{i}\pi k}\mathrm{e}^{\mathrm{i}\frac{\pi}{2}kb^2} \\ &\quad \prod_{\ell=0}^{|k|-1}\left(\frac{1+\mathrm{e}^{\mathrm{i}\frac{\pi}{2}\mathrm{sgn}(k)b^2(4\ell+1)}\mathrm{e}^{\mathrm{sgn}(k)2\xi}\mathrm{e}^{\sqrt{2}q}}{1+\mathrm{e}^{\mathrm{i}\frac{\pi}{2}\mathrm{sgn}(k)b^2(4\ell+3)}\mathrm{e}^{-\mathrm{sgn}(k)2\xi}\mathrm{e}^{\sqrt{2}q}}\right)\end{aligned} \tag{3.2.52}$$

where $\hbar = \pi b^2$ and $k \in \mathbb{Z}$. When we take

$$b^2 = \frac{n}{m} \in \mathbb{Q}_{>0}\,, \qquad\qquad n,m \in \mathbb{N}_{>0} \text{ and coprime}\,, \qquad\qquad \text{and } k = \pm m\,, \tag{3.2.53}$$

then this simplifies further to

$$\begin{aligned}&\frac{U\big(x,q\pm\mathrm{i}\sqrt{2}\pi n\big)E\big(q\pm\mathrm{i}\sqrt{2}\pi n\big)}{U(x,q)E(q)} = \\ &\qquad (-1)^{(n+1)m}\,\mathrm{e}^{\pm\mathrm{i}\frac{\pi}{2}n}\mathrm{e}^{\mp 2m\xi}\mathrm{e}^{\pm 2mx}\mathrm{e}^{\mp\sqrt{2}mq}\left(\frac{1-(-1)^m\,\mathrm{e}^{\mathrm{i}\frac{\pi}{2}n}\mathrm{e}^{2m\xi}\mathrm{e}^{\sqrt{2}mq}}{1-(-1)^m\,\mathrm{e}^{-\mathrm{i}\frac{\pi}{2}n}\mathrm{e}^{-2m\xi}\mathrm{e}^{\sqrt{2}mq}}\right)^{\pm}.\end{aligned} \tag{3.2.54}$$

Hence we find that the integrand defining ψ_0 in (3.2.51) is quasi-periodic in the sense of the quasi-periodic integrand lemma of subsection 3.2.2. Following the lemma, we can rewrite (3.2.51) as

$$\begin{aligned}\psi_0(x) = \left(\int_{\mathbb{R}+\mathrm{i}0} - \int_{\mathbb{R}+\mathrm{i}\sqrt{2}\pi n+\mathrm{i}0}\right)\mathrm{d}q \\ \frac{U(x,q)E(q)}{1-(-1)^{(n+1)m}\,\mathrm{e}^{\mathrm{i}\frac{\pi}{2}n}\mathrm{e}^{-2m\xi}\mathrm{e}^{2mx}\mathrm{e}^{-\sqrt{2}mq}\left(\frac{1-(-1)^m\mathrm{e}^{\mathrm{i}\frac{\pi}{2}n}\mathrm{e}^{2m\xi}\mathrm{e}^{\sqrt{2}mq}}{1-(-1)^m\mathrm{e}^{-\mathrm{i}\frac{\pi}{2}n}\mathrm{e}^{-2m\xi}\mathrm{e}^{\sqrt{2}mq}}\right)}\,.\end{aligned} \tag{3.2.55}$$

The integrand above is a meromorphic function of q with a finite number of poles inside the integration contour and an essential singularity at infinity. Note furthermore from (3.2.43) that the integrand decays exponentially inside the whole contour for $\mathrm{Re}(q) \to \pm\infty$. Hence, we can close the contour at complex infinity and the integral reduces to a sum over the residues of the poles.

[5] The observation that the eigenfunctions are entire was also made in [6], based on a computation of ψ_N for several $N \in \mathbb{N}$ for $\xi = 0$ and $\hbar = 2\pi$ [6, eqs. (2.95), (2.96)]. See also [7, eqs. (4.20), (4.21)] for the case $\xi = 0$, $\hbar = 4\pi$ and $\hbar = 2\pi/3$.

To simplify the discussion, we will assume that either $\xi \neq 0$ or $n \in (2\mathbb{N}+1)$.[6] There are potential poles of the integrand coming from E at (A.2.7)

$$q = \pm\sqrt{2}\xi \pm \mathrm{i}\sqrt{2}\pi\left(\left(k+\frac{1}{2}\right)+\frac{n}{m}\left(\ell+\frac{1}{4}\right)\right), \qquad k,\ell \in \mathbb{N}, \tag{3.2.56}$$

and all the poles inside the integration contour in (3.2.55) are simple as a direct consequence of the observation made around (A.2.15). However, for each such pole of E there is a coinciding simple pole for the denominator in (3.2.55), and hence the integrand in (3.2.55) is analytic around these points. The only poles inside the integration contour are hence coming from the roots of the denominator and are located at

$$\begin{aligned}\sqrt{2}mq_{\pm,k}(x) = \ln\Bigg[&(-1)^m\,\mathrm{e}^{\mathrm{i}\frac{\pi}{2}n}\left(\frac{\mathrm{e}^{2m\xi}}{2}\right)\mathrm{e}^{mx}\Bigg((-1)^{n(m+1)}\,\mathrm{e}^{mx}+\mathrm{e}^{-mx}\\ &\pm \mathrm{sgn}\Big(\arg\Big(x+\mathrm{i}\frac{\pi}{2}\Big)\Big)\sqrt{\Big((-1)^{n(m+1)}\,\mathrm{e}^{mx}+\mathrm{e}^{-mx}\Big)^2-(-1)^{nm}\,4\mathrm{e}^{-4m\xi}}\Bigg)\Bigg]+\mathrm{i}2\pi k\,,\end{aligned} \tag{3.2.57}$$

where $k \in \mathbb{Z}$ should be such that $0 < \mathrm{Im}(q_{\pm,k}(x)) \leqslant \sqrt{2}\pi n$ and we use the convention $\mathrm{sgn}(0) = -1$. It is important for later to note that these points are by construction a solution to

$$\begin{aligned}U(x,q_{\pm,k}(x))\,E(q_{\pm,k}(x)) &= U\Big(x,q_{\pm,k}(x)+\mathrm{i}\sqrt{2}\pi n\Big)\,E\Big(q_{\pm,k}(x)+\mathrm{i}\sqrt{2}\pi n\Big)\\ &= U(x,q_{\pm,k+nm}(x))E(q_{\pm,k+nm}(x))\,.\end{aligned} \tag{3.2.58}$$

The residues corresponding with (3.2.57) and coming from the denominator are given by

$$\begin{aligned}\mathrm{Res}_{\pm}(x) = &\frac{1}{2\sqrt{2}m}\\ &\pm\frac{\mathrm{sgn}\big(\arg\big(x+\mathrm{i}\frac{\pi}{2}\big)\big)}{2\sqrt{2}m}\left(\frac{(-1)^{n(m+1)}\,\mathrm{e}^{mx}-\mathrm{e}^{-mx}}{\sqrt{\Big((-1)^{n(m+1)}\,\mathrm{e}^{mx}+\mathrm{e}^{-mx}\Big)^2-(-1)^{nm}\,4\mathrm{e}^{-4m\xi}}}\right).\end{aligned} \tag{3.2.59}$$

It should be noted that the particular choice of branches in (3.2.57) and (3.2.59) is to some extent purely conventional. However, we will relate q_+ and q_- in (3.2.63), and for this purpose, it is important to use the particular choice made in (3.2.57) and (3.2.59), or something equivalent. In the end, we find that (3.2.51) is given by[7]

$$\psi_0(x) = \omega_{0,+}(x) + \omega_{0,-}(x), \tag{3.2.60}$$

[6] The derivation for $\xi = 0$ and $n \in 2\mathbb{N}_{>0}$ is done analogously, yielding the same result as obtained by taking the $\xi \to 0$ limit for $n \in 2\mathbb{N}_{>0}$ on the solution (3.2.60). This case agrees with the results of [6, 7], see also subsection A.1.2.

[7] The subscript $\pm$ in $\omega_\pm$ is logically independent of the superscript $\pm$ in $\omega^\pm$ that appeared in (3.2.47).

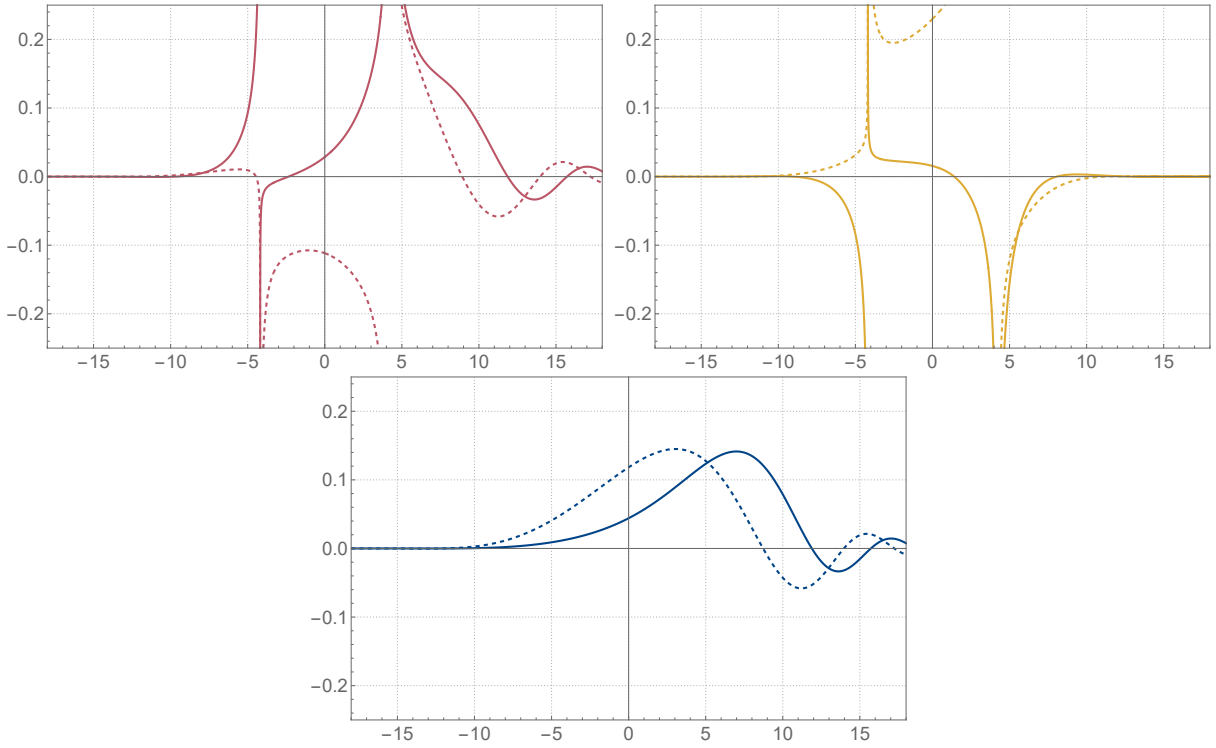

Figure 3.1. From top left to bottom: the first term $\omega_{0,+}$ on the right-hand side of (3.2.60), the second term $\omega_{0,-}$, and their sum ψ_0 for $\xi = -7/4$ and $\hbar = 4\pi$. The solid and dashed lines correspond to the real and imaginary parts, respectively.

$$\omega_{0,\pm}(x) = \mathrm{i}2\pi \mathrm{Res}_{\pm}(x) \sum_{k=0}^{nm-1} U(x, q_{\pm,k}(x)) E(q_{\pm,k}(x)) \,, \tag{3.2.61}$$

where $\hbar = \pi b^2 = \pi n/m$ with $n, m \in \mathbb{N}_{>0}$ and coprime. It is noteworthy that $\omega_{0,\pm}$ and hence ψ_0 can be expressed entirely in terms of elementary functions and the classical dilogarithm Li_2 by using (A.2.13). See figure 3.1 for some plots of the functions defined above.

Let us look at the analytic properties of $\omega_{0,\pm}$ and ψ_0. Note first that $\omega_{0,\pm}$ and ψ_0 are analytic along the logarithmic branch cut of $q_{\pm,k}$, since crossing the branch simply amounts to shifting the range of k in the sum in (3.2.60), which doesn't affect $\omega_{0,\pm}$ or ψ_0 by (3.2.58). Note furthermore that ψ_0 is analytic along the square root branches of $q_{\pm,k}$ and $\mathrm{Res}_{\pm}$ as well, since crossing the branches simply interchanges the $\pm$-signs. The only remaining potential singularities are the branch points of the logarithm in $q_{\pm,k}$ and the square roots, and the poles of $E\left(q_{\pm,k}\left(x\right)\right)$. The logarithmic branch point of $q_{\pm,k}$ is never realized, and the square root branch points in $\mathrm{Res}_{\pm}\left(x\right)$ cancel between the $\omega_{0,\pm}$. Furthermore, the poles of E are never reached by $q_{\pm,k}$ when either $\xi \neq 0$ or $n \in (2\mathbb{N}+1)$ as we assumed.[8] Hence, we conclude that $\psi_0\left(x\right)$ is an entire function of x, even though neither $\omega_{0,+}$ nor $\omega_{0,-}$ is entire, see figure 3.1. The same structure will reappear when we

[8]Though the $\xi \to 0$ limit for even n behaves well, see footnote 6.

express the eigenfunctions in terms of the grand potential of topological strings on local $\mathbb{F}_0$ in (3.3.35).

One can furthermore check that ψ_0 solves the difference equation associated with the quantized mirror curve at $\kappa = 0$, that is

$$\psi_0(x + \mathrm{i}\hbar) + \psi_0(x - \mathrm{i}\hbar) + 2\mathrm{e}^{2\xi}\cosh(x)\psi_0(x) = 0\,. \tag{3.2.62}$$

However, ψ_0 is not an eigenfunction of the quantized mirror curve, since it is not square integrable in the strip (3.2.5).

Let us end with the observation that (3.2.60) is a well-defined, entire function of x that solves (3.2.62) for all $b^2 = n/m \in \mathbb{Q}_{>0}$, also $b^2 \leqslant 2$, even though the original integral transform as given in (3.2.51) is only well-defined for $b^2 > 2$.

Relating the two terms for $N = 0$ and $\hbar \in \pi\mathbb{Q}_{>0}$

We now want to show that (3.2.60) can be written as in (3.2.50) for $N = 0$. For all $x \in \mathbb{C}$, $\xi \in \mathbb{R}$, coprime $n, m \in \mathbb{N}_{>0}$, and $k \in \mathbb{Z}$,[9] one finds the following relation for (3.2.57) and (3.2.59)

$$q_{\pm,k}(x) = -q_{\mp,-k-\ell}(-x - \mathrm{i}\pi)\,, \qquad \mathrm{Res}_{\pm}(x) = \mathrm{Res}_{\mp}(-x - \mathrm{i}\pi)\,, \tag{3.2.63}$$

where $\ell \in \{-1, 0, +1\}$ should be chosen appropriately according to the branches. It should be noted that this symmetry is only visible upon the specific choice of the branch structure we made in (3.2.57) and (3.2.59). One can use the parity structure for q in (3.2.44) to rewrite

$$\begin{aligned} U(x, q_{\pm,k}(x))E\left(q_{\pm,k}(x)\right) &= U(x, -q_{\mp,-k-\ell}(-x - \mathrm{i}\pi))E(-q_{\mp,-k-\ell}(-x - \mathrm{i}\pi)) \\ &= \exp\left(\frac{\mathrm{i}}{\hbar}\frac{\pi^2}{2} + \frac{\pi x}{\hbar}\right)U(-x - \mathrm{i}\pi, q_{\mp,-k-\ell}(-x - \mathrm{i}\pi))E(q_{\mp,-k-\ell}(-x - \mathrm{i}\pi))\,. \end{aligned} \tag{3.2.64}$$

Note that at the level of $\omega_{0,\mp}$ we can replace $q_{\mp,-k-\ell}$ by $q_{\mp,k}$ because of (3.2.58). Hence, we find that (3.2.60) can be written as

$$\begin{aligned} \psi_0(x) &= \omega_{0,+}(x) + \exp\left(\frac{\mathrm{i}}{\hbar}\frac{\pi^2}{2} + \frac{\pi x}{\hbar}\right)\omega_{0,+}(-x - \mathrm{i}\pi) \\ &= \exp\left(\frac{\mathrm{i}}{\hbar}\frac{\pi^2}{2} + \frac{\pi x}{\hbar}\right)\omega_{0,-}(-x - \mathrm{i}\pi) + \omega_{0,-}(x)\,, \end{aligned} \tag{3.2.65}$$

which is precisely the conjectured structure in (3.2.50), here for $N = 0$ and $\hbar \in \pi\mathbb{Q}_{>0}$.

[9] The branches in (3.2.57) have to be chosen differently when $x = -\mathrm{i}\pi/2$.

3.2.5 The 't Hooft expansion

An important way to test the conjectured structure in (3.2.50) is by analysing $\psi_N^{\pm}(x)$ (3.2.42) in a 't Hooft limit. This limit was studied in detail in [6, sec. 3] for the case $\xi = 0$, see also [171]. We will closely follow their approach and use it to argue for the structure in (3.2.50). The 't Hooft limit is defined by taking

$$\hbar, N, \xi, |q|, |x| \to +\infty\,, \tag{3.2.66}$$

while keeping the following ratio's constant,

$$\lambda = \frac{N}{\hbar}\,, \qquad \xi_D = \frac{2\pi}{\hbar}\xi\,, \qquad q_D = \frac{2\pi}{\hbar}q\,, \qquad x_D = \frac{2\pi}{\hbar}x\ . \tag{3.2.67}$$

Preparation

Later on, we will need the solutions of the classical mirror curve (3.2.1) in the matrix model coordinates q, p (3.2.8) and the topological string coordinates x, y, which read

$$\begin{aligned} \mathrm{e}^{p_\sigma(q,\xi,\kappa)/\sqrt{2}} &= P_\sigma\left(\mathrm{e}^{q/\sqrt{2}}, \xi, \kappa\right), \\ \mathrm{e}^{y_\sigma(x,\xi,\kappa)} &= Y_\sigma\left(\mathrm{e}^{x}, \xi, \kappa\right), \end{aligned} \tag{3.2.68}$$

where $\sigma = \pm 1$ and

$$\begin{aligned} P_\pm(Q,\xi,\kappa) &= \frac{-\mathrm{e}^{-\xi}\kappa \pm \sqrt{\left(\mathrm{e}^{-\xi}\kappa\right)^2 - 4\left(\mathrm{e}^{\xi}Q + \mathrm{e}^{-\xi}Q^{-1}\right)\left(\mathrm{e}^{-\xi}Q + \mathrm{e}^{\xi}Q^{-1}\right)}}{2\mathrm{e}^{\xi}\left(\mathrm{e}^{\xi}Q + \mathrm{e}^{-\xi}Q^{-1}\right)}\,, \\ Y_\pm(X,\xi,\kappa) &= -\left(\frac{\mathrm{e}^{2\xi}}{2}\left(X + \frac{1}{X}\right) + \frac{\kappa}{2}\right) \pm \sqrt{\left(\frac{\mathrm{e}^{2\xi}}{2}\left(X + \frac{1}{X}\right) + \frac{\kappa}{2}\right)^2 - 1}\,. \end{aligned} \tag{3.2.69}$$

Let us also introduce the convenient shorthand notation

$$p_\pm(q_D) = p_\pm(q_D, \xi_D, \kappa_D)\,, \qquad y_\pm(x_D) = y_\pm(x_D, \xi_D, \kappa_D)\,. \tag{3.2.70}$$

As we discuss below (3.2.74), there is an implicit definition of κ_D in terms of λ and ξ_D.

In matrix model coordinates

Let us now consider 't Hooft limit as defined in (3.2.66) and (3.2.67) on the matrix model

$$E(q)\Psi_N(q)/Z(N,\hbar)\,, \tag{3.2.71}$$

where the relevant functions are defined in equations (3.2.11), (3.2.15), (3.2.18), and below. One finds the asymptotic expansion [65]

$$\begin{aligned} E(q) &\simeq \exp\left(\frac{\mathrm{i}}{g_s}\mathcal{E}_0(q_D) + \mathcal{E}_1(q_D) + \mathcal{O}(g_s)\right), \\ \frac{E(q)\Psi_N(q)}{Z(N)} &\simeq \exp\left(\frac{\mathrm{i}}{g_s}\mathcal{T}_0(q_D) + \mathcal{T}_1(q_D) + \mathcal{O}(g_s)\right) \end{aligned} \tag{3.2.72}$$

The precise form of the functions $\mathcal{T}_1$ and $\mathcal{E}_1$ is not essential for our discussion. Thus, we focus on the leading-order terms. Using the quasi-classical expansion of the quantum dilogarithm (A.2.18) gives

$$\mathcal{E}_0(q_D) = \mathrm{i}\pi\xi_D - \mathrm{i}\pi\frac{q_D}{\sqrt{2}} - 2\mathrm{Li}_2\left(-\mathrm{i}\mathrm{e}^{q_D/\sqrt{2}}\mathrm{e}^{-\xi_D}\right) + 2\mathrm{Li}_2\left(\mathrm{i}\mathrm{e}^{q_D/\sqrt{2}}\mathrm{e}^{\xi_D}\right) . \tag{3.2.73}$$

The computation of $\mathcal{T}_0$ is more involved and requires various matrix model techniques developed in [6, sec. 3.2] and [65, 171]. Following [6, sec. 3.2] we get

$$\mathcal{T}_0(q_D) = \int^{q_D} p_\sigma(q'_D)\mathrm{d}q'_D + \mathrm{i}\pi\xi_D \tag{3.2.74}$$

where p_σ is defined through (3.2.68) and (3.2.70). The correct sign $\sigma = \sigma(q_D) \in \{\pm\}$ depends on the region of the complex q_D-plane. However, we will not need it for what follows. In (3.2.74), we implicitly use the matrix model relation between the 't Hooft coupling λ and κ_D. This relation is obtained as follows:

- There is an explicit relation between the 't Hooft coupling λ and the endpoints of the eigenvalue density, denoted by $a^\pm$. For our matrix model, this relation is given in [65, eqs. (2.76)–(2.80)].
- The endpoints of the cuts, $a^\pm$, are related to the mirror curve parameters ξ_D and κ_D as

$$a^{\pm 2} = a^{\pm 2}(\xi_D, \kappa_D) = \frac{\mathrm{e}^{-2\xi_D}\kappa_D^2}{8} - \cosh(2\xi_D) \pm \sqrt{\left(\frac{\mathrm{e}^{-2\xi_D}\kappa_D^2}{8} - \cosh(2\xi_D)\right)^2 - 1} . \tag{3.2.75}$$

  These correspond to the branch points of the mirror curve in the (p, q) coordinates.

By combining the above points, we obtain an explicit relation between κ_D, ξ_D, and λ, leading to (3.2.74). We refer to [65] for more details.

In outer topological string coordinates

We are interested in the 't Hooft limit of (3.2.42). By recalling the conventions (3.2.46) we have

$$\frac{\psi_N(x)}{Z(N)} = \int_{\mathbb{R}} \mathrm{d}q\, U(x,q)\frac{E(q)\Psi_N(q)}{Z(N)} = \int_{\mathbb{R}} \mathrm{d}q_D\, \frac{U^D(x_D, q_D)}{\sqrt{2\pi g_s}}\frac{E^D(q_D)\Psi_N^D(q_D)}{Z(N)} , \tag{3.2.76}$$

where we defined for future convenience

$$E^D(q_D) = E\left(\frac{2\pi}{g_s}q_D\right) , \qquad \Psi_N^D(q_D) = \Psi_N\left(\frac{2\pi}{g_s}q_D\right) , \tag{3.2.77}$$

$$U^D(x_D, q_D) = \sqrt{\frac{(2\pi)^3}{g_s}}U\left(\frac{2\pi}{g_s}x_D, \frac{2\pi}{g_s}q_D\right) . \tag{3.2.78}$$

The 't Hooft limit of (3.2.76) becomes then a simple application of the stationary phase method. The essential ingredient is the saddle point equation,

$$\partial_{q_D} F\left(x_D, q_D\right) + \mathcal{T}_0'\left(q_D\right) = -\sqrt{2}(x_D - \xi_D) + q_D + p_\sigma(q_D) = 0\,, \tag{3.2.79}$$

where we defined from (3.2.41)

$$F\left(x_D, q_D\right) = \frac{x_D^2}{2} - \sqrt{2}\left(x_D - \xi_D\right) q_D + \frac{q_D^2}{2}\,. \tag{3.2.80}$$

This should then be solved to find $q^D(x_D)$. Note that the saddle point equation is precisely the transformation of x in the canonical transformation (3.2.8), which is a direct consequence of the construction of U (3.2.41) [6, sec. 2.5] and the form of $\mathcal{T}_0$ in (3.2.74). Combining this with the transformation of y in (3.2.8) and using the fact that p_σ and y_σ in (3.2.68) are both solutions of the classical mirror curve (3.2.1) yields,[10]

$$q_\pm^D\left(x_D\right) = \frac{\sqrt{2}}{2}\left(x_D - y_\pm\left(x_D\right)\right)\,, \qquad |\mathrm{Im}(x_D)| < 2\pi\,,\ \xi_D \in \mathbb{R}\,, \tag{3.2.81}$$

where $y_\pm$ is given in (3.2.68) and (3.2.70). Note that the restriction on x_D is the usual domain restriction of the eigenfunctions (3.2.5) in the dual variables. Observe that $q_\pm^D$ has a simple parity symmetry,

$$q_\pm^D(x_D) = -q_\mp^D(-x_D)\,, \tag{3.2.82}$$

which will be important soon.

As a result of the stationary phase method one finds [172, ch. 5]

$$\frac{\psi_N\left(x\right)}{Z\left(N\right)} \simeq \sum_{\sigma\in\{\pm\}} \left(\frac{U^D\left(x_D, q_\sigma^D(x_D)\right)}{\sqrt{-\mathrm{i}\left(\mathcal{T}_0 + F\right)''\left(q_\sigma^D(x_D)\right)}} \frac{E^D(q_\sigma^D(x_D))\Psi_N^D(q_\sigma^D(x_D))}{Z\left(N\right)} + \mathcal{O}\left(g_s\right) \right)\,. \tag{3.2.83}$$

It should be noted that we didn't make the 't Hooft limit expansion in g_s explicit, and the functions involved are still complicated functions of g_s. However, the form given above is the most convenient one to understand the relation between the saddles.[11] We found in (3.2.82) that $q_\pm^D$ has a simple parity symmetry and one can see that the denominator has similarly

$$\left(\mathcal{T}_0 + F\right)''\left(q_\pm^D(x_D)\right) = p_\pm^{D\prime}(q_\pm^D(x_D)) + 1 = \frac{\sqrt{2}}{q_\pm^{D\prime}(x_D)} = \left(\mathcal{T}_0 + F\right)''\left(q_\mp^D(-x_D)\right)\,, \tag{3.2.84}$$

where the second equality follows from the x_D derivative of the saddle point equation (3.2.79). We can then use the parity symmetries of the functions involved to get rid of the

[10] Up to an integer multiple of $\mathrm{i}\sqrt{2}\pi$ if we are outside the strip $|\mathrm{Im}(x_D)| < 2\pi$.

[11] See [6, sec. 3.3, app. A] for an explicit construction of the subleading order in the 't Hooft limit.

minus sign in front of the $q_{\mp}^{D}(-x_D)$ in (3.2.82) to find that the saddles are related by

$$\frac{U^D\left(x_D, q_{\pm}^D(x_D)\right)}{\sqrt{-\mathrm{i}\left(\mathcal{T}_0+F\right)''\left(q_{\pm}^D(x_D)\right)}}\frac{E^D(q_{\pm}^D(x_D))\Psi_N^D(q_{\pm}^D(x_D))}{Z\left(N\right)} = \\ (-1)^N\,\mathrm{e}^{\mathrm{i}\frac{g_s}{8}}\mathrm{e}^{\frac{x_D}{2}}\frac{U^D\left(-x_D-\mathrm{i}\frac{g_s}{2}, q_{\mp}^D(-x_D)\right)}{\sqrt{-\mathrm{i}\left(\mathcal{T}_0+F\right)''\left(q_{\mp}^D(-x_D)\right)}}\frac{E^D(q_{\mp}^D(-x_D))\Psi_N^D(q_{\mp}^D(-x_D))}{Z\left(N\right)}\,. \quad (3.2.85)$$

It is then again a consequence of the saddle point equation (3.2.79) that we can shift the argument of $q_{\mp}(-x_D)$ as well to get

$$\frac{U^D\left(x_D, q_{\pm}^D(x_D)\right)}{\sqrt{-\mathrm{i}\left(\mathcal{T}_0+F\right)''\left(q_{\pm}^D(x_D)\right)}}\frac{E^D(q_{\pm}^D(x_D))\Psi_N^D(q_{\pm}^D(x_D))}{Z\left(N\right)} = (-1)^N\,\mathrm{e}^{\mathrm{i}\frac{g_s}{8}}\mathrm{e}^{\frac{x_D}{2}} \\ \frac{U^D\left(-x_D-\mathrm{i}\frac{g_s}{2}, q_{\mp}^D(-x_D-\mathrm{i}\frac{g_s}{2})\right)}{\sqrt{-\mathrm{i}\left(\mathcal{T}_0+F\right)''\left(q_{\mp}^D(-x_D-\mathrm{i}\frac{g_s}{2})\right)}}\frac{E^D(q_{\mp}^D(-x_D-\mathrm{i}\frac{g_s}{2}))\Psi_N^D(q_{\mp}^D(-x_D-\mathrm{i}\frac{g_s}{2}))}{Z\left(N\right)}+\mathcal{O}(g_s)\,, \quad (3.2.86)$$

which is precisely the proposed structure (3.2.50) in the dual variables, up to potential corrections of $\mathcal{O}(g_s)$. Note that factors like $\exp\left(\mathrm{i}g_s/8\right)$ or the shifts of the argument of $q_{\pm}^D$ are not visible at this level, but are part of the $\mathcal{O}(g_s)$ corrections.

3.3 The TS/ST correspondence for local $\mathbb{F}_0$

In this section, we first review some aspects of the TS/ST correspondence for the closed string sector and then discuss the generalization to the open string sector. We focus on the particular case where the toric CY threefold is local $\mathbb{F}_0$.

3.3.1 The quantum mirror map and Wilson loop

Mirror symmetry plays an important role in the TS/ST correspondence, with one of its key components being the quantum mirror map. Originally introduced from a geometrical perspective, this map was defined as the quantization of the A-period in the mirror curve [8, 23]. Subsequently, it was understood that, from a geometric engineering perspective, this map could be identified with a Wilson loop in a corresponding five-dimensional gauge theory, see [29, 32, 79, 173].

The quantum mirror map for local $\mathbb{F}_0$ is given in [8, sec. 7.2] or [174, eq. (3.58)]. The first few orders in a large μ expansion are

$$t_B(\hbar) = 2\mu - 2\left(\mathrm{e}^{4\xi}+1\right)\mathrm{e}^{-2\mu} - \left(3\mathrm{e}^{8\xi}+2\left(\mathrm{e}^{\mathrm{i}\hbar}+4+\mathrm{e}^{-\mathrm{i}\hbar}\right)\mathrm{e}^{4\xi}+3\right)\mathrm{e}^{-4\mu}+\mathcal{O}\left(\mathrm{e}^{-6\mu}\right) \quad (3.3.1)$$

where $\kappa = \exp\left(\mu\right)$ and ξ are the complex moduli of the mirror curve (3.2.1). We will also use

$$t_F\left(\hbar\right) = t_B\left(\hbar\right) - 4\xi\,. \quad (3.3.2)$$

If we sent $\hbar \to 0$ we recover the classical mirror map relating the Kähler parameters of local $\mathbb{F}_0$, to the complex moduli μ and ξ. For example, if $\xi = 0$ the classical mirror map is simply given by

$$t_B(0) = 2\mu - 4\,\mathrm{e}^{-2\mu}\,{}_4F_3\left[\begin{matrix} 1,\,1,\,\frac{3}{2},\,\frac{3}{2} \\ 2,\,2,\,2 \end{matrix}\middle|\, 16\,\mathrm{e}^{-2\mu}\right], \tag{3.3.3}$$

where ${}_4F_3$ is the generalized hypergeometric function.

From the perspective of geometric engineering, topological string theory on local $\mathbb{F}_0$ engineers a five-dimensional, $\mathcal{N} = 1$, SU(2) SYM theory in the Ω-background [118, 120]. In this gauge theory context, the quantum mirror map corresponds to the inverse of the Wilson loop in the fundamental representation. The latter can be computed via supersymmetric localization [29, 79] and the first few terms read

$$\begin{aligned} W(t_F, t_B, \hbar) = {} & \mathrm{e}^{t_F/2} + \mathrm{e}^{-t_F/2} + \left[\frac{\left(\mathrm{e}^{t_F/2} + \mathrm{e}^{-t_F/2}\right)}{\left(1 - \mathrm{e}^{\mathrm{i}\hbar}\mathrm{e}^{-t_F}\right)\left(1 - \mathrm{e}^{-\mathrm{i}\hbar}\mathrm{e}^{-t_F}\right)}\right]\mathrm{e}^{-t_B} + \\ & \left[\frac{\mathrm{e}^{-2t_F}\left(\mathrm{e}^{t_F/2} + \mathrm{e}^{-t_F/2}\right)}{\left(1 - \mathrm{e}^{\mathrm{i}2\hbar}\mathrm{e}^{-t_F}\right)\left(1 - \mathrm{e}^{\mathrm{i}\hbar}\mathrm{e}^{-t_F}\right)^3\left(1 - \mathrm{e}^{-\mathrm{i}\hbar}\mathrm{e}^{-t_F}\right)^3\left(1 - \mathrm{e}^{-\mathrm{i}2\hbar}\mathrm{e}^{-t_F}\right)}\Big(-\left(3\mathrm{e}^{\mathrm{i}\hbar} + 4 + 3\mathrm{e}^{-\mathrm{i}\hbar}\right)\right. \\ & \left. + \left(\mathrm{e}^{\mathrm{i}2\hbar} + \mathrm{e}^{\mathrm{i}\hbar} + 1 + \mathrm{e}^{-\mathrm{i}\hbar} + \mathrm{e}^{-\mathrm{i}2\hbar}\right)\left(\mathrm{e}^{t_F} + \mathrm{e}^{-t_F}\right)\Big)\right]\mathrm{e}^{-2t_B} + \mathcal{O}\left(\mathrm{e}^{-3t_B}\right) \end{aligned} \tag{3.3.4}$$

where $t_{B,F}$ are the Kähler parameters. We refer to [124, eq. (3.22)] for the full definition in this specific example. It is easily verified that setting

$$t_B = t_B(\hbar)\,, \qquad\qquad t_F = t_F(\hbar)\,, \tag{3.3.5}$$

in equation (3.3.4) gives

$$W(t_F(\hbar), t_B(\hbar), \hbar) = \mathrm{e}^{-2\xi}\kappa\,. \tag{3.3.6}$$

One can easily check, at least numerically, that both expansions in (3.3.1) and in (3.3.4) are convergent, see e.g. [124, 174].

3.3.2 The closed string sector and the spectral determinant

Let us first review some important elements of the TS/ST correspondence for the closed string sector [4, 5], see [175, 176] for a review. Note that we focus on the specific case where the CY threefold is local $\mathbb{F}_0$.

One feature of the TS/ST correspondence is that, on the topological string side, the relevant quantities involve a special combination of refined topological string partition functions in the GV ($-\epsilon_1 = \epsilon_2 = g_s$) and NS limit ($\epsilon_1 \to 0, \epsilon_2 = \hbar$) respectively with the relation

$$g_s = \frac{4\pi^2}{\hbar}\,. \tag{3.3.7}$$

The arguments of these two sets of special functions are typically rescaled with respect to each other. Hence, it is convenient to define

$$\alpha^D = \left(\frac{2\pi}{\hbar}\right)\alpha\,. \tag{3.3.8}$$

The self-dual, or maximally supersymmetric point, is defined at $\hbar = g_s = 2\pi$ [4, 102].

The main quantity is the closed topological string grand potential $\mathrm{J}(\mu,\xi,\hbar)$. This quantity encapsulates both perturbative and non-perturbative contributions to the closed topological string free energy near the large radius point [4, 174, 177]. More precisely, we have

$$\mathrm{J}(\mu,\xi,\hbar) = \mathrm{A}\left(\xi,\hbar\right) + \mathrm{J}_{\mathrm{p}}\left(\mu,\xi,\hbar\right) + \mathrm{J}_{\text{1-loop}}\left(\mu,\xi,\hbar\right) + \mathrm{J}_{\mathrm{inst}}(\mu,\xi,\hbar)\,. \tag{3.3.9}$$

Let us define these functions:

- We denote with $\mathrm{A}\left(\xi,\hbar\right)$ the constant map contribution whose closed-form reads [65, 178]

$$\mathrm{A}\left(\xi,\hbar\right) = \frac{4\xi^3}{3\pi\hbar} + \frac{\hbar\xi}{12\pi} + A_c\left(\frac{\hbar}{\pi}\right) - F_{\mathrm{CS}}\left(\xi,\hbar\right)\,, \tag{3.3.10}$$

$$A_c\left(k\right) = \frac{2\zeta\left(3\right)}{\pi^2 k}\left(1-\frac{k^3}{16}\right) + \left(\frac{k}{\pi}\right)^2\int_0^{+\infty}\mathrm{d}x\;\frac{x}{\mathrm{e}^{kx}-1}\ln\left(1-\mathrm{e}^{-2x}\right)\,, \tag{3.3.11}$$

$$\begin{aligned} F_{\mathrm{CS}}\left(\xi,g\right) = {}& \frac{\hbar^2}{8\pi^4}\left[\mathrm{Li}_3\left(-\mathrm{e}^{2\left(\frac{2\pi}{\hbar}\right)\xi}\right) + \mathrm{Li}_3\left(-\mathrm{e}^{-2\left(\frac{2\pi}{\hbar}\right)\xi}\right) - 2\zeta\left(3\right)\right] \\ & + \int_0^{+\infty}\mathrm{d}x\;\frac{x}{\mathrm{e}^{2\pi x}-1}\ln\left[\frac{\sinh^2\left(\frac{\pi^2 x}{\hbar}\right)}{\sinh^2\left(\frac{\pi^2 x}{\hbar}\right)+\cosh^2\left(\left(\frac{2\pi}{\hbar}\right)\xi\right)}\right]\,, \end{aligned} \tag{3.3.12}$$

  where Li_3 is the polylogarithm of order 3 and ζ is the Riemann zeta function.

- The polynomial part J_{p} is given by

$$\mathrm{J}_{\mathrm{p}}\left(\mu,\xi,\hbar\right) = \frac{t_B^3\left(\hbar\right)}{12\pi\hbar} - \frac{\xi t_B^2\left(\hbar\right)}{2\pi\hbar} + \left(\frac{\pi}{6\hbar}-\frac{\hbar}{24\pi}\right)t_B\left(\hbar\right) - \frac{\pi\xi}{3\hbar}\,, \tag{3.3.13}$$

  where the quantum mirror map $t_B\left(\hbar\right)$ is given in (3.3.1).

- The one-loop part consists of two contributions: one coming from the one-loop part of the free energy in the NS phase and one being the one-loop part of the free energy in the GV phase of the Ω-background. The sum of these two contributions reads then

$$\begin{aligned} \mathrm{J}_{\text{1-loop}}\left(\mu,\xi,\hbar\right) = {}& \sum_{k=1}^{+\infty}\left[\frac{1}{2\pi k^2}\cot\left(\hbar\frac{k}{2}\right)\left(1+kt_F\left(\hbar\right)\right) + \frac{\hbar}{4\pi k}\csc^2\left(\hbar\frac{k}{2}\right)\right]\mathrm{e}^{-kt_F(\hbar)} \\ & - \sum_{k=1}^{+\infty}\frac{1}{2k}\csc^2\left(\left(\frac{4\pi^2}{\hbar}\right)\frac{k}{2}\right)\mathrm{e}^{-k\left(\frac{2\pi}{\hbar}\right)t_F(\hbar)}\,, \end{aligned} \tag{3.3.14}$$

where $t_F(\hbar)$ is related μ and ξ via (3.3.2). This can be written in closed form in $t_F(\hbar)$ when $\hbar = 2\pi\,(n/m)$ with $n, m \in \mathbb{N}_{>0}$ coprime,

$$\begin{aligned}
&\mathrm{J}_{\text{1-loop}}(\mu,\xi,\hbar) = \\
&\left(\frac{2\pi^2\left(m^2-n^2\right)+3m^2t_F^2(\hbar)}{12\pi^2nm^2}\right)\ln\left(1-\mathrm{e}^{-mt_F(\hbar)}\right)-\frac{t_F(\hbar)\,\mathrm{Li}_2\left(\mathrm{e}^{-mt_F(\hbar)}\right)}{2\pi^2nm}-\frac{\mathrm{Li}_3\left(\mathrm{e}^{-mt_F(\hbar)}\right)}{2\pi^2nm^2} \\
&+\sum_{k=1}^{m-1}\frac{\csc^2\left(\hbar\frac{k}{2}\right)}{4\pi k}\mathrm{e}^{-kt_F(\hbar)}\left\{\left[\hbar+\left(\frac{1}{k}+t_F(\hbar)\right)\sin(\hbar k)\right]{}_3F_2\left[\begin{matrix}1,\,\frac{k}{m},\,\frac{k}{m}\\ 1+\frac{k}{m},\,1+\frac{k}{m}\end{matrix}\middle|\,\mathrm{e}^{-mt_F(\hbar)}\right]\right. \\
&\left.+\left(\frac{k/m}{(1+k/m)^2}\right)\mathrm{e}^{-mt_F(\hbar)}\left[\hbar+t_F(\hbar)\sin(\hbar k)\right]{}_3F_2\left[\begin{matrix}2,\,1+\frac{k}{m},\,1+\frac{k}{m}\\ 2+\frac{k}{m},\,2+\frac{k}{m}\end{matrix}\middle|\,\mathrm{e}^{-mt_F(\hbar)}\right]\right\} \\
&-\sum_{k=1}^{n-1}\frac{\csc^2\left(\left(\frac{4\pi^2}{\hbar}\right)\frac{k}{2}\right)}{2k}\mathrm{e}^{-k\left(\frac{2\pi}{\hbar}\right)t_F(\hbar)}\,{}_2F_1\left[\begin{matrix}1,\,\frac{k}{n}\\ 1+\frac{k}{n}\end{matrix}\middle|\,\mathrm{e}^{-n\left(\frac{2\pi}{\hbar}\right)t_F(\hbar)}\right], \qquad (3.3.15)
\end{aligned}$$

where Li_q is the polylogarithm of order q, and ${}_pF_q$ is the generalized hypergeometric function. It is interesting to note that (3.3.14) also admits the following integral representation [14, eq. (3.9)]

$$\begin{aligned}
&\mathrm{J}_{\text{1-loop}}(\mu,\xi,\hbar) = -\frac{\hbar^2}{8\pi^4}\mathrm{Li}_3\left(\mathrm{e}^{-\left(\frac{2\pi}{\hbar}\right)t_F(\hbar)}\right)+ \\
&\quad 2\,\mathrm{Re}\int_0^{\infty\mathrm{e}^{\mathrm{i}0}}\mathrm{d}x\;\frac{x}{\mathrm{e}^{2\pi x}-1}\ln\left(1-2\cosh\left(\left(\frac{4\pi^2}{\hbar}\right)x\right)\mathrm{e}^{-\left(\frac{2\pi}{\hbar}\right)t_F(\hbar)}+\mathrm{e}^{-2\left(\frac{2\pi}{\hbar}\right)t_F(\hbar)}\right). \qquad (3.3.16)
\end{aligned}$$

- The instanton part of the grand potential also consists of two parts: one coming from the instanton part of the NS free energy, and one being the instanton part of the GV free energy. Together, they read

$$\begin{aligned}
\mathrm{J}_{\text{inst}}(\mu,\xi,\hbar) &= F_{\text{inst}}^{\text{GV}}\left(\left(\frac{2\pi}{\hbar}\right)t_F(\hbar),\left(\frac{2\pi}{\hbar}\right)t_B(\hbar),\frac{4\pi^2}{\hbar}\right) \\
&\quad+\left(-\frac{1}{2\pi}+\frac{t_F(\hbar)}{2\pi}\partial_{t_F}+\frac{t_B(\hbar)}{2\pi}\partial_{t_B}+\frac{\hbar}{2\pi}\partial_\hbar\right)F_{\text{inst}}^{\text{NS}}\left(t_F(\hbar),t_B(\hbar),\hbar\right) \qquad (3.3.17)
\end{aligned}$$

where $F_{\text{inst}}^{\text{NS}}$ is the instanton part of the 5d Nekrasov free energy in the NS limit, and $F_{\text{inst}}^{\text{GV}}$ is similarly the instanton part of the 5d Nekrasov free energy in the GV limit. The leading order reads

$$F_{\text{inst}}^{\text{NS}}(t_F,t_B,\hbar) = \left[\frac{\mathrm{i}\left(1+\mathrm{e}^{\mathrm{i}\hbar}\right)}{\left(1-\mathrm{e}^{\mathrm{i}\hbar}\right)\left(1-\mathrm{e}^{\mathrm{i}\hbar}\mathrm{e}^{-t_F}\right)\left(1-\mathrm{e}^{-\mathrm{i}\hbar}\mathrm{e}^{-t_F}\right)}\right]\mathrm{e}^{-t_B}+\mathcal{O}\left(\mathrm{e}^{-2\,t_B}\right), \qquad (3.3.18)$$

$$F_{\text{inst}}^{\text{GV}}(t_F,t_B,g_s) = \left[\frac{2\mathrm{e}^{\mathrm{i}g_s}}{\left(1-\mathrm{e}^{\mathrm{i}g_s}\right)^2\left(1-\mathrm{e}^{-t_F}\right)^2}\right]\mathrm{e}^{-t_B}+\mathcal{O}\left(\mathrm{e}^{-2\,t_B}\right), \qquad (3.3.19)$$

and the all order constructions can be found in section A.3, equations (A.3.12) and (A.3.15) respectively.

Note that the NS contributions in $\mathrm{J}_{\text{1-loop}}$ (3.3.14) and J_{inst} (3.3.17) are perturbative in $\hbar$ for fixed $t_{B,F}$, but non-perturbative in $g_s = 4\pi^2/\hbar$ for fixed $t^D_{B,F} = (2\pi/\hbar)\, t_{B,F}$. Vice versa, the GV contributions in $\mathrm{J}_{\text{1-loop}}$ (3.3.14) and J_{inst} (3.3.17) are perturbative in g_s for fixed $t^D_{B,F}$, but non-perturbative in $\hbar = 4\pi^2/g_s$ for fixed $t_{B,F} = (2\pi/g_s)\, t^D_{B,F}$. The specific combination of GV and NS free energies in (3.3.9) provides a genuinely non-perturbative completion of both quantities. Indeed, the NS and GV functions are not well-defined functions of $\hbar$ or g_s when considered separately. Each of them individually exhibits a dense set of poles along the real $\hbar$ or g_s line, making them ill-defined. However, these poles cancel in the combinations (3.3.14) and (3.3.17), and the resulting function is perfectly well-defined for any value of $\hbar$ or g_s.

It is well known that, given an asymptotic series, its non-perturbative completion is not unique; additional conditions are required to fix it. In the context of the TS/ST correspondence, these conditions are provided by the spectral theory of the quantized mirror curve. In particular, the non-perturbative completion defined by the TS/ST correspondence is the unique one that correctly reproduces the spectrum and eigenfunctions of the operator associated with the quantum mirror curve, which in turn is related to an underlying relativistic quantum integrable systems. The same non-perturbative completion was also used in ABJM theory [174, 179], where it successfully captures non-perturbative effects in its corresponding string dual [180]. Nevertheless, other completions are possible in principle; see for instance [181, 182] for an alternative proposal, and [183] for a broader discussion of non-perturbative completions in topological string theory and their interplay with resurgence.

From the perspective of spectral theory, it is natural to consider the grand-canonical ensemble. One of the key statements of the TS/ST correspondence is then that

$$\det\left(1+\kappa\rho\right) = \sum_{k\in\mathbb{Z}} \mathrm{e}^{\mathrm{J}(\mu+\mathrm{i}2\pi k,\xi,\hbar)}\,, \qquad\qquad \kappa = \exp\left(\mu\right)\,, \tag{3.3.20}$$

where ρ is the operator in (3.2.12) and J is the grand potential of (3.3.9). An important point is that (3.3.20) is entire in the full κ plane, therefore all the singularities in the closed string moduli space are smoothed out, and the full quantity is background independent. To extract the partition function around specific points in the moduli space, we need to expand (3.3.20) accordingly. For instance, expanding around $\kappa = \infty$ leads to the large radius expansion. Expanding around the orbifold point $\kappa = 0$ gives [4, 65, 157]

$$\det\left(1+\kappa\rho\right) = \sum_{N=0}^{\infty} \kappa^N Z\left(N,\hbar\right)\,, \tag{3.3.21}$$

where $Z(N,\hbar)$ is defined in (3.2.15). It is a distinctive feature of this construction that even though one expands the determinant around the orbifold point $\kappa = 0$, the coefficients $Z(N,\hbar)$ actually encode the non-perturbative partition function in the conifold frame.

3.3.3 The open string sector and the eigenfunctions

Let us now turn to the open sector of the topological string. As before, we focus on the example of local $\mathbb{F}_0$. The grand potential for the open topological string in the presence of a toric D-brane on an external leg of the toric diagram was introduced in [6, 7]. Here, we follow the formulation in [1, app. A], where the resummation in the open string modulus x is also performed.

The open string grand potential is

$$\mathrm{J}^{\mathrm{open}}(x,\mu,\xi,\hbar) = \mathrm{J}^{\mathrm{open}}_{\mathrm{p}}(x,\xi,\hbar) + \mathrm{J}^{\mathrm{open}}_{\text{1-loop}}(x,\mu,\xi,\hbar) + \mathrm{J}^{\mathrm{open}}_{\mathrm{inst}}(x,\mu,\xi,\hbar)\ , \tag{3.3.22}$$

where μ is the closed string modulus, ξ is the mass parameter, and x is the open string modulus. The functions appearing on the right-hand side of (3.3.22) are defined as follows:

- The polynomial part in x is

$$\mathrm{J}^{\mathrm{open}}_{\mathrm{p}}(x,\xi,\hbar) = -\frac{\mathrm{i}}{\hbar}2\xi x - \frac{\mathrm{i}}{\hbar}\frac{x^2}{2} + \frac{1}{2}\left(\frac{2\pi}{\hbar}-1\right)x\,. \tag{3.3.23}$$

- The one loop part is given by [1, eq. (A.24)]

$$\begin{aligned}&\mathrm{J}^{\mathrm{open}}_{\text{1-loop}}(x,\mu,\xi,\hbar) = \\ &\ln\Phi_\beta\left(\frac{1}{2\pi\beta}\left(-x-\frac{t_F(\hbar)}{2}\right)+\mathrm{i}\frac{\beta}{2}\right)+\ln\Phi_\beta\left(\frac{1}{2\pi\beta}\left(-x+\frac{t_F(\hbar)}{2}\right)+\mathrm{i}\frac{\beta}{2}\right)\end{aligned} \tag{3.3.24}$$

  where $\hbar = 2\pi\beta^2$ and $\ln\Phi_\beta$ is the logarithm of Faddeev's non-compact quantum dilogarithm, see subsection A.2.2. One can express (3.3.24) in closed form in terms of elementary functions and the classical dilogarithm Li_2 if $\hbar \in 2\pi\mathbb{Q}_{>0}$, by using (A.2.13). This 1-loop part of the grand potential consists again of contributions from both the NS and GV free energies, just as in the closed sector. See [1, app. A] for details.

- The instanton part $\mathrm{J}^{\mathrm{open}}_{\mathrm{inst}}$ consists also of a part coming from the NS free energy, and a part coming from the GV free energy

$$\begin{aligned}\mathrm{J}^{\mathrm{open}}_{\mathrm{inst}}(x,\mu,\xi,\hbar) &= F^{\mathrm{open}}_{\mathrm{NS,inst}}(x,t_F(\hbar),t_B(\hbar),\hbar)\\ &\quad + F^{\mathrm{open}}_{\mathrm{GV,inst}}\left(\left(\frac{2\pi}{\hbar}\right)x,\left(\frac{2\pi}{\hbar}\right)t_F(\hbar),\left(\frac{2\pi}{\hbar}\right)t_B(\hbar),\frac{4\pi^2}{\hbar}\right)\ .\end{aligned} \tag{3.3.25}$$

  Here, $F^{\mathrm{open}}_{\mathrm{NS,inst}}$ represents the NS limit of the refined open topological string free energy associated with a brane inserted on the outer leg of the toric diagram:

$$\begin{aligned}&F^{\mathrm{open}}_{\mathrm{NS,inst}}(x,t_F,t_B,\hbar) = \\ &\frac{\mathrm{e}^{\mathrm{i}\hbar}\mathrm{e}^{\frac{t_F}{2}-x}\left(1+\mathrm{e}^{-t_F}+\mathrm{e}^{\mathrm{i}\hbar}\left(1+\mathrm{e}^{\mathrm{i}\hbar}\right)\mathrm{e}^{-\frac{t_F}{2}-x}\right)\mathrm{e}^{-t_B}}{\left(1-\mathrm{e}^{\mathrm{i}\hbar}\right)\left(1-\mathrm{e}^{\mathrm{i}\hbar}\mathrm{e}^{-t_F}\right)\left(1-\mathrm{e}^{-\mathrm{i}\hbar}\mathrm{e}^{-t_F}\right)\left(1+\mathrm{e}^{\mathrm{i}\hbar}\mathrm{e}^{\frac{t_F}{2}-x}\right)\left(1+\mathrm{e}^{\mathrm{i}\hbar}\mathrm{e}^{-\frac{t_F}{2}-x}\right)}+\mathcal{O}\left(\mathrm{e}^{-2t_B}\right),\end{aligned} \tag{3.3.26}$$

and the all order definition is given in section A.3, equation (A.3.12). Similarly, $F^{\text{open}}_{\text{GV,inst}}$ is the open topological string free energy corresponding to a brane inserted in the outer leg of the toric diagram:

$$F^{\text{open}}_{\text{GV,inst}}(x,t_F,t_B,g_s) = \\ -\frac{\mathrm{e}^{\mathrm{i}\frac{g_s}{2}}\mathrm{e}^{\frac{t_F}{2}-x}\left(1+\mathrm{e}^{-t_F}-2\mathrm{e}^{\mathrm{i}\frac{g_s}{2}}\mathrm{e}^{-\frac{t_F}{2}-x}\right)}{\left(1-\mathrm{e}^{\mathrm{i}g_s}\right)\left(1-\mathrm{e}^{-t_F}\right)^2\left(1-\mathrm{e}^{\mathrm{i}\frac{g_s}{2}}\mathrm{e}^{\frac{t_F}{2}-x}\right)\left(1-\mathrm{e}^{\mathrm{i}\frac{g_s}{2}}\mathrm{e}^{-\frac{t_F}{2}-x}\right)}\mathrm{e}^{-t_B}+\mathcal{O}\left(\mathrm{e}^{-2t_B}\right), \tag{3.3.27}$$

and the all order expression for (3.3.27) can be found in section A.3, equation (A.3.15).

Similar to what was observed in the closed string sector, the role of the NS partition function in (3.3.22) in the open sector is also purely non-perturbative in g_s, and it plays a crucial role in cancelling the poles in g_s of the GV part and making the full expression well-defined. Hence, (3.3.22) provides a well-defined non-perturbative completion for the open topological string partition function around the large radius frame. On the other side, from the spectral theory perspective, the perturbative contributions in $\hbar = 4\pi^2/g_s$ are captured by the NS partition function in (3.3.22), whereas the GV part remains purely non-perturbative in $\hbar$. We refer to [6, 7] for further details.

Note that $\exp\left(J^{\text{open}}_{\text{1-loop}}\right)$ has poles at

$$x = \pm\frac{t_F(\hbar)}{2} - \mathrm{i}2\pi\left(n-\frac{1}{2}\right) - \mathrm{i}\hbar m\,, \qquad n\in\mathbb{N}_{>0},\, m\in\mathbb{N}\,, \tag{3.3.28}$$

and similarly, $\exp\left(J^{\text{open}}_{\text{inst}}\right)$ has poles coming from $F^{\text{open}}_{\text{NS,inst}}$ and $F^{\text{open}}_{\text{GV,inst}}$ respectively when

$$\begin{aligned} x &= \pm\frac{t_F(\hbar)}{2} + \mathrm{i}2\pi\left(m-\frac{1}{2}\right) + \mathrm{i}\hbar n\,, && n\in\mathbb{N}_{>0},\, m\in\mathbb{Z}\,, \\ x &= \pm\frac{t_F(\hbar)}{2} + \mathrm{i}2\pi\left(n-\frac{1}{2}\right) + \mathrm{i}\hbar m\,, && n\in\mathbb{N}_{>0},\, m\in\mathbb{Z}\,. \end{aligned} \tag{3.3.29}$$

Note that only the poles with $n \leqslant N$ occur at order $\exp\left(-N\,t_B\right)$ in $F^{\text{open}}_{\text{NS,inst}}$ or $F^{\text{open}}_{\text{GV,inst}}$. These poles should be related to the transition from the external to the internal leg of the toric diagram, and they do not disappear in the open string grand potential $\mathrm{J}^{\text{open}}(x,\mu,\xi,\hbar)$.

Now we want to relate (3.3.22) to the eigenfunctions of the quantum mirror curve (3.2.3). It is important to emphasize that there are numerous ways to construct formal solutions to (3.2.3). For instance, consider

$$\exp\left[\mathrm{J}^{\text{open}}_{\text{p}}(x,\xi,\hbar) + \mathrm{J}^{\text{open}}_{\text{1-loop}}(x,\mu,\xi,\hbar) + F^{\text{open}}_{\text{NS,inst}}\left(x,t_F(\hbar),t_B(\hbar),\hbar\right)\right]. \tag{3.3.30}$$

While this expression formally satisfies (3.2.3), it is not a well-defined function for $\hbar\in\mathbb{R}_{>0}$ due to the dense set of poles at $\hbar\in\pi\mathbb{Q}$, and it fails to satisfy the analytic properties

required by a proper eigenfunction as discussed below (3.2.3). The exponential of (3.3.22) on the other hand, as well as each individual term in (3.3.35), would give a well-defined solution to the difference equation for all $\hbar \in \mathbb{R}_{>0}$. However, it does not have the correct analytical properties or asymptotic behaviour to be in the domain of the quantized mirror curve. Hence, it does not qualify as an eigenfunction either.

To construct proper eigenfunctions, it is useful to introduce the full grand potential, which is defined as

$$\mathrm{J}(x,\mu,\xi,\hbar) = \mathrm{J}(\mu,\xi,\hbar) + \mathrm{J}^{\mathrm{open}}(x,\mu,\xi,\hbar)\,. \tag{3.3.31}$$

It was conjectured in [6, 7] that one of the terms in the sum (3.1.5) should be given by

$$\sum_{k\in\mathbb{Z}} \mathrm{e}^{\mathrm{J}(x,\mu+\mathrm{i}2\pi k,\xi,\hbar)}\,. \tag{3.3.32}$$

Building on the structure found in (3.2.48) for the second term, we can now express the full eigenfunctions of the quantum mirror curve (3.2.2) in a compact form:

$$\psi(x,\kappa) = \sum_{k\in\mathbb{Z}} \sum_{\sigma\in\{1,2\}} \mathrm{e}^{\mathrm{J}_\sigma(x,\mu+\mathrm{i}2\pi k,\xi,\hbar)}\,, \qquad \kappa = \mathrm{e}^{\mu}\,, \tag{3.3.33}$$

$$\mathrm{J}_1(x,\mu,\xi,\hbar) = \mathrm{J}(x,\mu,\xi,\hbar)\,, \qquad \mathrm{J}_2(x,\mu,\xi,\hbar) = \frac{\mathrm{i}}{\hbar}\frac{\pi^2}{2} + \frac{\pi x}{\hbar} + \mathrm{J}(-x-\mathrm{i}\pi,\mu+\mathrm{i}\pi,\xi,\hbar)\,. \tag{3.3.34}$$

Hence, the eigenfunctions are simply

$$\boxed{\psi(x,\kappa) = \sum_{k\in\mathbb{Z}} \left(\mathrm{e}^{\mathrm{J}(x,\mu+\mathrm{i}2\pi k,\xi,\hbar)} + \mathrm{e}^{\frac{\mathrm{i}}{\hbar}\frac{\pi^2}{2}+\frac{\pi x}{\hbar}+\mathrm{J}(-x-\mathrm{i}\pi,\mu+\mathrm{i}\pi+\mathrm{i}2\pi k,\xi,\hbar)}\right)}\,. \tag{3.3.35}$$

According to our construction, these are well-defined functions for all $x,\kappa \in \mathbb{C}$, $\xi \in \mathbb{R}$ and $\hbar \in \mathbb{R}_{>0}$, which are *entire* in x and solve the difference equation (3.2.3) for any value of the parameters, and which are the true, square-integrable eigenfunctions of the quantum mirror curve when $\kappa = -\exp(E_n)$ coincides with a value in the spectrum. We do not have a rigorous proof of this, but there are many non-trivial tests. See figure 3.2, figure 3.3, and subsection A.5.1 for some graphical representations of (3.3.35).

Let us make some comments on this result:

- The grand potential $\mathrm{J}(x,\mu,\xi,\hbar)$ is defined in the large-radius frame, corresponding to placing a brane on the outer leg of the toric diagram. It is therefore expected that $\mathrm{J}(x,\mu,\xi,\hbar)$ has poles in x: it is associated with a specific patch of the open-string moduli space and is not background independent. Starting from $\mathrm{J}(x,\mu,\xi,\hbar)$ and moving to a different patch in the moduli space requires performing a modular transformation followed by an analytic continuation.

  In contrast, the non-perturbative completion that we propose — given in equation (3.3.35) — is an entire function of both the open modulus x and the closed moduli.

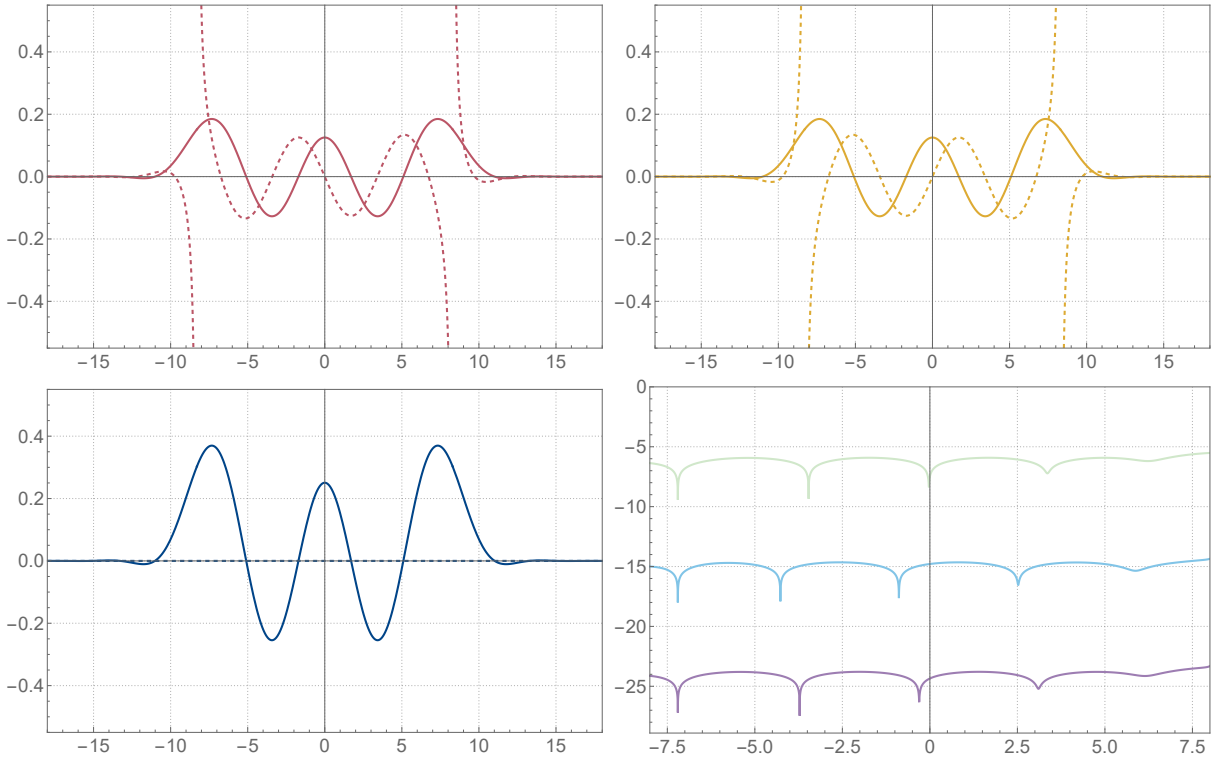

Figure 3.2. The on-shell eigenfunction from topological strings for $\xi = -16/53$ and $\hbar = 8\pi/3$ at energy $E = E_4 \approx 7.69$. Top left: the $\sigma = 1$ term in (3.3.33). Top right: the $\sigma = 2$ term in (3.3.33). Bottom left: the full eigenfunction ψ as given in (3.3.35), after normalization. Bottom right: the absolute difference between the analytical and numerical eigenfunctions, including 0 (green), 2 (blue), and 4 (violet) instantons in the small $\exp(-t_B)$ expansion of ψ. The plot on the bottom right uses a logarithmic scale with base 10. The solid and dashed lines correspond to the real and imaginary parts, respectively.

In this sense, equation (3.3.35) is background independent: we can simply expand it around any desired point in the moduli space, such as the large-radius or orbifold regions, and directly recover the corresponding open-string partition function valid in that particular frame.

At the technical level, such background independence is obtained by the summation over k and the summation over σ in (3.3.33) and (3.3.35). Indeed, as we reviewed in the introduction, the summation over k in equation (3.3.20) smooths all the singularities in the closed-string moduli space, parametrized by κ, yielding an entire function in κ. The sum over σ in equation (3.3.35) plays an analogous role for the open-string modulus x: each of the two terms in (3.3.33) and (3.3.35) individually has singularities in x, but these are smoothed out once the two contributions are combined and the sum over k is performed. This property holds even off-shell, i.e. for $\kappa \neq -\mathrm{e}^{E_n}$. Geometrically, it was argued in [6, 7] that such a sum over σ should correspond to a sum over the two sheets of the mirror curve.

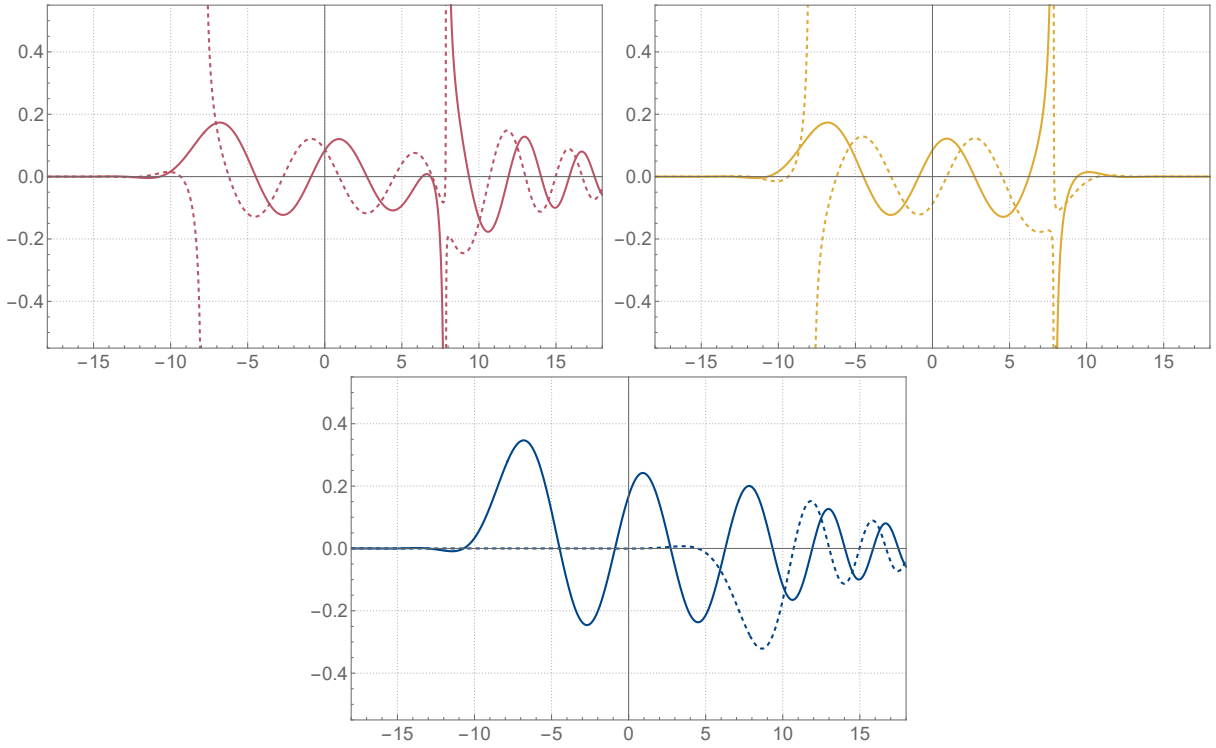

Figure 3.3. The off-shell eigenfunction from topological strings for $\xi = -16/53$ and $\hbar = 8\pi/3$ at energy $E = 225/31$, which is between E_3 and E_4. From top left to bottom: the $\sigma = 1$ term in (3.3.33), the $\sigma = 2$ term in (3.3.33), and the complete eigenfunction ψ in (3.3.35), after normalization. The solid and dashed lines correspond to the real and imaginary parts, respectively.

- As can be seen in figure 3.2 and in subsection A.5.1, when evaluated on-shell, the two terms in (3.3.35) have the same real part along the real line, which is pole-free, while having opposite imaginary parts, with poles that cancel in the sum.
- An important part of the statement is that the sums in (3.3.35) are convergent. The instanton expansion of $\mathrm{J}_{\mathrm{inst}}$ and the sum over the shifts $k \in \mathbb{Z}$ are both essentially expansions in $\exp\left(-t_B\left(\hbar\right)\right)$, and the mirror map $t_B\left(\hbar\right)$ is itself is given as an expansion in large κ. Hence, one can think of this as a convergent semi-classical expansion. For $\hbar \in 2\pi\mathbb{Q}_{>0}$ numerical evidence suggests that the convergence of this series is compact, that is uniform on every compact subset of the complex x-plane, but only pointwise near complex infinity. For $\hbar \in 2\pi\left(\mathbb{R}_{>0} \setminus \mathbb{Q}_{>0}\right)$ the convergence near $x \in \pm t_F\left(\hbar\right)/2 + \mathrm{i}\mathbb{R}$ may be only pointwise as well.

Let us end with a few words about the evidence in favour of (3.3.35). Many tests that do no directly involve the $\sigma = 2$ term as written in (3.3.33) were done in [6, 7]. Let us in particular mention the closed form solutions they wrote down for $\xi = 0$, $\hbar = 2\pi$, for which one can explicitly check the pole cancellation. Strong numerical evidence for our proposal (3.3.35) comes from diagonalizing the quantum mirror curve in the basis of the harmonic

oscillator as in [184], and comparing the resulting numerical eigenfunctions with (3.3.35). See also the explanation at the beginning of subsection A.5.1. Another non-trivial test of (3.3.35) comes from the so-called standard and dual four-dimensional limits. These are interesting stories in their own right, which we will discuss next.

3.4 Four-dimensional limits

It is well-known that topological string theory on local CY manifolds can be used to geometrically engineer four-dimensional $\mathcal{N}=2$ theories [118, 120]. In the case of a local $\mathbb{F}_0$ geometry, the corresponding four-dimensional gauge theory is $\mathcal{N}=2$, SU(2) SYM. In this section, we study the four-dimensional limit of the open TS/ST correspondence. There are two distinct four-dimensional limits one can implement: the standard limit, discussed in subsection 3.4.1, and the dual limit, presented in subsection 3.4.2.

3.4.1 The standard four-dimensional limit

Let us consider the mirror curve for local $\mathbb{F}_0$ (3.2.1). In the standard 4d limit, the parameters of the curve scale as [118]

$$x = R x_{4\mathrm{d}}\,, \qquad \mathrm{e}^{2\xi} = \frac{1}{\sqrt{t}R^2}\,, \qquad \kappa = \frac{1}{\sqrt{t}R^2}\left(-2-R^2E\right)\,, \qquad \hbar = R\epsilon\,, \tag{3.4.1}$$

and the limit is taken as $R\to 0$. In this limit, (3.2.2) becomes the Fourier transformed modified Mathieu operator

$$\mathrm{O}_{\mathrm{FMa}} = \sqrt{t}\left(\mathrm{e}^{\hat{y}}+\mathrm{e}^{-\hat{y}}\right)+\hat{x}^2\,, \qquad [\hat{x},\hat{y}]=\mathrm{i}\epsilon\,, \qquad t,\epsilon>0\,, \tag{3.4.2}$$

where we omit the subscripts 4d in the variable x for the sake of notation. The corresponding eigenvalue equation reads

$$\sqrt{t}\left(\phi(x-\mathrm{i}\epsilon,E)+\phi(x+\mathrm{i}\epsilon,E)\right)+x^2\phi(x,E)-E\phi(x,E)=0\,. \tag{3.4.3}$$

If we perform a Fourier transform on (3.4.2), i.e. we exchange position and momentum operator, we obtain the modified Mathieu operator in the standard form

$$\left(\sqrt{t}\left(\mathrm{e}^{q}+\mathrm{e}^{-q}\right)-\epsilon^2\partial_q^2-E\right)\widehat{\phi}(q,E)=0\,. \tag{3.4.4}$$

The eigenfunctions of (3.4.3) and (3.4.4) are related by a Fourier transform,

$$\widehat{\phi}(q,E)=\int_{\mathbb{R}}\mathrm{d}x\,\mathrm{e}^{\mathrm{i}qx/\epsilon}\,\phi(x,E)\,. \tag{3.4.5}$$

The quantization condition for the spectrum of (3.4.2) is derived analogously to the one for (3.2.2), i.e. by imposing analytic continuation within the strip (3.2.5), and requiring square integrability of $\phi(x,E)$. On the other hand, for the Fourier transformed operator

(3.4.4), this corresponds to square integrability of $\widehat{\phi}(q, E)$. The energy spectrum is then discrete and the same for both operators.

For the sake of notation, we work at $\epsilon = 1$. The ϵ-dependence can be reinstated by appropriately shifting the variable as follows:

- For the modified Mathieu operator (3.4.4), we can work at $\epsilon = 1$ and then re-install the ϵ dependence by shifting

$$t \to t/\epsilon^4 \,, \qquad\qquad E \to E/\epsilon^2 \,. \tag{3.4.6}$$

- For the Fourier transformed modified Mathieu (3.4.2) (3.4.3), we can work at $\epsilon = 1$ and then re-install the ϵ dependence by shifting

$$x \to x/\epsilon \,, \qquad\qquad t \to t/\epsilon^4 \,, \qquad\qquad E \to E/\epsilon^2 \,. \tag{3.4.7}$$

Result

The standard four-dimensional limit (3.4.1) was examined in the context of the closed TS/ST correspondence in [41, 55, 185]. In [41] it was shown that in this limit (3.3.20) gives

$$\det\left(1 - E\,\mathrm{O}_{\mathrm{FMa}}^{-1}\right) = A(t)\left(\frac{\sinh\left(\frac{\mathrm{i}}{2}\partial_\sigma F_{\mathrm{NS}}^{\mathrm{4d}}(\sigma, t)\right)}{\mathrm{i}\sinh\left(2\pi\sigma\right)}\right) \,, \tag{3.4.8}$$

where $A(t)$ is a normalization constant independent of E, chosen such that the left-hand side, when evaluated at $E = 0$, equals 1. In (3.4.8), we note by $F_{\mathrm{NS}}^{\mathrm{4d}}$ the full, four-dimensional NS free energy associated with $\mathcal{N} = 2$, SU (2) SYM

$$\begin{aligned} F_{\mathrm{NS}}^{\mathrm{4d}}\left(\sigma, t\right) = &-\psi^{(-2)}(1 - \mathrm{i}2\sigma) - \psi^{(-2)}(1 + \mathrm{i}2\sigma) - \sigma^2 \ln\left(t\right) \\ &- \left(\frac{2}{4\sigma^2 + 1}\right) t - \left(\frac{20\sigma^2 - 7}{4\left(4\sigma^2 + 1\right)^3\left(\sigma^2 + 1\right)}\right) t^2 + \mathcal{O}\left(t^3\right) \,, \end{aligned} \tag{3.4.9}$$

where $\psi^{(-2)}$ is the polygamma function of order -2. Higher orders in the t expansion can be found in (A.3.30) and according to the all order expression (A.3.28). The variable σ and the energy E are related via the quantum Matone relation [99, 100]

$$E = -t\partial_t F_{\mathrm{NS}}^{\mathrm{4d}}\left(\sigma, t\right) \,, \qquad\qquad 2\sigma \notin \mathrm{i}\mathbb{Z} \setminus \{0\} \,. \tag{3.4.10}$$

This relation is the 4d limit of the Wilson loop (3.3.4), and is hence the 4d equivalent of the quantum mirror map, relating the gauge theory and spectral parameters to each other. The quantization condition for the operator spectrum, determined by the vanishing of the determinant (3.4.8), exactly reproduces the NS quantization condition [22]:

$$\partial_\sigma F_{\mathrm{NS}}^{\mathrm{4d}}(\sigma, t) = 2\pi(n + 1) \,, \qquad\qquad n \in \mathbb{N} \,, \tag{3.4.11}$$

see also [44, 53] and reference therein. For a fixed value of t, we denote by $\{\sigma_n\}_{n\geqslant 0}$ the solution to (3.4.11). These give the energy spectrum of the operator (3.4.3) via the quantum Matone relation (3.4.10).

Implementing the four-dimensional limit (3.4.1) on the eigenfunction expression appearing on the right-hand side of (3.3.35) gives (see section 3.4.1)

$$\sum_{k\in\mathbb{Z}}\left(\mathrm{e}^{\mathrm{J}(x,\mu+\mathrm{i}2\pi k,\xi,\hbar)}+\mathrm{e}^{\frac{\mathrm{i}}{\hbar}\frac{\pi^2}{2}+\frac{\pi x}{\hbar}+\mathrm{J}(-x-\mathrm{i}\pi,\mu+\mathrm{i}\pi+\mathrm{i}2\pi k,\xi,\hbar)}\right)\to\phi_1(x,\sigma,t)+\phi_2(x,\sigma,t)\,,\tag{3.4.12}$$

where[12]

$$\boxed{\phi_1(x,\sigma,t)=-\mathrm{i}\exp\left(\frac{\mathrm{i}}{4}\partial_\sigma F^{\mathrm{4d}}_{\mathrm{NS}}(\sigma,t)\right)t^{-\mathrm{i}\frac{x}{2}}\Gamma\left(\mathrm{i}\left(x+\sigma\right)\right)\Gamma\left(\mathrm{i}\left(x-\sigma\right)\right)Z^{\mathrm{2d/4d}}_{\mathrm{NS,inst}}\left(-x,\sigma,t\right)\,,}\tag{3.4.13}$$

$$\boxed{\phi_2(x,\sigma,t)=\phi_1(-x,\sigma,t)\left[\frac{\mathrm{e}^{-\frac{\mathrm{i}}{2}\partial_\sigma F^{\mathrm{4d}}_{\mathrm{NS}}(\sigma,t)}\left(\mathrm{e}^{2\pi x}-\mathrm{e}^{2\pi\sigma}\right)-\mathrm{e}^{\frac{\mathrm{i}}{2}\partial_\sigma F^{\mathrm{4d}}_{\mathrm{NS}}(\sigma,t)}\left(\mathrm{e}^{2\pi x}-\mathrm{e}^{-2\pi\sigma}\right)}{\mathrm{e}^{2\pi\sigma}-\mathrm{e}^{-2\pi\sigma}}\right]\,,}\tag{3.4.14}$$

with $Z^{\mathrm{2d/4d}}_{\mathrm{NS,inst}}$ denoting the instanton part of the NS function in the presence of a surface defect

$$Z^{\mathrm{2d/4d}}_{\mathrm{NS,inst}}\left(x,\sigma,t\right)=1+\left[\frac{1+2(\mathrm{i}x+1)}{(1+4\sigma^2)\left((\mathrm{i}x+1)^2+\sigma^2\right)}\right]t+\mathcal{O}\left(t^2\right).\tag{3.4.15}$$

Higher-order terms are provided in (A.3.31), while the full all-order definition is given in (A.3.29). We obtain then the following eigenfunction of (3.4.3)

$$\boxed{\phi(x,E,t)=\phi_1(x,\sigma,t)+\phi_2(x,\sigma,t)\,,}\tag{3.4.16}$$

where E and σ are related as in (3.4.10). Let us make some comments on the above result.

- The finite difference equation (3.4.3) has extensive families of formal solutions. For instance, both functions (3.4.14) and (3.4.13) are solutions to the Fourier transform Mathieu equation (3.4.3). Each of these functions is meromorphic, with poles located at $x=\pm\sigma+\mathrm{i}\ell$, where $\ell\in\mathbb{Z}$. However, what makes the solution (3.4.16) special is that in the summation, all poles cancel, yielding a final expression that is entire in x, even when evaluated at generic values of the energy. The factor in the square brackets in (3.4.14) is crucial for this to happen.

- Although the symmetric structure of the two contributions from (3.2.48) is lost in the 4d limit, the key feature that remains is that only the sum (3.4.16) of these two contributions is entire in x.

[12] The overall normalization $-\mathrm{i}\exp\left(\frac{\mathrm{i}}{4}\partial_\sigma F_{\mathrm{NS}}\left(\sigma,t\right)\right)$ was added so that the on-shell eigenfunctions are real.

- When we evaluate the above eigenfunctions (3.4.16), (3.4.14), (3.4.13) on-shell, i.e. on the locus (3.4.11), we obtain

$$\begin{aligned}\phi(x,E_n,t) = (-1)^n\, \mathrm{e}^{\mathrm{i}\frac{\pi}{2}n} t^{\frac{\mathrm{i}x}{2}}\, \Gamma\left(\mathrm{i}\left(-x+\sigma_n\right)\right) \Gamma\left(\mathrm{i}\left(-x-\sigma_n\right)\right) Z^{\text{2d/4d}}_{\text{NS,inst}}\left(x,\sigma_n,t\right) \\ + \mathrm{e}^{\mathrm{i}\frac{\pi}{2}n} t^{-\frac{\mathrm{i}x}{2}}\, \Gamma\left(\mathrm{i}\left(x+\sigma_n\right)\right) \Gamma\left(\mathrm{i}\left(x-\sigma_n\right)\right) Z^{\text{2d/4d}}_{\text{NS,inst}}\left(-x,\sigma_n,t\right)\,, \end{aligned} \tag{3.4.17}$$

  which is the well-known form of the eigenfunctions obtained in [27, 30, 32, 35, 36]. Notice that the relation between the two terms in (3.4.17) once again exhibits the same symmetry structure as in (3.2.48).

- Let us now consider the asymptotic behaviour of (3.4.14) and (3.4.13) for $\mathrm{Re}(x) \to \pm\infty$ with constant $\mathrm{Im}(x)$. The non-trivial asymptotics is determined by the part involving Γ functions as well as the term inside the square brackets in (3.4.14). For $\phi^{(1)}$, we get an exponential decay in both directions

$$\left|\phi^{(1)}\left(x+\mathrm{i}y,\sigma,t\right)\right| \propto \mathrm{e}^{\mp\pi x-(1+2y)\ln(\pm x)}\left(1+\mathcal{O}\left(\frac{1}{x}\right)\right)\,, \qquad x\to\pm\infty\,, \tag{3.4.18}$$

  for any constant $y \in \mathbb{R}$. For $\phi^{(2)}$, we have instead

$$\left|\phi^{(2)}\left(x+\mathrm{i}y,\sigma,t\right)\right| \propto \begin{cases} \left(\frac{\sinh\left(\frac{\mathrm{i}}{2}\partial_\sigma F^{\text{4d}}_{\text{NS}}(\sigma,t)\right)}{\mathrm{i}\sinh(2\pi\sigma)}\right) \mathrm{e}^{+\pi x-(1-2y)\ln(x)}\left(1+\mathcal{O}\left(\frac{1}{x}\right)\right)\,, & x\to+\infty \\ \left(\frac{\sinh\left(\frac{\mathrm{i}}{2}\partial_\sigma F^{\text{4d}}_{\text{NS}}(\sigma,t)-2\pi\sigma\right)}{\mathrm{i}\sinh(2\pi\sigma)}\right) \mathrm{e}^{+\pi x-(1-2y)\ln(-x)}\left(1+\mathcal{O}\left(\frac{1}{x}\right)\right)\,, & x\to-\infty \end{cases} \tag{3.4.19}$$

  for any constant $y \in \mathbb{R}$. The overall trigonometric terms come from the factor in square brackets in (3.4.14). Hence, the complete eigenfunction is square-integrable if and only if

$$\frac{\sinh\left(\frac{\mathrm{i}}{2}\partial_\sigma F^{\text{4d}}_{\text{NS}}\left(\sigma,t\right)\right)}{\mathrm{i}\sinh\left(2\pi\sigma\right)} = 0\,, \tag{3.4.20}$$

  which is precisely the vanishing of the Fredholm determinant (3.4.8).[13]

Derivation

Here we derive (3.4.12). We are interested in the standard 4d limit (3.4.1) of the eigenfunctions as they appear in terms of the gauge theory grand potential in (3.3.35). The scaling of the complex structure parameters as given in (3.4.1) corresponds to the following scaling of the Kähler parameters

$$t_B\left(\hbar\right) = -\ln\left(t\hbar^4\right) + 2\sigma\hbar\,, \qquad t_F\left(\hbar\right) = 2\sigma\hbar\,, \tag{3.4.21}$$

[13] Note that each of the two terms themselves are never square-integrable for all $y \in \mathbb{R}$ due to the simple poles at $x+\mathrm{i}y = \pm\sigma + \mathrm{i}k$ for $k \in \mathbb{Z}$.

and in addition, the negative sign of κ in (3.4.1) is reflected in a shift

$$t_{B,F}(\hbar) \to t_{B,F}(\hbar) - \mathrm{i}2\pi\,. \tag{3.4.22}$$

The standard 4d limit is then taking $\hbar \to 0$ from above while keeping $x_{4\mathrm{d}}$, σ and t fixed with $\mathrm{Re}(\sigma)$, $t > 0$.

We will not keep track of the overall normalization of the 5d eigenfunctions, since we didn't fix it in the first place. Hence, we can freely choose an overall normalization, and it turns out that normalizing the eigenfunctions (3.3.35) as

$$\mathrm{e}^{-\mathrm{J}(\mu,\xi,\hbar)} \sum_{k\in\mathbb{Z}} \left(\mathrm{e}^{\mathrm{J}(x,\mu+\mathrm{i}\pi(2k-1),\xi,\hbar)} + \mathrm{e}^{\frac{\mathrm{i}}{\hbar}\frac{\pi^2}{2}+\frac{\pi x}{\hbar}+\mathrm{J}(-x-\mathrm{i}\pi,\mu+\mathrm{i}\pi(2k),\xi,\hbar)} \right), \tag{3.4.23}$$

will be a convenient choice.[14]

Let us first look at the closed sector, closely following [41, 185]. One gets for the polynomial part of the closed grand potential (3.3.13)

$$\begin{aligned}\mathrm{J}_{\mathrm{p}}(\mu+\mathrm{i}\pi\ell,\xi,\hbar) - \mathrm{J}_{\mathrm{p}}(\mu,\xi,\hbar) = \\ \frac{\pi\ell^2\ln(t\hbar^4)}{2\hbar} - \mathrm{i}\frac{\pi^2\ell(2\ell^2-1)}{3\hbar} - \mathrm{i}\ell\sigma\ln\left(t\hbar^4\right) - 2\pi\ell^2\sigma + \mathcal{O}(\hbar)\,,\end{aligned} \tag{3.4.24}$$

where $\ell = 2k-1$ for the first term and $\ell = 2k$ for the second term. Hence, one can see that the dominating contributions in the sum over the shifts $k \in \mathbb{Z}$ are given by $k = 0, 1$ for the first term and by $k = 0$ term for the second term. One can already note that this gives a trivial closed sector contribution for the second term, due to our normalization. The 4d limit for the 1-loop and instanton part of the closed grand potential can be dealt with as done in [41, 185] and one finds

$$\begin{aligned}\mathrm{J}(\mu\pm\mathrm{i}\pi,\xi,\hbar) - \mathrm{J}(\mu,\xi,\hbar) = \\ \frac{\pi}{2}\frac{\ln(t\hbar^4)}{\hbar} \mp \mathrm{i}\frac{\pi}{2} \pm \frac{\mathrm{i}}{2}\partial_\sigma F^{4\mathrm{d}}_{\mathrm{NS}}(t,\sigma) - \ln\left(\mathrm{e}^{2\pi\sigma} - \mathrm{e}^{-2\pi\sigma}\right) + \mathcal{O}(\hbar)\,.\end{aligned} \tag{3.4.25}$$

where the 4d NS free energy is given in (3.4.9).

Let us now turn our attention to the open sector. The polynomial part of the open grand potential (3.3.23) can be dealt with straightforwardly. To take the standard 4d limit on the 1-loop part (3.3.24) it is useful to first use the quasi-periodicity of the quantum dilogarithm (A.2.12) to write[15]

$$\begin{aligned}\mathrm{J}^{\text{open}}_{\text{1-loop}}(x,\mu\pm\mathrm{i}\pi,\xi,\hbar) = -2\ln(\hbar) - \ln\left(x_{4\mathrm{d}}^2-\sigma^2\right) - 2\pi x_{4\mathrm{d}} + \ln\left(\mathrm{e}^{2\pi x_{4\mathrm{d}}} - \mathrm{e}^{\mp 2\pi\sigma}\right) + \\ \ln\Phi_\beta\left[\beta(\sigma - x_{4\mathrm{d}}) + \frac{\mathrm{i}}{2}\left(\beta^{-1}-\beta\right)\right] + \ln\Phi_\beta\left[\beta(-\sigma - x_{4\mathrm{d}}) + \frac{\mathrm{i}}{2}\left(\beta^{-1}-\beta\right)\right] + \mathcal{O}(\hbar)\,,\end{aligned} \tag{3.4.26}$$

[14] Interchanging the sum over k with the limit is quite subtle, since the sum is not always uniformly converging in x. However, we will not go into this issue and simply note that interchanging the sum and limit in this case gives a perfectly well-behaved answer in line with our expectations.

[15] When implementing the limit we assume for simplicity $2\,|\mathrm{Im}(x\pm\sigma)| < 1$. However, the final result extends to all values of x in the complex plane.

$$\mathrm{J}^{\text{open}}_{\text{1-loop}}(-x-\mathrm{i}\pi,\mu,\xi,\hbar)=-2\ln(\hbar)-\ln\left(x_{4\mathrm{d}}^2-\sigma^2\right)+$$
$$\ln\Phi_\beta\left[\beta\left(\sigma+x_{4\mathrm{d}}\right)+\frac{\mathrm{i}}{2}\left(\beta^{-1}-\beta\right)\right]+\ln\Phi_\beta\left[\beta\left(-\sigma+x_{4\mathrm{d}}\right)+\frac{\mathrm{i}}{2}\left(\beta^{-1}-\beta\right)\right]+\mathcal{O}(\hbar)\,, \tag{3.4.27}$$

with $\beta=\sqrt{\hbar/2\pi}$. In the end, we are interested in the exponential of the grand potential, so all equalities are modulo integer multiples of $\mathrm{i}2\pi$. Let us introduce a variable z which is

$$z=\frac{1}{2}\pm\mathrm{i}\left(x_{4\mathrm{d}}\pm\sigma\right)\,, \tag{3.4.28}$$

with the signs chosen independently and $2\left|\mathrm{Im}(x\pm\sigma)\right|<1$ or $0<\mathrm{Re}(z)<1$. To compute the expansion of the quantum dilogarithms in (3.4.26) and (3.4.27), we use the integral representations in (A.2.16) and (A.2.17). We find that

$$\ln\Phi_\beta\left(\frac{\mathrm{i}}{2}\beta^{-1}-\mathrm{i}\beta z+\mathcal{O}\left(\beta^3\right)\right)=$$
$$-\mathrm{i}\frac{\pi}{12\beta^2}+z\ln\left(2\pi\beta^2\right)-\frac{\ln(2\pi)}{2}+\mathrm{i}\frac{\pi}{2}z+\ln\Gamma\left(z+\frac{1}{2}\right)+\mathcal{O}\left(\beta^2\right)\,. \tag{3.4.29}$$

Combining the polynomial and 1-loop parts of the grand potential one finds

$$\mathrm{J}^{\text{open}}_{\mathrm{p}}(x,\xi,\hbar)+\mathrm{J}^{\text{open}}_{\text{1-loop}}(x,\mu\pm\mathrm{i}\pi,\xi,\hbar)=-\frac{\mathrm{i}\pi^2}{3\hbar}-\ln(2\pi\hbar)-\mathrm{i}\frac{\pi}{2}$$
$$+\ln\Gamma\left(\mathrm{i}\left(-x_{4\mathrm{d}}+\sigma\right)\right)+\ln\Gamma\left(\mathrm{i}\left(-x_{4\mathrm{d}}-\sigma\right)\right)+\mathrm{i}\frac{x_{4\mathrm{d}}}{2}\ln(t)+\ln\left(\mathrm{e}^{2\pi x_{4\mathrm{d}}}-\mathrm{e}^{\mp 2\pi\sigma}\right)+\mathcal{O}(\hbar) \tag{3.4.30}$$

$$\frac{\mathrm{i}}{\hbar}\frac{\pi^2}{2}+\frac{\pi}{\hbar}x+\mathrm{J}^{\text{open}}_{\mathrm{p}}(-x-\mathrm{i}\pi,\xi,\hbar)+\mathrm{J}^{\text{open}}_{\text{1-loop}}(-x-\mathrm{i}\pi,\mu,\xi,\hbar)=\frac{\pi}{2}\frac{\ln\left(t\hbar^4\right)}{\hbar}-\frac{\mathrm{i}\pi^2}{3\hbar}-\ln(2\pi\hbar)$$
$$+\ln\Gamma\left(\mathrm{i}\left(x_{4\mathrm{d}}+\sigma\right)\right)+\ln\Gamma\left(\mathrm{i}\left(x_{4\mathrm{d}}-\sigma\right)\right)-\mathrm{i}\frac{x}{2}\ln(t)+\mathcal{O}(\hbar)\,. \tag{3.4.31}$$

Regarding the instanton part for the open sector, one can see that the NS part is a rational function of $\exp\left(x-t_F/2\right)$, $\exp\left(-t_F\right)$ and $\exp\left(-t_B\right)$. Hence, the shifts of $t_{B,F}$ by $\mathrm{i}4\pi k$ act trivially, and the only difference between the first and second term is a change in the sign of x. The GV part, on the other hand, vanishes in the standard 4d limit. The resulting defect instanton partition function can be found in (A.3.34).

Hence, putting all parts of the grand potential for both the closed and open sectors together gives an overall divergent factor

$$\frac{\pi}{2}\frac{\ln\left(t\hbar^4\right)}{\hbar}-\frac{\mathrm{i}\pi^2}{3\hbar}-\ln(2\pi\hbar)\,, \tag{3.4.32}$$

so that, after appropriate normalization, (3.4.23) reduces to (3.4.14), (3.4.13) and (3.4.16) in the standard 4d limit (3.4.21).

3.4.2 The dual four-dimensional limit

A few years ago, [14, 63] showed that, starting from the quantum mirror curve (3.2.7), one can implement another scaling limit to connect with the four-dimensional gauge theory. In this limit, we take

$$4\xi = 4\pi \mathrm{i}\sigma - \frac{2\pi}{R}\ln\left(R^4 t\right)\,, \qquad \mathrm{e}^{-2\xi}\kappa = 2\cos(2\pi\sigma)\,, \qquad \hbar = \frac{4\pi^2}{R}\,, \tag{3.4.33}$$

and send $R \to 0$. One of the key differences between the limits (3.4.1) and (3.4.33) is that in (3.4.1), we take $\hbar \to 0$, whereas in (3.4.33), we take $\hbar \to \infty$. Hence, we refer to (3.4.33) as the "dual" four-dimensional limit.

Applying the scaling (3.4.33) and taking the limit $R \to 0$ on the operator kernel (3.2.12) yields the integral operator $\rho_{\mathrm{GV}} : \; L^2(\mathbb{R}) \to L^2(\mathbb{R})$ with kernel [14]

$$\rho_{\mathrm{GV}}\left(q,p\right) = \frac{\mathrm{e}^{-4t^{1/4}\cosh q}\mathrm{e}^{-4t^{1/4}\cosh p}}{\cosh\left(\frac{q-p}{2}\right)}\,, \tag{3.4.34}$$

and we look for square-integrable eigenfunctions

$$\int_{\mathbb{R}} \mathrm{d}p\; \rho_{\mathrm{GV}}(q,p)\widehat{\varphi}_n(p,\widehat{E}_n,t) = \widehat{E}_n\widehat{\varphi}_n(q,\widehat{E}_n,t)\,. \tag{3.4.35}$$

Interestingly, (3.4.34) first appeared in the literature in the 1970s in studies of the 2d Ising model and the theory of Painlevé equations, see [58, 61, 72, 186]. We will refer to it as McCoy-Tracy-Wu operator. The connection between the quantum mirror curve (3.2.7) and the Painlevé kernel (3.4.34) made it possible to prove the TS/ST correspondence for local $\mathbb{F}_0$ in this particular dual 4d limit [14]. See also [15] for the generalization to all $Y^{N,0}$ geometries.

The spectral problem (3.4.35) was solved in [1], where it was shown that the eigenfunctions can be explicitly computed using the partition function of four-dimensional, $\mathcal{N}=2$, SU (2) supersymmetric Yang-Mills theory in the GV (or self-dual) phase of the Ω-background ($-\epsilon_1 = \epsilon_2 = 1$), with the inclusion of a surface defect. More precisely we have [1]

$$\begin{aligned}\widehat{\varphi}(q,\widehat{E}_n,t) = \int_{\mathbb{R}} \mathrm{d}x\; \mathrm{e}^{\mathrm{i}2qx}\sum_{k\in\mathbb{Z}}\Bigg(&Z^{\mathrm{2d/4d}}_{\mathrm{GV}}\left(x,k+\frac{1}{2}+\mathrm{i}\widehat{\sigma}_n,t\right)Z^{\mathrm{4d}}_{\mathrm{GV}}\left(k+\frac{1}{2}+\mathrm{i}\widehat{\sigma}_n,t\right)\\ &+Z^{\mathrm{2d/4d}}_{\mathrm{GV}}\left(-x-\frac{\mathrm{i}}{2},k+\mathrm{i}\widehat{\sigma}_n,t\right)Z^{\mathrm{4d}}_{\mathrm{GV}}\left(k+\mathrm{i}\widehat{\sigma}_n,t\right)\Bigg)\,,\end{aligned} \tag{3.4.36}$$

$$\widehat{E}_n = 2\pi\,\mathrm{sech}\left(2\pi\widehat{\sigma}_n\right)\,, \tag{3.4.37}$$

where the gauge theory partition function of the defect is given by (2.6.4), (2.6.1),

$$Z^{\mathrm{2d/4d}}_{\mathrm{GV}}(x,\sigma,t) = t^{\mathrm{i}\frac{x}{2}}\Gamma\left(-\mathrm{i}x-\sigma+\frac{1}{2}\right)\Gamma\left(-\mathrm{i}x+\sigma+\frac{1}{2}\right)Z^{\mathrm{2d/4d}}_{\mathrm{GV,inst}}(x,\sigma,t)\,, \tag{3.4.38}$$

$$Z^{\text{2d/4d}}_{\text{GV,inst}}(x,\sigma,t) = 1 - \left[\frac{\widetilde{x}}{2\sigma^2\left(\widetilde{x}^2-\sigma^2\right)}\right] t + \left[\frac{\widetilde{x}\left(\widetilde{x}+1\right)^2 - \widetilde{x}\left(10\widetilde{x}^2+19\widetilde{x}+10\right)\sigma^2 + \left(8\widetilde{x}^2+30\widetilde{x}+9\right)\sigma^4}{4\sigma^4\left(4\sigma^2-1\right)^2\left(\widetilde{x}^2-\sigma^2\right)\left(\left(\widetilde{x}+1\right)^2-\sigma^2\right)}\right] t^2 + \mathcal{O}\left(t^3\right) , \quad (3.4.39)$$

with $\widetilde{x} = \mathrm{i}x + 1/2$ and higher orders in the t expansion can be found from the definition (A.3.32). The $\widehat{\sigma}_n \in \mathbb{R} \setminus \{0\}$ are solutions to (2.3.8)

$$\sum_{k\in\mathbb{Z}} Z^{\text{4d}}_{\text{GV}}\left(k+\frac{1}{2}+\mathrm{i}\widehat{\sigma}_n, t\right) = 0\,, \quad (3.4.40)$$

and $Z^{\text{4d}}_{\text{GV}}(\sigma,t)$ is the Nekrasov function in the GV-phase of the Ω-background (2.3.10)

$$Z^{\text{4d}}_{\text{GV}}(\sigma,t) = \frac{t^{\sigma^2}}{G(1-2\sigma)G(1+2\sigma)}\left(1+\frac{t}{2\sigma^2}+\frac{\left(8\sigma^2+1\right)t^2}{4\sigma^2\left(4\sigma^2-1\right)^2}+\mathcal{O}(t^3)\right) , \quad (3.4.41)$$

with G the Barnes G-function, and higher orders in the instanton expansion can be found in (A.3.33) and according to (A.3.32). The Fourier transform in (3.4.36) can be interpreted exactly as in (3.4.5). Indeed, we can represent the kernel (3.4.34) in operator form as

$$\mathrm{e}^{-4t^{1/4}\cosh\hat{q}}\frac{1}{\cosh\left(\frac{\hat{p}}{2}\right)}\mathrm{e}^{-4t^{1/4}\cosh\hat{q}}\,, \qquad [\hat{q},\hat{p}] = \mathrm{i}2\pi\,. \quad (3.4.42)$$

By exchanging momentum and position operator according to the transformation

$$\begin{pmatrix}\hat{x}\\ \hat{y}\end{pmatrix} = \begin{pmatrix}0 & \frac{1}{4\pi}\\ -4\pi & 0\end{pmatrix}\begin{pmatrix}\hat{q}\\ \hat{p}\end{pmatrix} , \quad (3.4.43)$$

we obtain the Fourier transformed operator whose eigenfunctions are given by

$$\varphi(x,\widehat{E}_n,t) = \sum_{k\in\mathbb{Z}}\left(Z^{\text{2d/4d}}_{\text{GV}}\left(x,k+\frac{1}{2}+\mathrm{i}\widehat{\sigma}_n,t\right)Z^{\text{4d}}_{\text{GV}}\left(k+\frac{1}{2}+\mathrm{i}\widehat{\sigma}_n,t\right) + Z^{\text{2d/4d}}_{\text{GV}}\left(-x-\frac{\mathrm{i}}{2},k+\mathrm{i}\widehat{\sigma}_n,t\right)Z^{\text{4d}}_{\text{GV}}\left(k+\mathrm{i}\widehat{\sigma}_n,t\right)\right) . \quad (3.4.44)$$

3.4.3 Relating modified Mathieu to McCoy-Tracy-Wu

From the preceding discussion, we see that:

1. The eigenfunctions and spectrum of the (Fourier transformed) modified Mathieu operator (3.4.4) are determined by gauge theory partition functions in the NS phase of the Ω background.

2. The eigenfunctions and spectrum of the (Fourier transformed) McCoy–Tracy–Wu operator (3.4.34) are determined by gauge theory partition functions in the GV phase of the Ω background.

It was first shown in [111], based on [110],[16] that these two phases of the Ω background can be related by using the Nakajima-Yoshioka blowup equations [188]. This relation was extended to partition functions in the presence of surface defects in [112, 113]. It is therefore natural to ask whether we can relate the eigenfunctions and the spectra of (3.4.4) and (3.4.34).

The spectrum

For the modified Mathieu equation the spectrum E_n is given in terms of σ_n (3.4.10), which is a solution of (3.4.11) [22], while for the McCoy-Tracy-Wu operator the spectrum $\widehat{E}_n$ is given in terms of $\widehat{\sigma}_n$ (3.4.37), which is a solution of (3.4.40) [14]. Using the NS limit of blowup equations without defects, it follows that solutions of (3.4.11) are mapped to solutions of (3.4.40), that is [111, 115]

$$\sigma_n = \widehat{\sigma}_n \,. \tag{3.4.45}$$

This gives a direct, but non-trivial relation between the spectra of the two operators above, namely

$$\boxed{\begin{array}{ll} \text{modified Mathieu:} & E_n = -t\partial_t F^{\text{4d}}_{\text{NS}}\left(\sigma_n, t\right) \\ \text{McCoy-Tracy-Wu:} & \widehat{E}_n = 2\pi\,\text{sech}(2\pi\sigma_n) \end{array}} \,. \tag{3.4.46}$$

Note that the relation between the energy and σ is much simpler in the McCoy-Tracy-Wu case. The spectra of the two operators are hence related by

$$E_n = -t\partial_t F^{\text{4d}}_{\text{NS}}\left(\frac{1}{2\pi}\text{arcsech}\left(\frac{\widehat{E}_n}{2\pi}\right), t\right) \,. \tag{3.4.47}$$

Let us emphasize that much of the derivation of (3.4.47) from [14, 41, 115] is fully rigorous, as it is based on several well-established results: the AGT correspondence [85], which was later proven in [189, 190]; the Kyiv formula for the Painlevé tau function [191], subsequently proven in [68, 69, 148]; the Nakajima–Yoshioka blowup relation derived and proven in [188]; the special solution to the Painlevé III_3 equation constructed in [58, 59]; and the convergence of the NS function [192]. While many of these results were originally conjectural, they have all been proven by now. What is not rigorously established yet is that $\widehat{\sigma}_n = (1/2\pi)\,\text{arcsech}(\widehat{E}_n/2\pi)$ with $\widehat{E}_n \in]0, 2\pi[$ lies within the radius of convergence of $t\partial_t F^{\text{4d}}_{\text{NS}}\left(\widehat{\sigma}_n, t\right)$[17].

The eigenfunctions

One can verify that the modified Mathieu and the McCoy–Tracy–Wu operators commute. Since the modified Mathieu operator possesses a self-adjoint, trace-class inverse, and the

[16] In [110], the relationship between GV invariants and the NS phase of the Ω-background was used to express the quantization condition of [4] in a more symmetric form [187].

[17] We recall that $F^{\text{4d}}_{\text{NS}}(\sigma, t)$ is defined by a power series in t, whose radius of convergence is finite and may depend on σ.

McCoy–Tracy–Wu operator is itself self-adjoint and trace-class, it follows that they admit a common L^2-orthonormal basis of eigenfunctions. Indeed, we can also check numerically, that

$$\boxed{\frac{\phi(x,E_n,t)}{\phi(x_0,E_n,t)}=\frac{\varphi(x,\widehat{E}_n,t)}{\varphi(x_0,\widehat{E}_n,t)}} \tag{3.4.48}$$

where $\varphi(x,\widehat{E}_n,t)$ are the Fourier transformed eigenfunctions of the McCoy-Tracy-Wu operator in (3.4.44), $\phi(x,E_n,t)$ are the Fourier transformed eigenfunctions of the modified Mathieu operator (3.4.16) and x_0 is some arbitrary point which is not a zero of the eigenfunctions. The equality (3.4.48) should follow from taking the NS limit of the blowup equations in the presence of surface defect [112]. A detailed study will appear elsewhere. Note that for (3.4.48) to hold, we must evaluate both sides on-shell, i.e. at (3.4.46), (3.4.11). For generic values of E, $\widehat{E}$ (3.4.48) does not hold.

The operators

Let us now use the relation between the spectrum and the eigenfunctions of the modified Mathieu operator (3.4.4) and McCoy-Tracy-Wu operator (3.4.34) to find a relation between the operators themselves. To avoid subtleties related to the domain of definition, it is convenient to work with bounded operators.

We denote by $\rho_{\rm NS}$ the trace class inverse of the modified Mathieu operator[18]

$$-\frac{1}{4}\partial_q^2+\sqrt{t}(\mathrm{e}^{2q}+\mathrm{e}^{-2q})\,. \tag{3.4.49}$$

As discussed previously, the modified Mathieu operator and $\rho_{\rm GV}$ admit a common basis of eigenfunctions. Consequently, the same holds for $\rho_{\rm NS}$ and $\rho_{\rm GV}$. Hence, by employing their spectral decompositions together with the relation between their spectra given in (3.4.47), it follows immediately that

$$\boxed{\rho_{\rm NS}=\mathfrak{F}\left(\rho_{\rm GV}\right)\,,} \tag{3.4.50}$$

$$\boxed{\mathfrak{F}\ :\ \Sigma\left(\rho_{\rm GV}\right)\to\Sigma\left(\rho_{\rm NS}\right)\ :\ E\mapsto\left(-t\partial_t F^{\rm 4d}_{\rm NS}\left(\frac{1}{2\pi}\mathrm{arcsech}\left(\frac{E}{2\pi}\right),t\right)\right)^{-1}\,,} \tag{3.4.51}$$

where $F^{\rm 4d}_{\rm NS}$ is defined by (3.4.9) and (A.3.28), $\Sigma\left(\rho\right)\subset\mathbb{R}_{\geqslant 0}$ is the spectrum of ρ, and $\mathfrak{F}\left(\rho\right)$ should be understood in the functional calculus sense [193, def. 7.13]. Note that $\mathfrak{F}$ is strictly increasing on $\Sigma\left(\rho_{\rm GV}\right)$, hence $\mathfrak{F}^{-1}$ is also well-defined on $\Sigma\left(\rho_{\rm NS}\right)$.

3.5 Outlook and open questions

Many open questions remain; we summarize some of them below.

[18] There is a factor of 2 multiplying q compared to (3.4.4), which arises from the factor of 2 in the unitary transformation of the eigenfunctions in (3.4.36).

- Non-perturbative effects in the context of the closed TS/ST correspondence have been analysed from a resurgence perspective in [169, 181, 194–199], see [176] for a review and a more exhaustive list of references. It would be interesting to explore the open version of the TS/ST correspondence through the lens of resurgence, particularly the role that the special combinations (3.3.35) and (3.4.16) may play in the context of exact WKB [197, 198, 200–202], as well as the connection with quantum modularity [203].

- In subsection 3.4.3, we numerically demonstrated an explicit relation between the on-shell eigenfunctions of the modified Mathieu operator and the McCoy-Tracy-Wu operator. It should be possible to derive this relation analytically using blowup equations in the presence of surface defects. The proof will appear elsewhere.

- Over the years, many formal solutions to the functional difference equation (3.2.3) have been constructed using topological string/gauge theory partition functions. However, most of these proposals are not well-defined for $\hbar \in \mathbb{R}_{>0}$ and, moreover, they do not satisfy the analytic properties required for the eigenfunctions of the relativistic Toda lattice, discussed below (3.2.3). To our knowledge, the only exceptions are [6, 7, 32].

  The constructions in [6, 7] are specific to the self-dual point $\hbar = 2\pi$ with $\xi = 0$. Our proposal naturally reduces to theirs when these parameter values are imposed.

  On the other hand, the connection to [32] is less straightforward. A key distinction between (3.3.35) and the eigenfunctions in [32] is that our functions in (3.3.35) remain entire even off-shell, whereas those in [32] exhibit poles at specific values of x. It would be interesting to understand this better, e.g. via blowup equations.

- In the closed version of the TS/ST correspondence, the sum over integers on the right-hand side of (3.1.3) has an interpretation in the context of q-isomonodromic tau functions [64]. It would be interesting to explore whether the special combinations of the two terms in (3.3.35) carry any particular meaning from the perspective of q-isomonodromic deformations.

- Another point for future investigation is the relation to fibre-base duality, i.e. invariance under exchange of t_B and t_F. This corresponds to the transformation $\xi, \kappa \to -\xi, \mathrm{e}^{-2\xi}\kappa$ at the level of the complex moduli. One can verify that the Fredholm determinant (3.1.3) remains invariant under this duality. It would be interesting to explore how this duality manifests at the level of the special eigenfunctions (3.3.35) we constructed.

See also the conclusion and outlook in chapter 5.

Chapter 4

Eigenfunctions of finite difference Schrödinger equations

Building on the previous two chapters and [6, 7], we now turn our attention to finite difference analogues of the Schrödinger equation with an arbitrary polynomial potential. These operators are quantized Seiberg-Witten curves of four-dimensional, $\mathcal{N} = 2$, SU(N) SYM and the eigenfunctions are given in terms of the partition functions in the Nekrasov-Shatashvili limit. This chapter bundles work that originally appeared in [3], which is joint work with Alba Grassi and Tommaso Pedroni.

4.1 Introduction

Exactly solvable models have been playing a central role in quantum mechanics, providing profound insights into its mathematical structure and phenomenology. Over the past decade, advances in topological string theory and supersymmetric gauge theory have uncovered many new examples of solvable quantum spectral problems, often arising from the quantization of mirror curves; see [175, 176] for a review and a list of references. Regarding quantities that encode the energy spectrum (such as exact quantization conditions, Fredholm determinants and spectral traces) the situation is now well understood for operators associated with mirror curves of arbitrary genus. In contrast, much less is known about the corresponding eigenfunctions, particularly for mirror curves of genus greater than one, which are related to gauge theories with higher-rank gauge groups.

We will consider the finite difference operator

$$\mathrm{H}_N = 2\Lambda^N \cosh(\mathrm{p}) + V_N(\mathrm{x})\,, \qquad [\mathrm{x},\mathrm{p}] = \mathrm{i}\hbar\,, \tag{4.1.1}$$

where $V_N(x) = \sum_{k=0}^{N-1}(-1)^k h_k\, x^{N-k}$ is a generic polynomial potential of degree N. This system can be regarded as a deformation of the standard quantum-mechanical anharmonic oscillator

$$\mathrm{p}^2 + V_N(\mathrm{x})\,, \qquad [\mathrm{x},\mathrm{p}] = \mathrm{i}\hbar\,. \tag{4.1.2}$$

As we will show, the deformation (4.1.1) has a remarkable property: it defines a spectral problem that is exactly solvable in terms of explicit analytic functions. This stands in sharp contrast to the quantum anharmonic oscillator (4.1.2), for which no explicit, closed-form analytic expressions for the eigenfunctions are known[1].

The exact solvability of (4.1.1) originates from a beautiful connection with supersymmetric gauge theory. In particular, the operator (4.1.1) can be identified with a quantization[2] of the Seiberg–Witten (SW) curve associated with four-dimensional $\mathcal{N} = 2$, SU(N) super Yang–Mills (SYM) theory [8, 22, 23, 56]. This correspondence provides access to powerful tools from supersymmetric localization [22] and topological string theory [4], enabling the explicit computation of spectral quantities via Nekrasov–Shatashvili (NS) functions. By contrast, from the perspective of supersymmetric QFT, the differential operator (4.1.2) is related to Argyres–Douglas theories [31, 46, 206, 207], which are non-Lagrangian. Consequently, at present there is no known analogue of NS functions for these theories, and explicit closed-form expressions for the eigenfunctions and other spectral quantities remain out of reach (for progress in this direction, see e.g. [44, 208–212]).

The deformed Hamiltonian (4.1.1) was first analysed in [55] and later in [41], where an exact quantization condition for the energy spectrum, together with the associated Fredholm determinant, was derived. Interestingly, the same deformed Hamiltonian also appears in the context of the $T\bar{T}$ deformation [213]. In this work, we provide explicit analytic formulas for the eigenfunctions of the operator (4.1.1), valid for arbitrary polynomial potentials $V_N(x)$ and capturing both bound and resonant states.

The eigenvalue equation associated with the Hamiltonian (4.1.1) is the finite-difference equation

$$\Lambda^N \left(\psi(x + \mathrm{i}\hbar, \boldsymbol{h}) + \psi(x - \mathrm{i}\hbar, \boldsymbol{h})\right) + V_N(x)\psi(x, \boldsymbol{h}) = E\psi(x, \boldsymbol{h})\,. \tag{4.1.3}$$

Difference equations of this type typically admit many formal solutions. The solutions we construct are singled out by the following properties:

1. For *generic* values of the parameters h_k and the energy E, our solutions solve (4.1.3) and are entire in x. It is worth emphasizing that this is highly non-trivial for a finite-difference equation. In our construction, the entireness ultimately follows from background independence in topological string theory: the special eigenfunctions we construct arise as specific limits of non-perturbative open topological string partition functions, obtained via the open topological string/spectral theory (TS/ST) correspondence [2, 6, 7]. We refer to these as *off-shell* eigenfunctions. Their explicit expressions are given in (4.2.25) for N even and in (4.2.31) for N odd.

[1] One notable exception occurs when $N = 6$ and the potential takes the form $V_6(x) = x^6 + 2b\,x^4 + \big(b^2 - (4m + 2p + 3)\big)x^2$, with $m \in \mathbb{N}_{>0}$ and $p \in \{0, 1\}$. In this case, certain special eigenfunctions can be constructed explicitly; see, e.g. [204].

[2] When quantizing such a curve [8, 23, 56], one must decide which variable plays the role of position and which that of its conjugate momentum. Our convention differs from the standard one by a Fourier transform; as a result, the quantized curve is a difference equation rather than a higher order differential equation [48, 205].

2. For generic values of E, the off-shell solutions are not square-integrable. They become L^2-normalizable (physical) eigenfunctions only at the discrete set of energies $\{E_k\}_{k\geqslant 0}$ determined by the quantization condition of [55]. We refer to the eigenfunctions evaluated at these energies as *on-shell* eigenfunctions.

3. As noted in [55], the deformed Hamiltonian (4.1.1) displays several novel features not present in the standard Schrödinger Hamiltonian (4.1.2).

   For instance, when N is even, (4.1.1) admits degenerate ground states at special values of the moduli h_k. Moreover, the oscillation theorem [214, thm. 3.5] that applies to the standard Hamiltonian (4.1.2) no longer holds for the deformed Hamiltonian (4.1.1).

   Similarly, when N is odd, there are specials values of the moduli h_k for which (4.1.1) admits L^2-normalizable eigenfunctions with real energies, even tough the potential is unbounded from below.

Let us also note that the difference equation (4.1.3) arises in the integrability context as the Baxter equation of the N-particle closed quantum Toda lattice [27, 215–218]. In that setting, one imposes very specific boundary conditions on the solutions, beyond just square-integrability. As a consequence, the solutions considered in [27, 215–218] exist only at special values of the parameters h_k with $k = 2, \cdots, N$. We will return to this point in section 4.3.

4.2 The spectral problem and its solution

4.2.1 The spectral problem

We consider the following quantum Hamiltonian[3]:

$$\mathrm{H}_N = \Lambda^N \left(\mathrm{e}^{\mathrm{p}} + \mathrm{e}^{-\mathrm{p}}\right) + V_N(\mathrm{x})\,, \qquad [\mathrm{x},\mathrm{p}] = \mathrm{i}\hbar\,, \qquad \Lambda, \hbar \in \mathbb{R}_{>0}\,, \tag{4.2.1}$$

where the potential takes the form

$$V_N(x) = \sum_{k=0}^{N-1} (-1)^k\, h_k\, x^{N-k}\,, \qquad h_k \in \mathbb{R}\,, \tag{4.2.2}$$

and, without loss of generality, we set $h_1 = 0$ and $h_0 = 1$. The eigenvalue equation associated with (4.2.1) is a difference equation and reads[4]

$$\Lambda^N \left(\psi(x + \mathrm{i}\hbar, \boldsymbol{h}) + \psi(x - \mathrm{i}\hbar, \boldsymbol{h})\right) + V_N(x)\psi(x, \boldsymbol{h}) = E\psi(x, \boldsymbol{h})\,, \tag{4.2.3}$$

[3]The restriction $\Lambda, \hbar \in \mathbb{R}_{>0}$ and $h_k \in \mathbb{R}$ is not essential: the solutions we construct remain well-defined even for other choices of the parameters. However, this assumption simplifies the discussion of the operator's spectral properties, and we will adopt this convention.

[4]To simplify notation, we suppress the explicit dependence of the eigenfunctions on Λ and $\hbar$.

where $\boldsymbol{h}$ contains $h_2, \cdots, h_N$ with

$$h_N = (-1)^{N-1} E\,, \tag{4.2.4}$$

and E plays the role of energy. We remark that the nature of this equation depends on whether N is even or odd.

N even: confining potential. When N is even, the potential $V_N(x)$ is confining. For $h_k \in \mathbb{R}$, the operator H_N is self-adjoint, with domain given by the Friedrichs extension of

$$\{\, \psi \in L^2(\mathbb{R}) \mid \psi \in D_1 \cap D_2 \,\}\,, \tag{4.2.5}$$

where

$$D_1 = \left\{ \psi \in L^2(\mathbb{R}) \;\middle|\; V_N(x)\psi\,(x) \in L^2(\mathbb{R}) \right\}\,, \tag{4.2.6}$$

and D_2 consists of all $\psi \in L^2(\mathbb{R})$ that admit an analytic continuation to the strip

$$\{\, x \in \mathbb{C} \mid |\mathrm{Im}(x)| < \hbar \,\}, \tag{4.2.7}$$

such that $\psi(x + \mathrm{i}y) \in L^2(\mathbb{R})$ for all fixed $-\hbar < y < \hbar$, and for which the limits

$$\lim_{y \to \hbar^-} \psi(x \pm \mathrm{i}y) \tag{4.2.8}$$

exist in the sense of convergence in $L^2(\mathbb{R})$. It was shown in [125], based on [12], that H_N has a purely discrete spectrum corresponding to bound states. Numerically, the spectrum and eigenfunctions can be computed via Hamiltonian truncation in the harmonic oscillator basis.

N odd: unbounded potential. When N is odd, the potential $V_N(x)$ is confining as $x \to +\infty$ but unbounded from below as $x \to -\infty$. As a consequence, the spectrum of H_N generically contains resonances with complex energies. Such potentials have been studied numerically for the standard Schrödinger equation (4.1.2) using the method of complex dilation [219], and rigorous analyses of resonances are available in [220–222]. As emphasized in [55], complex dilation can be applied directly to the deformed Hamiltonian (4.2.1); this is the numerical method we adopt here. Let us briefly recall the main idea. For N odd, the eigenfunctions of (4.2.1) decay only as a power law as $x \to -\infty$. Consequently, numerical diagonalization in the harmonic oscillator basis converges poorly since Hamiltonian truncation is best suited to exponentially decaying wavefunctions. Therefore, to improve convergence, we perform a small complex rotation of the position and momentum operators by an angle θ. This yields the rotated Hamiltonian

$$\mathrm{H}_{N,\theta} = 2\Lambda^N \cosh\!\left(\mathrm{e}^{-\mathrm{i}\theta}\mathrm{p}\right) + V_N(\mathrm{e}^{\mathrm{i}\theta}\mathrm{x})\,, \tag{4.2.9}$$

which admits exponentially decaying, square-integrable eigenfunctions

$$\psi_n^{(\theta)}(x, \boldsymbol{h}) \tag{4.2.10}$$

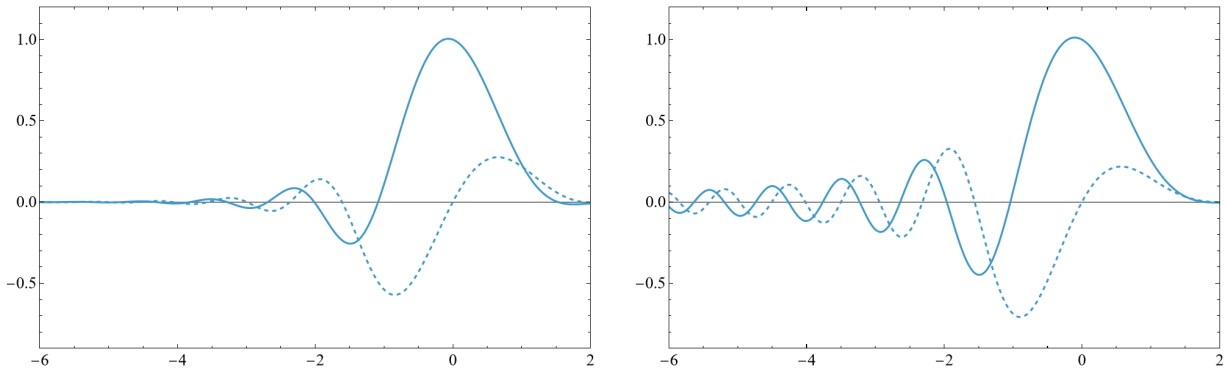

Figure 4.1. Numerical ground state eigenfunction ($E_0 \approx 0.54151 + \mathrm{i}\,0.25905$) of (4.2.1) with $V_3(x) = x^3$, obtained via complex dilation. Left: rotated eigenfunction $\psi_0^\theta(x, \boldsymbol{h})$. Right: true eigenfunction $\psi_0(x, \boldsymbol{h}) = \psi_0^\theta(\mathrm{e}^{-\mathrm{i}\theta}x, \boldsymbol{h})$. Here we set $\Lambda = 1/2$, $\hbar = 1$ and $\theta = -1/10$. The eigenfunction is normalized so that $\psi_0(0, \boldsymbol{h}) = 1$. Solid lines denote the real part; dashed lines denote the imaginary part.

with complex eigenvalues. Therefore, $\psi_n^{(\theta)}(x, \boldsymbol{h})$ can be computed efficiently by diagonalizing (4.2.9) in the harmonic oscillator basis. The eigenfunctions of the original Hamiltonian (4.2.1) are then obtained by analytic continuation:

$$\psi_n(x, \boldsymbol{h}) = \psi_n^{(\theta)}(\mathrm{e}^{-\mathrm{i}\theta}x, \boldsymbol{h})\,. \tag{4.2.11}$$

An explicit example is shown in figure 4.1 for the cubic potential $V_3(x) = x^3$. One observes the exponential decay of the rotated eigenfunctions (4.2.10) (left), in contrast with the slower power-law decay of the true eigenfunctions (4.2.11) (right). In the next section, we construct explicit solutions to (4.2.3) for arbitrary N. These solutions are entire in x for generic values of the energy E and of the potential parameters h_k, $k = 2, \ldots, N-1$, and we refer to them as *off-shell* eigenfunctions. As we will see, such solutions become square-integrable wavefunctions only when E satisfies an appropriate quantization condition. The corresponding eigenfunctions, evaluated at these discrete energy values, will be denoted as *on-shell* eigenfunctions.

4.2.2 The generalized Matone relations

The explicit construction of our eigenfunctions is based on the open TS/ST correspondence [2, 6, 7]. A key lesson from studying spectral problems through the lens of supersymmetric gauge theory and topological strings is that eigenfunctions — and spectral quantities more generally — take a simpler form when written in terms of the Coulomb branch (or Kähler) parameters $\{a_I\}_{I=1}^{N-1}$, rather than the complex moduli $\{h_k\}_{k=2}^{N}$ that appear in the potential. The map relating the two sets of parameters has a precise geometrical meaning: it is known as the quantum mirror map [8, 23, 24]. In the framework of five-dimensional $\mathcal{N} = 1$ supersymmetric gauge theory, the inverses of these maps are interpreted as Wilson

loops expectation values [29, 79], and in the four-dimensional limit they reduce to the (generalized) Matone relations [55, 99, 100]. At leading order in Λ, we have

$$\boxed{h_k = s_{(1^k)}(a_I) + \mathcal{O}\big(\Lambda^N\big)\,,} \tag{4.2.12}$$

where s_R denotes the Schur polynomial associated with the Young tableau R, and (1^k) refers to the tableau consisting of k rows and k boxes. We refer to (4.2.12) as generalized Matone relation. Explicit examples are:

$$\begin{aligned} h_2 &= -\frac{1}{2}\sum_{I=1}^{N} a_I^2 + \mathcal{O}(\Lambda^N)\,, \\ h_3 &= \frac{1}{3}\sum_{I=1}^{N} a_I^3 + \mathcal{O}(\Lambda^N)\,, \\ h_4 &= \frac{1}{8}\left(\left(\sum_{I=1}^{N} a_I^2\right)^2 - 2\sum_{I=1}^{N} a_I^4\right) + \mathcal{O}(\Lambda^N)\,. \end{aligned} \tag{4.2.13}$$

The complete expression for the map, including all orders in Λ (which also depend on $\hbar$), is reviewed in section A.3.3; see in particular equation (A.3.52). One can invert (4.2.12), (A.3.52) and obtain an expression for a_I as a function of h_k, Λ and $\hbar$. Geometrically, the quantities $a_I(\boldsymbol{h}, \Lambda, \hbar)$, for $I = 1, \ldots, N-1$, represent the quantum A-periods associated with the SW curve

$$2\Lambda^N \cosh(p) + V_N(x) = E, \qquad x, p \in \mathbb{C}\,, \tag{4.2.14}$$

see [8, 23, 24].

4.2.3 The eigenfunctions

In this section, we present an explicit, analytic and exact expression for the eigenfunctions of (4.2.3). As noted in the introduction, (4.2.3) coincides with a quantization of the SW curve (4.2.14) describing the low-energy dynamics of four-dimensional $\mathcal{N} = 2$, SU(N) SYM. It is therefore natural to expect that the eigenfunctions inherit an SU(N) structure. We thus begin by recalling a few representation-theoretic notions related to SU(N).

Let $\mathcal{W}_N$ denote the Weyl group of SU(N). Consider a vector

$$\boldsymbol{v} = \sum_{I=1}^{N} v_I\, \boldsymbol{e}_I\,, \tag{4.2.15}$$

where $\boldsymbol{e}_I$ are the weights of the fundamental representation (see section A.4 for our conventions). The Weyl orbit of $\boldsymbol{v}$ is defined by

$$\mathcal{W}_N \cdot \boldsymbol{v} \;=\; \{\, w(\boldsymbol{v}) \mid w \in \mathcal{W}_N \,\}\,, \tag{4.2.16}$$

where the Weyl group acts on the weights of the fundamental representation $\boldsymbol{e}_I$ by permutation. We define

$$\boldsymbol{\gamma} = \frac{1}{2}\sum_{I=1}^{N}(-1)^{I-1}\boldsymbol{e}_I = \sum_{k=1}^{N-1}(-1)^{k-1}\boldsymbol{\lambda}_k\,, \tag{4.2.17}$$

where $\boldsymbol{\lambda}_k$ is a fundamental weight (A.4.1), and organize the Coulomb branch parameters a_I of $\mathcal{N}=2$, SU(N) SYM into the vector

$$\boldsymbol{a} = \sum_{I=1}^{N} a_I \boldsymbol{e}_I\,, \qquad\qquad \sum_{I=1}^{N} a_I = 0\,. \tag{4.2.18}$$

The parameters $a_I \equiv a_I(h_2,\cdots,h_N,\Lambda,\hbar)$ provide a convenient way to encode the potential parameters h_k, as explained around (4.2.12) and (A.3.52). It is also useful to introduce the linear map

$$\boldsymbol{r}(\boldsymbol{a}) = -\sum_{I=1}^{N} a_{N-I+1}\,\boldsymbol{e}_I\,. \tag{4.2.19}$$

The starting point of our construction is the so-called defect partition function:

$$\boxed{Z_D(x,\boldsymbol{a},\Lambda,\hbar) = \left(\frac{\Lambda}{\hbar}\right)^{\mathrm{i}N\frac{x}{\hbar}} \mathrm{e}^{\pi\left(1+\frac{N}{2}\right)\frac{x}{\hbar}} \left\{\prod_{I=1}^{N}\Gamma\left(\mathrm{i}\left(\frac{\boldsymbol{e}_I\cdot\boldsymbol{a}-x}{\hbar}\right)\right)\right\} Z_D^{\mathrm{inst}}\left(x,\boldsymbol{a},\Lambda,\hbar\right)\,,} \tag{4.2.20}$$

where the instanton part Z_D^{inst} is defined in (A.3.44). It is known [27–30, 32, 33] that this function provides a formal solution to the difference equation (4.2.3). However, Z_D as in (4.2.20) is not entire in x since it has poles at

$$x = a_I + \mathrm{i}\hbar k\,, \qquad\qquad k\in\mathbb{Z}\,, \qquad\qquad I\in\{1,\ldots,N\}\,. \tag{4.2.21}$$

Hence, one cannot use only the function (4.2.20) to construct square integrable eigenfunctions. In what follows, we will combine two copies of (4.2.20) with an additional function in such a way that the resulting expression becomes entire in x for *arbitrary* values of a_I, and hence *arbitrary* values of h_k. The function we shall use is

$$\boxed{\mathcal{P}_{\boldsymbol{n}}(x,\boldsymbol{a},\Lambda,\hbar) = \frac{\mathrm{e}^{\left(\frac{\mathrm{i}}{\hbar}\partial_{\boldsymbol{a}}F_{\mathrm{NS}} - \pi\frac{\boldsymbol{a}}{\hbar}\mathbb{1}_{2\mathbb{N}+1}(N)\right)\cdot\boldsymbol{n}}}{\prod_{\boldsymbol{\alpha}\in\Delta_+}\left(2\sinh\left(\frac{\pi\boldsymbol{a}\cdot\boldsymbol{\alpha}}{\hbar}\right)\right)^{(\boldsymbol{n}\cdot\boldsymbol{\alpha})^2}} \prod_{I=1}^{N}\left(1-\mathrm{e}^{\frac{2\pi}{\hbar}(\boldsymbol{a}\cdot\boldsymbol{e}_I-x)}\right)^{\frac{1}{2}-n_I}\,,} \tag{4.2.22}$$

$$\boldsymbol{n} = \sum_{I=1}^{N} n_I\boldsymbol{e}_I\,, \qquad\qquad n_I\in\left\{-\frac{1}{2},+\frac{1}{2}\right\}\,, \tag{4.2.23}$$

where $\mathbb{1}_{2\mathbb{N}+1}(N)$ is the indicator function vanishing for N even, Δ_+ is the set of positive roots (A.4.3), the $\boldsymbol{e}_I$ are the weights of the fundamental representation in (A.4.1), and $\boldsymbol{n}$

is a particular element in the weight lattice, see later. The dual quantum period is given by[5]

$$\frac{\mathrm{i}}{\hbar}\partial_{\boldsymbol{a}}F_{\mathrm{NS}} = \sum_{I=1}^{N}\frac{\mathrm{i}}{\hbar}\frac{\partial F_{\mathrm{NS}}^{\mathrm{inst}}}{\partial a_I}\boldsymbol{e}_I - \sum_{\boldsymbol{\alpha}\in\Delta_+}\left[\mathrm{i}\,\frac{\pi}{2} + \mathrm{i}\,2\left(\boldsymbol{\alpha}\cdot\frac{\boldsymbol{a}}{\hbar}\right)\ln\left(\frac{\Lambda}{\hbar}\right) + \ln\left(\frac{\Gamma\left(1-\mathrm{i}\left(\boldsymbol{\alpha}\cdot\frac{\boldsymbol{a}}{\hbar}\right)\right)}{\Gamma\left(1+\mathrm{i}\left(\boldsymbol{\alpha}\cdot\frac{\boldsymbol{a}}{\hbar}\right)\right)}\right)\right]\boldsymbol{\alpha} \tag{4.2.24}$$

where $F_{\mathrm{NS}}^{\mathrm{inst}}$ is defined in (A.3.41). Note that the difference equation (4.2.3) acts trivially on the functions $\mathcal{P}_{\boldsymbol{n}}$ (4.2.22).

Using the building blocks (4.2.20) and (4.2.22), we obtain the following entire, off-shell solutions to the difference equation (4.2.3).

N even: confining potential. For N even, where the potential is confining, we have:

$$\begin{aligned}\psi_N^{\mathrm{even}}(x,\boldsymbol{h}) = Z_D(x,\boldsymbol{a},\Lambda,\hbar)\sum_{\boldsymbol{n}\in\mathcal{W}_N\cdot\boldsymbol{\gamma}}\mathcal{P}_{\boldsymbol{n}}(x,\boldsymbol{a},\Lambda,\hbar)\\ +\mathrm{i}\,\mathrm{e}^{\frac{2\pi x}{\hbar}}Z_D(-x,\boldsymbol{r}(\boldsymbol{a}),\Lambda,\hbar)\sum_{\boldsymbol{n}\in\mathcal{W}_N\cdot(\boldsymbol{\gamma}+\boldsymbol{e}_N)}\mathcal{P}_{\boldsymbol{n}}(-x,\boldsymbol{r}(\boldsymbol{a}),\Lambda,\hbar)\,,\end{aligned} \tag{4.2.25}$$

where we recall that $\boldsymbol{r}(\boldsymbol{a})$ is defined in (4.2.19), and $\boldsymbol{a}$ is related to $\boldsymbol{h}$ via the generalized Matone relations; see (4.2.12) and (A.3.52).[6] We will refer to the first and second terms in (4.2.25) as saddles, reflecting their origin in topological string theory [2, 6, 7], see section 4.4.

Let us now analyse the asymptotic behaviour of (4.2.25). For N even, the Weyl orbit of $\boldsymbol{\gamma}$ contains $\binom{N}{N/2}$ elements, while the orbit of $\boldsymbol{\gamma}+\boldsymbol{e}_N$ contains $\binom{N}{N/2-1}$ elements. Moreover, in this case the number of non-trivial factors appearing in the product in (4.2.22) equals $N/2$ for elements in the orbit of $\boldsymbol{\gamma}$, and $N/2-1$ for those in the orbit of $\boldsymbol{\gamma}+\boldsymbol{e}_N$. This leads to the following exponentially growing behaviour as $x\to+\infty$:

$$\psi_N^{\mathrm{even}}(x,\boldsymbol{h}) \simeq \mathrm{e}^{\frac{\pi|x|}{\hbar}}\left(\frac{2\pi\hbar}{|x|}\right)^{\frac{N}{2}}u_N(x)\sum_{\boldsymbol{n}\in\mathcal{W}_N\cdot\boldsymbol{\gamma}}\frac{\exp\left(\frac{\mathrm{i}}{\hbar}\,\partial_{\boldsymbol{a}}F_{\mathrm{NS}}\cdot\boldsymbol{n}\right)}{\prod_{\boldsymbol{\alpha}\in\Delta_+}\left(2\sinh\left(\frac{\pi\boldsymbol{a}\cdot\boldsymbol{\alpha}}{\hbar}\right)\right)^{(\boldsymbol{n}\cdot\boldsymbol{\alpha})^2}}\,, \tag{4.2.26}$$

where $u_N(x)$ is an x-dependent factor of unit modulus,

$$u_N(x) = \mathrm{e}^{\mathrm{i}\frac{\pi}{4}N}\left(\frac{\mathrm{e}\,\Lambda\,\hbar}{|x|}\right)^{\mathrm{i}N\frac{|x|}{\hbar}}\,. \tag{4.2.27}$$

[5] The derivatives w.r.t a_I are taken before imposing the constraint $\sum_{I=1}^{N}a_I=0$.

[6] Note that $\mathcal{W}_N\cdot\boldsymbol{\gamma}=\mathcal{W}_N\cdot\boldsymbol{\lambda}_{N/2}$ and $\mathcal{W}_N\cdot(\boldsymbol{\gamma}+\boldsymbol{e}_N)=\mathcal{W}_N\cdot\boldsymbol{\lambda}_{(N/2)+1}$ for N even, with $\boldsymbol{\lambda}_{N/2},\boldsymbol{\lambda}_{(N/2)+1}\in\Lambda_w$ fundamental weights.

On the other hand, as $x \to -\infty$, we obtain exponential suppression:

$$\psi_N^{\text{even}}(x,\boldsymbol{h}) \simeq \mathrm{e}^{-\frac{\pi|x|}{\hbar}} \left(\frac{2\pi\hbar}{|x|}\right)^{\frac{N}{2}} \left(u_N^{-1}(x) \sum_{\boldsymbol{n}\in\mathcal{W}_N\cdot\boldsymbol{\gamma}} \frac{\exp\left(\frac{\mathrm{i}}{\hbar}\,\partial_{\boldsymbol{a}} F_{\text{NS}}\cdot\boldsymbol{n}\right)}{\prod_{\boldsymbol{\alpha}\in\Delta_+}\left(2\sinh\left(\frac{\pi\boldsymbol{a}\cdot\boldsymbol{\alpha}}{\hbar}\right)\right)^{(\boldsymbol{n}\cdot\boldsymbol{\alpha})^2}} \right.$$
$$\left. \cdot \prod_{I=1}^{N} \left(-\mathrm{e}^{\frac{2\pi\boldsymbol{a}\cdot\boldsymbol{e}_I}{\hbar}}\right)^{\frac{1}{2}-n_I} + u_N(x) \sum_{\boldsymbol{n}\in\mathcal{W}_N\cdot(\boldsymbol{\gamma}+\boldsymbol{e}_N)} \frac{\exp\left(\frac{\mathrm{i}}{\hbar}\,\partial_{\boldsymbol{r}(\boldsymbol{a})} F_{\text{NS}}\cdot\boldsymbol{n}\right)}{\prod_{\boldsymbol{\alpha}\in\Delta_+}\left(2\sinh\left(\frac{\pi\boldsymbol{r}(\boldsymbol{a})\cdot\boldsymbol{\alpha}}{\hbar}\right)\right)^{(\boldsymbol{n}\cdot\boldsymbol{\alpha})^2}} \right) . \tag{4.2.28}$$

Therefore, although (4.2.25) is entire in x, it is generically not square-integrable unless we impose:

$$\sum_{\boldsymbol{n}\in\mathcal{W}_N\cdot\boldsymbol{\gamma}} \exp\left(\tfrac{\mathrm{i}}{\hbar}\,\partial_{\boldsymbol{a}} F_{\text{NS}}\cdot\boldsymbol{n}\right) \prod_{\boldsymbol{\alpha}\in\Delta_+}\left(2\sinh\left(\tfrac{\pi\boldsymbol{a}\cdot\boldsymbol{\alpha}}{\hbar}\right)\right)^{-(\boldsymbol{n}\cdot\boldsymbol{\alpha})^2} \;=\; 0\,, \tag{4.2.29}$$

which coincides with the quantization condition obtained in [55] by explicitly constructing the Fredholm determinant. Note that, we are implicitly using the generalized Matone relations (4.2.12) to write $\boldsymbol{a} = \boldsymbol{a}(\boldsymbol{h})$. Hence, (4.2.29) is a quantization condition for the energy E. After imposing this condition, the on-shell eigenfunctions at $x \to +\infty$ behave as:

$$\psi_N^{\text{even}}(x,\boldsymbol{h})\Big|_{(4.2.29)} \simeq \mathrm{e}^{-\frac{\pi|x|}{\hbar}} \left(\frac{2\pi\hbar}{|x|}\right)^{\frac{N}{2}} \left(u_N(x)c_N^{(1)}(\boldsymbol{a},\Lambda,\hbar) + u_N^{-1}(x)c_N^{(2)}(\boldsymbol{a},\Lambda,\hbar)\right)\Big|_{(4.2.29)}\,, \tag{4.2.30}$$

for some coefficients $c_N^{(i)}$ which can be easily obtained from (4.2.25).

N odd: unbounded potential. For N odd, the potential is unbounded from below as $x \to -\infty$ and we find the following entire off-shell solution to (4.2.3):

$$\boxed{\begin{aligned}\psi_N^{\text{odd}}(x,\boldsymbol{h}) = Z_D(x,\boldsymbol{a},\Lambda,\hbar) \sum_{\boldsymbol{n}\in\mathcal{W}_N\cdot\boldsymbol{\gamma}} \mathcal{P}_{\boldsymbol{n}}(x,\boldsymbol{a},\Lambda,\hbar) \\ + \mathrm{e}^{\frac{\pi x}{\hbar}} Z_D(-x,\boldsymbol{r}(\boldsymbol{a}),\Lambda,\hbar) \sum_{\boldsymbol{n}\in\mathcal{W}_N\cdot\boldsymbol{\gamma}} \mathcal{P}_{\boldsymbol{n}}(-x,\boldsymbol{r}(\boldsymbol{a}),\Lambda,\hbar)\,,\end{aligned}} \tag{4.2.31}$$

where, again, we recall that $\boldsymbol{r}(\boldsymbol{a})$ is defined in (4.2.19) and $\boldsymbol{a}$ is related to $\boldsymbol{h}$ via the generalized Matone relations; see (4.2.12).[7] Once more, we will refer to the first and second terms in (4.2.31) as saddles. Let us now analyse the asymptotic behaviour of this solution. For N odd, the Weyl orbit of $\boldsymbol{\gamma}$ contains $\binom{N}{(N-1)/2}$ elements. In this case, the number of non-trivial factors appearing in the product in equation (4.2.22) is $(N-1)/2$. Hence, as $x \to +\infty$ we obtain the following exponentially growing behaviour:

$$\psi_N^{\text{odd}}(x,\boldsymbol{h}) \simeq \mathrm{e}^{\frac{\pi|x|}{\hbar}} \left(\frac{2\pi\hbar}{|x|}\right)^{\frac{N}{2}} u_N(x) \sum_{\boldsymbol{n}\in\mathcal{W}_N\cdot\boldsymbol{\gamma}} \frac{\exp\left(\left(\frac{\mathrm{i}}{\hbar}\,\partial_{\boldsymbol{a}} F_{\text{NS}} - \frac{\pi\boldsymbol{a}}{\hbar}\right)\cdot\boldsymbol{n}\right)}{\prod_{\boldsymbol{\alpha}\in\Delta_+}\left(2\sinh\left(\frac{\pi\boldsymbol{a}\cdot\boldsymbol{\alpha}}{\hbar}\right)\right)^{(\boldsymbol{n}\cdot\boldsymbol{\alpha})^2}}\,. \tag{4.2.32}$$

[7] Note that $\mathcal{W}_N\cdot\boldsymbol{\gamma} = \mathcal{W}_N\cdot\boldsymbol{\lambda}_{(N+1)/2}$ for N odd, with $\boldsymbol{\lambda}_{(N+1)/2} \in \Lambda_w$ a fundamental weight.

On the other hand, we find a power-law decay when $x \to -\infty$,

$$\psi_N^{\text{odd}}(x, \boldsymbol{h}) \simeq \left(\frac{2\pi\hbar}{|x|}\right)^{\frac{N}{2}} u_N(x) \sum_{\boldsymbol{n}\in\mathcal{W}_N\cdot\boldsymbol{\gamma}} \frac{\exp\left(\left(\frac{\mathrm{i}}{\hbar}\partial_{\boldsymbol{f}(\boldsymbol{a})}F_{\text{NS}} - \frac{\pi \boldsymbol{f}(\boldsymbol{a})}{\hbar}\right)\cdot\boldsymbol{n}\right)}{\prod_{\boldsymbol{\alpha}\in\Delta_+}\left(2\sinh\left(\frac{\pi \boldsymbol{f}(\boldsymbol{a})\cdot\boldsymbol{\alpha}}{\hbar}\right)\right)^{(\boldsymbol{n}\cdot\boldsymbol{\alpha})^2}}\,. \tag{4.2.33}$$

Let us emphasize that, although the behaviour at $x \to -\infty$ is only power-law, it is still square-integrable. In contrast, the exponential growth at $x \to +\infty$ must be eliminated to achieve square-integrability, which requires imposing:

$$\sum_{\boldsymbol{n}\in\mathcal{W}_N\cdot\boldsymbol{\gamma}} \frac{\exp\left(\left(\frac{\mathrm{i}}{\hbar}\,\partial_{\boldsymbol{a}}F_{\text{NS}} - \frac{\pi\boldsymbol{a}}{\hbar}\right)\cdot\boldsymbol{n}\right)}{\prod_{\boldsymbol{\alpha}\in\Delta_+}\left(2\sinh\left(\frac{\pi\boldsymbol{a}\cdot\boldsymbol{\alpha}}{\hbar}\right)\right)^{(\boldsymbol{n}\cdot\boldsymbol{\alpha})^2}} = 0\,. \tag{4.2.34}$$

Once again, this is precisely the quantization condition found in [55]. After imposing this condition, we find that as $x \to +\infty$:

$$\psi_N^{\text{odd}}(x, \boldsymbol{h})\Big|_{(4.2.34)} \simeq \mathrm{e}^{-\frac{\pi|x|}{\hbar}} \left(\frac{2\pi\hbar}{|x|}\right)^{\frac{N}{2}} \left(u_N(x)c_N^{(3)}(\boldsymbol{a}, \Lambda, \hbar) + u_N^{-1}(x)c_N^{(4)}(\boldsymbol{a}, \Lambda, \hbar)\right)\Big|_{(4.2.34)}\,, \tag{4.2.35}$$

for some coefficients $c_N^{(i)}$ which can be easily worked out from (4.2.25).

We conclude this section with a few remarks on the expressions (4.2.25) and (4.2.31).

1. Whereas the Schrödinger equation (4.2.1) admits only entire solutions, this is not the case for the difference equations associated with the deformed operator (4.1.1). For instance, each of the two terms in (4.2.25) and (4.2.31) is, by itself, a solution of (4.2.3), but each presents poles at

$$x = a_I + \mathrm{i}\hbar n, \quad n \in \mathbb{Z}. \tag{4.2.36}$$

   Only for the special linear combinations (4.2.25) and (4.2.31) do these poles cancel, yielding a function that is entire in x[8] for generic values of the parameters h_k, $i = 2, \ldots, N$.

2. As noted in [55], there are special values of the moduli h_k, those corresponding to eigenvalues of the quantum Toda Hamiltonians, at which the spectrum and eigenfunctions exhibit striking features. For N even, certain eigenstates, including the ground state, become degenerate, i.e. tunnelling is suppressed at these special points. A similar phenomenon occurs for N odd. For generic values of h_k, the energies associated with square-integrable solutions are complex. Nevertheless, at these special values of h_k, the eigenfunctions exhibit enhanced exponential decay as $x \to -\infty$, and the corresponding energies are real, despite the potential being unbounded from below. We will return to these special points in section 4.3.

[8] Although we do not have a rigorous proof of this statement, we have tested it for $N = 2, 3, 4, 5, 6$ up to three orders in the Λ expansion.

3. Another noteworthy property of the deformed Hamiltonian (4.2.3) is that its bound states violate the standard oscillation theorem [214, thm. 3.5]. For the deformed Schrödinger equation (4.2.3) it is no longer true that the n^{th} eigenfunction has n zeroes, even if the potential is confining. This behaviour occurs even for the simplest potential $V_2(x) = x^2$, see [2].[9] This violation is evident from the oscillatory asymptotics (4.2.28) and (4.2.30), see also figure 4.4 for a graphical representation.

4. Eigenfunctions are defined up to an overall normalization. In our conventions, we choose the normalization so that the asymptotic behaviour (4.2.26) and (4.2.32) reproduces the Fredholm determinant of the corresponding spectral problem as computed in [41, 55]. This choice is natural from the perspective of the TS/ST correspondence, where eigenfunctions are required to be entire both in the open and closed string moduli. However, as we discuss in section 4.3, this normalization is not convenient for studying the Toda points.

5. By evaluating (4.2.25) for $N = 2$ we recover [2, eq. (4.16)].

6. For N odd, the asymptotic expression (4.2.33) exhibits an outgoing oscillatory behaviour as $x \to -\infty$, characteristic of resonant states (see also figure 4.2).

4.2.4 Examples

Cubic potentials

Let us consider the $N = 3$ case:

$$\mathrm{H}_3 = 2\,\Lambda^3 \cosh(\mathrm{p}) + \mathrm{x}^3 + h_2\,\mathrm{x}\,. \tag{4.2.37}$$

The potential is unbounded from below, and for generic values of h_k the spectrum contains resonant states with complex energies. Such resonances always occur in complex-conjugate pairs, and throughout this chapter we focus on those having a positive imaginary part of the energy. For $N = 3$, the Weyl orbit of $\boldsymbol{\gamma}$ is given by:

$$\mathcal{W}_N \cdot \boldsymbol{\gamma} = \left\{ \tfrac{1}{2}\big(\boldsymbol{e}_1 - \boldsymbol{e}_2 + \boldsymbol{e}_3\big),\ \tfrac{1}{2}\big(\boldsymbol{e}_1 + \boldsymbol{e}_2 - \boldsymbol{e}_3\big),\ \tfrac{1}{2}\big(-\boldsymbol{e}_1 + \boldsymbol{e}_2 + \boldsymbol{e}_3\big) \right\}. \tag{4.2.38}$$

Examples of on-shell eigenfunctions are shown in figure 4.2, figure A.9, figure A.10 and figure A.11. In figure 4.2, we consider the case $h_2 = 0$ and focus on the third excited state, with complex energy:

$$E_3 \approx 3.951964 + \mathrm{i}\,4.473061\,. \tag{4.2.39}$$

Through the generalized Matone relations, this corresponds to:

$$a_1 \approx 1.473672 + \mathrm{i}\,0.395307, \quad a_2 \approx -0.394390 - \mathrm{i}\,1.473919. \tag{4.2.40}$$

[9] A similar phenomenon has been observed for difference equations arising in the context of the open TS/ST correspondence [2, 6, 7].

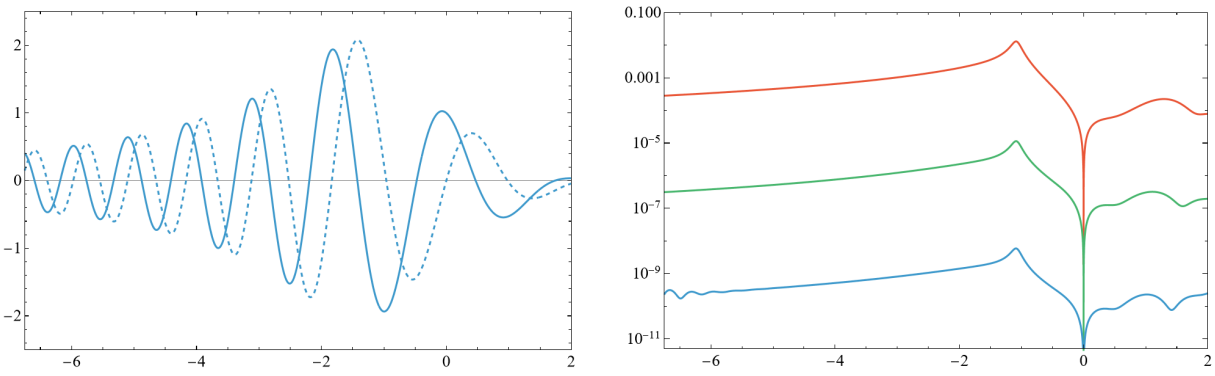

Figure 4.2. Left: third excited state of the $V_3(x)$ potential with $h_2 = 0$, $\hbar = 1$, and $\Lambda = \frac{1}{2}$. Dashed lines denote the imaginary part of the eigenfunction, while solid lines denote the real part. Right: difference between the numerical eigenfunction and the analytic expression from (4.2.25). The coloured curves show the effect of including an increasing number of terms in the Λ-expansion of the eigenfunction: red (0 terms), green (1 term), blue (2 terms).

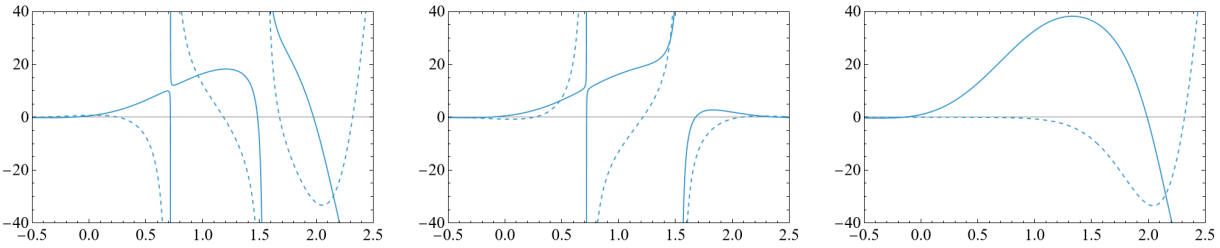

Figure 4.3. Off-shell eigenfunction of the potential $V_3(x)$ with $h_2 = -4$, $h_3 = -2.5$, $\hbar = 1$ and $\Lambda = 2/5$. From left to right: first saddle, second saddle and the full eigenfunction given by (4.2.31). Dashed lines denote the imaginary part, while solid lines denote the real part.

The power-law decay of the on-shell wavefunctions as $x \to -\infty$ is particularly evident in this figure. Similarly, figure A.9, figure A.10 and figure A.11 illustrate the ground, first and second excited state for $h_2 = -5$, $h_2 = -3$ and $h_2 = 2$ respectively.

Each figure shows excellent agreement between the analytic expression (4.2.31) and the numerical results obtained via complex dilation. In addition, figure A.10 clearly shows the cancellation of poles between the two terms in (4.2.31). Finally, an example of off-shell eigenfunction is shown in figure 4.3. The figure also clearly shows that each individual saddle in (4.2.25) develops poles, whereas the complete sum is free of singularities. Since we are off-shell, the resulting eigenfunction does not belong to $L^2(\mathbb{R})$.

Quartic potentials

Let us consider the $N = 4$ Hamiltonian:

$$\mathrm{H}_4 = 2\,\Lambda^4 \cosh(\mathrm{p}) + \mathrm{x}^4 + h_2\,\mathrm{x}^2 - h_3\,\mathrm{x}\,. \tag{4.2.41}$$

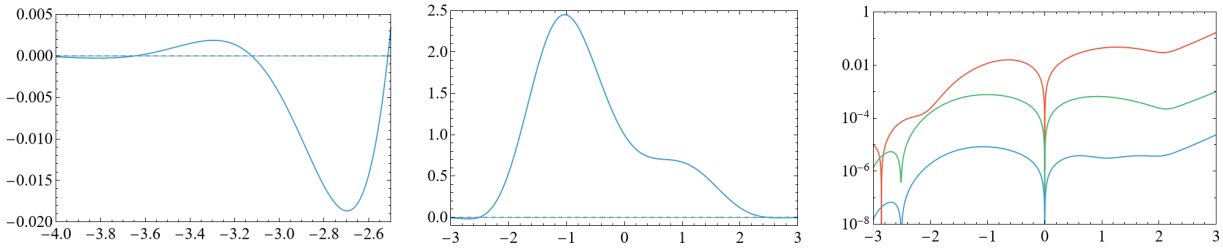

Figure 4.4. The ground state of the $V_4(x)$ potential with $h_2 = -3$, $h_3 = -0.1$, $\Lambda = (1/2)^{1/2}$ and $\hbar = 1$; the corresponding energy is $E_0 \approx -0.527521$. Dashed lines represent the imaginary part of the eigenfunction, while solid lines represent the real part. Left: illustration of the failure of the oscillation theorem. Centre: eigenfunction obtained from (4.2.25). Right: difference between the numerical eigenfunction and the analytic expression from (4.2.25). The coloured curves show the effect of including an increasing number of terms in the Λ-expansion of the eigenfunction: red (0 terms), green (1 term), blue (2 terms).

In this case, the potential is confining and the operator has a purely real and discrete spectrum, corresponding to bound states. The Weyl orbits of $\boldsymbol{\gamma}$ and $\boldsymbol{\gamma} + \boldsymbol{e}_N$ are, respectively:

$$\begin{aligned}\mathcal{W}_N \cdot \boldsymbol{\gamma} = \Big\{ &\frac{1}{2}(\boldsymbol{e}_1 - \boldsymbol{e}_2 + \boldsymbol{e}_3 - \boldsymbol{e}_4),\ \frac{1}{2}(\boldsymbol{e}_1 - \boldsymbol{e}_2 - \boldsymbol{e}_3 + \boldsymbol{e}_4),\\ &\frac{1}{2}(\boldsymbol{e}_1 + \boldsymbol{e}_2 - \boldsymbol{e}_3 - \boldsymbol{e}_4),\ \frac{1}{2}(-\boldsymbol{e}_1 + \boldsymbol{e}_2 + \boldsymbol{e}_3 - \boldsymbol{e}_4),\\ &\frac{1}{2}(-\boldsymbol{e}_1 + \boldsymbol{e}_2 - \boldsymbol{e}_3 + \boldsymbol{e}_4),\ \frac{1}{2}(-\boldsymbol{e}_1 - \boldsymbol{e}_2 + \boldsymbol{e}_3 + \boldsymbol{e}_4)\Big\},\end{aligned} \tag{4.2.42}$$

$$\begin{aligned}\mathcal{W}_N \cdot (\boldsymbol{\gamma} + \boldsymbol{e}_N) = \Big\{ &\frac{1}{2}(\boldsymbol{e}_1 - \boldsymbol{e}_2 + \boldsymbol{e}_3 + \boldsymbol{e}_4),\ \frac{1}{2}(\boldsymbol{e}_1 + \boldsymbol{e}_2 - \boldsymbol{e}_3 + \boldsymbol{e}_4),\\ &\frac{1}{2}(\boldsymbol{e}_1 + \boldsymbol{e}_2 + \boldsymbol{e}_3 - \boldsymbol{e}_4),\ \frac{1}{2}(-\boldsymbol{e}_1 + \boldsymbol{e}_2 + \boldsymbol{e}_3 + \boldsymbol{e}_4)\Big\}.\end{aligned} \tag{4.2.43}$$

Examples of on-shell solutions are shown in figure 4.4, figure A.12 and figure A.13. In figure 4.4, we exhibit the ground state eigenfunction for $h_2 = -3$ and $h_3 = -0.1$, corresponding to the eigenvalue:

$$E_0 \approx -0.527521. \tag{4.2.44}$$

Through the generalized Matone relations, this corresponds to:

$$a_1 \approx 0.446118, \qquad a_2 \approx 1.656437, \qquad a_3 \approx -1.694744. \tag{4.2.45}$$

In this figure, the quartic potential is a slight deformation of the symmetric double well (the symmetric case has $h_2 < 0$ and $h_3 = 0$), and the corresponding ground state clearly reflects this small asymmetry. Similarly, figure A.12 and figure A.13 show the first and second excited state for $h_2 = 3.5$, $h_3 = 0$ and $h_2 = 1.2$, $h_3 = -4.7$, respectively. Again,

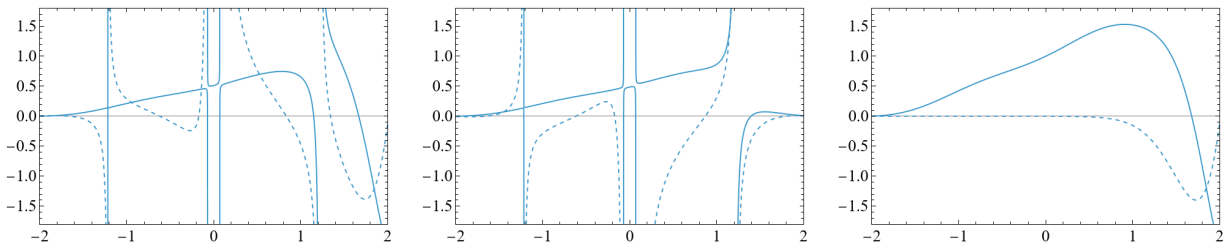

Figure 4.5. Off-shell eigenfunction of the potential $V_4(x)$ with $h_2 = -1.6$, $h_3 = 0.45$, $h_4 = 0.06$, $\hbar = 1$ and $\Lambda = 13/23$. From left to right: first saddle, second saddle and the full eigenfunction given by (4.2.25). Dashed lines represent the imaginary part, while solid lines the real part.

each figure shows excellent agreement between the analytic expression (4.2.25) and the results obtained by numerically diagonalizing the Hamiltonian (4.2.41). The cancellation of poles is clearly visible for the on-shell eigenfunction in figure A.12 and in the off-shell eigenfunction in figure 4.5. In the latter case, the resulting eigenfunction does not belong to $L^2(\mathbb{R})$, being off-shell.

4.3 Comments on the Toda points

So far, we have discussed the spectral problem (4.2.3) from the standpoint of standard quantum mechanics, wherein one first constructs entire off-shell solutions and then imposes square-integrability as a boundary condition.

However, there is another way to view (4.2.3), namely from the perspective of integrability. Indeed, the difference equation (4.2.3) is closely related to the Baxter equation for the quantum SU(N) Toda lattice [215–218], namely

$$(\mathrm{i}\Lambda)^N Q(x+\mathrm{i}\hbar) + (-\mathrm{i}\Lambda)^N Q(x-\mathrm{i}\hbar) - V_N(x)Q(x) = EQ(x)\,. \tag{4.3.1}$$

In this setting, one looks for entire solutions to (4.3.1) such that:

$$Q(x) \in L^2(\mathbb{R}) \quad \text{with} \quad Q(x) \simeq \mathrm{e}^{-\frac{N\pi}{2\hbar}|x|}, \qquad x \to \pm\infty\,. \tag{4.3.2}$$

By defining:

$$Q(x) = \left(\sum_{n_i \in S} d_i \mathrm{e}^{-\frac{2\pi x n_i}{\hbar}}\right) \mathrm{e}^{-\frac{\pi(N+2)}{2\hbar}x}\psi(x)\,, \quad S \subset \mathbb{Z}, \quad d_i \in \mathbb{C}\,, \tag{4.3.3}$$

it is easy to show that $Q(x)$ solves (4.3.1) for any choice of $S \subset \mathbb{Z}$. However, the mapping between the Baxter solution (4.3.2) and our solutions (4.2.25), (4.2.31) requires a particular choice of S. We will address this question in a separate work [223].

Nevertheless, even after taking (4.3.3) into account, one can see that for generic values of the potential parameters h_k ($k = 1, \ldots, N-1$), the on-shell eigenfunctions (4.2.25) and

(4.2.31) do not reproduce (4.3.2). For odd N, this follows directly from the fact that the asymptotics of (4.2.31) are outgoing with power-law decay on one side and exponentially decaying on the other, with a rate which is independent on N. Likewise, for N even, this follows from the fact that the decay behaviour of (4.2.25) as $x \to \pm\infty$ is the same for both plus and minus infinity, and it is independent of N. This is in line with the works of [215–218], where they found that eigenfunctions satisfying (4.3.2) exist only for special values of the moduli h_k, $k = 2, \ldots, N$. We refer to these distinguished values as *Toda points* and denote them by h_k^{T}, $k = 2, \ldots, N$. This, in turn, means that for (4.3.2) to hold, one must impose simultaneously $N-1$ quantization conditions, thereby quantizing all the h_k, $k = 2, \ldots, N$. This was nicely illustrated in [218]. From the gauge theory perspective, it was found in [22, 24, 27] that the quantization conditions determining the Toda points are (following the notation of [55]):

$$\frac{\mathrm{i}}{\hbar}\frac{\partial F_{\mathrm{NS}}}{\partial \boldsymbol{a}} = \mathrm{i}2\pi\boldsymbol{\ell} + \mathrm{i}\pi\boldsymbol{\rho}\,, \tag{4.3.4}$$

where $\boldsymbol{\ell}$ encodes the quantum numbers,

$$\boldsymbol{\ell} = \sum_{k=1}^{N-1} \ell_k \boldsymbol{\lambda}_k\,, \qquad \ell_k \in \mathbb{N}\,, \qquad \boldsymbol{\rho} = \sum_{I=1}^{N} (N-I)\,\boldsymbol{e}_I\,, \tag{4.3.5}$$

and $\boldsymbol{\rho}$ is a constant vector. It is important to note that (4.3.4) is a vector equation: it consists of $N-1$ quantization conditions for the a_I, the corresponding solutions being denoted by $\boldsymbol{a}(\boldsymbol{\ell})$. After using the generalized Matone relations (4.2.12) and (A.3.52), these translate into $N-1$ quantization conditions for the complex moduli h_k, $k = 2, \ldots, N$. In other words, it constrains the h_k to lie at the Toda points, which we denote by $h_k^{\mathrm{T}}(\boldsymbol{\ell})$. This stands in sharp contrast with standard quantum mechanics, where square-integrability imposes only a single quantization condition, namely (4.2.29) for N even and (4.2.34) for N odd. This condition quantises the energy E, while the other parameters h_k, $k = 2, \ldots, N-1$, in the potential remain free. However, as shown in [55], if the h_k satisfy the Toda quantization conditions (4.3.4), they automatically satisfy the quantum mechanical quantization conditions (4.2.29), (4.2.34). Hence, the Toda points correspond to special loci in our quantum mechanical problem, where eigenfunctions have an enhanced decay. As discussed above, this enhancement also comes together with some interesting phenomena, such as degeneracies among bound states. It is then natural to ask how these phenomena are captured by our explicit eigenfunctions (4.2.25) and (4.2.31).

Let us first review what is known about the Toda eigenfunction (4.3.2) from a gauge-theoretic perspective. It was found in [27, 32] that, in gauge-theoretic language, the eigenfunctions of the Toda Baxter equation (4.3.1) take the form:

$$Q(x, \boldsymbol{h}^T(\boldsymbol{\ell})) = \mathrm{e}^{-\frac{\pi(N+2)}{\hbar}x} Z_D(x, \boldsymbol{a}(\boldsymbol{\ell}), \Lambda, \hbar) + \xi\, \mathrm{e}^{\frac{\pi(N+2)}{\hbar}x} Z_D(-x, -\boldsymbol{a}(\boldsymbol{\ell}), \Lambda, \hbar), \tag{4.3.6}$$

where $\boldsymbol{a}(\boldsymbol{\ell})$ are solutions to the $N-1$ quantization conditions (4.3.4). The factor ξ in (4.3.6) is an x-independent function that should ensure the cancellation of poles between

the two terms in (4.3.6). It was shown in [27] that the existence of such *x-independent function* is guaranteed only if $\boldsymbol{a} = \boldsymbol{a}(\boldsymbol{\ell})$, where $\boldsymbol{a}(\boldsymbol{\ell})$ are solutions to (4.3.4). For example, in the $SU(2)$ case there is only a single quantum number ℓ, and one finds:

$$\xi = (-1)^{\ell} \,. \tag{4.3.7}$$

Hence, we can see another important difference between (4.3.6) and (4.2.25), (4.2.31):

- Our eigenfunctions (4.2.25) and (4.2.31) are entire in x for generic values of $\boldsymbol{a}$, i.e. generic values of h_k, $k = 2, \ldots, N$. In this case, no quantization condition is required to guarantee pole cancellation. This is made possible by the x-dependent factor appearing inside the sums over the Weyl orbit in (4.2.25) and (4.2.31).
- The eigenfunctions constructed in [27, 32] are pole-free only if $\boldsymbol{a} \equiv \boldsymbol{a}(\boldsymbol{\ell})$, where the $\boldsymbol{a}(\boldsymbol{\ell})$ are fixed by the $N-1$ quantization conditions (4.3.4). This is because ξ in (4.3.6) is assumed to be x-independent.

Given these considerations, let us examine what happens to the eigenfunctions (4.2.25) and (4.2.31) once we restrict to the Toda points, that is, upon imposing the $N-1$ quantization conditions (4.3.4). Let us first consider the case of even $N > 2$.[10] We find that the following special combinations vanish identically:

$$\sum_{\boldsymbol{n} \in \mathcal{W}_N \cdot \boldsymbol{\gamma}} \frac{\exp\left(\mathrm{i}(2\pi \boldsymbol{\ell} + \pi \boldsymbol{\rho}) \cdot \boldsymbol{n}\right)}{\prod_{\boldsymbol{\alpha} \in \Delta_+} \left(2 \sinh\left(\frac{\pi \boldsymbol{a} \cdot \boldsymbol{\alpha}}{\hbar}\right)\right)^{(\boldsymbol{n} \cdot \boldsymbol{\alpha})^2}} \prod_{I=1}^{N} \left(\mathrm{e}^{\frac{2\pi x}{\hbar}} - \mathrm{e}^{\frac{2\pi \boldsymbol{a} \cdot \boldsymbol{e}_I}{\hbar}}\right)^{\frac{1}{2} - n_I} = 0 \,, \tag{4.3.8}$$

$$\sum_{\boldsymbol{n} \in \mathcal{W}_N \cdot (\boldsymbol{\gamma} + \boldsymbol{e}_N)} \frac{\exp\left(\mathrm{i}(2\pi \boldsymbol{\ell} + \pi \boldsymbol{\rho}) \cdot \boldsymbol{n}\right)}{\prod_{\boldsymbol{\alpha} \in \Delta_+} \left(2 \sinh\left(\frac{\pi \boldsymbol{a} \cdot \boldsymbol{\alpha}}{\hbar}\right)\right)^{(\boldsymbol{n} \cdot \boldsymbol{\alpha})^2}} \prod_{I=1}^{N} \left(\mathrm{e}^{\frac{2\pi x}{\hbar}} - \mathrm{e}^{\frac{2\pi \boldsymbol{a} \cdot \boldsymbol{e}_I}{\hbar}}\right)^{\frac{1}{2} - n_I} = 0 \,. \tag{4.3.9}$$

Likewise, for N odd we have:

$$\sum_{\boldsymbol{n} \in \mathcal{W}_N \cdot \boldsymbol{\gamma}} \frac{\exp\left(\mathrm{i}\left(2\pi \boldsymbol{\ell} + \pi \boldsymbol{\rho} + \mathrm{i}\frac{\pi}{\hbar} \boldsymbol{a}\right) \cdot \boldsymbol{n}\right)}{\prod_{\boldsymbol{\alpha} \in \Delta_+} \left(2 \sinh\left(\frac{\pi \boldsymbol{a} \cdot \boldsymbol{\alpha}}{\hbar}\right)\right)^{(\boldsymbol{n} \cdot \boldsymbol{\alpha})^2}} \prod_{I=1}^{N} \left(\mathrm{e}^{\frac{2\pi x}{\hbar}} - \mathrm{e}^{\frac{2\pi \boldsymbol{a} \cdot \boldsymbol{e}_I}{\hbar}}\right)^{\frac{1}{2} - n_I} = 0 \,. \tag{4.3.10}$$

This means that, strictly speaking, the eigenfunctions (4.2.25), (4.2.31) vanish at the Toda points. However, since the two terms in the sums (4.2.25) and (4.2.31) go to zero at the same rate, an appropriate normalization can be introduced to obtain a non-vanishing result. A more detailed analysis will be presented in [223].

4.4 Derivation from the TS/ST correspondence

In this section, we derive (4.2.25) and (4.2.31) from the TS/ST correspondence [2, 4–7].

[10] For $N = 2$ these sums do not vanish, see [2].

4.4.1 Open TS/ST for the $Y^{N,0}$ geometries

We consider the toric Calabi–Yau threefolds obtained as crepant resolutions of the $Y^{N,0}$ singularities, which geometrically engineer $\mathcal{N}=1$, SU(N) SYM in five dimensions or $\mathcal{N}=2$, SU(N) SYM in four dimensions [118, 120]. The associated mirror curve [118] has the form:

$$\Lambda^N \left(\mathrm{e}^{y}+\mathrm{e}^{-y}\right)+\sum_{\ell=0}^{N}\kappa_\ell\,\mathrm{e}^{\left(\frac{N}{2}-\ell\right)x}=0 \tag{4.4.1}$$

where Λ and κ_ℓ are the complex moduli, and we can set without loss of generality $\kappa_0 = 1 = \kappa_N$. It is also useful to introduce the chemical potentials μ_ℓ by

$$\kappa_\ell=\mathrm{e}^{\mu_\ell}\,, \qquad\qquad \ell\in\{1,\dots,N-1\} \tag{4.4.2}$$

and the Batyrev coordinates as

$$z_k=\frac{\kappa_{k-1}\kappa_{k+1}}{\kappa_k^2}\,, \qquad k\in\{1,\dots,N-1\}\,, \qquad z_N=\frac{\Lambda^{2N}}{\kappa_0\kappa_N}\,. \tag{4.4.3}$$

The complex moduli κ_ℓ are related to the Kähler parameters t_k through the mirror maps [224]. Our conventions for the classical mirror maps are as follows:

$$t_k=\sum_{\ell=1}^{N-1}C_{k\ell}\mu_\ell+\mathcal{O}(z_i)\,, \qquad k\in\{1,\dots,N-1\}\,, \qquad t_N=-\ln(z_N)\,, \tag{4.4.4}$$

where $C_{k\ell}$ is the Cartan matrix of SU(N).

Within the TS/ST correspondence, we consider the quantization of the mirror curve (4.4.1). Upon quantization, this curve is promoted to a difference equation [8, 22, 23, 56]:

$$\Lambda^N\left(\varphi(x+\mathrm{i}\hbar,\boldsymbol{\kappa})+\varphi(x-\mathrm{i}\hbar,\boldsymbol{\kappa})\right)+\sum_{\ell=0}^{N}\kappa_\ell\,\mathrm{e}^{\left(\frac{N}{2}-\ell\right)x}\varphi(x,\boldsymbol{\kappa})=0\,, \tag{4.4.5}$$

and, simultaneously, the classical Kähler parameters t_k are replaced by their quantum counterparts, giving rise to the quantum mirror maps [8, 23], which we denote by

$$t_k(\hbar)\,, \qquad\qquad k\in\{1,\dots,N-1\}\,. \tag{4.4.6}$$

We refer to [15, 185] for explicit expressions of the quantum mirror maps for the $Y^{N,0}$ geometries. In the limit $\hbar\to 0$, (4.4.6) reduces to the classical mirror map (4.4.4). For the geometries under consideration, the quantum mirror maps can also be interpreted as the inverses of Wilson loop VEVs of five-dimensional $\mathcal{N}=1$ SYM in the NS limit [29, 79]. Explicit expressions for the relevant Wilson loop VEVs in the case of $Y^{N,0}$ geometries can be found in [15, app. D]. In this context, it is often convenient to introduce the 5d Coulomb branch parameters[11]:

$$a_I, \qquad I\in\{1,\dots,N\}\,, \qquad \sum_{I=1}^{N}a_I=0\,, \tag{4.4.7}$$

[11] We are using the same notation for the 5d and 4d Coulomb branch parameters. The distinction should be clear from the context.

which parametrize the VEVs of the complexified scalars in the vector multiplet of 5d SYM, compactified on $\mathbb{R}^4 \times \mathbb{S}^1$. These are related to the quantum mirror maps by

$$t_k(\hbar) = a_k - a_{k+1}, \qquad k \in \{1, \dots, N-1\}\,, \tag{4.4.8}$$

or equivalently, inverting the relations, by

$$a_I = \sum_{\ell=1}^{I-1} \left(-\frac{\ell}{N}\right) t_\ell(\hbar) + \sum_{\ell=I}^{N-1} \left(\frac{N-\ell}{N}\right) t_\ell(\hbar)\,. \tag{4.4.9}$$

Given the underlying SU(N) structure, it is convenient to organize these parameters as

$$\boldsymbol{t} = \sum_{I=1}^{N} a_I\, \boldsymbol{e}_I = \sum_{k=1}^{N-1} t_k(\hbar)\, \boldsymbol{\lambda}_k\,, \tag{4.4.10}$$

where $\boldsymbol{e}_I$ are the weights of the fundamental representation and $\boldsymbol{\lambda}_k$ denote the fundamental weights, see section A.4 for details on the conventions.

The TS/ST correspondence for the $Y^{N,0}$ Calabi–Yau geometries has been studied in the closed string sector in [15, 55, 63, 185]. In this work, we also consider the open sector, extending the results of [2, 6, 7] to this class of geometries. A central object in the correspondence is the full grand potential, which we denote by

$$\mathrm{J}(x, \boldsymbol{t}, \Lambda, \hbar) \;=\; \mathrm{J}^{\text{closed}}(\boldsymbol{t}, \Lambda, \hbar) \;+\; \mathrm{J}^{\text{open}}(x, \boldsymbol{t}, \Lambda, \hbar)\,. \tag{4.4.11}$$

The closed topological string grand potential $\mathrm{J}^{\text{closed}}(\boldsymbol{t}, \Lambda, \hbar)$ is constructed from a specific combination of the refined topological string partition function in the Gopakumar–Vafa (GV) limit and in the NS limit [4, 5, 174]. For the $Y^{N,0}$ geometries, the explicit expression is given in [55, p. 19]. The open topological string grand potential $\mathrm{J}^{\text{open}}(x, \boldsymbol{t}, \Lambda, \hbar)$ has an analogous structure, but it involves instead the open string partition functions [2, 6, 7]. More concretely, for the $Y^{N,0}$ geometries we have:

$$\mathrm{J}^{\text{open}}(x, \boldsymbol{t}, \Lambda, \hbar) = \mathrm{J}^{\text{open}}_{\text{p}}(x, \Lambda, \hbar) + \mathrm{J}^{\text{open}}_{\text{1-loop}}(x, \boldsymbol{t}, \Lambda, \hbar) + \mathrm{J}^{\text{open}}_{\text{inst}}(x, \boldsymbol{t}, \Lambda, \hbar)\,. \tag{4.4.12}$$

Here, the polynomial part is given by

$$\mathrm{J}^{\text{open}}_{\text{p}}(x, \Lambda, \hbar) = \mathrm{i}\ln\!\left(\Lambda^N\right) \frac{x}{\hbar} + \pi \frac{x}{\hbar} - \frac{N}{4}\, x \left(1 + \mathrm{i}\frac{x}{\hbar}\right)\,. \tag{4.4.13}$$

This term is obtained by analysing the large-x behaviour of (4.4.5) and demanding that $\exp \mathrm{J}^{\text{open}}_{\text{p}}$ provides a formal solution in the large-x asymptotic regime. This procedure fixes the form of (4.4.13) up to an $\mathrm{i}\hbar$ periodic factor $\sim \exp\left(\frac{2\pi}{\hbar} x\right)$, which is then fixed with hindsight by requiring the cancellation of poles between the two terms in (4.4.15). The one-loop contribution takes the form [2, 32]

$$\exp\!\left(\mathrm{J}^{\text{open}}_{\text{1-loop}}(x, \boldsymbol{t}, \Lambda, \hbar)\right) = \prod_{I=1}^{N} \Phi_b\left(\frac{-x + \boldsymbol{e}_I \cdot \boldsymbol{t} + \mathrm{i}\pi b^2}{2\pi b}\right)\,, \qquad \hbar = 2\pi b^2, \tag{4.4.14}$$

where Φ_b is Faddeev's non-compact quantum dilogarithm, see subsection A.2.2. Finally, the instanton contribution $\mathrm{J}^{\text{open}}_{\text{inst}}(x, \boldsymbol{t}, \Lambda, \hbar)$ is built from a specific combination of the refined open topological string partition function on the $Y^{N,0}$ geometry, taken in the GV and NS limits, see [6, sec. 4.1], [7, sec. 2.2] and [2, sec. 3.3].

From the topological string perspective, the open string grand potential (4.4.12) provides a non-perturbative completion of the open topological string free energy in the large-radius frame. This quantity, however, is not background independent and moreover develops poles at finite values of x, which is identified with the open string modulus. To remedy this, it was shown in [2, 6, 7] that one must consider a particular linear combination of the form:

$$\varphi(x, \boldsymbol{\kappa}) = \sum_{s\in\{-1,+1\}} \sum_{\boldsymbol{n}\in Q_{N-1}} \exp\left[\mathrm{J}_s\left(x, \boldsymbol{t} + \mathrm{i}2\pi\boldsymbol{n}, \Lambda, \hbar\right)\right], \tag{4.4.15}$$

where Q_{N-1} is the root lattice defined in (A.4.4) and $\mathrm{J}_+(x, \boldsymbol{t}, \Lambda, \hbar) = \mathrm{J}(x, \boldsymbol{t}, \Lambda, \hbar)$, while J_- is obtained from J_+ by a suitable transformation, as we will see later. Note that in (4.4.15) we are implicitly using the quantum mirror maps (4.4.6) relating $\boldsymbol{\kappa}$ to the quantum Kähler parameters $\boldsymbol{t}$. In the topological string theory, both summations in (4.4.15) are essential to achieve background independence in the open and closed string moduli. Indeed, the sum over $\boldsymbol{n}$ renders the expression entire in the closed string moduli $\boldsymbol{\kappa}$, while the sum over s ensures entireness in the open modulus x. From the perspective of spectral theory, equation (4.4.15) is particularly significant, as it provides an exact entire solution to the quantum mirror curve associated with the underlying Calabi-Yau geometry. Although formal solutions to the quantum mirror curve can be constructed in various ways, (4.4.15) stands out due to its analyticity in both the open modulus x and the closed moduli $\boldsymbol{\kappa}$. Moreover, when evaluated on-shell, it yields genuine square-integrable eigenfunctions, see [2, 6, 7] for more details.

An important open question in the context of the open TS/ST correspondence is the precise characterization of the second term in (4.4.15). In [6, 7] it was suggested that intuitively this has to do with moving to a different sheet of the mirror curve. In practice, however, it is challenging to implement this explicitly, that is, to find a simple explicit relation between J_+ and J_-. For local $\mathbb{F}_0$, this problem was successfully solved in [2], where, using insights from Painlevé equations [1], it was shown that the two terms are simply related by shifts of the complex moduli and of the variable x. At the level of the mirror curve, these shifts are characterized by the fact that they leave the curve itself invariant. Let us now apply the same idea to (4.4.1). We consider transformations of the form

$$x \to s\,x - \mathrm{i}2\pi\frac{k_x}{N}\,, \qquad y \to \frac{1}{s}\,y - \mathrm{i}\pi k_y\,, \qquad k_x, k_y \in \mathbb{Z}\,, \qquad k_x + k_y \in 2\mathbb{Z}\,, \tag{4.4.16}$$

combined with a corresponding transformation of the moduli μ_ℓ, which we will introduce below. Drawing inspiration from the example of local $\mathbb{F}_0$ [2] and the Toda lattice [27, 32], it is natural to choose $s = -1$. The classical curve is then invariant if and only if the

closed moduli transform as

$$\mu_\ell \to \mu_{N-\ell} - \mathrm{i}2\pi\frac{k_x \ell}{N}\,. \tag{4.4.17}$$

Following again the analogy with local $\mathbb{F}_0$ [2], we set $k_x = 1 = k_y$. This gives

$$\boxed{\varphi(x,\boldsymbol{\kappa}) = \varphi_+(x,\boldsymbol{\kappa}) + \exp\left(\frac{\mathrm{i}}{\hbar}\frac{\pi^2}{N} + \pi\frac{x}{\hbar}\right)\varphi_+\left(-x - \mathrm{i}\frac{2\pi}{N},\, \widetilde{\boldsymbol{\kappa}}\right),} \tag{4.4.18}$$

$$\varphi_+(x,\boldsymbol{\kappa}) = \sum_{\boldsymbol{n}\in Q_{N-1}} \mathrm{e}^{\mathrm{J}(x,\boldsymbol{t}+\mathrm{i}2\pi\boldsymbol{n},\Lambda,\hbar)}. \tag{4.4.19}$$

where $\boldsymbol{\kappa} = \{\kappa_1, \cdots, \kappa_{N-1}\}$, $\widetilde{\boldsymbol{\kappa}} = \{\widetilde{\kappa}_1, \cdots, \widetilde{\kappa}_{N-1}\}$ with $\widetilde{\kappa}_\ell = \kappa_{N-\ell}\,\mathrm{e}^{-\mathrm{i}\frac{2\pi}{N}\ell}$. Let us also note that, after applying the quantum mirror map, the transformation (4.4.17) is equivalent to

$$\boldsymbol{t} \to \boldsymbol{r}(\boldsymbol{t}) + \mathrm{i}2\pi k_x \boldsymbol{e}_N\,, \qquad \boldsymbol{r}(\boldsymbol{t}) = \sum_{k=1}^{N-1} t_{N-k}\boldsymbol{\lambda}_k = -\sum_{I=1}^{N} a_{N-I+1}\boldsymbol{e}_I\,. \tag{4.4.20}$$

We have carried out preliminary tests of (4.4.18) for $N = 4$. The next section, provides further evidence in favour of (4.4.18) for generic N, and is the origin of our proposal in subsection 4.2.3.

4.4.2 The four-dimensional limit

Topological string theory on the $Y^{N,0}$ geometries provides a framework to engineer four-dimensional $\mathcal{N} = 2$, SU(N) SYM [118, 120]. To realize this setup, one performs a specific geometric limit, usually called the four-dimensional limit. In this section, we show that, after carrying out this limit, the eigenfunctions (4.4.18) reduce to (4.2.25) and (4.2.31), respectively. The computation of the four-dimensional limit of the eigenfunctions mirrors that for the spectral determinant in [55, Sec. 5], which we follow closely. To take the limit on the mirror curve, we need a different parametrization from the one used in (4.4.1). The reparametrization is implemented by some simple shifts, see also the discussion in [55, sec. 5]. Combining these shifts with the natural scaling one finds that the four-dimensional limit is

$$x \to Rx - \mathrm{i}\frac{\pi}{N}\mathbb{1}_{2\mathbb{N}+1}(N)\,, \quad \boldsymbol{t} \to R\boldsymbol{a} + \mathrm{i}2\pi\boldsymbol{\gamma}\,, \quad \Lambda^{2N} \to (-)^N (R\Lambda)^{2N}\,, \quad \hbar \to R\hbar\,, \tag{4.4.21}$$

and then $R \to 0$ from above, with $\boldsymbol{\gamma}$ defined in (4.2.17). One can check that, by taking this limit, the quantum mirror curve (4.4.5) reduces to the quantum Seiberg-Witten curve of four-dimensional $\mathcal{N} = 2$ SU(N) SYM (4.2.3).

For simplicity, we set the four-dimensional reduced Planck constant $\hbar$ to 1. We can reintroduce it by sending $(x, \boldsymbol{a}, \Lambda) \to (x/\hbar, \boldsymbol{a}/\hbar, \Lambda/\hbar)$ at the end. The four-dimensional limit acts similarly on both terms in the right-hand side of (4.4.18). Hence, it is convenient

to introduce the variables $s \in \{-1,+1\}$ and $k_x = k_y = k \in \{0,1\}$, and look at the $R \to 0$ limit of

$$\sum_{\boldsymbol{n}\in Q_{N-1}} \exp\Bigg[-\mathrm{J}^{\mathrm{closed}}\Big(R\boldsymbol{a} + \mathrm{i}2\pi\boldsymbol{\gamma}, \mathrm{e}^{-\mathrm{i}\frac{\pi}{2}\frac{\mathbb{1}_{2\mathbb{N}+1}(N)}{N}} R\Lambda, R\Big) + \mathrm{i}\frac{\pi^2}{N}\frac{k^2}{R} - sk\pi\left(x - \mathrm{i}\frac{\pi}{N}\frac{\mathbb{1}_{2\mathbb{N}+1}(N)}{R}\right) + \mathrm{J}\Big(sRx - \mathrm{i}\frac{\pi}{N}\left(2k + s\mathbb{1}_{2\mathbb{N}+1}(N)\right), R\boldsymbol{r}_s(\boldsymbol{a}) + \mathrm{i}2\pi\boldsymbol{w}, \mathrm{e}^{-\mathrm{i}\frac{\pi}{2}\frac{\mathbb{1}_{2\mathbb{N}+1}(N)}{N}} R\Lambda, R\Big)\Bigg], \quad (4.4.22)$$

where we introduced the convenient notation

$$\boldsymbol{r}_s(\boldsymbol{t}) = \begin{cases} \boldsymbol{r}(\boldsymbol{t}) & s = -1 \\ \boldsymbol{t} & s = +1 \end{cases}, \qquad \boldsymbol{w} = \boldsymbol{\gamma} + \left(\frac{1-s}{2}\right)\mathbb{1}_{2\mathbb{N}}(N)\,\boldsymbol{e}_N + \boldsymbol{n}\,. \quad (4.4.23)$$

The first term on the right-hand side of (4.4.18) is then given by $s = 1$ and $k = 0$, while the second term corresponds to $s = -1$ and $k = 1$. Note that we normalized the eigenfunctions by the x-independent constant $\exp\left(\mathrm{J}^{\mathrm{closed}}\right)$, which is convenient in the four-dimensional limit [55]. In (4.4.23), we have already used the fact that

$$\boldsymbol{r}(\boldsymbol{\gamma}) + \boldsymbol{e}_N + \boldsymbol{m} = (-1)^N\boldsymbol{\gamma} + \boldsymbol{e}_N + \boldsymbol{m} = \boldsymbol{\gamma} + \mathbb{1}_{2\mathbb{N}}(N)\,\boldsymbol{e}_N + \boldsymbol{n}\,, \quad (4.4.24)$$

where $\boldsymbol{n}, \boldsymbol{m} \in Q_{N-1}$ are related by a simple shift of the origin of the root lattice Q_{N-1} when N is odd, and are instead equal when N is even.

The leading terms and the closed part

The key observation in the four-dimensional limit is that only finitely many of the $\boldsymbol{n} \in Q_{N-1}$ appearing in the sum (4.4.22) contribute. As discussed below, which $\boldsymbol{n}$ dominate is determined by the polynomial part of the closed grand potential.

Let us first consider the shifts of $\boldsymbol{r}_s(\boldsymbol{t})$ by $\mathrm{i}2\pi\boldsymbol{w}$ in (4.4.22). We introduce $\boldsymbol{\beta}$ for future convenience,

$$\boldsymbol{\beta} = \boldsymbol{\gamma} + \left(\frac{1-s}{2}\right)\mathbb{1}_{2\mathbb{N}}(N)\,\boldsymbol{e}_N\,, \qquad \boldsymbol{w} = \boldsymbol{\beta} + \boldsymbol{n}\,. \quad (4.4.25)$$

The polynomial part of the closed grand potential then scales as

$$\mathrm{J}^{\mathrm{closed}}_{\mathrm{p}}\Big(R\boldsymbol{r}_s(\boldsymbol{a}) + \mathrm{i}2\pi\boldsymbol{w}, \mathrm{e}^{-\mathrm{i}\frac{\pi}{2}\frac{\mathbb{1}_{2\mathbb{N}+1}(N)}{N}} R\Lambda, R\Big) = 2\pi N\boldsymbol{w}^2\frac{\ln(R)}{R} + \left[\pi\boldsymbol{w}^2\ln\left(\Lambda^{2N}\right) + \mathrm{i}\pi^2\left(\frac{1}{3}\sum_{\boldsymbol{\alpha}\in\Delta_+}\left[\boldsymbol{\alpha}\cdot\boldsymbol{w} - 2\left(\boldsymbol{\alpha}\cdot\boldsymbol{w}\right)^3\right] + \boldsymbol{w}^2\mathbb{1}_{2\mathbb{N}+1}(N)\right)\right]\frac{1}{R} - \mathrm{i}2N\left(\boldsymbol{w}\cdot\boldsymbol{r}_s(\boldsymbol{a})\right)\ln(R) + \mathcal{O}\left(R^0\right). \quad (4.4.26)$$

This is the only part of the total grand potential in (4.4.22) with an $\boldsymbol{n}$-dependent divergence of order $\ln(R)/R$; all other contributions are subleading. Therefore, this part determines

which terms in the sum (4.4.22) survive. The $R \to 0$ limit of (4.4.22) is then dominated by the minima of the positive definite form

$$\boldsymbol{w}^2 = (\boldsymbol{n} + \boldsymbol{\beta})^2 \ . \tag{4.4.27}$$

These are precisely the elements of the Weyl orbit of $\boldsymbol{\beta}$ [55], that is we have minima for[12]

$$\boldsymbol{w} \in \mathcal{W}_N \cdot \boldsymbol{\beta} \, . \tag{4.4.28}$$

For the rest of the closed part, the limit works exactly as outlined in [55]. From the closed 1-loop part we have

$$\begin{aligned} \mathrm{J}^{\text{closed}}_{\text{1-loop}}\Big(R\boldsymbol{r}_s(\boldsymbol{a}) + \mathrm{i}2\pi\boldsymbol{w}, \mathrm{e}^{-\mathrm{i}\frac{\pi}{2}\frac{\mathbb{1}_{2\mathbb{N}+1}(N)}{N}} R\Lambda, R\Big) = \\ \mathrm{i}\frac{\pi^2}{3}\left(\sum_{\boldsymbol{\alpha}\in\Delta_+} \boldsymbol{\alpha}\cdot\boldsymbol{w}\right)\frac{1}{R} + \mathrm{i}2N\left(\boldsymbol{w}\cdot\boldsymbol{r}_s(\boldsymbol{a})\right)\ln\left(R\right) + \mathcal{O}\big(R^0\big) \, , \end{aligned} \tag{4.4.29}$$

while the instanton part is regular. This means that for the second term in (4.4.18), i.e. for $s = -1$, we get an extra divergent factor which is the exponential of

$$\begin{aligned} \Big[\mathrm{J}^{\text{closed}}\Big(R\boldsymbol{r}(\boldsymbol{a}) + \mathrm{i}2\pi\left(\boldsymbol{\gamma} + \mathbb{1}_{2\mathbb{N}}(N)\boldsymbol{e}_N\right), \mathrm{e}^{-\mathrm{i}\frac{\pi}{2}\frac{\mathbb{1}_{2\mathbb{N}+1}(N)}{N}} R\Lambda, R\Big) - \\ \mathrm{J}^{\text{closed}}\Big(R\boldsymbol{a} + \mathrm{i}2\pi\boldsymbol{\gamma}, \mathrm{e}^{-\mathrm{i}\frac{\pi}{2}\frac{\mathbb{1}_{2\mathbb{N}+1}(N)}{N}} R\Lambda, R\Big)\Big] = -2\pi\mathbb{1}_{2\mathbb{N}}(N)\frac{\ln\left(R\right)}{R} - \frac{\pi}{N}\mathbb{1}_{2\mathbb{N}}(N)\frac{\ln\left(\Lambda^{2N}\right)}{R} \\ + \mathcal{O}\big(R^0\big) \, . \end{aligned} \tag{4.4.30}$$

The $\mathcal{O}(R^0)$ contribution coming from the closed sector can then be obtained directly from [55, p. 34], and the standard four-dimensional limit becomes

$$\begin{aligned} \lim_{R\to 0}\,(4.4.22) \propto \sum_{\boldsymbol{w}\in\mathcal{W}_N\cdot\boldsymbol{\beta}} \frac{\exp\left(\left(\mathrm{i}\partial_{\boldsymbol{a}} F_{\text{NS}} - \pi\boldsymbol{a}\mathbb{1}_{2\mathbb{N}+1}(N)\right)\cdot\boldsymbol{w}\right)}{\prod_{\boldsymbol{\alpha}\in\Delta_+}\left(2\sinh\left(\pi\boldsymbol{a}\cdot\boldsymbol{\alpha}\right)\right)^{(\boldsymbol{w}\cdot\boldsymbol{\alpha})^2}} \cdot \lim_{R\to 0}\mathrm{e}^{\left(\frac{1-s}{2}\right)(4.4.30) + \mathrm{i}\frac{\pi^2}{N}\frac{k^2}{R}} \\ \cdot \lim_{R\to 0}\mathrm{e}^{-sk\pi\left(x - \mathrm{i}\frac{\pi}{N}\frac{\mathbb{1}_{2\mathbb{N}+1}(N)}{R}\right) + \mathrm{J}^{\text{open}}\left(sRx - \mathrm{i}\frac{\pi}{N}(2k + s\mathbb{1}_{2\mathbb{N}+1}(N)), R\boldsymbol{r}_s(\boldsymbol{a}) + \mathrm{i}2\pi\boldsymbol{w}, \mathrm{e}^{-\mathrm{i}\frac{\pi}{2}\frac{\mathbb{1}_{2\mathbb{N}+1}(N)}{N}} R\Lambda, R\right)} \, . \end{aligned} \tag{4.4.31}$$

It should be noted that the proportionality constant we are neglecting here is finite and independent of x, s and k. Hence, it is an overall constant of the eigenfunctions and the same for both saddles. One can compare with [55, p. 34].

[12] Note that with $\boldsymbol{w} = \sum_I w_I \boldsymbol{e}_I$ and $\boldsymbol{\beta} = \sum_I \beta_I \boldsymbol{e}_I$ we have the constraint $\sum_I w_I = \sum_I \beta_I$. Let us now take $\beta_I \in \{\pm 1/2\}$ and hence $w_I \in \mathbb{Z} + 1/2$ for convenience. One can see that $\boldsymbol{w}^2 = \sum_I w_I^2 - \left(\sum_I \beta_I\right)^2/N$, which gets minimized for $w_I \in \{\pm 1/2\}$, and since $\sum_I w_I = \sum_I \beta_I$ we find that the w_I's should be a permutation of the β_I's. This means exactly that $\boldsymbol{w} \in \mathcal{W}_N \cdot \boldsymbol{\beta}$.

The open part

One finds for the open polynomial part:

$$\begin{aligned}
&\mathrm{i}\frac{\pi^2}{N}\frac{k^2}{R}-sk\pi\left(x-\mathrm{i}\frac{\pi}{N}\frac{\mathbb{1}_{2\mathbb{N}+1}(N)}{R}\right)+\mathrm{J}_{\mathrm{p}}^{\mathrm{open}}\left(sRx-\mathrm{i}\frac{\pi}{N}\left(2k+s\mathbb{1}_{2\mathbb{N}+1}(N)\right),\mathrm{e}^{-\mathrm{i}\frac{\pi}{2}\frac{\mathbb{1}_{2\mathbb{N}+1}(N)}{N}}R\Lambda,R\right)\\
&=\begin{cases}2\pi k\frac{\ln(R)}{R}+2\pi\frac{k}{N}\frac{\ln(\Lambda^N)}{R}+\mathrm{i}sNx\ln(R)+\mathrm{i}\frac{\pi}{2}k+\mathrm{i}sx\ln\left(\Lambda^N\right)+s\pi\left(1-2k\right)x\\ \pi\frac{\ln(R)}{R}+\frac{\frac{\pi}{N}\ln(\Lambda^N)-\mathrm{i}\frac{5}{4}\frac{\pi^2}{N}}{R}+\mathrm{i}sNx\ln(R)+\mathrm{i}\frac{\pi}{4}+\mathrm{i}sx\ln\left(\Lambda^N\right)+s\pi\left(1-k\right)x\end{cases}
\end{aligned}\tag{4.4.32}$$

up to $\mathcal{O}(R)$ corrections, and where the first case is for N even and the second for N odd. We will come back to the divergent terms near the end of the section.

For the open 1-loop part, we need the $b\to 0$ limit of

$$\begin{aligned}
&\Phi_b\left(-b\left(sx-\boldsymbol{e}_I\cdot\boldsymbol{r}_s\left(\boldsymbol{a}\right)\right)+\mathrm{i}\frac{b}{2}+\mathrm{i}\left(\boldsymbol{e}_I\cdot\boldsymbol{w}+\frac{k}{N}+s\frac{\mathbb{1}_{2\mathbb{N}+1}(N)}{2N}\right)b^{-1}\right)\\
&\qquad=\Phi_b\left(-\mathrm{i}\left(\frac{1}{2}-w_I\right)b^{-1}+\mathrm{i}b+\mathrm{i}\frac{b^{-1}}{2}-\mathrm{i}bz_I\right)\,,
\end{aligned}\tag{4.4.33}$$

where $b=\sqrt{R/2\pi}$ and we used that

$$\boldsymbol{e}_I\cdot\boldsymbol{w}-\frac{1}{2}+\frac{k}{N}+s\frac{\mathbb{1}_{2\mathbb{N}+1}(N)}{2N}=-\left(\frac{1}{2}-w_I\right)\,,\qquad z_I=\frac{1}{2}-\mathrm{i}\left(sx-\boldsymbol{e}_I\cdot\boldsymbol{r}_s\left(\boldsymbol{a}\right)\right)\,,\tag{4.4.34}$$

with $\boldsymbol{w}=\sum_I w_I\boldsymbol{e}_I$. It should be noted that $1/2-w_I$ is either 0 or 1. Using the quasi-periodicity of the quantum dilogarithm (A.2.11) under shifts of $\mathrm{i}b$ and $-\mathrm{i}b^{-1}$ gives

$$\begin{aligned}
&\Phi_b\left(-\mathrm{i}\left(\frac{1}{2}-w_I\right)b^{-1}+\mathrm{i}b+\mathrm{i}\frac{b^{-1}}{2}-\mathrm{i}bz_I\right)\\
&\qquad=\frac{\left(1+\left(\frac{1}{2}-w_I\right)\exp\left(-\mathrm{i}2\pi z_I\right)\right)}{1-\exp\left(\mathrm{i}2\pi b^2\left(z_I-\frac{1}{2}\right)\right)}\Phi_b\left(\mathrm{i}\frac{b^{-1}}{2}-\mathrm{i}bz_I\right)\,.
\end{aligned}\tag{4.4.35}$$

Expanding around $b\to 0$ and using [2, eq. (4.29)], we find

$$\begin{aligned}
&\frac{\left(1+\left(\frac{1}{2}-w_I\right)\exp\left(-\mathrm{i}2\pi z_I\right)\right)}{1-\exp\left(\mathrm{i}2\pi b^2\left(z_I-\frac{1}{2}\right)\right)}\Phi_b\left(\mathrm{i}\frac{b^{-1}}{2}-\mathrm{i}bz_I\right)=\exp\left(-\mathrm{i}\frac{\pi}{12}b^{-2}+\left(z_I-1\right)\ln\left(2\pi b^2\right)\right)\\
&\qquad\frac{\mathrm{i}}{\sqrt{2\pi}}\left(1+\left(\frac{1}{2}-w_I\right)\exp\left(-\mathrm{i}2\pi z_I\right)\right)\exp\left(\mathrm{i}\frac{\pi}{2}z_I\right)\Gamma\left(z_I-\frac{1}{2}\right)\left(1+\mathcal{O}\left(b^2\right)\right)
\end{aligned}\tag{4.4.36}$$

where we also used the integral representations of the quantum dilogarithm (A.2.16) and of the log gamma function (A.2.17). The leading contribution from the 1-loop part in the

four-dimensional limit is then

$$\begin{aligned}\lim_{R\to 0}\exp\left[\mathrm{J}^{\text{open}}_{\text{1-loop}}\left(sRx-\mathrm{i}\frac{\pi}{N}\left(2k+s\mathbb{1}_{2\mathbb{N}+1}(N)\right),R\boldsymbol{r}_s(\boldsymbol{a})+\mathrm{i}2\pi\boldsymbol{w},R\right)\right]\\ =\left(\frac{\mathrm{e}^{\mathrm{i}\frac{3\pi}{4}}}{\sqrt{2\pi}}\right)^N\exp\left(-\mathrm{i}\frac{\pi^2}{6}\frac{N}{R}-N\left(\frac{1}{2}+\mathrm{i}sx\right)\ln\left(R\right)\right)\exp\left(s\frac{\pi}{2}Nx\right)\\ \prod_{I=1}^{N}\left\{1-\left(\frac{1}{2}-w_I\right)\exp\left(-2\pi\left[sx-\boldsymbol{e}_I\cdot\boldsymbol{r}_s\left(\boldsymbol{a}\right)\right]\right)\right\}\Gamma\left(-\mathrm{i}\left[sx-\boldsymbol{e}_I\cdot\boldsymbol{r}_s\left(\boldsymbol{a}\right)\right]\right)\end{aligned}\tag{4.4.37}$$

Regarding the instanton part, the contributions from the 5d GV free energy vanish in the 4d limit, while the contributions from the 5d NS free energy lead directly to their 4d counterparts [119, 121]. This is exactly as noted in [55] for the closed sector and in [2] for the open sector in the $N=2$ case. That is

$$\begin{aligned}\lim_{R\to 0}\exp\left[\mathrm{J}^{\text{open}}_{\text{inst}}\left(sRx-\mathrm{i}\frac{\pi}{N}\left(2k+s\mathbb{1}_{2\mathbb{N}+1}(N)\right),R\boldsymbol{r}_s(\boldsymbol{a})+\mathrm{i}2\pi\boldsymbol{w},\mathrm{e}^{-\mathrm{i}\frac{\pi}{2}\frac{\mathbb{1}_{2\mathbb{N}+1}(N)}{N}}R\Lambda,R\right)\right]\\ =Z^{\text{inst}}_{\text{D}}\left(sx,\boldsymbol{f}_{\boldsymbol{s}}(\boldsymbol{a}),\Lambda,1\right)\end{aligned}\tag{4.4.38}$$

We remark that there are no divergences coming from the instanton part.

Let us briefly come back to the divergent factors. For N odd, we have no divergences coming from the closed part of the grand potential, and only an overall, x-independent divergence coming from the open part. This can be dealt with by introducing an appropriate, overall normalization. For N even on the other hand, the polynomial part of the closed grand potential gives rise to a divergent constant for the second saddle (4.4.30) that is not present for the first saddle. However, this gets exactly cancelled by the divergences from the polynomial part of the open grand potential (4.4.32), leaving only an x-independent, overall divergent factor. This can again be dealt with by an appropriate overall normalization.

The result of the four-dimensional limit

Hence, up to an x-independent, divergent overall factor, we obtain for both saddles

$$\mathrm{e}^{\mathrm{i}\frac{\pi}{2}k\mathbb{1}_{2\mathbb{N}}(N)}\mathrm{e}^{-s\pi(1+\mathbb{1}_{2\mathbb{N}}(N))kx}Z_D\left(sx,\boldsymbol{r}_s(\boldsymbol{a}),\Lambda,1\right)\sum_{\boldsymbol{w}\in\mathcal{W}_N\cdot\boldsymbol{\beta}}\mathcal{P}_{\boldsymbol{w}}\left(sx,\boldsymbol{r}_s(\boldsymbol{a}),\Lambda,1\right)\tag{4.4.39}$$

where we have $s=1$ and $k=k_x=k_y=0$ for the first saddle, while $s=-1$ and $k=k_x=k_y=1$ for the second saddle. We used the expressions[13]

$$Z_D\left(x,\boldsymbol{a},\Lambda,1\right)=\mathrm{e}^{\mathrm{i}\ln(\Lambda^N)x+\pi\left(\frac{N}{2}+1\right)x}\left(\prod_{I=1}^{N}\Gamma(\mathrm{i}\left[\boldsymbol{e}_I\cdot\boldsymbol{a}-x\right])\right)Z^{\text{inst}}_{\text{D}}(x,\boldsymbol{a},\Lambda,1)\tag{4.4.40}$$

[13]Note that $\mathcal{P}_{\boldsymbol{w}}$ in (4.4.41) is indeed equal to (4.2.22), since $1/2-w_I$ is either 0 or 1.

$$\mathcal{P}_{\boldsymbol{w}}\left(x,\boldsymbol{a},\Lambda,1\right)=\frac{\mathrm{e}^{\mathrm{i}\partial_{\boldsymbol{a}}F_{\mathrm{NS}}\cdot\boldsymbol{w}-\pi\boldsymbol{a}\cdot\boldsymbol{w}\mathbb{1}_{2\mathbb{N}+1}(N)}}{\prod_{\boldsymbol{\alpha}\in\Delta_+}\left(2\sinh\left(\pi\boldsymbol{a}\cdot\boldsymbol{\alpha}\right)\right)^{(\boldsymbol{w}\cdot\boldsymbol{\alpha})^2}}\prod_{I=1}^{N}\left(1-\left(\frac{1}{2}-w_I\right)\mathrm{e}^{2\pi(\boldsymbol{e}_I\cdot\boldsymbol{a}-x)}\right) \tag{4.4.41}$$

$$\boldsymbol{\beta}=\boldsymbol{\gamma}+\left(\frac{1-s}{2}\right)\mathbb{1}_{2\mathbb{N}}(N)\,\boldsymbol{e}_N \tag{4.4.42}$$

The number of non-trivial factors in (4.4.41) is $N/2$ for $s=1$ and $(N-2)/2$ for $s=-1$ when N is even, and $(N-1)/2$ when N is odd. This can be verified directly from the expression of $\boldsymbol{\beta}$ in (4.4.42). Let us end with the comment that

$$\left(\frac{1}{2}-w_I\right)=\frac{1}{2}-\boldsymbol{e}_I\cdot\boldsymbol{w}-\left(\frac{k}{N}+s\frac{\mathbb{1}_{2\mathbb{N}+1}(N)}{2N}\right)=\frac{1}{2}-\boldsymbol{e}_I\cdot\boldsymbol{w}-\left(\frac{1-s\mathbb{1}_{2N}(N)}{2N}\right) \tag{4.4.43}$$

where the latter two expressions are coordinate invariant and independent of the choice $w_I\in\{\pm1/2\}$, and they are always 0 or 1.

4.5 Outlook and open questions

Our analysis opens up several directions for future investigation, some of which we briefly outline below.

- It would be interesting to investigate how our solutions (4.4.18), (4.2.25) and (4.2.31) emerge from a resurgent analysis of the open-string wavefunction and an exact WKB analysis; see for instance [197, 198, 200–202, 225].

- The deformed Hamiltonian (4.1.1) exhibits several novel spectral features absent in standard Schrödinger operators. Due to its difference-equation nature, the usual oscillation theorem [214, thm. 3.5] does not apply. Moreover, the system can display ground-state degeneracies and, remarkably, bound states with real energies even in potentials unbounded from below. These phenomena reveal a rich and unconventional spectral structure whose physical interpretation deserves further study. A detailed analysis of these aspects will be presented in a forthcoming work [223, 226].

- It is important to undertake a mathematical study of the spectral properties of (4.1.1) for odd N. Indeed, when the potential is confining (N even), the spectral properties of the corresponding difference operators have been analysed rigorously in [125], where it was shown that such operators are self-adjoint on a suitable domain and possess a purely discrete spectrum. See also [227] for extensions to certain complex potentials. It would be meaningful to extend this type of rigorous analysis to the case of potentials unbounded from below. See also [220, 221] for some discussion on the case of the standard Schrödinger operator.

- It was pointed out in [14, 63] that there exists another four-dimensional limit, the so-called dual 4d limit, which can be implemented on the mirror curve (4.4.1) and leads

to a family of integral operators. The corresponding spectral problems make contact with the 4D gauge theory in the self-dual phase of the Ω-background, rather than the NS-phase, as is the case for the spectral problems studied in this chapter. For $N = 2$, this limit on the eigenfunctions was analysed in [1, 2], where a new functional relation between the modified Mathieu and the McCoy-Tracy-Wu operators was found. It would be interesting to extend this analysis to $N > 2$ in light of our new results on the eigenfunction.

See also the conclusion and outlook in chapter 5.

Chapter 5

Conclusion and outlook

In chapter 2, we have argued that the eigenfunctions of the operator (2.1.1) are computed by surface defects in $\mathcal{N} = 2$, SU(N) SYM in the self-dual phase of the four-dimensional Ω-background ($\epsilon_1 + \epsilon_2 = 0$). This result, together with [14, 15, 63], extends the correspondence between 4d $\mathcal{N} = 2$ theories and spectral theory to a new class of operators. In addition, we have expressed the eigenfunctions of these operators in closed form via a matrix model average (2.2.2). This provides a representation for the surface defect partition function which resums both the instanton and the ϵ expansions. In this way, we have a manifest interpolation from the weak to the strong coupling region. In particular, the strong coupling expansion in $1/\Lambda$ (exact in ϵ and a_D) corresponds to the expansion of the matrix model around its Gaussian point, and hence, it is obtained straightforwardly.

In chapter 3, we formulated the open topological string/spectral theory correspondence for local $\mathbb{F}_0$, by generalizing [6, 7] away from the self-dual point. Focusing on local $\mathbb{F}_0$, our main result is encapsulated in (3.3.35). From the perspective of topological string theory, the right-hand side provides a non-perturbative, background-independent formulation of the open topological string partition function, which is entire in both the closed string modulus κ and the open string modulus x. From the viewpoint of the quantum mirror curve, what makes (3.3.35) particularly significant is that it provides a solution to the corresponding difference equation (3.1.7) which is entire, even off-shell. When evaluated on-shell, this solution gives the eigenfunctions of the relativistic two-particle Toda lattice. We explored the implications of our construction (3.3.35) in both the standard [118] and dual [14] four-dimensional limits, where the quantum mirror curves reduce to the (Fourier-transformed) Mathieu operator (3.4.2) and the McCoy-Tracy-Wu operator (3.4.34), respectively. In the standard 4d limit, our construction provides entire off-shell eigenfunctions of the Fourier-transformed Mathieu operator (3.1.7), expressed as special combinations of NS functions in the presence of 2d/4d surface defects, see (3.4.16). When evaluated on-shell, these solutions reproduce the known results [27, 28, 30, 32, 33, 35, 36, 39, 40]. On the other hand, in the dual 4d limit, our result (3.3.35) reproduces the expression of [1], where the eigenfunctions of the McCoy-Tracy-Wu operator are obtained through a special

combination of 2d/4d surface defects in the GV phase of the background Ω. Notably, we find that the eigenfunctions of the Mathieu and the McCoy-Tracy-Wu operators, when evaluated on-shell, are the same. This gives an explicit functional relation between the two operators, see (3.4.50).

In chapter 4, we generalized the construction to the family of $Y^{N,0}$ toric Calabi–Yau geometries. Following the general framework of [2, 6, 7], we constructed a background-independent quantity, given in equation (4.4.18), which plays the role of non-perturbative open topological string partition function. This object is entire in both the open and closed string moduli and provides an exact analytic solution to the difference equation obtained by quantizing the mirror curve of the $Y^{N,0}$ geometry. The resulting wavefunction becomes square-integrable only at discrete energy values, where it reproduces the physical eigenfunctions of the associated operator. We then analysed the four-dimensional limit of this construction. In this limit, the quantum mirror curve (4.4.5) reduces to the deformed quantum-mechanical Hamiltonian (4.1.1), which can be regarded as a deformation of the standard Schrödinger operator with an arbitrary polynomial potential. Through the open TS/ST correspondence, we derived explicit analytic expressions for the corresponding eigenfunctions, given in equations (4.2.25) and (4.2.31). These functions are entire in x for arbitrary values of the moduli h_k and become L^2-normalizable only for a discrete set of values of the energy, in perfect agreement with the quantization conditions previously derived in [55].

Let us end with some interesting open questions

- It is important to establish a rigorous analytic proof of our results, such as demonstrating that the eigenfunctions are entire in x for generic values of the parameters.

- In section 3.2.3 we used a simple integration lemma to compute the first fermionic spectral trace when $\hbar \in 2\pi\mathbb{Q}_{>0}$. It is then natural to ask whether the same can be done for generic $N \in \mathbb{N}$. Unfortunately, for $N \geqslant 2$ not all integrands are quasi-periodic in the right sense, so that one cannot use the same trick. Nevertheless, it would be an interesting problem to solve, and it could be a useful step towards a rigorous proof for the closed TS/ST correspondence for local $\mathbb{F}_0$.

- It would be interesting to generalize our construction of the eigenfunctions of the finite difference Schrödinger operator (4.1.1) to other four-dimensional quantum mirror curves, including those associated with SW theories with matter or with different gauge groups. Such extensions could reveal new classes of solvable quantum systems. Moreover, they could provide further insights into the open TS/ST correspondence.

- The open version of the TS/ST correspondence was understood for local $\mathbb{F}_0$, local $\mathbb{P}^2$, and the $\mathbb{C}^3/\mathbb{Z}_5$ orbifold at $\hbar = 2\pi$ in [6, 7], and we now have a proposal for the $Y^{N,0}$ geometries as well at any $\hbar$. However, we are still working on a case by case basis, while the closed version of the TS/ST correspondence has a clear construction

of any toric CY threefold. The ingredient that is missing for open TS/ST is a good understanding of the pole cancellation in x. The structure of the proposal in section 4.4 suggest that the answer could be hidden among simple symmetries of the mirror curve.

- Understanding the eigenfunctions of the usual Schrödinger equation with arbitrary polynomial potential would be a wonderful application of our results. However, as pointed out in [55, sec. 6], this requires an analytic continuation of our eigenfunctions away from the semi-classical region, which we cannot straightforwardly carry out with current techniques.

We hope to report on some of these points in the future.

Appendix A

Appendices

A.1 Extra notes

A.1.1 Matrix model and eigenfunction identities for the Painlevé kernel

In this appendix, we argue for the equivalence between the identities (2.6.5) and (2.6.6)[1]. Our strategy is similar to the one used in the context of ABJM theory, see e.g. [228] and reference therein.

Let us start by writing (2.6.5) as

$$\int_{\mathbb{R}+\mathrm{i}\sigma_*} \mathrm{d}\sigma \frac{\tan(2\pi\sigma)}{(2\cos(2\pi\sigma))^N}\left(Z^{\mathrm{II}}_{\mathrm{tot}}(q,t,\sigma)+Z^{\mathrm{II}}_{\mathrm{tot}}\left(-q-\frac{\mathrm{i}}{2},t,\sigma+\frac{1}{2}\right)\right) = \mathrm{i}\frac{2^{11/12}\sqrt{\pi}t^{3/16}}{\mathrm{e}^{3\zeta'(-1)}\mathrm{e}^{4\sqrt{t}}(4\pi)^N}\int_{\mathbb{R}}\mathrm{d}x\ \mathrm{e}^{-\mathrm{i}2qx}\mathrm{e}^{-4t^{1/4}\cosh x+x2}\Psi_N(\mathrm{e}^x,t), \quad (A.1.1)$$

where we have absorbed the $(-1)^N$ into a shift of σ, and σ_* is a strictly positive number which guarantees that the integration contour on the left-hand side of (A.1.1) does not hit the poles of $Z^{\mathrm{II}}_{\mathrm{tot}}$. This is the case if $0<\sigma_*<|\mathrm{Re}(q)|\neq 0$. If $\mathrm{Re}(q)=0$, one can take σ_* to be any strictly positive number as in footnote 12. For the sake of notation, let us define

$$f(N)=\mathrm{i}\frac{2^{11/12}\sqrt{\pi}t^{3/16}}{\mathrm{e}^{3\zeta'(-1)}\mathrm{e}^{4\sqrt{t}}(4\pi)^N}\int_{\mathbb{R}}\mathrm{d}x\ \mathrm{e}^{-\mathrm{i}2qx}\mathrm{e}^{-4t^{1/4}\cosh x+\frac{x}{2}}\Psi_N(\mathrm{e}^x,t)\,, \quad (A.1.2)$$

$$g(\sigma)=Z^{\mathrm{II}}_{\mathrm{tot}}(q,t,\sigma)+Z^{\mathrm{II}}_{\mathrm{tot}}\left(-q-\frac{\mathrm{i}}{2},t,\sigma+\frac{1}{2}\right)\,, \quad (A.1.3)$$

so that (A.1.1) becomes

$$f(N)=\int_{\mathbb{R}}\mathrm{d}\sigma\frac{\tan(2\pi(\sigma+\mathrm{i}\sigma_*))}{[2\cos(2\pi(\sigma+\mathrm{i}\sigma_*))]^N}g(\sigma+\mathrm{i}\sigma_*) = \int_{-1/2}^{1/2}\mathrm{d}\sigma\frac{\tan(2\pi(\sigma+\mathrm{i}\sigma_*))}{[2\cos(2\pi(\sigma+\mathrm{i}\sigma_*))]^N}\sum_{k\in\mathbb{Z}}g(\sigma+\mathrm{i}\sigma_*+k)\ . \quad (A.1.4)$$

[1] We will not be rigorous in switching the order of sums and integrals since all the quantities are conjecturally convergent.

Note that the second equality in (A.1.4) assumes some good analytic properties of g, for instance, g is such that the sum over n on the right-hand side of (A.1.4) is convergent. This is the case for (A.1.2). Furthermore, it is part of our conjecture that the function $\sum_{k\in\mathbb{Z}} g(\sigma + \mathrm{i}\sigma_* + k)$ is not only well-defined but also an entire function of σ. Hence, we are free to deform the integration path in (A.1.4) to any path $\mathcal{C}_{\{-1/2,1/2\}}$, beginning at $\sigma = -1/2$ and ending at $\sigma = 1/2$, as long as we don't cross the poles coming from the tangent when $\sigma + \mathrm{i}\sigma_* \in \mathbb{Z}/2 + 1/2$. Consider then the change of variables given by

$$\mu : \mathcal{C}_{\{-\frac{1}{2},\frac{1}{2}\}} \to]-\pi,\pi[: \sigma \mapsto \mu(\sigma) = -\mathrm{i}\ln\left[\frac{\cos(2\pi(\sigma + \mathrm{i}\sigma_*))}{2\pi}\right], \tag{A.1.5}$$

which is well-defined for a suitable choice of $\mathcal{C}_{\{-1/2,1/2\}}$. Then, we have for the integral that

$$\frac{1}{2\pi}\int_{-\pi}^{\pi} \mathrm{d}\mu \exp(-\mathrm{i}\mu N)\cdots = -\mathrm{i}(2\pi)^N \int_{-1/2}^{1/2} \mathrm{d}\sigma \frac{\tan(2\pi(\sigma + \mathrm{i}\sigma_*))}{[\cos(2\pi(\sigma + \mathrm{i}\sigma_*))]^N}\cdots, \tag{A.1.6}$$

and hence, we can rewrite (A.1.4) as

$$-\mathrm{i}(4\pi)^N f(N) = \frac{1}{2\pi}\int_{-\pi}^{\pi} \mathrm{d}\mu \exp(-\mathrm{i}\mu N)\sum_{k\in\mathbb{Z}} g(\sigma(\mu) + \mathrm{i}\sigma_* + k), \tag{A.1.7}$$

where $\sigma(\mu)$ is the inverse of (A.1.5). Note that the integral on the right-hand side gives the N-th Fourier coefficient of the function $\sum_{k\in\mathbb{Z}} g(\sigma(\mu) + \mathrm{i}\sigma_* + k)$. The full Fourier series leads then to

$$\begin{aligned} -\mathrm{i}\sum_{N\in\mathbb{N}} (4\pi)^N \exp(\mathrm{i}\nu N) f(N) &= \sum_{N\in\mathbb{Z}} \frac{\exp(\mathrm{i}\nu N)}{2\pi}\int_{-\pi}^{\pi} \mathrm{d}\mu \exp(-\mathrm{i}\mu N)\sum_{k\in\mathbb{Z}} g(\sigma(\mu) + \mathrm{i}\sigma_* + k) \\ &= \sum_{k\in\mathbb{Z}} g(\sigma(\nu) + \mathrm{i}\sigma_* + k). \end{aligned} \tag{A.1.8}$$

where the last equality holds whenever the Fourier series on the previous line is convergent. We expect this to be true in our case even though we do not have a rigorous proof. We also used that $f(-N) = 0$ for $N \in \mathbb{N}\setminus\{0\}$.

To go in the opposite direction from (A.1.8) to (A.1.4), one can apply Cauchy's residue theorem. Using the notation

$$\kappa = \exp(\mathrm{i}\nu) = \frac{\cos(2\pi(\sigma + \mathrm{i}\sigma_*))}{2\pi} \tag{A.1.9}$$

one can multiply both sides in (A.1.8) by $1/\kappa^{N+1}$ and integrate over κ along an anticlockwise contour of radius 1 centered at the origin to arrive at

$$\begin{aligned} (2\pi)(4\pi)^N f(N) &= \oint \frac{\mathrm{d}\kappa}{\kappa^{N+1}} \sum_{k\in\mathbb{Z}} g(\sigma(-\mathrm{i}\ln(\kappa)) + \mathrm{i}\sigma_* + k) \\ &= \mathrm{i}\int_{-\pi}^{\pi} \mathrm{d}\nu \exp(-\mathrm{i}\nu N)\sum_{k\in\mathbb{Z}} g(\sigma(\nu) + \mathrm{i}\sigma_* + k) \end{aligned} \tag{A.1.10}$$

which is equivalent to (A.1.7) and hence by (A.1.6) to (A.1.4). We can conclude that (A.1.4) and (A.1.8) are indeed equivalent, provided f and g have good analytic properties, which we assume to be the case.

A.1.2 Comment on $\xi = 0$, $\hbar = 2\pi$ for finite difference modified Mathieu

The eigenfunctions of (3.2.7) for $\xi = 0$ and $\hbar = 2\pi$ were studied extensively in [6, 7]. The explicit expression for $\psi_0(x)$ can be found in [6, eqs. (2.95), (2.96)]. However, when written in the form given in [6, eqs. (2.95), (2.96)], the structure presented in (3.2.50) is not immediately apparent. In this appendix, we clarify the reasons for this.

Let us consider the $\xi \to 0$ limit when $\hbar = 2\pi$ of (3.2.60). In this case one gets

$$\sqrt{2} q_{\pm,k}(x) = \ln\left[e^x \left(\frac{e^x + e^{-x} \pm \operatorname{sgn}\left(\arg\left(x + i\frac{\pi}{2}\right)\right)\sqrt{(e^x - e^{-x})^2}}{2} \right)\right] + i2\pi k\,, \tag{A.1.11}$$

and it should be noted that the important symmetry $q_{\pm,k}(x) = -q_{\mp,-k}(-x - i\pi) \bmod i2\pi$ is still present. Let us now write the two terms (3.2.60) explicitly for $x \in \mathbb{R}$ and $\hbar = 2\pi$. We find that

$$\begin{aligned} \omega_{0,+}(x) &= i2\pi \lim_{\xi\to 0}\left(\operatorname{Res}_+(x) \sum_{k=0}^{1} U(x, q_{+,k}(x)) E(q_{+,k}(x)) \right) \\ &= \begin{cases} -\frac{1}{\sqrt{\pi}} e^{ix^2/4\pi} \left(\frac{e^x}{e^{2x}-1}\right) & \text{if } x < 0\,, \\ \frac{e^{i\pi/4}}{\sqrt{2\pi}} e^{-ix^2/4\pi} \left(\frac{e^x(e^x - i)}{e^{2x}-1}\right) & \text{if } x > 0\,, \end{cases} \end{aligned} \tag{A.1.12}$$

$$\begin{aligned} \omega_{0,-}(x) &= i2\pi \lim_{\xi\to 0}\left(\operatorname{Res}_-(x) \sum_{k=0}^{1} U(x, q_{-,k}(x)) E(q_{-,k}(x)) \right) \\ &= \begin{cases} \frac{e^{i\pi/4}}{\sqrt{2\pi}} e^{-ix^2/4\pi} \left(\frac{e^x(e^x - i)}{e^{2x}-1}\right) & \text{if } x < 0\,, \\ -\frac{1}{\sqrt{\pi}} e^{ix^2/4\pi} \left(\frac{e^x}{e^{2x}-1}\right) & \text{if } x > 0\,, \end{cases} \end{aligned} \tag{A.1.13}$$

and $\omega_{0,\pm}(x)$ diverges when $x = 0$ but the sum $\psi_0(x)$ is still well-defined. One finds for all $x \in \mathbb{R}$ that

$$\psi_0(x) = \omega_{0,+}(x) + \omega_{0,-}(x) = \frac{e^{i\pi/4}}{\sqrt{2\pi}} e^{-ix^2/4\pi} \left(\frac{e^x(e^x - i)}{e^{2x} - 1} \right) - \frac{1}{\sqrt{\pi}} e^{ix^2/4\pi} \left(\frac{e^x}{e^{2x} - 1} \right)\,, \tag{A.1.14}$$

which is indeed the same expression as in [6, eq. (2.95)-(2.96)]. However, if we were to start from the final expression on the right-hand side of (A.1.14), we would not see the general structure (3.2.50) which is instead manifest when $\xi \neq 0$.

A.1.3 The dual four-dimensional limit

Consider the following reparametrization of the Kähler parameters [14, p. 5]

$$X = \exp(g_s x)\,, \qquad Q_B = g_s^4 t\,, \qquad Q_F = \exp(2g_s i\sigma)\,, \tag{A.1.15}$$

where as before $q = \exp(\mathrm{i} g_s)$ and $q^S = \exp\left(\mathrm{i}(2\pi)^2/g_s\right)$. The four-dimensional limit is then $g_s \to 0$ with x, t and σ and kept fixed. In terms of more familiar gauge theoretic quantities, one has

$$x = \frac{y}{2\epsilon}\,, \qquad t = \left(\frac{\Lambda}{\epsilon}\right)^4\,, \qquad \sigma = \mathrm{i}\frac{a}{2\epsilon}\,, \tag{A.1.16}$$

where ϵ corresponds to the Ω-background parameter in the self-dual phase, Λ is the instanton counting parameter and, a is the Coulomb branch parameter or equivalently the A-period of the underlying Seiberg-Witten geometry. The parameter y corresponds to the position of the defect. Note also that the variable x is called q in the main text.

The instanton part of the type II defect as obtained from this limit is given in (A.3.32) and reads to second order in t

$$\begin{aligned} Z^{\mathrm{II}}_{\mathrm{inst}}(x,t,\sigma) = 1 &- \left[\frac{\widetilde{x}}{2\sigma^2\left(\widetilde{x}^2-\sigma^2\right)}\right] t \\ &+ \left[\frac{\widetilde{x}\left(\widetilde{x}+1\right)^2 - \widetilde{x}\left(10\widetilde{x}^2+19\widetilde{x}+10\right)\sigma^2 + \left(8\widetilde{x}^2+30\widetilde{x}+9\right)\sigma^4}{4\sigma^4\left(4\sigma^2-1\right)^2\left(\widetilde{x}^2-\sigma^2\right)\left(\left(\widetilde{x}+1\right)^2-\sigma^2\right)}\right] t^2 + \mathcal{O}\left(t^3\right)\,, \end{aligned} \tag{A.1.17}$$

where we used for the sake of readability

$$\widetilde{x} = \mathrm{i}x + \frac{1}{2}\,. \tag{A.1.18}$$

We checked (A.1.17) against [32, eqs A.3-A.13] up to and including order t^2, and found perfect agreement[2]. On the other hand, one can see that the NS instanton part of the topological string vanishes in the same four-dimensional limit.

In the 4d limit, the polynomial part of the open grand potential reduces to

$$Z^{\mathrm{II},(\mathrm{p})}(x) = \lim_{g_s\to 0} Z^{(\mathrm{p})}\left(\exp(g_s x), g_s\right) = \exp(-\pi x) = \exp\left(-\pi\frac{y}{2\epsilon}\right). \tag{A.1.19}$$

Looking at the 1-loop part of the open grand potential and the reparametrization (A.1.15), one can see that

$$-\mathrm{e}^{2\pi b^{-1} z_\pm} = \mathrm{e}^{-g_s(x\pm\mathrm{i}\sigma)}, \tag{A.1.20}$$

and using the integral representation of Faddeev's quantum dilogarithm (A.2.16) gives

$$\ln\left(\Phi_b(z_\pm)\right) = -\mathrm{i}\frac{\mathrm{Li}_2\left(\mathrm{e}^{-g_s(x\pm\mathrm{i}\sigma)}\right)}{g_s} - \mathrm{i}\int_0^{+\infty}\frac{\mathrm{d}t}{1+\mathrm{e}^{2\pi t}}\ln\left(\frac{1-\mathrm{e}^{-g_s(x\pm\mathrm{i}\sigma)}\mathrm{e}^{-g_s t}}{1-\mathrm{e}^{-g_s(x\pm\mathrm{i}\sigma)}\mathrm{e}^{g_s t}}\right). \tag{A.1.21}$$

[2]Looking at the product of the instanton parts of the Nekrasov (2.3.10) and defect (2.6.1), (A.1.17), partition functions, one finds equality with the "chiral defect" [32, eq A.7] if $\sigma_{[32]} = -\epsilon(\widetilde{x}-1)$, and with the "anti-chiral" defect [32, eq A.10] if $\sigma_{[32]} = \epsilon(\widetilde{x}-1)$. Note that since we are working in the self-dual phase of the Ω-background, we have $\epsilon = \epsilon_1 = -\epsilon_2$.

The expansion of for $g_s \to 0$ from above

$$-\mathrm{i}\frac{\mathrm{Li}_2\left(\mathrm{e}^{-g_s(x\pm\mathrm{i}\sigma)}\right)}{g_s} = -\mathrm{i}\frac{\pi^2}{6}\frac{1}{g_s} - \mathrm{i}\,(x\pm\mathrm{i}\sigma)\ln(g_s) - \mathrm{i}\,(x\pm\mathrm{i}\sigma)\left[\ln(x\pm\mathrm{i}\sigma)-1\right] + \mathcal{O}(g_s)\,, \tag{A.1.22}$$

$$-\mathrm{i}\int_0^{+\infty}\frac{\mathrm{d}t}{1+\mathrm{e}^{2\pi t}}\ln\left(\frac{1-\mathrm{e}^{-g_s(x\pm\mathrm{i}\sigma)}\mathrm{e}^{-g_s t}}{1-\mathrm{e}^{-g_s(x\pm\mathrm{i}\sigma)}\mathrm{e}^{g_s t}}\right) = -\mathrm{i}\int_0^{+\infty}\frac{\mathrm{d}t}{1+\mathrm{e}^{2\pi t}}\ln\left(\frac{x\pm\mathrm{i}\sigma+t}{x\pm\mathrm{i}\sigma-t}\right) + \mathcal{O}(g_s)\,, \tag{A.1.23}$$

The divergent terms in (A.1.22) can be dealt with properly in the context of the open TS/ST correspondence [2], but we will simply drop them. By using the integral representation of the Gamma function, we get [229, p. 8]

$$\begin{aligned}
&-\mathrm{i}\int_0^{+\infty}\frac{\mathrm{d}t}{1+\mathrm{e}^{2\pi t}}\ln\left(\frac{x\pm\mathrm{i}\sigma+t}{x\pm\mathrm{i}\sigma-t}\right) = -2\int_0^{+\infty}\frac{\mathrm{d}t}{1+\mathrm{e}^{2\pi t}}\arctan\left(\frac{t}{-\mathrm{i}\,(x\pm\mathrm{i}\sigma)}\right)\\
&= \mathrm{i}\,(x\pm\mathrm{i}\sigma)\ln\left(-\mathrm{i}\,(x\pm\mathrm{i}\sigma)\right) - \mathrm{i}\,(x\pm\mathrm{i}\sigma) - \frac{\ln(2\pi)}{2} + \ln\Gamma\left(-\mathrm{i}\,(x\pm\mathrm{i}\sigma)+\frac{1}{2}\right)\,,
\end{aligned} \tag{A.1.24}$$

where $\ln\Gamma$ is the log Gamma function. Hence, we get

$$\lim_{g_s\to 0}\ln\left(\Phi_b\left(z_\pm\right)\right) = \ln\Gamma\left(-\mathrm{i}\,(x\pm\mathrm{i}\sigma)+\frac{1}{2}\right) - \frac{\ln(2\pi)}{2} + \frac{\pi}{2}(x\pm\mathrm{i}\sigma)\,, \tag{A.1.25}$$

and combining with (A.1.19) gives the perturbative part of the type II defect partition function

$$\begin{aligned}
Z^{\mathrm{II}}_{\mathrm{pert}}(x,\sigma) &= \lim_{g_s\to 0} Z^{(\mathrm{p})}_{\mathbb{F}_0}\left(\exp(g_s x), g_s\right) Z^{1\text{-loop}}_{\mathbb{F}_0}\left(\exp(g_s x), \exp(2g_s\mathrm{i}\sigma), g_s\right)\\
&= \frac{\Gamma\left(-\mathrm{i}\,(x-\mathrm{i}\sigma)+\frac{1}{2}\right)\Gamma\left(-\mathrm{i}\,(x+\mathrm{i}\sigma)+\frac{1}{2}\right)}{2\pi}\,.
\end{aligned} \tag{A.1.26}$$

The product of the perturbative (A.1.26) and instanton (A.1.17) (A.1.18) parts gives us then the complete partition function for the type II defect in 4d, $\mathcal{N}=2$, SU(2) super Yang-Mills[3],

$$Z^{\mathrm{II}}(x,t,\sigma) = \exp\left(\frac{\mathrm{i}}{2}x\ln(t)\right)\Gamma\left(-\mathrm{i}x-\sigma+\frac{1}{2}\right)\Gamma\left(-\mathrm{i}x+\sigma+\frac{1}{2}\right)Z^{\mathrm{II}}_{\mathrm{inst}}(x,t,\sigma)\,. \tag{A.1.27}$$

Note that we use a slightly different notation compared to the main text: what we call x here is called q elsewhere.

A.2 Special functions

A.2.1 Elliptic integrals

For the elliptic integrals, we follow the conventions of *Wolfram Mathematica* [230–233]. The notation in [137, pp. 8-10] is slightly different and we denote their elliptic integrals

[3] We choose for the four-dimensional partition function a normalization that does not include the $1/2\pi$. In addition, the relation between eigenfunctions of the integral kernel (2.3.5) and the defect partition function (A.1.27) makes it convenient to include an extra factor $\exp(\mathrm{i}x\ln(t)/2)$ in the latter.

with a tilde. In particular, we have the normal or incomplete elliptic integral of the first kind for $k^2 \in \mathbb{R}$, $-\pi/2 < \phi < \pi/2$ and $k^2 \sin^2(\phi) < 1$, [231], [137, eq. 110.02],

$$\mathrm{F}\left(\phi\middle|k^2\right) = \int_0^\phi \frac{\mathrm{d}\theta}{\sqrt{1-k^2\sin^2(\theta)}} = \widetilde{F}(\phi,k)\,, \tag{A.2.1}$$

the normal or incomplete elliptic integral of the second kind for $k^2 < 1$ and $-\pi/2 < \phi < \pi/2$, [232], [137, eq. 110.03],

$$\mathrm{E}\left(\phi\middle|k^2\right) = \int_0^\phi \mathrm{d}\theta\sqrt{1-k^2\sin^2(\theta)} = \widetilde{E}(\phi,k)\,, \tag{A.2.2}$$

and the normal or incomplete elliptic integral of the third kind for $k^2, \alpha^2 \in \mathbb{R}$, $-\pi/2 < \phi < \pi/2$ and $k^2\sin^2(\phi) < 1$, [233], [137, eq. 110.04],

$$\Pi\left(\alpha^2;\phi\middle|k^2\right) = \int_0^\phi \frac{\mathrm{d}\theta}{\left(1-\alpha^2\sin^2(\theta)\right)\sqrt{1-k^2\sin^2(\theta)}} = \widetilde{\Pi}\left(\phi,\alpha^2,k\right). \tag{A.2.3}$$

The complete elliptic integrals are obtained by taking $\phi = \pi/2$,

$$\mathrm{K}\left(k^2\right) = \mathrm{F}\left(\frac{\pi}{2}\middle|k^2\right), \qquad \mathrm{E}\left(k^2\right) = \mathrm{E}\left(\frac{\pi}{2}\middle|k^2\right), \qquad \Pi\left(\alpha^2\middle|k^2\right) = \Pi\left(\alpha^2;\frac{\pi}{2}\middle|k^2\right). \tag{A.2.4}$$

The complete elliptic integrals of the first and second kind are analytic on $\mathbb{C}$ apart from a branch cut along the positive real line for $k^2 \geqslant 1$, and the complete elliptic integral of the third kind is analytic on $\mathbb{C}^2$ apart from similar branch cuts for $k^2, \alpha^2 \geqslant 1$ [230, 232, 233].

We also need a Jacobi elliptic function sn which is an inverse of the incomplete elliptic integral of the first kind [137, p. 18],

$$\mathrm{sn}\left(v\middle|k^2\right), \qquad \mathrm{sn}\left(\mathrm{F}\left(\phi\middle|k^2\right)\middle|k^2\right) = \sin(\phi)\,, \tag{A.2.5}$$

which is sometimes called the sine amplitude.

A.2.2 Faddeev's non-compact quantum dilogarithm

Good summaries of the properties of Faddeev's non-compact quantum dilogarithm $\Phi_b(z)$ can be found in the appendices of [11, 168] and the more comprehensive [170, app. A].

The defining representation of the quantum dilogarithm is often taken to be [170, eq. (42)]

$$\Phi_b(z) = \exp\left(\frac{1}{4}\int_{\mathbb{R}+\mathrm{i}0} \frac{\mathrm{e}^{-\mathrm{i}2zu}}{\sinh(bu)\sinh(b^{-1}u)}\frac{\mathrm{d}u}{u}\right), \qquad 2\left|\mathrm{Im}(z)\right| < \left|\mathrm{Re}\left(b+b^{-1}\right)\right|. \tag{A.2.6}$$

It can be analytically continued to a meromorphic function of z on the whole complex plane with poles and roots at [170, eq. (45)]

$$z = \begin{cases} +\mathrm{i}\left[\left(k+\frac{1}{2}\right)b + \left(\ell+\frac{1}{2}\right)b^{-1}\right] & \text{poles} \\ -\mathrm{i}\left[\left(k+\frac{1}{2}\right)b + \left(\ell+\frac{1}{2}\right)b^{-1}\right] & \text{roots} \end{cases}, \qquad k,\ell \in \mathbb{N}\,, \tag{A.2.7}$$

and with an essential singularity at complex infinity [170, p. 34]. One can determine the order of the poles and roots when $b^2 \in \mathbb{Q}_{>0}$, based on [168, eq. (21)], as we do around (A.2.15). The parameter b is in general such that $b^2 \in \mathbb{C}\backslash\mathbb{R}_{\leqslant 0}$, but we are mostly interested in $b^2 > 0$, since this corresponds to $\hbar, g_s > 0$. The asymptotic behaviour of the quantum dilogarithm is given by [170, eq. (46)]

$$\Phi_b(z) \simeq \begin{cases} \Phi_b^2(0)\exp\left(\mathrm{i}\pi z^2\right) & \mathrm{Re}(z) \gg 1 \\ 1 & \mathrm{Re}(z) \ll -1 \end{cases}, \qquad \mathrm{Re}(b) > 0\,, \tag{A.2.8}$$

and the asymptotic behaviour elsewhere in the complex z-plane can be found in [170, eq. (46)].

The non-compact quantum dilogarithm has some important symmetries. There is an inversion and parity symmetry in b [170, p. 34],

$$\Phi_b\left(z\right) = \Phi_{b^{-1}}\left(z\right) = \Phi_{-b}\left(z\right) \tag{A.2.9}$$

and the following behaviour under a parity transformation for z [170, eq. (47)] [168, p. 16],

$$\Phi_b\left(z\right)\Phi_b\left(-z\right) = \Phi_b^2\left(0\right)\exp\left(\mathrm{i}\pi z^2\right)\,, \qquad \Phi_b\left(0\right) = \exp\left(\mathrm{i}\frac{\pi}{24}\left(b^2 + b^{-2}\right)\right)\,. \tag{A.2.10}$$

One has furthermore that $\overline{\Phi_b(z)} = 1/\Phi_b(\overline{z})$ whenever $b \in \mathbb{R}\setminus\{0\}$ or $|b| = 1$. Another important property for us is the quasi-periodicity in z [170, eq. (48)] [168, eq. (77)],

$$\Phi_b(z + sib^{\pm}) = \left(1 + \mathrm{e}^{s\mathrm{i}\pi b^{\pm 2}}\mathrm{e}^{2\pi b^{\pm} z}\right)^{-s}\Phi_b(z)\,, \tag{A.2.11}$$

where $s \in \{\pm 1\}$. One has similarly

$$\Phi_b(z + \mathrm{i}kb^{\pm}) = \left\{\prod_{n=0}^{|k|-1}\left(1 + \mathrm{e}^{\mathrm{sgn}(k)\mathrm{i}\pi(2n+1)b^{\pm 2}}\mathrm{e}^{2\pi b^{\pm} z}\right)^{-\mathrm{sgn}(k)}\right\}\Phi_b(z)\,, \qquad k \in \mathbb{Z}\,, \tag{A.2.12}$$

by applying $|k|$ times (A.2.11).

One can express the non-compact quantum dilogarithm in terms of elementary functions and the classical dilogarithm when $b^2 \in \mathbb{Q}_{>0}$ [168, eqs. 9, 11, 21],

$$\Phi_b\left(z\right) = \frac{\exp\left[\frac{\mathrm{i}}{2\pi nm}\mathrm{Li}_2(\exp\left(\widetilde{z}\right)) + \left(1 + \frac{\mathrm{i}}{2\pi nm}\widetilde{z}\right)\ln\left(1 - \exp\left(\widetilde{z}\right)\right)\right]}{D_m\left(\exp\left(\frac{\widetilde{z}}{m}\right);\exp\left(\mathrm{i}2\pi\frac{n}{m}\right)\right)D_n\left(\exp\left(\frac{\widetilde{z}}{n}\right);\exp\left(\mathrm{i}2\pi\frac{m}{n}\right)\right)}\,, \tag{A.2.13}$$

$$D_k\left(X;q\right) = \prod_{\ell=1}^{k-1}\left(1 - q^{\ell}X\right)^{\ell/k}\,, \qquad \widetilde{z} = 2\pi\sqrt{nm}z + \mathrm{i}\pi\left(n+m\right)\,, \qquad b^2 = \frac{n}{m}\,, \tag{A.2.14}$$

where $n, m \in \mathbb{N}_{>0}$ are coprime. It should be noted that this is a representation of the meromorphic quantum dilogarithm in terms of multivalued functions. One can use (A.2.13) to check that the poles and roots of the quantum dilogarithm (A.2.7) located at

$$z = \pm\mathrm{i}\left[\left(km + r + \frac{1}{2}\right)b + \left(\ell n + s + \frac{1}{2}\right)b^{-1}\right]\,, \qquad b^2 = \frac{n}{m}\,, \tag{A.2.15}$$

are of order $1+k+\ell$, where $k,\ell\in\mathbb{N}$ and $r\in\mathbb{N}_{<m}$, $s\in\mathbb{N}_{<n}$, and the upper, plus sign is for the poles and the lower, minus sign for the roots.

When taking the 4d limits the following representation of Faddeev's quantum dilogarithm comes in useful [181, eqs. (3.2)-(3.8)][4]

$$\ln\Phi_b(z)=-\frac{\mathrm{i}}{2\pi b^2}\mathrm{Li}_2\left(-\mathrm{e}^{2\pi bz}\right)-\mathrm{i}\int_0^{+\infty}\frac{\mathrm{d}u}{1+\mathrm{e}^{2\pi u}}\ln\left(\frac{1+\mathrm{e}^{2\pi bz-2\pi b^2u}}{1+\mathrm{e}^{2\pi bz+2\pi b^2u}}\right),\tag{A.2.16}$$

under the condition that $2\left|\mathrm{Im}(z)\right|<b^{-1}$ when $b>0$.[5] In taking the standard or dual 4d limit on the integral representation above, one may use the following integral representation of the log gamma function [229, p. 8],

$$\ln\Gamma\left(z+\frac{1}{2}\right)=\frac{\ln(2\pi)}{2}-z+z\ln(z)-2\int_0^{+\infty}\frac{\mathrm{d}u}{1+\mathrm{e}^{2\pi u}}\arctan\left(\frac{u}{z}\right),\qquad \mathrm{Re}(z)>0\,,\tag{A.2.17}$$

which can be obtained from Binet's second formula for the log gamma function.

From [170, eqs. 65, 67] one also has the following asymptotic expansion

$$\ln\Phi_b\left(\frac{z}{2\pi b}\right)\simeq\sum_{n=0}^{\infty}\left(\mathrm{i}2\pi b^2\right)^{2n-1}\frac{B_{2n}(1/2)}{(2n)!}\partial_z^{2n}\mathrm{Li}_2(-\mathrm{e}^z)=-\frac{\mathrm{i}}{2\pi b^2}\mathrm{Li}_2(-\mathrm{e}^z)+\mathcal{O}\left(b^2\right),\tag{A.2.18}$$

when $b\to 0$ and where $B_n(1/2)$ are the Bernoulli polynomials evaluated at $1/2$.

A.3 Special functions from topological strings

Here, we summarize the all-order construction of the instanton partition function or instanton free energy for the relevant gauge theories.

One can go from the instanton partition function to the free energy by

$$Z(Q)=\sum_{n\in\mathbb{N}}\frac{Z_n}{n!}Q^n\qquad\qquad F(Q)=\ln\left(Z(Q)\right)=\sum_{n\in\mathbb{N}_{>0}}\frac{F_n}{n!}Q^n\tag{A.3.1}$$

where F_n is given by Faà di Bruno's formula

$$F_n=\sum_{m=1}^{n}(-1)^{m-1}\ (m-1)!\ B_{n,m}\left(Z_1,\cdots,Z_{n-m+1}\right),\tag{A.3.2}$$

and the $B_{n,m}$ are the partial or incomplete, exponential Bell polynomials, BellY in *Wolfram Mathematica*.

[4] There appears to be a constant term missing in [181, eqs. (3.2)-(3.8)].

[5] One can note from the behaviour under shifts of z by $\mathrm{i}b^{-1}$ that the representation above has a limited domain of validity: the quantum dilogarithm is quasi-periodic under such shifts while the same shifts act trivially on the right-hand side above. Some numerical checks seem to suggest that the representation above is only valid for $2\left|\mathrm{Im}(z)\right|<b^{-1}$ when $\mathrm{Re}(z)\geqslant 0$.

A.3.1 Topological vertex for local $\mathbb{F}_0$ / five-dimensional, SU(2) SYM

We summarize the refined open topological vertex for local $\mathbb{F}_0$ as presented in [1, app. A.1], which follows [234]. See [121, 235] for earlier works.

A Young diagram, or partition, μ is given by

$$\mu = \{\mu_1, \mu_2, \mu_3, \cdots \mid \forall\, k, \ell \in \mathbb{N}_{>0} : (\mu_k \in \mathbb{N}) \wedge (k \leqslant \ell \Rightarrow \mu_k \geqslant \mu_\ell)\} \,. \tag{A.3.3}$$

We denote by μ^t the transposed Young diagram

$$\mu^t = \left\{\mu_1^t, \mu_2^t, \mu_3^t, \cdots \mid \forall\, k \in \mathbb{N}_{>0} : \mu_k^t = |\{\ell \in \mathbb{N}_{>0} \mid \mu_\ell \geqslant k\}|\right\} \,. \tag{A.3.4}$$

For any pair $k, \ell \in \mathbb{N}_{>0}$ we say that $(k, \ell) \in \mu$ if $1 \leqslant \ell \leqslant \mu_k$ and we define

$$|\mu| = \sum_{k=1}^{+\infty} \mu_k \,, \qquad\qquad ||\mu||^2 = \sum_{k=1}^{+\infty} \mu_k^2 \,. \tag{A.3.5}$$

Let μ, ν be two Young diagrams and define

$$Z_\mu\left(r_1, r_2\right) = \prod_{(k,\ell)\in\mu} \left(1 - r_2^{\mu_k - \ell} r_1^{\mu_\ell^t - k + 1}\right)^{-1} \,, \qquad ||Z_\mu\left(r_1, r_2\right)||^2 = Z_{\mu^t}\left(r_1, r_2\right) Z_\mu\left(r_2, r_1\right) \,, \tag{A.3.6}$$

where $r_1 = \exp\left(\mathrm{i}\epsilon_1\right)$ and $r_2 = \exp\left(-\mathrm{i}\epsilon_2\right)$, with $\epsilon_{1,2}$ the Ω-background parameters. Note the different sign in the definition of $r_{1,2}$. Define then the Nekrasov factors as [234, eq. (A.7)]

$$N_{\mu,\nu}\left(Q; r_1, r_2\right) = \prod_{(k,\ell)\in\nu} \left(1 - Q\, r_2^{\nu_k - \ell} r_1^{\mu_\ell^t - k + 1}\right) \prod_{(k,\ell)\in\mu} \left(1 - Q\, r_2^{-\mu_k + \ell - 1} r_1^{-\nu_\ell^t + k}\right) \,, \tag{A.3.7}$$

as well as the combination

$$\begin{aligned} C_{\mu,\nu}\left(Q_X, Q_F, r_1, r_2\right) = \Bigg(& N_{\mu^t,\nu}\left(Q_F; r_1^{-1}, r_2^{-1}\right) N_{\mu^t,\nu}\left(Q_F \frac{r_1}{r_2}; r_1^{-1}, r_2^{-1}\right)\Bigg)^{-1} \\ & \frac{N_{\emptyset,\mu^t}\left(Q_X \frac{r_1^2}{r_2}; r_1^{-1}, r_2^{-1}\right)}{N_{\emptyset,\mu^t}\left(Q_X \frac{r_1}{r_2}; r_1^{-1}, r_2^{-1}\right)} \frac{N_{\emptyset,\nu}\left(Q_X Q_F \frac{r_1^2}{r_2}; r_1^{-1}, r_2^{-1}\right)}{N_{\emptyset,\nu}\left(Q_X Q_F \frac{r_1}{r_2}; r_1^{-1}, r_2^{-1}\right)} \,, \end{aligned} \tag{A.3.8}$$

where $\emptyset$ is the empty partition and $Q_{X,F}$ is related to the Kähler parameter of the brane and the fibre respectively. The "*open-closed t-brane partition function*" for local $\mathbb{F}_0$ is then given by [234, p. 50, eq. (5.4)]

$$\begin{aligned} & Z_{\text{inst}}^{\text{open}-\text{closed}}\left(Q_X, Q_F, Q_B, r_1, r_2\right) = \\ & \sum_{n\in\mathbb{N}} Q_B^n \sum_{m=0}^{n} \sum_{\substack{|\mu|=m \\ |\nu|=n-m}} r_1^{||\nu^t||^2} r_2^{||\mu^t||^2} ||Z_\mu\left(r_1, r_2\right)||^2 ||Z_\nu\left(r_2, r_1\right)||^2 C_{\mu,\nu}\left(Q_X, Q_F, r_1, r_2\right) \,, \end{aligned} \tag{A.3.9}$$

where Q_B is related to the Kähler parameter of the base. The closed partition function is then obtained by setting $Q_X = 0$, that is

$$Z_{\text{inst}}\left(Q_F, Q_B, r_1, r_2\right) = Z_{\text{inst}}^{\text{open}-\text{closed}}\left(0, Q_F, Q_B, r_1, r_2\right) . \tag{A.3.10}$$

Finally we define the t-brane instanton partition function for local $\mathbb{F}_0$ by [234, p. 50, eq. (5.7)]

$$Z_{\text{inst}}^{\text{open}}\left(Q_X, Q_F, Q_B, r_1, r_2\right) = \frac{Z_{\text{inst}}^{\text{open}-\text{closed}}\left(Q_X, Q_F, Q_B, r_1, r_2\right)}{Z_{\text{inst}}\left(Q_F, Q_B, r_1, r_2\right)} . \tag{A.3.11}$$

Two particular phases of the refined topological vertex are of interest to us: the self-dual or Gopakumar-Vafa (GV) phase $\epsilon_1 + \epsilon_2 = 0$ or $r_1 = r_2$, and the Nekrasov-Shatashvili (NS) phase $\epsilon_1 \to 0$ or $r_1 \to 1$. For the NS phase we have

$$\begin{aligned} F_{\text{inst}}^{\text{NS}}\left(t_F, t_B, \hbar\right) &= \lim_{\epsilon_1 \to 0} \left(-\epsilon_1\right) F_{\text{inst}}\left(\mathrm{e}^{-t_F}, \mathrm{e}^{-t_B}, \mathrm{e}^{\mathrm{i}\epsilon_1}, \mathrm{e}^{-\mathrm{i}\hbar}\right) , \\ F_{\text{NS,inst}}^{\text{open}}\left(x, t_F, t_B, \hbar\right) &= \lim_{\epsilon_1 \to 0} F_{\text{inst}}^{\text{open}}\left(-\mathrm{e}^{-\mathrm{i}\epsilon_1/2}\mathrm{e}^{t_F/2}\mathrm{e}^{-x}, \mathrm{e}^{-t_F}, \mathrm{e}^{-t_B}, \mathrm{e}^{\mathrm{i}\epsilon_1}, \mathrm{e}^{-\mathrm{i}\hbar}\right) . \end{aligned} \tag{A.3.12}$$

Numerically, one can see that the series expansions in t_B of the above quantities are convergent,[6] but, to our knowledge, at present there is not a rigorous mathematical proof. At leading order we have

$$F_{\text{inst}}^{\text{NS}}\left(t_F, t_B, \hbar\right) = \left[\frac{\mathrm{i}\left(1 + \mathrm{e}^{\mathrm{i}\hbar}\right)}{\left(1 - \mathrm{e}^{\mathrm{i}\hbar}\right)\left(1 - \mathrm{e}^{-\mathrm{i}\hbar}\mathrm{e}^{-t_F}\right)\left(1 - \mathrm{e}^{\mathrm{i}\hbar}\mathrm{e}^{-t_F}\right)}\right] \mathrm{e}^{-t_B} + \mathcal{O}\left(\mathrm{e}^{-2\,t_B}\right) , \tag{A.3.13}$$

$$\begin{aligned} &F_{\text{NS,inst}}^{\text{open}}\left(x, t_F, t_B, \hbar\right) = \\ &\left[\frac{\mathrm{e}^{\mathrm{i}2\hbar}\mathrm{e}^{\frac{t_F}{2}-x}\left(1 + \mathrm{e}^{-t_F} + \mathrm{e}^{\mathrm{i}\hbar}\left(1 + \mathrm{e}^{\mathrm{i}\hbar}\right)\mathrm{e}^{-t_F}\mathrm{e}^{\frac{t_F}{2}-x}\right)}{\left(1 - \mathrm{e}^{\mathrm{i}\hbar}\right)\left(1 - \mathrm{e}^{\mathrm{i}\hbar}\mathrm{e}^{-t_F}\right)\left(\mathrm{e}^{\mathrm{i}\hbar} - \mathrm{e}^{-t_F}\right)\left(1 + \mathrm{e}^{\mathrm{i}\hbar}\mathrm{e}^{-\frac{t_F}{2}-x}\right)\left(1 + \mathrm{e}^{\mathrm{i}\hbar}\mathrm{e}^{\frac{t_F}{2}-x}\right)}\right] \mathrm{e}^{-t_B} + \mathcal{O}\left(\mathrm{e}^{-2\,t_B}\right) \end{aligned} \tag{A.3.14}$$

For the GV phase we have similarly

$$\begin{aligned} F_{\text{inst}}^{\text{GV}}\left(t_F, t_B, g_s\right) &= F_{\text{inst}}\left(\mathrm{e}^{-t_F}, \mathrm{e}^{-t_B}, \mathrm{e}^{-\mathrm{i}g_s}, \mathrm{e}^{-\mathrm{i}g_s}\right) \\ F_{\text{GV,inst}}^{\text{open}}\left(x, t_F, t_B, g_s\right) &= F_{\text{inst}}^{\text{open}}\left(\mathrm{e}^{\mathrm{i}g_s/2}\mathrm{e}^{t_F/2}\mathrm{e}^{-x}, \mathrm{e}^{-t_F}, \mathrm{e}^{-t_B}, \mathrm{e}^{-\mathrm{i}g_s}, \mathrm{e}^{-\mathrm{i}g_s}\right) . \end{aligned} \tag{A.3.15}$$

The series expansion in t_B of the above quantities is convergent. In the case of $F_{\text{inst}}^{\text{GV}}$, this was rigorously demonstrated in [68].[7] The proof for $F_{\text{GV,inst}}^{\text{open}}$ follows analogously. The leading order reads then

$$F_{\text{inst}}^{\text{GV}}\left(t_B, t_F, g_s\right) = \left[\frac{2\mathrm{e}^{\mathrm{i}g_s}}{\left(1 - \mathrm{e}^{\mathrm{i}g_s}\right)^2\left(1 - \mathrm{e}^{-t_F}\right)^2}\right] \mathrm{e}^{-t_B} + \mathcal{O}\left(\mathrm{e}^{-2\,t_B}\right) , \tag{A.3.16}$$

[6] There are some issues when $\hbar$ is real, but these are resolved once F_{NS} and F_{GV} are combined in the definition of topological string grand potential J, as discussed in the main text.

[7] There are some issues when g_s is real, but these are resolved once F_{NS} and F_{GV} are combined in the definition of topological string grand potential J, as discussed in the main text.

$$F^{\text{open}}_{\text{GV,inst}}\left(x,t_F,t_B,g_s\right)=$$
$$\left[\frac{\mathrm{e}^{\mathrm{i}\frac{g_s}{2}}\mathrm{e}^{\frac{t_F}{2}-x}\left(2\mathrm{e}^{\mathrm{i}\frac{g_s}{2}}\mathrm{e}^{-\frac{t_F}{2}-x}-1-\mathrm{e}^{-t_F}\right)}{\left(1-\mathrm{e}^{\mathrm{i}g_s}\right)\left(1-\mathrm{e}^{-t_F}\right)^2\left(1-\mathrm{e}^{\mathrm{i}\frac{g_s}{2}}\mathrm{e}^{\frac{t_F}{2}-x}\right)\left(1-\mathrm{e}^{\mathrm{i}\frac{g_s}{2}}\mathrm{e}^{-\frac{t_F}{2}-x}\right)}\right]\mathrm{e}^{-t_B}+\mathcal{O}\left(\mathrm{e}^{-2\,t_B}\right), \quad \text{(A.3.17)}$$

for the closed and open parts respectively.

A.3.2 Four-dimensional, $\mathcal{N}=2$, SU(2) SYM

Consider the following four-dimensional limit for the variables in the previous section [118, 236]

$$Q_X=\exp\left(-R\left(z-a+\mathrm{i}\epsilon_1^{4\mathrm{d}}\right)\right) \qquad Q_F=\exp\left(-2Ra\right) \qquad Q_B=R^4t \quad \text{(A.3.18)}$$

$$\epsilon_{1,2}=R\epsilon_{1,2}^{4\mathrm{d}}\,, \qquad R\to 0\,. \quad \text{(A.3.19)}$$

This is the same scaling as for the standard variables in the standard 4d limit, (3.4.1), (3.4.21), and (3.4.22), and the same scaling as for the dual variables in the dual 4d limit, (3.4.33). This gives for (A.3.6)

$$Z^{4\mathrm{d}}_{\mu}\left(\epsilon_1,\epsilon_2\right)=\prod_{(k,\ell)\in\mu}\left(\left(\mu_k-\ell\right)\epsilon_2-\left(\mu^t_\ell-k+1\right)\epsilon_1\right)^{-1}, \quad \text{(A.3.20)}$$

$$\left|\left|Z^{4\mathrm{d}}_{\mu}\left(\epsilon_1,\epsilon_2\right)\right|\right|^2=Z^{4\mathrm{d}}_{\mu^t}\left(\epsilon_1,\epsilon_2\right)Z^{4\mathrm{d}}_{\mu}\left(\epsilon_2,\epsilon_1\right), \quad \text{(A.3.21)}$$

while the Nekrasov factors (A.3.7) become

$$N^{4\mathrm{d}}_{\mu,\nu}\left(\alpha;\epsilon_1,\epsilon_2\right)=\prod_{(k,\ell)\in\nu}\left(\left(\nu_k-\ell\right)\epsilon_2-\left(\mu^t_\ell-k+1\right)\epsilon_1+\mathrm{i}\alpha\right)$$
$$\prod_{(k,\ell)\in\mu}\left(\left(-\mu_k+\ell-1\right)\epsilon_2-\left(-\nu^t_\ell+k\right)\epsilon_1+\mathrm{i}\alpha\right), \quad \text{(A.3.22)}$$

and similarly

$$C^{4\mathrm{d}}_{\mu,\nu}\left(a,\epsilon_1,\epsilon_2\right)=\left(N^{4\mathrm{d}}_{\mu^t,\nu}\left(2a;\epsilon_1,\epsilon_2\right)N^{4\mathrm{d}}_{\mu^t,\nu}\left(2a-\mathrm{i}\left(\epsilon_1+\epsilon_2\right);\epsilon_1,\epsilon_2\right)\right)^{-1}, \quad \text{(A.3.23)}$$

$$C^{2\mathrm{d}/4\mathrm{d}}_{\mu,\nu}\left(z,a,\epsilon_1,\epsilon_2\right)=C^{4\mathrm{d}}_{\mu,\nu}\left(a,\epsilon_1,\epsilon_2\right)$$
$$\frac{N^{4\mathrm{d}}_{\emptyset,\mu^t}\left(z-a-\mathrm{i}\left(\epsilon_1+\epsilon_2\right);\epsilon_1,\epsilon_2\right)}{N^{4\mathrm{d}}_{\emptyset,\mu^t}\left(z-a-\mathrm{i}\epsilon_2;\epsilon_1,\epsilon_2\right)}\frac{N^{4\mathrm{d}}_{\emptyset,\nu}\left(z+a-\mathrm{i}\left(\epsilon_1+\epsilon_2\right);\epsilon_1,\epsilon_2\right)}{N^{4\mathrm{d}}_{\emptyset,\nu}\left(z+a-\mathrm{i}\epsilon_2;\epsilon_1,\epsilon_2\right)}. \quad \text{(A.3.24)}$$

Hence we find for the complete 2d/4d defect instanton partition function in a generic phase of the Ω-background

$$Z^{4\mathrm{d}}_{\text{inst}}\left(a,t,\epsilon_1,\epsilon_2\right)=\sum_{n\in\mathbb{N}}t^n\sum_{m=0}^{n}\sum_{\substack{|\mu|=m\\|\nu|=n-m}}\left(-1\right)^n\left|\left|Z^{4\mathrm{d}}_{\mu}\left(\epsilon_1,\epsilon_2\right)\right|\right|^2\left|\left|Z^{4\mathrm{d}}_{\nu}\left(\epsilon_2,\epsilon_1\right)\right|\right|^2C^{4\mathrm{d}}_{\mu,\nu}\left(a,\epsilon_1,\epsilon_2\right), \quad \text{(A.3.25)}$$

$$Z^{\mathrm{D}}_{\mathrm{inst}}\left(z,a,t,\epsilon_1,\epsilon_2\right)=$$
$$\sum_{n\in\mathbb{N}}t^n\sum_{m=0}^{n}\sum_{\substack{|\mu|=m\\|\nu|=n-m}}(-1)^n\,||Z^{4\mathrm{d}}_{\mu}\left(\epsilon_1,\epsilon_2\right)||^2||Z^{4\mathrm{d}}_{\nu}\left(\epsilon_2,\epsilon_1\right)||^2C^{2\mathrm{d}/4\mathrm{d}}_{\mu,\nu}\left(z,a,\epsilon_1,\epsilon_2\right)\,, \tag{A.3.26}$$

$$Z^{2\mathrm{d}/4\mathrm{d}}_{\mathrm{inst}}\left(z,a,t,\epsilon_1,\epsilon_2\right)=\frac{Z^{\mathrm{D}}_{\mathrm{inst}}\left(z,a,t,\epsilon_1,\epsilon_2\right)}{Z^{4\mathrm{d}}_{\mathrm{inst}}\left(a,t,\epsilon_1,\epsilon_2\right)}\,. \tag{A.3.27}$$

The NS limit as used in subsection 3.4.1 is then given by

$$F^{4\mathrm{d}}_{\mathrm{NS,inst}}\left(\sigma,t\right)=\lim_{\epsilon_1\to0}\left(-\epsilon_1\right)F^{4\mathrm{d}}_{\mathrm{inst}}\left(\sigma,t,\epsilon_1,1\right)\,, \tag{A.3.28}$$

$$Z^{2\mathrm{d}/4\mathrm{d}}_{\mathrm{NS,inst}}\left(x,\sigma,t\right)=\lim_{\epsilon_1\to0}Z^{2\mathrm{d}/4\mathrm{d}}_{\mathrm{inst}}\left(x-\mathrm{i}\frac{\epsilon_1}{2},\sigma,t,\epsilon_1,1\right)\,. \tag{A.3.29}$$

The convergence of (A.3.28) as series in t for $2\sigma\neq\epsilon_1\mathbb{Z}$ follows from [192]. Similar arguments should hold for (A.3.29) as well. The first few terms of the NS limit are

$$F^{4\mathrm{d}}_{\mathrm{NS,inst}}\left(\sigma,t\right)=-\left[\frac{2}{4\sigma^2+1}\right]t-\left[\frac{20\sigma^2-7}{4\left(4\sigma^2+1\right)^3\left(\sigma^2+1\right)}\right]t^2$$
$$-\left[\frac{4\left(144\sigma^4-232\sigma^2+29\right)}{3\left(4\sigma^2+1\right)^5\left(\sigma^2+1\right)\left(4\sigma^2+9\right)}\right]t^3+\mathcal{O}\left(t^4\right)\,, \tag{A.3.30}$$

$$Z^{2\mathrm{d}/4\mathrm{d}}_{\mathrm{NS,inst}}\left(x,\sigma,t\right)=1+\left[\frac{1-2\widetilde{x}}{\left(1+4\sigma^2\right)\left(\widetilde{x}^2+\sigma^2\right)}\right]t+$$
$$\left[\frac{5+9\widetilde{x}-27\widetilde{x}^2+14\widetilde{x}^3+(91-10\widetilde{x}(17+2\widetilde{x}(-7+2\widetilde{x})))\sigma^2+4(-7+2\widetilde{x})(-5+4\widetilde{x})\sigma^4}{4\left(1+4\sigma^2\right)^3\left(1+\sigma^2\right)\left(\widetilde{x}^2+\sigma^2\right)\left((\widetilde{x}-1)^2+\sigma^2\right)}\right]t^2$$
$$+\mathcal{O}\left(t^3\right) \tag{A.3.31}$$

where $\widetilde{x}=-\mathrm{i}x-1$.

For the GV phase we define

$$\begin{aligned}Z^{2\mathrm{d}/4\mathrm{d}}_{\mathrm{GV,inst}}\left(x,\sigma,t\right)=&Z^{2\mathrm{d}/4\mathrm{d}}_{\mathrm{inst}}\left(x+\frac{\mathrm{i}}{2},\mathrm{i}\sigma,t,-1,1\right)\,,\\ Z^{4\mathrm{d}}_{\mathrm{GV,inst}}=&Z^{4\mathrm{d}}_{\mathrm{inst}}\left(\mathrm{i}\sigma,t,-1,1\right)\end{aligned} \tag{A.3.32}$$

The convergence of (A.3.32) as a series in t for $2\mathrm{i}\sigma\notin\mathbb{Z}$ follows from [97]. The first few orders of the GV phase (A.3.32) are given by

$$Z^{4\mathrm{d}}_{\mathrm{GV,inst}}\left(\sigma,t\right)=1+\left[\frac{1}{2\sigma^2}\right]t+\left[\frac{8\sigma^2+1}{4\sigma^2\left(4\sigma^2-1\right)^2}\right]t^2+\left[\frac{8\sigma^4-5\sigma^2+3}{24\sigma^2\left(4\sigma^2-1\right)^2\left(\sigma^2-1\right)^2}\right]t^3$$
$$+\left[\frac{256\sigma^8-832\sigma^6+972\sigma^4-177\sigma^2+81}{384\sigma^4\left(4\sigma^2-1\right)^2\left(\sigma^2-1\right)^2\left(4\sigma^2-9\right)^2}\right]t^4+\mathcal{O}\left(t^5\right)\,, \tag{A.3.33}$$

$$Z^{\text{2d/4d}}_{\text{GV,inst}}(x,\sigma,t) = 1 - \left[\frac{\widetilde{x}}{2\sigma^2\left(\widetilde{x}^2-\sigma^2\right)}\right] t + \left[\frac{\widetilde{x}\left(\widetilde{x}+1\right)^2 - \widetilde{x}\left(10\widetilde{x}^2+19\widetilde{x}+10\right)\sigma^2 + \left(8\widetilde{x}^2+30\widetilde{x}+9\right)\sigma^4}{4\sigma^4\left(4\sigma^2-1\right)^2\left(\widetilde{x}^2-\sigma^2\right)\left(\left(\widetilde{x}+1\right)^2-\sigma^2\right)}\right] t^2 + \mathcal{O}\left(t^3\right), \quad \text{(A.3.34)}$$

where we used $\widetilde{x} = \mathrm{i}x + 1/2$ for convenience.

A.3.3 Four-dimensional, $\mathcal{N} = 2$, SU(N) SYM

The Nekrasov–Shatashvili (NS) functions capture physical information about supersymmetric gauge theories in the NS limit of the gravitational Ω-background, with the case relevant here being four-dimensional $\mathcal{N} = 2$, SU(N) SYM. It is convenient to organize the Coulomb branch parameters a_I into the vector[8]

$$\boldsymbol{a} = \sum_{I=1}^{N} a_I \boldsymbol{e}_I, \qquad \sum_{I=1}^{N} a_I = 0\,, \quad \text{(A.3.35)}$$

where $\boldsymbol{e}_I$ are the weights of the fundamental representation of SU(N) (see section A.4 for our conventions).

Note on convention: when dealing with Nekrasov functions, the term "instanton partition function" refers to the instantons of the supersymmetric gauge theory that appear in localization computations [18, 20, 94, 95, 237]. These should not be confused with quantum-mechanical instantons.

The NS free energy Let $\boldsymbol{Y} = (Y_1, \ldots, Y_N)$ denote an N-tuple of Young diagrams, each one being equivalently specified by an ordered partition $Y = (y_1, y_2, \ldots)$, $y_1 \geqslant y_2 \geqslant \cdots \geqslant 0$. The total size of the N-tuple is given by

$$\ell(\boldsymbol{Y}) = \sum_{I=1}^{N} |Y_I|, \qquad |Y| = \sum_{i\geqslant 1} y_i. \quad \text{(A.3.36)}$$

For a box $s = (i,j) \in Y$, we define the arm and leg lengths as

$$A_Y(s) = y_i - j, \qquad L_Y(s) = y_j^T - i, \quad \text{(A.3.37)}$$

where $Y^T = \left(y_1^T, y_2^T, \ldots\right)$ denotes the transposed partition. Let Y, W be two Young diagrams, we introduce the building block

$$N_{Y,W}(z;\epsilon_1,\epsilon_2) = \prod_{s\in Y}\left(z - \epsilon_1 L_W(s) + \epsilon_2\left(A_Y(s)+1\right)\right) \prod_{t\in W}\left(z + \epsilon_1\left(L_Y(t)+1\right) - \epsilon_2 A_W(t)\right). \quad \text{(A.3.38)}$$

The 4d instanton Nekrasov partition function for this gauge theory is given by [18, 20, 94, 95, 237]

$$Z^{\text{inst}}(\boldsymbol{a},\Lambda,\epsilon_1,\epsilon_2) = \sum_{\boldsymbol{Y}} \left((-1)^N \Lambda^{2N}\right)^{\ell(\boldsymbol{Y})} \mathcal{Z}_{\boldsymbol{Y}}(\boldsymbol{a},\epsilon_1,\epsilon_2)\,, \quad \text{(A.3.39)}$$

[8] The a_I parameters here are denoted by α_I in [55].

with

$$\mathcal{Z}_{\boldsymbol{Y}}(\boldsymbol{a},\epsilon_1,\epsilon_2) = \prod_{I,J=1}^{N} \frac{1}{N_{Y_I,Y_J}(a_I - a_J;\epsilon_1,\epsilon_2)}\,. \tag{A.3.40}$$

The instanton part of the NS free energy is then defined as

$$F^{\text{inst}}_{\text{NS}}(\boldsymbol{a},\Lambda,\hbar) = \mathrm{i}\hbar \lim_{\epsilon_2\to 0} \epsilon_2 \ln Z^{\text{inst}}(\boldsymbol{a},\Lambda,\mathrm{i}\hbar,\epsilon_2). \tag{A.3.41}$$

The first few orders in the Λ expansion of (A.3.41) for N = 2, 3 and 4 are provided in the accompanying file `ancillary_file.nb`. Note that the functions (A.3.39) and (A.3.41) are expressed as series in Λ. These series are, however, convergent; see, e.g. [97, 98, 192].

The NS partition function in presence of a surface defect In the presence of a type-II chiral defect, the partition function was computed in [29, 79] and is nicely summarized in [32, app. A]. By evaluating the residues in these expressions explicitly, the partition function can be written as

$$Z^{(c),\text{inst}}_{2d/4d}(x,\boldsymbol{a},\Lambda,\epsilon_1,\epsilon_2) = \sum_{\boldsymbol{Y}} \left((-1)^N\Lambda^{2N}\right)^{\ell(\boldsymbol{Y})} \mathcal{Z}_{\boldsymbol{Y}}(\boldsymbol{a},\epsilon_1,\epsilon_2)\, \mathcal{Z}^{(c)}_{\boldsymbol{Y}}(x,\boldsymbol{a},\epsilon_1,\epsilon_2)\,, \tag{A.3.42}$$

where the defect factor is

$$\mathcal{Z}^{(c)}_{\boldsymbol{Y}}(x,\boldsymbol{a},\epsilon_1,\epsilon_2) = \prod_{I=1}^{N} \prod_{(i,j)\in Y_I} \frac{a_I - x + i\,\epsilon_1 + j\,\epsilon_2}{a_I - x + i\,\epsilon_1 + (j-1)\epsilon_2}. \tag{A.3.43}$$

Here x denotes the two-dimensional twisted mass parameter. We then define the full instanton defect partition function in the NS limit as

$$Z^{\text{inst}}_{\text{D}}(x,\boldsymbol{a},\Lambda,\hbar) = \lim_{\epsilon_2\to 0} \frac{Z^{(c),\text{inst}}_{2d/4d}(x,\boldsymbol{a},\Lambda,\mathrm{i}\hbar,\epsilon_2)}{Z^{\text{inst}}(\boldsymbol{a},\Lambda,\mathrm{i}\hbar,\epsilon_2)}\,. \tag{A.3.44}$$

The Wilson loops Another ingredient we need is the four-dimensional limit of Wilson-loop expectation values [29, 79]; here we closely follow [55]. As before, let us write an N-tuple of Young diagrams as $\boldsymbol{Y} = (Y_1,\ldots,Y_N)$. We define the equivariant Chern character as

$$\mathrm{Ch}_{\boldsymbol{Y}}(\boldsymbol{a},\epsilon_1,\epsilon_2) = \mathcal{W} - (1-\mathrm{e}^{R\epsilon_1})(1-\mathrm{e}^{R\epsilon_2})\mathcal{V}_{\boldsymbol{Y}}\,, \tag{A.3.45}$$

where

$$\begin{aligned} \mathcal{W} &= \sum_{I=1}^{N} \mathrm{e}^{Ra_I}, \\ \mathcal{V}_{\boldsymbol{Y}} &= \sum_{I=1}^{N} \mathrm{e}^{R\alpha_I} \sum_{(k,l)\in Y_I} \mathrm{e}^{(k-1)R\epsilon_1+(l-1)R\epsilon_2}\,. \end{aligned} \tag{A.3.46}$$

In the $R\to 0$ limit, $\mathcal{W}$ behaves as

$$\mathrm{Ch}_{\boldsymbol{Y}}(\boldsymbol{a},\epsilon_1,\epsilon_2) = N + \sum_{k\geqslant 2} \mathcal{C}^{(k)}_{\boldsymbol{Y}}(\boldsymbol{a},\epsilon_1,\epsilon_2)\, R^k, \tag{A.3.47}$$

where, for example:

$$\begin{aligned}\mathcal{C}^{(2)}_{\boldsymbol{Y}}(\boldsymbol{a},\epsilon_1,\epsilon_2) &= \frac{1}{2}\sum_{I=1}^{N} a_I^2 - \epsilon_1\epsilon_2 \ell\left(\boldsymbol{Y}\right),\\ \mathcal{C}^{(3)}_{\boldsymbol{Y}}(\boldsymbol{a},\epsilon_1,\epsilon_2) &= \frac{1}{6}\sum_{I=1}^{N} a_I^3 - \epsilon_1\epsilon_2\left(\frac{\epsilon_1+\epsilon_2}{2}\ell\left(\boldsymbol{Y}\right) + \epsilon_1\sum_{I=1}^{N} c_2\left(Y_I^T\right)\right.\\ &\qquad \left. +\epsilon_2\sum_{I=1}^{N} c_2\left(Y_I\right) + \sum_{I=1}^{N} a_I\left|Y_I\right|\right),\end{aligned} \tag{A.3.48}$$

while

$$c_2\left(Y\right) = \frac{1}{2}\sum_{i\geqslant 1} y_i\left(y_i-1\right). \tag{A.3.49}$$

We define the "4d Wilson loops" as

$$\mathrm{W}^{(k)}(\boldsymbol{a},\Lambda,\epsilon_1,\epsilon_2) = \frac{1}{Z^{\mathrm{inst}}}\sum_{\boldsymbol{Y}}((-1)^N\Lambda^{2N})^{\ell(\boldsymbol{Y})}\,\mathcal{C}^{(k)}_{\boldsymbol{Y}}(\boldsymbol{a},\epsilon_1,\epsilon_2)\,Z_{\boldsymbol{Y}}(\boldsymbol{a},\epsilon_1,\epsilon_2). \tag{A.3.50}$$

Here we are interested in their NS limit, which we denote by

$$\mathrm{W}^{(k)}_{\mathrm{NS}}(\boldsymbol{a},\Lambda,\hbar) = \lim_{\epsilon_2\to 0}\mathrm{W}^{(k)}(\boldsymbol{a},\Lambda,\mathrm{i}\hbar,\epsilon_2), \quad k=1,\dots N-1. \tag{A.3.51}$$

These observables are directly related to the complex moduli parameters h_k appearing in the mirror curve, and they generalise the Matone relation to higher rank gauge theories. More precisely, we have

$$\boxed{h_j = \sum_{\boldsymbol{k}}\frac{(-1)^{|\boldsymbol{k}|-\ell(\boldsymbol{k})}}{z_{\boldsymbol{k}}}\mathrm{W}^{\boldsymbol{k}}_{\mathrm{NS}}(\boldsymbol{a},\Lambda,\hbar), \qquad j\in\{2,\cdots,N\}} \tag{A.3.52}$$

where $\boldsymbol{k}=(0,k_2,\cdots)$ satisfies

$$\ell(\boldsymbol{k}) = \sum_{m\geqslant 2} m k_m = j\,, \tag{A.3.53}$$

and we used

$$\mathrm{W}^{\boldsymbol{k}}_{\mathrm{NS}}(\boldsymbol{a},\Lambda,\hbar) = \prod_{j\geqslant 1}(j!\mathrm{W}^{(j)}_{\mathrm{NS}}(\boldsymbol{a},\Lambda,\hbar))^{k_j}\,, \quad z_{\boldsymbol{k}} = \prod_{j\geqslant 1} k_j! j^{k_j}\,, \quad |\boldsymbol{k}| = \sum_m k_m\,. \tag{A.3.54}$$

Hence, for instance:[9]

$$\begin{aligned} h_2 &= -\,\mathrm{W}^{(2)}_{\mathrm{NS}},\\ h_3 &= 2\mathrm{W}^{(3)}_{\mathrm{NS}},\\ h_4 &= \tfrac{1}{2}\big(\mathrm{W}^{(2)}_{\mathrm{NS}}\big)^2 - 6\mathrm{W}^{(4)}_{\mathrm{NS}},\\ h_5 &= -2\,\mathrm{W}^{(2)}_{\mathrm{NS}}\mathrm{W}^{(3)}_{\mathrm{NS}} + 24\mathrm{W}^{(5)}_{\mathrm{NS}},\\ h_6 &= -\tfrac{1}{6}\big(\mathrm{W}^{(2)}_{\mathrm{NS}}\big)^3 + 6\mathrm{W}^{(2)}_{\mathrm{NS}}\mathrm{W}^{(4)}_{\mathrm{NS}} + 2\big(\mathrm{W}^{(3)}_{\mathrm{NS}}\big)^2 - 120\mathrm{W}^{(6)}_{\mathrm{NS}}. \end{aligned} \tag{A.3.55}$$

[9] We omit the dependence on $(\boldsymbol{a},\Lambda,\hbar)$ in $W^{(2)}_{\mathrm{NS}}$ for brevity.

The first few orders in the Λ expansion of h_j for $N = 2$, 3 and 4 are provided in the accompanying file `ancillary_file.nb`. One can further check that

$$\mathrm{W}^{(2)}_{\mathrm{NS}} = -\frac{1}{N}\Lambda\partial_\Lambda F_{\mathrm{NS}} \tag{A.3.56}$$

giving rise to the usual quantum Matone relation [99, 100].

A.4 The $\mathfrak{su}(N)$ root system

Let us introduce some objects from the Lie algebra $\mathfrak{su}\,(N)$:

$$\begin{cases} \{\boldsymbol{b}_I\}_{I\in\{1,\cdots,N\}} & \text{standard euclidean orthonormal basis;} \\ \{\boldsymbol{e}_I\}_{I\in\{1,\cdots,N\}} & \text{weights of the fundamental representation;} \\ \{\boldsymbol{\lambda}_k\}_{k\in\{1,\cdots,N-1\}} & \text{fundamental weights, basis of the weight lattice;} \\ \{\boldsymbol{\alpha}_\ell\}_{\ell\in\{1,\cdots,N-1\}} & \text{simple roots, dual to the fundamental weights;} \end{cases} \tag{A.4.1}$$

These quantities are related to each other by:

$$\boldsymbol{e}_I = \boldsymbol{b}_I - \frac{1}{N}\sum_{J=1}^{N}\boldsymbol{b}_J\,, \qquad \boldsymbol{\alpha}_k = \boldsymbol{e}_k - \boldsymbol{e}_{k+1} = \boldsymbol{b}_k - \boldsymbol{b}_{k+1}\,, \qquad \boldsymbol{\lambda}_k = \sum_{I=1}^{k}\boldsymbol{e}_I\,, \tag{A.4.2a}$$

$$\boldsymbol{b}_I\cdot\boldsymbol{b}_J = \delta_{I,J}\,, \qquad \boldsymbol{e}_I\cdot\boldsymbol{e}_J = \delta_{I,J} - \frac{1}{N}\,, \tag{A.4.2b}$$

$$\boldsymbol{\alpha}_k\cdot\boldsymbol{\alpha}_l = C_{k,\ell} = -\delta_{k,\ell-1} + 2\delta_{k,\ell} - \delta_{k,\ell+1}\,, \qquad \boldsymbol{\lambda}_k\cdot\boldsymbol{\alpha}_l = \delta_{k,\ell}\,, \tag{A.4.2c}$$

where $C_{k,\ell}$ is the SU(N) Cartan matrix. The set of positive roots is given by:

$$\Delta^+ = \left\{\boldsymbol{\alpha}_{k,\ell} = \boldsymbol{e}_k - \boldsymbol{e}_\ell \,\middle|\, 1\leqslant k<\ell\leqslant N\right\}, \tag{A.4.3}$$

while the root lattice is denoted by:

$$Q_{N-1} = \left\{\sum_{\ell=1}^{N-1} m_\ell\boldsymbol{\alpha}_\ell \,\middle|\, m_\ell\in\mathbb{Z}\right\} = \left\{\sum_{I=1}^{N} m_I\boldsymbol{e}_I \,\middle|\, m_I\in\mathbb{Z}\wedge\sum_{I=1}^{N} m_I = 0\right\}. \tag{A.4.4}$$

In our construction of the eigenfunctions, we also need

$$\boldsymbol{\gamma} = \frac{1}{2}\sum_{I=1}^{N}(-1)^{I-1}\boldsymbol{e}_I = \sum_{k=1}^{N-1}(-1)^{k-1}\boldsymbol{\lambda}_k = \frac{1}{2}\sum_{\ell=1}^{N-1}\left(\mathbb{1}_{2\mathbb{N}+1}(\ell) - \frac{\ell}{N}\mathbb{1}_{2\mathbb{N}+1}(N)\right)\boldsymbol{\alpha}_\ell\,. \tag{A.4.5}$$

A.5 Selected plots and numerical evidence

A.5.1 The finite difference modified Mathieu equation

Below, we plot (3.3.35) for various values of the parameters. For the on-shell eigenfunctions, we have always from top left to bottom right: the $\sigma = 1$ term in (3.3.33), the $\sigma = 2$ term in (3.3.33), the complete eigenfunction ψ in (3.3.35), after normalization, and the absolute difference between the analytical and numerical eigenfunctions for 0, 2 and 4 instantons, using a logarithmic scale with base 10. With "0, 2 and 4 instantons" we mean that we truncate the large t_B expansion of ψ up to terms of order $\exp\left(-n \min\left(1, (2\pi/\hbar)\right) t_B\right)$ where $n \in \{0, 2, 4\}$. The numerical eigenfunctions are obtained by diagonalizing in the basis of the harmonic oscillator, as in [184]. The peaks visible in the bottom-right plots of the figures occur at $x = \pm \mathrm{Re}(t_F(\hbar))/2$, where the $\sigma = 1$ and $\sigma = 2$ terms of (3.3.33) have poles. The convergence of the sum over k in (3.3.35) is slower near these points, leading to those peaks. For the off-shell eigenfunctions, we have similarly from top left to bottom: the $\sigma = 1$ term in (3.3.33), the $\sigma = 2$ term in (3.3.33), and the complete eigenfunction ψ in (3.3.35), after normalization. The solid and dashed lines correspond to the real and imaginary parts, respectively.

The case $\xi = -\ln(3)/3$ and $\hbar = 2\pi/3$

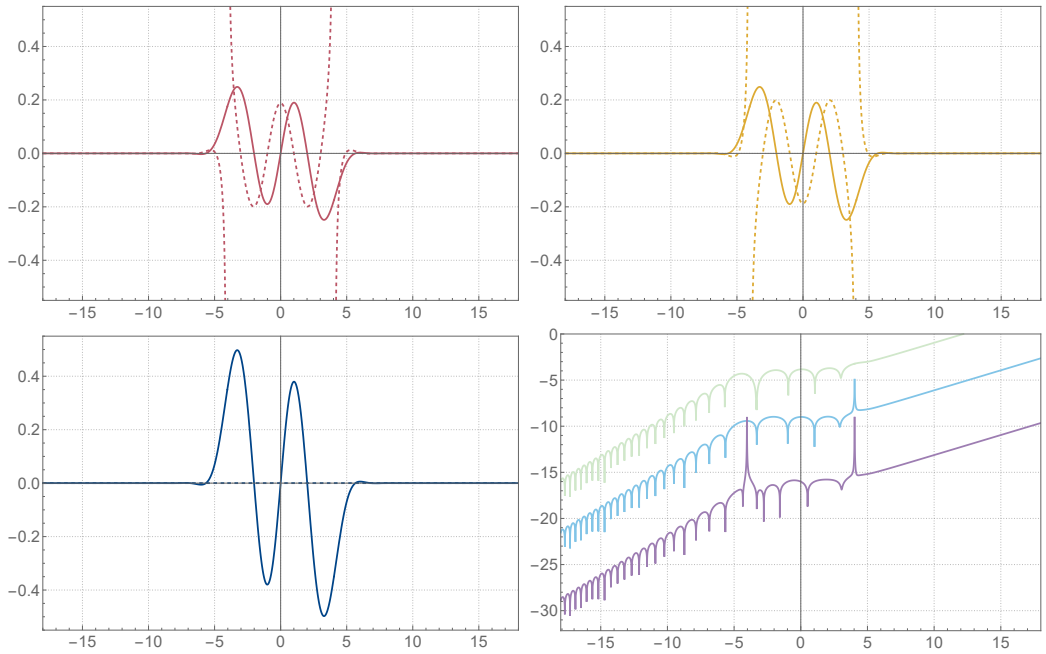

Figure A.1. The on-shell eigenfunction from topological strings for $\xi = -\ln(3)/3$ and $\hbar = 2\pi/3$ at energy $E = E_3 \approx 3.31$. See the explanation at the beginning of subsection A.5.1.

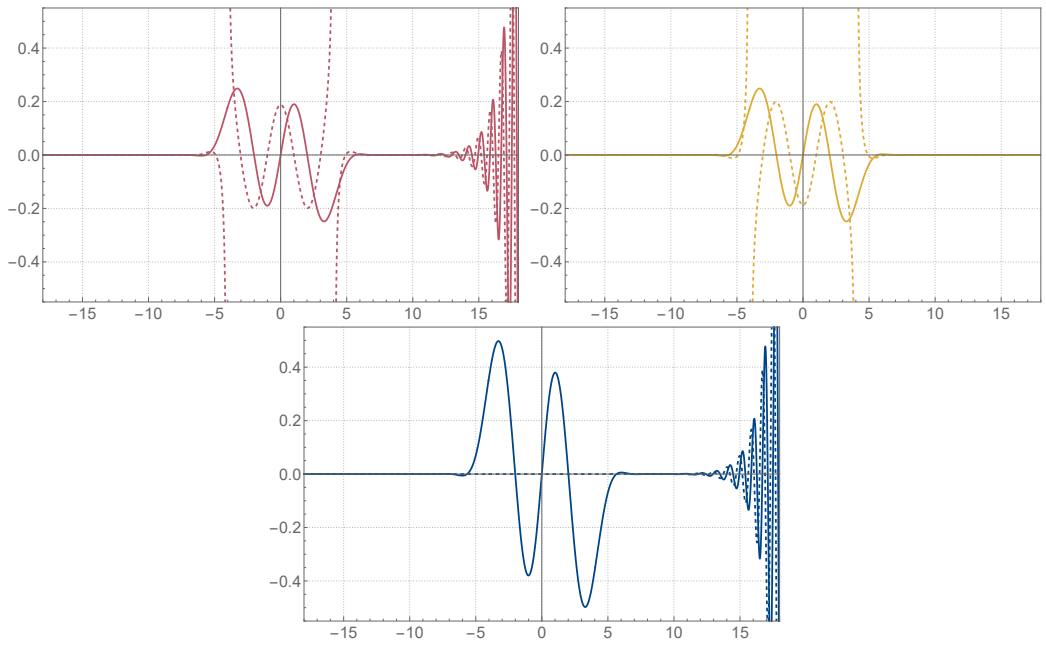

Figure A.2. The off-shell eigenfunction from topological strings for $\xi = -\ln(3)/3$ and $\hbar = 2\pi/3$ at energy $E = 40367/12209$, just below E_3. See the explanation at the beginning of subsection A.5.1.

The case $\xi = \sqrt{7}/4$ and $\hbar = 3\pi$

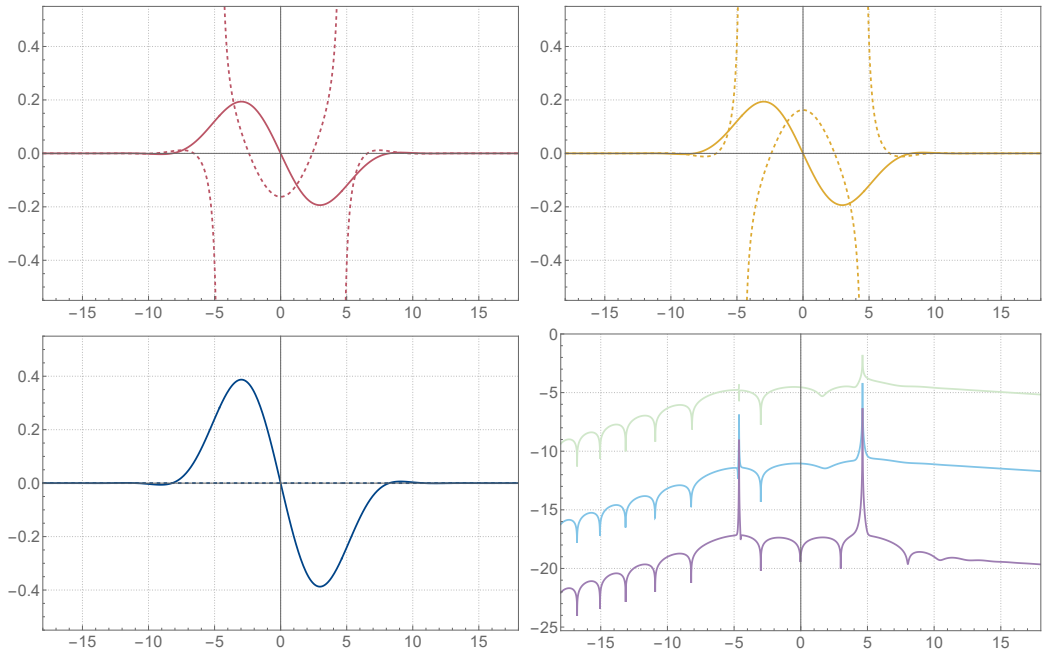

Figure A.3. The on-shell eigenfunction from topological strings for $\xi = \sqrt{7}/4$ and $\hbar = 3\pi$ at energy $E = E_1 \approx 5.95$. See the explanation at the beginning of subsection A.5.1.

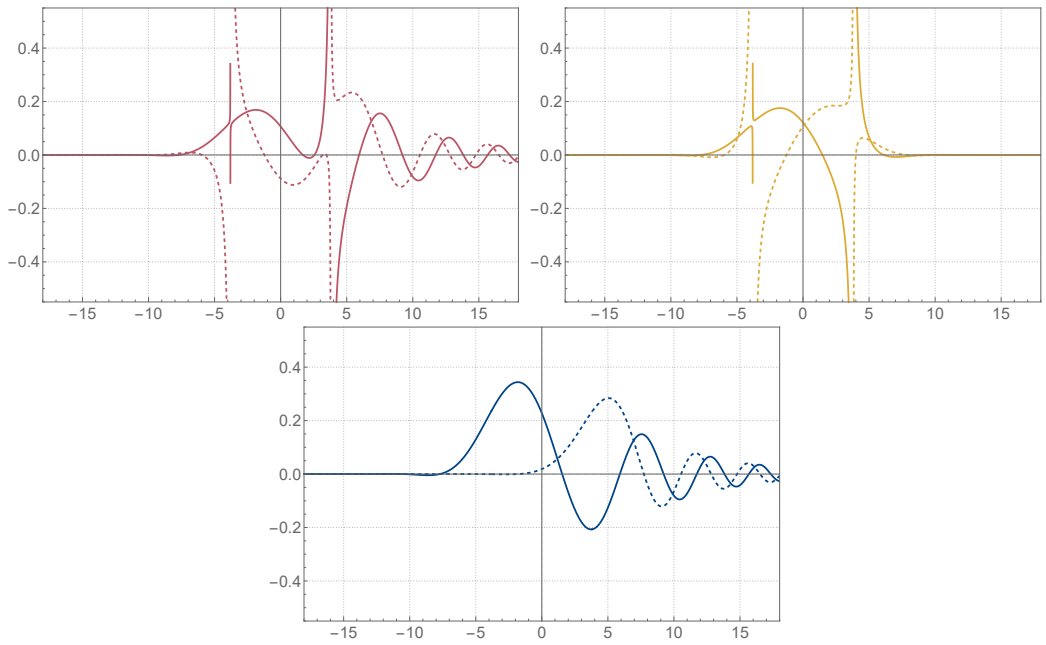

Figure A.4. The off-shell eigenfunction from topological strings for $\xi = \sqrt{7}/4$ and $\hbar = 3\pi$ at energy $E = 118/23$, which is between E_0 and E_1. See the explanation at the beginning of subsection A.5.1.

The case $\xi = 1/7$ and $\hbar = 5\pi/2$

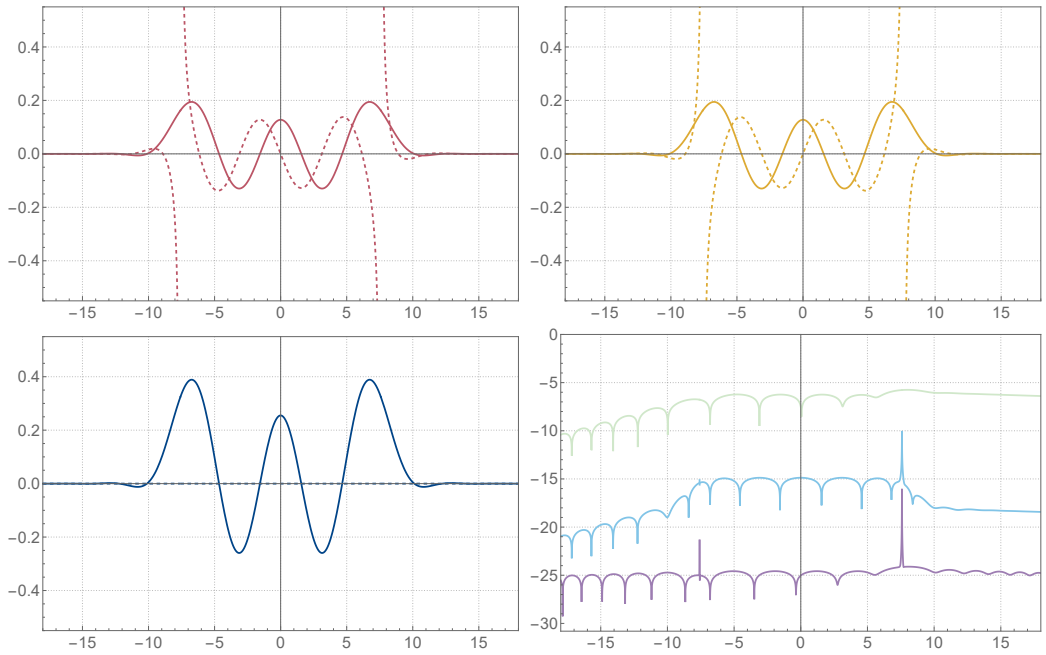

Figure A.5. The on-shell eigenfunction from topological strings for $\xi = 1/7$ and $\hbar = 5\pi/2$ at energy $E = E_4 \approx 7.87$. See the explanation at the beginning of subsection A.5.1.

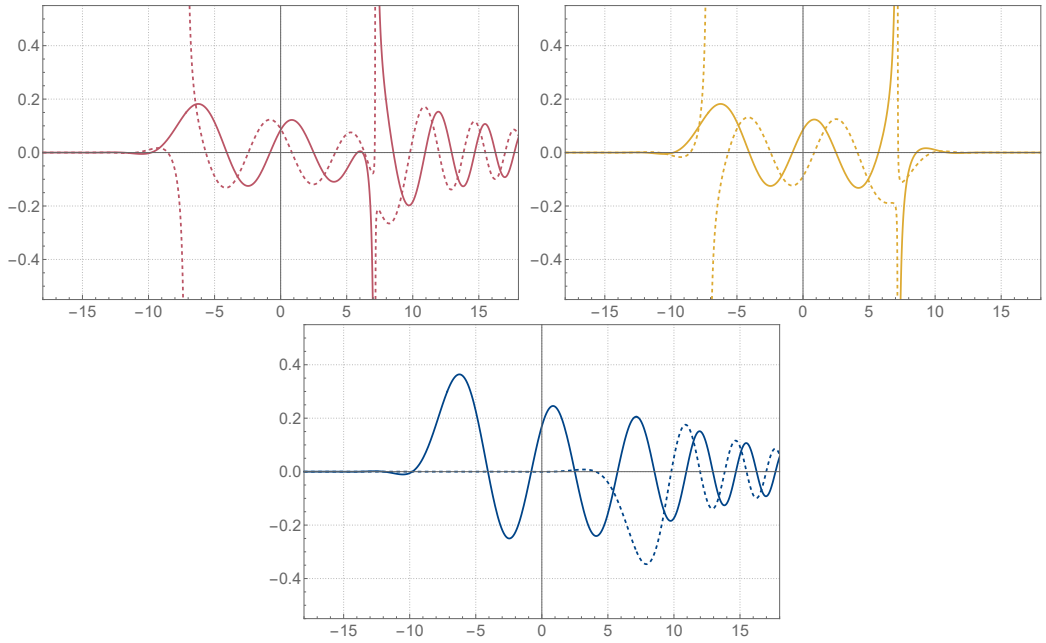

Figure A.6. The off-shell eigenfunction from topological strings for $\xi = 1/7$ and at energy $E = 149/20$, which is between E_3 and E_4. See the explanation at the beginning of subsection A.5.1.

The case $\xi = 2/3$ and $\hbar = 4\sqrt{2}$

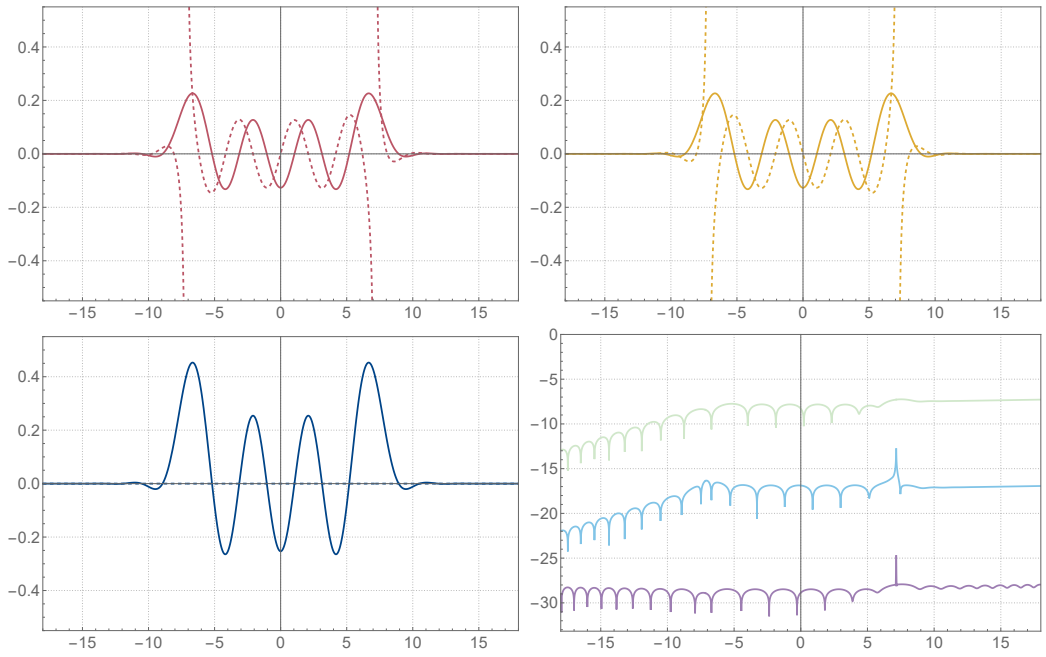

Figure A.7. The on-shell eigenfunction from topological strings for $\xi = 2/3$ and $\hbar = 4\sqrt{2}$ at energy $E = E_6 \approx 8.49$. See the explanation at the beginning of subsection A.5.1.

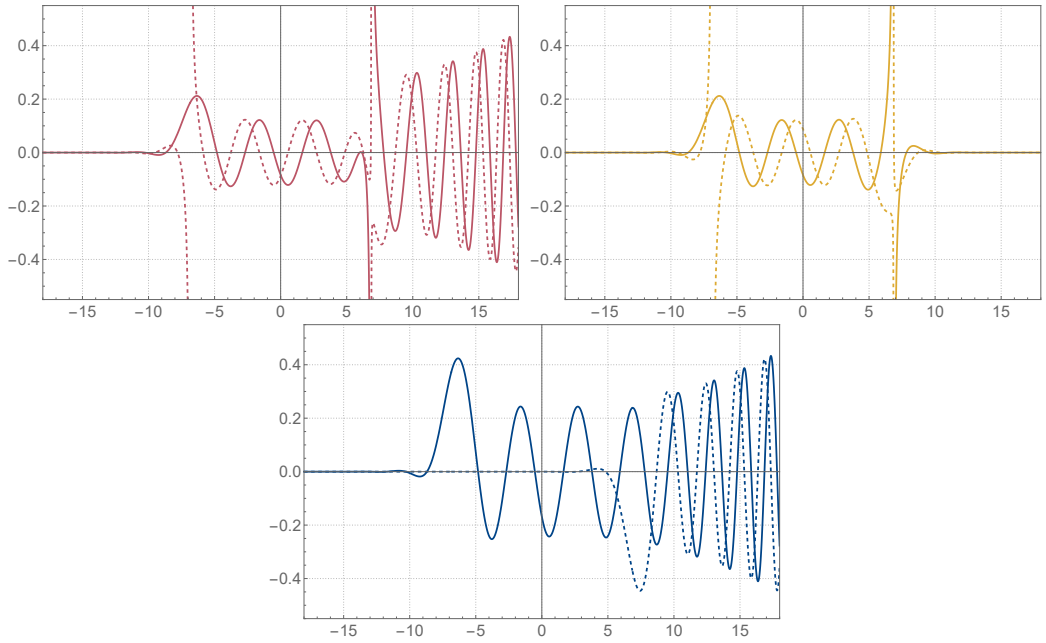

Figure A.8. The off-shell eigenfunction from topological strings for $\xi = 2/3$ and $\hbar = 4\sqrt{2}$ at energy $E = 172/21$, between E_5 and E_6. See the explanation at the beginning of subsection A.5.1.

A.5.2 The finite difference Schrödinger equations

In this appendix, we present additional numerical evidence supporting our results. We focus on the cubic and quartic potentials, displaying, for various choices of parameters, the ground, first, and second excited states for the cubic case, the first and second excited states for the quartic case.

In figure A.9 we show the ground-state wavefunction for the cubic potential for $h_2 = -5$. Due to the deep local minimum of the potential, the wavefunction closely resembles that of a bound state. In figure A.10 we show the first excited state for $h_2 = -3$, together with the two singular saddles, making the cancellation of poles in their sum evident. Finally, for the cubic case, figure A.11 shows the wavefunction corresponding to the second excited state for the cubic potential with $h_2 = 2$. In this case, the potential has no real stationary points, yet resonant eigenfunctions still exist. Moving on to the quartic case, in figure A.12 we show the wavefunction of the first excited state for the symmetric ($h_3 = 0$) single well potential with $h_2 = 3.5$, together with the two singular saddle contributions. The on-shell solution is antisymmetric and normalized to 1 at $x = 1/2$. Finally, figure A.13 displays the wavefunction corresponding to the second excited state of the quartic potential with $h_2 = 1.2$ and $h_3 = -4.7$. The corresponding potential is an asymmetric quartic single well with a unique minimum.

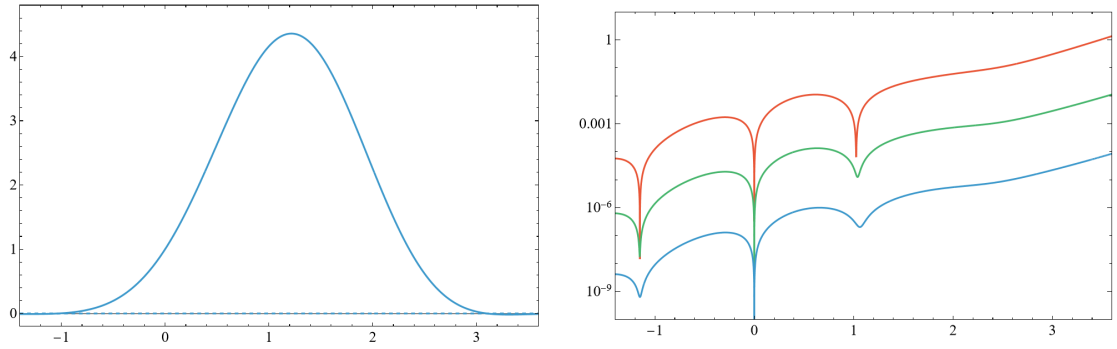

Figure A.9. Left: ground state of the $V_3(x)$ potential with $h_2 = -5$, $\hbar = 1$ and $\Lambda = (3/5)^{1/2}$; the corresponding complex energy is $E_0 \approx -1.855383 + \mathrm{i}\, 5.697572 \cdot 10^{-9}$. Dashed lines denote the imaginary part of the eigenfunction, while solid lines denote the real part. Right: difference between the numerical eigenfunction and the analytic expression from (4.2.31). The coloured curves show the effect of including an increasing number of terms in the Λ-expansion of the eigenfunction: red (0 terms), green (1 term), blue (2 terms).

The case of an odd potential

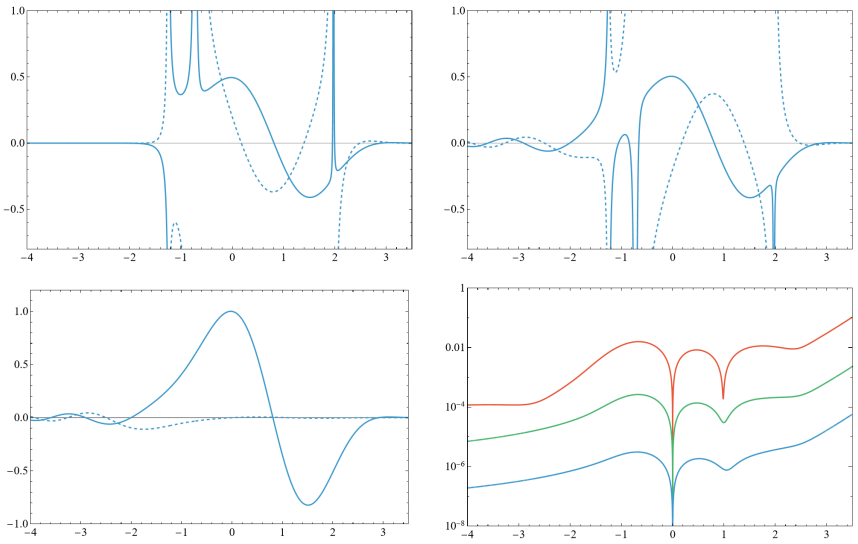

Figure A.10. The first excited state of the $V_3(x)$ potential with $h_2 = -3$, $\hbar = 1$, and $\Lambda = \frac{2}{3}$; the corresponding complex energy is $E_1 \approx 1.758084 + \mathrm{i}\,0.010614$. Dashed lines denote the imaginary part of the eigenfunction, while solid lines denote the real part. Top panels: first (left) and second (right) saddle contributions in the analytic expression (4.2.31), evaluated on-shell. The two functions develop poles individually, which cancel in the sum. Bottom left: full on-shell eigenfunction from (4.2.31). Bottom right: difference between the numerical eigenfunction and the analytic result from (4.2.31). The coloured curves show the effect of including an increasing number of terms in the Λ-expansion of the eigenfunction: red (0 terms), green (1 term), blue (2 terms).

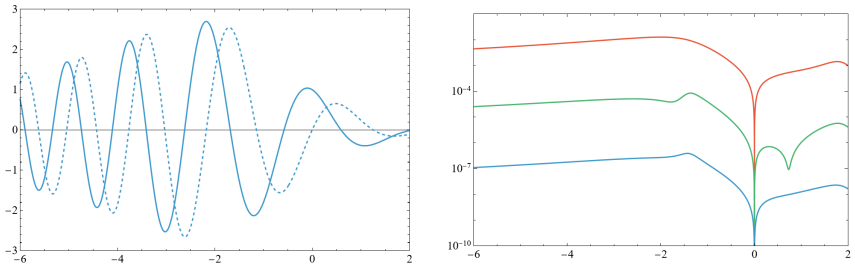

Figure A.11. Left: second excited state of the $V_3(x)$ potential with $h_2 = 2$, $\hbar = 1$ and $\Lambda = \frac{9}{10}$; the corresponding complex energy is $E_2 \approx 7.842147 + \mathrm{i}\,8.389762$. Dashed lines denote the imaginary part of the eigenfunction, while solid lines denote the real part. Right: difference between the numerical eigenfunction and the analytic expression from (4.2.31). The coloured curves show the effect of including an increasing number of terms in the Λ-expansion of the eigenfunction: red (0 terms), green (1 term), blue (2 terms).

The case of an even potential

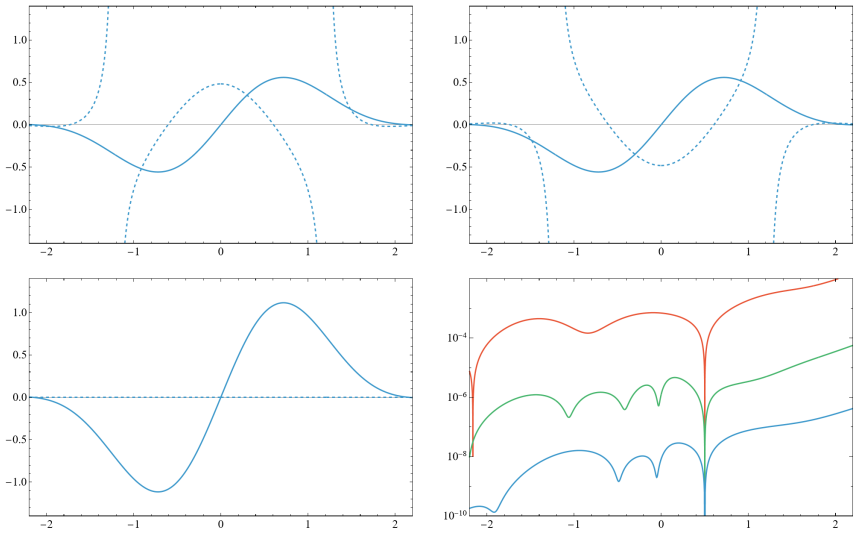

Figure A.12. First excited state of the symmetric $V_4(x)$ potential with $h_2 = 3.5$, $h_3 = 0$, $\hbar = 1$ and $\Lambda = \frac{7}{8}$; the corresponding energy is $E_1 \approx 7.324917$. Dashed lines denote the imaginary part of the eigenfunction, while solid lines denote the real part. Top panels: first (left) and second (right) saddle contributions in the analytic expression (4.2.25), evaluated on-shell. The two functions develop poles individually, which cancel in the sum. Bottom left: full on-shell eigenfunction from (4.2.25). Bottom right: difference between the numerical eigenfunction and the analytic result from (4.2.25). The coloured curves show the effect of including an increasing number of terms in the Λ-expansion of the eigenfunction: red (0 terms), green (1 term), blue (2 terms).

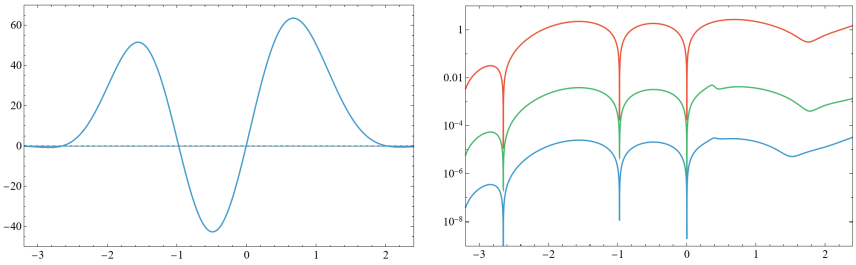

Figure A.13. Left: second excited state of the $V_4(x)$ potential with $h_2 = 1.2$, $h_3 = -4.7$, $\hbar = 1$ and $\Lambda = \frac{4}{5}$; the corresponding energy is $E_2 \approx 8.094909$. Dashed lines represent the imaginary part of the eigenfunction, while solid lines represent the real part. Right: difference between the numerical eigenfunction and the analytic expression from (4.2.25). The coloured curves show the effect of including an increasing number of terms in the Λ-expansion of the eigenfunction: red (0 terms), green (1 term), blue (2 terms).

Bibliography

[1] M. François and A. Grassi, *Painlevé Kernels and Surface Defects at Strong Coupling*, *Ann. Henri Poincaré* **26** (2025) 2117 [2310.09262].

[2] M. François and A. Grassi, *On the open TS/ST correspondence*, *arXiv preprints* (2025) [2503.21762].

[3] M. François, A. Grassi and T. Pedroni, *Eigenfunctions of deformed Schrödinger equations*, *arXiv preprints* (2025) [2511.10636].

[4] A. Grassi, Y. Hatsuda and M. Marino, *Topological Strings from Quantum Mechanics*, *Annales Henri Poincaré* **17** (2016) 3177 [1410.3382].

[5] S. Codesido, A. Grassi and M. Marino, *Spectral Theory and Mirror Curves of Higher Genus*, *Annales Henri Poincare* **18** (2017) 559 [1507.02096].

[6] M. Marino and S. Zakany, *Exact eigenfunctions and the open topological string*, *J. Phys.* **A50** (2017) 325401 [1606.05297].

[7] M. Marino and S. Zakany, *Wavefunctions, integrability, and open strings*, *JHEP* **05** (2019) 014 [1706.07402].

[8] M. Aganagic, M.C. Cheng, R. Dijkgraaf, D. Krefl and C. Vafa, *Quantum Geometry of Refined Topological Strings*, *JHEP* **1211** (2012) 019 [1105.0630].

[9] M. Reed and B. Simon, *Fourier analysis, self-adjointness*, vol. 2 of *Methods of modern mathematical physics*, Academic Press, San Diego, California (1975).

[10] K. Schmüdgen, *Unbounded Self-adjoint Operators on Hilbert Space*, no. 265 in Graduate Texts in Mathematics, Springer, Dordrecht (2012), 10.1007/978-94-007-4753-1.

[11] R. Kashaev and M. Marino, *Operators from mirror curves and the quantum dilogarithm*, *Commun. Math. Phys.* **346** (2016) 967 [1501.01014].

[12] A. Laptev, L. Schimmer and L.A. Takhtajan, *Weyl type asymptotics and bounds for the eigenvalues of functional-difference operators for mirror curves.*, *Geom. Funct. Anal.* **26** (2016) 288 [1510.00045].

[13] M. Reed and B. Simon, *Functional analysis*, vol. 1 of *Methods of modern mathematical physics*, Academic Press, San Diego, California, second ed. (1980).

[14] G. Bonelli, A. Grassi and A. Tanzini, *Seiberg–Witten theory as a Fermi gas*, *Lett. Math. Phys.* **107** (2017) 1 [1603.01174].

[15] P. Gavrylenko, A. Grassi and Q. Hao, *Connecting topological strings and spectral theory via non-autonomous Toda equations*, *arXiv preprints: High Energy Physics - Theory* (2023) [2304.11027].

[16] N. Seiberg and E. Witten, *Monopoles, duality and chiral symmetry breaking in N=2 supersymmetric QCD*, *Nucl. Phys.* **B431** (1994) 484 [hep-th/9408099].

[17] N. Seiberg and E. Witten, *Electric - magnetic duality, monopole condensation, and confinement in N=2 supersymmetric Yang-Mills theory*, *Nucl. Phys.* **B426** (1994) 19 [hep-th/9407087].

[18] G.W. Moore, N. Nekrasov and S. Shatashvili, *Integrating over Higgs branches*, *Commun. Math. Phys.* **209** (2000) 97 [hep-th/9712241].

[19] A. Losev, N. Nekrasov and S.L. Shatashvili, *Issues in topological gauge theory*, *Nucl.Phys.* **B534** (1998) 549 [hep-th/9711108].

[20] N.A. Nekrasov, *Seiberg-Witten prepotential from instanton counting*, *Adv.Theor.Math.Phys.* **7** (2004) 831 [hep-th/0206161].

[21] N. Nekrasov and A. Okounkov, *Seiberg-Witten theory and random partitions*, *Prog. Math.* **244** (2006) 525 [hep-th/0306238].

[22] N.A. Nekrasov and S.L. Shatashvili, *Quantization of Integrable Systems and Four Dimensional Gauge Theories*, in *XVIth International Congress On Mathematical Physics*, pp. 265–289, World Scientific, 2010, DOI [0908.4052].

[23] A. Mironov and A. Morozov, *Nekrasov Functions and Exact Bohr-Sommerfeld Integrals*, *JHEP* **1004** (2010) 040 [0910.5670].

[24] A. Mironov and A. Morozov, *Nekrasov Functions from Exact BS Periods: The Case of SU(N)*, *J. Phys. A* **43** (2010) 195401 [0911.2396].

[25] Y. Zenkevich, *Nekrasov prepotential with fundamental matter from the quantum spin chain*, *Physics Letters B* **701** (2011) 630 [1103.4843].

[26] N. Nekrasov, A. Rosly and S. Shatashvili, *Darboux coordinates, Yang-Yang functional, and gauge theory*, *Nucl. Phys. B Proc. Suppl.* **216** (2011) 69 [1103.3919].

[27] K.K. Kozlowski and J. Teschner, *TBA for the Toda chain*, in *New Trends in Quantum Integrable Systems*, pp. 195–219, World Scientific, 2010, DOI [1006.2906].

[28] L.F. Alday and Y. Tachikawa, *Affine SL(2) conformal blocks from 4d gauge theories*, *Lett. Math. Phys.* **94** (2010) 87 [1005.4469].

[29] D. Gaiotto and H.-C. Kim, *Surface defects and instanton partition functions*, *JHEP* **10** (2016) 012 [1412.2781].

[30] H. Kanno and Y. Tachikawa, *Instanton counting with a surface operator and the chain-saw quiver*, *JHEP* **06** (2011) 119 [1105.0357].

[31] D. Gaiotto, G.W. Moore and A. Neitzke, *Wall-crossing, Hitchin systems, and the WKB approximation*, *Adv. Math.* **234** (2013) 239 [0907.3987].

[32] A. Sciarappa, *Exact relativistic Toda chain eigenfunctions from Separation of Variables and gauge theory*, *JHEP* **10** (2017) 116 [1706.05142].

[33] S. Jeong, N. Lee and N. Nekrasov, *Intersecting defects in gauge theory, quantum spin chains, and Knizhnik-Zamolodchikov equations*, *JHEP* **10** (2021) 120 [2103.17186].

[34] S. Jeong, N. Lee and N. Nekrasov, *Parallel surface defects, Hecke operators, and quantum Hitchin system*, *arXiv e-prints: High Energy Physics - Theory* (2023) [2304.04656].

[35] S. Jeong and N. Nekrasov, *Opers, surface defects, and Yang-Yang functional*, *Adv. Theor. Math. Phys.* **24** (2020) 1789 [1806.08270].

[36] S. Jeong, *Splitting of surface defect partition functions and integrable systems*, *Nucl. Phys. B* **938** (2019) 775 [1709.04926].

[37] G. Bonelli, C. Iossa, D. Panea Lichtig and A. Tanzini, *Irregular Liouville Correlators and Connection Formulae for Heun Functions*, *Commun. Math. Phys.* **397** (2023) 635 [2201.04491].

[38] M. Piatek and A.R. Pietrykowski, *Solving Heun's equation using conformal blocks*, *Nucl. Phys. B* **938** (2019) 543 [1708.06135].

[39] L.F. Alday, D. Gaiotto, S. Gukov, Y. Tachikawa and H. Verlinde, *Loop and surface operators in N=2 gauge theory and Liouville modular geometry*, *JHEP* **2010** (2010) 113 [0909.0945].

[40] N. Drukker, J. Gomis, T. Okuda and J. Teschner, *Gauge Theory Loop Operators and Liouville Theory*, *JHEP* **1002** (2010) 057 [0909.1105].

[41] A. Grassi, J. Gu and M. Mariño, *Non-perturbative approaches to the quantum Seiberg-Witten curve*, *JHEP* **07** (2020) 106 [1908.07065].

[42] A. Grassi, Q. Hao and A. Neitzke, *Exact WKB methods in SU(2) $N_f = 1$*, *JHEP* **01** (2022) 046 [2105.03777].

[43] O. Lisovyy and A. Naidiuk, *Perturbative connection formulas for Heun equations*, *J. Phys. A* **55** (2022) 434005 [2208.01604].

[44] L. Hollands, P. Rüter and R.J. Szabo, *A geometric recipe for twisted superpotentials*, *JHEP* **12** (2021) 164 [2109.14699].

[45] L. Hollands and O. Kidwai, *Higher length-twist coordinates, generalized Heun's opers, and twisted superpotentials*, *Adv. Theor. Math. Phys.* **22** (2018) 1713 [1710.04438].

[46] D. Gaiotto, *Opers and TBA*, *arXiv preprints: High Energy Physics - Theory* (2014) [1403.6137].

[47] K. Ito, S. Kanno and T. Okubo, *Quantum periods and prepotential in $\mathcal{N} = 2$ SU(2) SQCD*, *JHEP* **08** (2017) 065 [1705.09120].

[48] F. Yan, *Exact WKB and the quantum Seiberg-Witten curve for 4d $N = 2$ pure SU(3) Yang-Mills. Abelianization*, *JHEP* **03** (2022) 164 [2012.15658].

[49] K. Imaizumi, *Quantum periods and TBA equations for $\mathcal{N} = 2$ $SU(2)$ $N_f = 2$ SQCD with flavor symmetry*, *Phys. Lett. B* **816** (2021) 136270 [2103.02248].

[50] L. Hollands and A. Neitzke, *Spectral Networks and Fenchel–Nielsen Coordinates*, *Lett. Math. Phys.* **106** (2016) 811 [1312.2979].

[51] A.-K. Kashani-Poor and J. Troost, *Pure $\mathcal{N} = 2$ super Yang-Mills and exact WKB*, *JHEP* **08** (2015) 160 [1504.08324].

[52] D. Fioravanti and D. Gregori, *Integrability and cycles of deformed $\mathcal{N} = 2$ gauge theory*, *Phys. Lett. B* **804** (2020) 135376 [1908.08030].

[53] L. Hollands and A. Neitzke, *Exact WKB and abelianization for the T_3 equation*, *Commun. Math. Phys.* **380** (2020) 131 [1906.04271].

[54] K. Ito, T. Kondo and H. Shu, *Wall-crossing of TBA equations and WKB periods for the third order ODE*, *Nucl. Phys. B* **979** (2022) 115788 [2111.11047].

[55] A. Grassi and M. Mariño, *A Solvable Deformation of Quantum Mechanics*, *SIGMA* **15** (2019) 025 [1806.01407].

[56] M. Aganagic, R. Dijkgraaf, A. Klemm, M. Marino and C. Vafa, *Topological strings and integrable hierarchies*, *Commun.Math.Phys.* **261** (2006) 451 [hep-th/0312085].

[57] A.A. Belavin, A.M. Polyakov and A.B. Zamolodchikov, *Infinite Conformal Symmetry in Two-Dimensional Quantum Field Theory*, *Nucl. Phys. B* **241** (1984) 333.

[58] B.M. McCoy, C.A. Tracy and T.T. Wu, *Painleve Functions of the Third Kind*, *J. Math. Phys.* **18** (1977) 1058.

[59] H. Widom, *Some classes of solutions to the Toda lattice hierarchy*, *Commun. Math. Phys.* **184** (1997) 653 [solv-int/9602001].

[60] C.A. Tracy and H. Widom, *Asymptotics of a Class of Solutions to the Cylindrical Toda Equations*, *Commun. Math. Phys* **190** (1998) 697 [solv-int/9701003].

[61] A.B. Zamolodchikov, *Painleve III and 2D polymers*, *Nucl.Phys.* **B432** (1994) 427 [hep-th/9409108].

[62] C.A. Tracy and H. Widom, *Proofs of two conjectures related to the thermodynamic Bethe ansatz*, *Commun. Math. Phys.* **179** (1996) 667 [solv-int/9509003].

[63] G. Bonelli, A. Grassi and A. Tanzini, *New results in $\mathcal{N} = 2$ theories from non-perturbative string*, *Annales Henri Poincaré* **19** (2018) 743 [1704.01517].

[64] G. Bonelli, A. Grassi and A. Tanzini, *Quantum curves and q-deformed Painlevé equations*, *Lett. Math. Phys.* **109** (2019) 1961 [1710.11603].

[65] R. Kashaev, M. Marino and S. Zakany, *Matrix Models from Operators and Topological Strings, 2*, *Annales Henri Poincare* **17** (2016) 2741 [1505.02243].

[66] O. Gamayun, N. Iorgov and O. Lisovyy, *Conformal field theory of Painlevé VI*, *JHEP* **10** (2012) 038 [1207.0787].

[67] O. Gamayun, N. Iorgov and O. Lisovyy, *How instanton combinatorics solves Painlevé VI, V and IIIs*, *J. Phys.* **A46** (2013) 335203 [1302.1832].

[68] M.A. Bershtein and A.I. Shchechkin, *q-deformed Painlevé τ function and q-deformed conformal blocks*, *J. Phys. A* **50** (2017) 085202 [1608.02566].

[69] N. Iorgov, O. Lisovyy and J. Teschner, *Isomonodromic tau-functions from Liouville conformal blocks*, *Commun. Math. Phys.* **336** (2015) 671 [1401.6104].

[70] M. Bershtein, P. Gavrylenko and A. Marshakov, *Cluster Toda chains and Nekrasov functions*, *Theor. Math. Phys.* **198** (2019) 157 [1804.10145].

[71] M.A. Bershtein and A.I. Shchechkin, *Bilinear equations on Painlevé τ functions from CFT*, *Commun. Math. Phys.* **339** (2015) 1021 [1406.3008].

[72] A. Grassi and M. Marino, *M-theoretic matrix models*, *JHEP* **1502** (2015) 115 [1403.4276].

[73] B. Eynard and M. Marino, *A Holomorphic and background independent partition function for matrix models and topological strings*, *J.Geom.Phys.* **61** (2011) 1181 [0810.4273].

[74] S. Gukov and P. Sulkowski, *A-polynomial, B-model, and Quantization*, *JHEP* **02** (2012) 070 [1108.0002].

[75] J.M. Maldacena, G.W. Moore, N. Seiberg and D. Shih, *Exact vs. semiclassical target space of the minimal string*, *JHEP* **10** (2004) 020 [hep-th/0408039].

[76] G. Borot and B. Eynard, *Geometry of Spectral Curves and All Order Dispersive Integrable System*, *SIGMA* **8** (2012) 100 [1110.4936].

[77] C. Kozcaz, S. Pasquetti and N. Wyllard, *A & B model approaches to surface operators and Toda theories*, *JHEP* **08** (2010) 042 [1004.2025].

[78] D. Gaiotto, S. Gukov and N. Seiberg, *Surface Defects and Resolvents*, *JHEP* **09** (2013) 070 [1307.2578].

[79] M. Bullimore, H.-C. Kim and P. Koroteev, *Defects and Quantum Seiberg-Witten Geometry*, *JHEP* **05** (2015) 095 [1412.6081].

[80] Y. Pan and W. Peelaers, *Intersecting Surface Defects and Instanton Partition Functions*, *JHEP* **07** (2017) 073 [1612.04839].

[81] A. Gorsky, B. Le Floch, A. Milekhin and N. Sopenko, *Surface defects and instanton–vortex interaction*, *Nucl. Phys. B* **920** (2017) 122 [1702.03330].

[82] M. Aganagic, A. Klemm and C. Vafa, *Disk instantons, mirror symmetry and the duality web*, *Z. Naturforsch. A* **57** (2002) 1 [hep-th/0105045].

[83] M. Aganagic and C. Vafa, *Mirror symmetry, D-branes and counting holomorphic discs*, *arXiv preprints* (2000) [hep-th/0012041].

[84] A.-K. Kashani-Poor, *The Wave Function Behavior of the Open Topological String Partition Function on the Conifold*, *JHEP* **04** (2007) 004 [hep-th/0606112].

[85] L.F. Alday, D. Gaiotto and Y. Tachikawa, *Liouville Correlation Functions from Four-dimensional Gauge Theories*, *Lett.Math.Phys.* **91** (2010) 167 [0906.3219].

[86] T. Dimofte, S. Gukov and L. Hollands, *Vortex Counting and Lagrangian 3-manifolds*, *Lett. Math. Phys.* **98** (2011) 225 [1006.0977].

[87] H. Awata, H. Fuji, H. Kanno, M. Manabe and Y. Yamada, *Localization with a Surface Operator, Irregular Conformal Blocks and Open Topological String*, *Adv. Theor. Math. Phys.* **16** (2012) 725 [1008.0574].

[88] M. Taki, *Surface Operator, Bubbling Calabi-Yau and AGT Relation*, *JHEP* **07** (2011) 047 [1007.2524].

[89] S.K. Ashok, M. Billo, E. Dell'Aquila, M. Frau, R.R. John and A. Lerda, *Modular and duality properties of surface operators in N=2* gauge theories*, *JHEP* **07** (2017) 068 [1702.02833].

[90] S.K. Ashok, M. Billo, E. Dell'Aquila, M. Frau, V. Gupta, R.R. John et al., *Surface operators, chiral rings and localization in $\mathcal{N}$ =2 gauge theories*, *JHEP* **11** (2017) 137 [1707.08922].

[91] S. Gukov, *Surface operators*, in *New Dualities of Supersymmetric Gauge Theories*, J. Teschner, ed., Mathematical Physics Studies, (Cham), pp. 223–259, Springer (2016), DOI [1412.7127].

[92] B. Eynard and N. Orantin, *Invariants of algebraic curves and topological expansion*, *Commun.Num.Theor.Phys.* **1** (2007) 347 [math-ph/0702045].

[93] A. Grassi, J. Kallen and M. Marino, *The topological open string wavefunction*, *Commun. Math. Phys.* **338** (2015) 533 [1304.6097].

[94] U. Bruzzo, F. Fucito, J.F. Morales and A. Tanzini, *Multiinstanton calculus and equivariant cohomology*, *JHEP* **0305** (2003) 054 [hep-th/0211108].

[95] R. Flume and R. Poghossian, *An Algorithm for the microscopic evaluation of the coefficients of the Seiberg-Witten prepotential*, *Int. J. Mod. Phys.* **A18** (2003) 2541 [hep-th/0208176].

[96] Y. Tachikawa, $\mathcal{N} = 2$ *Supersymmetric Dynamics for Pedestrians*, vol. 890 of *Lecture Notes in Physics*, Springer, Cham (2014), 10.1007/978-3-319-08822-8, [1312.2684].

[97] A. Its, O. Lisovyy and Y. Tykhyy, *Connection problem for the sine-gordon/painlevé iii tau function and irregular conformal blocks*, *Int. Math. Res. Notices* **2015** (2014) 8903 [1403.1235].

[98] P. Arnaudo, G. Bonelli and A. Tanzini, *On the convergence of Nekrasov functions*, *Ann. Henri Poincaré* **25** (2024) 2389–2425 [2212.06741].

[99] M. Matone, *Instantons and recursion relations in $\mathcal{N} = 2$ SUSY gauge theory*, *Phys. Lett.* **B357** (1995) 342 [hep-th/9506102].

[100] R. Flume, F. Fucito, J.F. Morales and R. Poghossian, *Matone's relation in the presence of gravitational couplings*, *JHEP* **04** (2004) 008 [hep-th/0403057].

[101] O. Lisovyy and et al., "-." Unpublished notes.

[102] S. Codesido, A. Grassi and M. Marino, *Exact results in N=8 Chern-Simons-matter theories and quantum geometry*, *JHEP* **1507** (2015) 011 [1409.1799].

[103] G. Bonelli, O. Lisovyy, K. Maruyoshi, A. Sciarappa and A. Tanzini, *On Painlevé/gauge theory correspondence*, *Lett. Math. Phys.* **107** (2017) pages 2359 [1612.06235].

[104] H. Nagoya, *Irregular conformal blocks, with an application to the fifth and fourth Painlevé equations*, *J. Math. Phys.* **56** (2015) 123505 [1505.02398].

[105] H. Nagoya, *Remarks on irregular conformal blocks and Painlevé III and II tau functions*, *arXiv e-prints: Mathematical Physics* (2018) [1804.04782].

[106] O. Lisovyy and J. Roussillon, *On the connection problem for Painlevé I*, *J. Phys. A* **50** (2017) 255202 [1612.08382].

[107] P. Gavrylenko, A. Marshakov and A. Stoyan, *Irregular conformal blocks, Painlevé III and the blow-up equations*, *JHEP* **12** (2020) 125 [2006.15652].

[108] M. Bershadsky, S. Cecotti, H. Ooguri and C. Vafa, *Holomorphic anomalies in topological field theories*, *Nucl.Phys.* **B405** (1993) 279 [hep-th/9302103].

[109] M.-x. Huang and A. Klemm, *Holomorphic Anomaly in Gauge Theories and Matrix Models*, *JHEP* **09** (2007) 054 [hep-th/0605195].

[110] K. Sun, X. Wang and M.-x. Huang, *Exact Quantization Conditions, Toric Calabi-Yau and Nonperturbative Topological String*, *JHEP* **01** (2017) 061 [1606.07330].

[111] A. Grassi and J. Gu, *BPS relations from spectral problems and blowup equations*, *Lett. Math. Phys.* **109** (2019) 1271 [1609.05914].

[112] S. Jeong and N. Nekrasov, *Riemann-Hilbert correspondence and blown up surface defects*, *JHEP* **12** (2020) 006 [2007.03660].

[113] N. Nekrasov, *Blowups in BPS/CFT correspondence, and Painlevé VI*, *Annales Henri Poincaré* (2023) 1 [2007.03646].

[114] M. Lencsés and F. Novaes, *Classical Conformal Blocks and Accessory Parameters from Isomonodromic Deformations*, *JHEP* **04** (2018) 096 [1709.03476].

[115] M. Bershtein, P. Gavrylenko and A. Grassi, *Quantum Spectral Problems and Isomonodromic Deformations*, *Commun. Math. Phys.* **393** (2022) 347 [2105.00985].

[116] B.C. da Cunha and J.a.P. Cavalcante, *Expansions for semiclassical conformal blocks*, *arXiv e-prints: High Energy Physics - Theory* (2022) [2211.03551].

[117] J. Gu, *Relations between Stokes constants of unrefined and Nekrasov-Shatashvili topological strings*, *arXiv e-prints: High Energy Physics - Theory* (2023) [2307.02079].

[118] S.H. Katz, A. Klemm and C. Vafa, *Geometric engineering of quantum field theories*, *Nucl.Phys.* **B497** (1997) 173 [hep-th/9609239].

[119] A. Iqbal and A.-K. Kashani-Poor, *SU(N) geometries and topological string amplitudes*, *Adv. Theor. Math. Phys.* **10** (2006) 1 [hep-th/0306032].

[120] A. Klemm, W. Lerche, P. Mayr, C. Vafa and N.P. Warner, *Selfdual strings and N=2 supersymmetric field theory*, *Nucl. Phys. B* **477** (1996) 746 [hep-th/9604034].

[121] A. Iqbal, C. Kozcaz and C. Vafa, *The Refined topological vertex*, *JHEP* **10** (2009) 069 [hep-th/0701156].

[122] M. Taki, *Refined Topological Vertex and Instanton Counting*, *JHEP* **03** (2008) 048 [0710.1776].

[123] S. Codesido, J. Gu and M. Marino, *Operators and higher genus mirror curves*, *JHEP* **02** (2017) 092 [1609.00708].

[124] A. Grassi and M. Marino, *The complex side of the TS/ST correspondence*, *J. Phys. A* **52** (2019) 055402 [1708.08642].

[125] A. Laptev, L. Schimmer and L.A. Takhtajan, *Weyl asymptotics for perturbed functional difference operators*, *Journal of Mathematical Physics* **60** (2019) 103505.

[126] K. Iwaki and A. Saenz, *Quantum Curve and the First Painleve Equation*, *SIGMA* **12** (2016) 011 [1507.06557].

[127] K. Iwaki, *2-Parameter τ-Function for the First Painlevé Equation: Topological Recursion and Direct Monodromy Problem via Exact WKB Analysis*, *Commun. Math. Phys.* **377** (2020) 1047 [1902.06439].

[128] O. Marchal and N. Orantin, *Isomonodromic deformations of a rational differential system and reconstruction with the topological recursion: the $\mathfrak{sl}_2$ case*, *J. Math. Phys.* **61** (2020) 061506 [1901.04344].

[129] O. Marchal and N. Orantin, *Quantization of hyper-elliptic curves from isomonodromic systems and topological recursion*, *J. Geom. Phys.* **171** (2022) 104407 [1911.07739].

[130] I.K. Kostov, *Solvable statistical models on a random lattice*, *Nucl. Phys. Proc. Suppl.* **45A** (1996) 13 [hep-th/9509124].

[131] I.K. Kostov, *O(n) Vector Model on a Planar Random Lattice: Spectrum of Anomalous Dimensions*, *Mod. Phys. Lett.* **A4** (1989) 217.

[132] I.K. Kostov and M. Staudacher, *Multicritical phases of the O(n) model on a random lattice*, *Nucl. Phys.* **B384** (1992) 459 [hep-th/9203030].

[133] I.K. Kostov, *Exact solution of the six vertex model on a random lattice*, *Nucl. Phys.* **B575** (2000) 513 [hep-th/9911023].

[134] B. Eynard and C. Kristjansen, *More on the exact solution of the O(n) model on a random lattice and an investigation of the case $|n| > 2$*, *Nucl. Phys.* **B466** (1996) 463 [hep-th/9512052].

[135] B. Eynard and C. Kristjansen, *Exact solution of the O(n) model on a random lattice*, *Nucl. Phys.* **B455** (1995) 577 [hep-th/9506193].

[136] T. Suyama, *On Large N Solution of N=3 Chern-Simons-adjoint Theories*, *Nucl. Phys. B* **867** (2013) 887 [1208.2096].

[137] P.F. Byrd and M.D. Friedman, *Handbook of Elliptic Integrals for Engineers and Scientists*, vol. 67 of *Die Grundlehren der mathematischen Wissenschaften*, Springer, Berlin, Heidelberg, Germany, second ed. (1971), 10.1007/978-3-642-65138-0.

[138] E. Witten, *Quantum background independence in string theory*, in *Conference on Highlights of Particle and Condensed Matter Physics (SALAMFEST)*, 6, 1993 [hep-th/9306122].

[139] M. Aganagic, V. Bouchard and A. Klemm, *Topological Strings and (Almost) Modular Forms*, *Commun.Math.Phys.* **277** (2008) 771 [hep-th/0607100].

[140] V. Bouchard, A. Klemm, M. Marino and S. Pasquetti, *Remodeling the B-model*, *Commun.Math.Phys.* **287** (2009) 117 [0709.1453].

[141] M. Marino, *Open string amplitudes and large order behavior in topological string theory*, *JHEP* **03** (2008) 060 [hep-th/0612127].

[142] B. Eynard and N. Orantin, *Computation of Open Gromov–Witten Invariants for Toric Calabi–Yau 3-Folds by Topological Recursion, a Proof of the BKMP Conjecture*, *Commun. Math. Phys.* **337** (2015) 483 [1205.1103].

[143] G. Borot and B. Eynard, *Enumeration of maps with self avoiding loops and the O(n) model on random lattices of all topologies*, *J. Stat. Mech.* **1101** (2011) P01010 [0910.5896].

[144] G. Borot, B. Eynard and N. Orantin, *Abstract loop equations, topological recursion and new applications*, *Commun. Num. Theor. Phys.* **09** (2015) 51 [1303.5808].

[145] Y. Hatsuda, S. Moriyama and K. Okuyama, *Exact Results on the ABJM Fermi Gas*, *JHEP* **10** (2012) 020 [1207.4283].

[146] G. Bonelli, F. Globlek and A. Tanzini, *Toda equations for surface defects in SYM and instanton counting for classical Lie groups*, *J. Phys. A* **55** (2022) 454004 [2206.13212].

[147] S. Cecotti, P. Fendley, K.A. Intriligator and C. Vafa, *A New supersymmetric index*, *Nucl. Phys. B* **386** (1992) 405 [hep-th/9204102].

[148] P. Gavrylenko and O. Lisovyy, *Fredholm Determinant and Nekrasov Sum Representations of Isomonodromic Tau Functions*, *Commun. Math. Phys.* **363** (2018) 1 [1608.00958].

[149] P. Gavrylenko and O. Lisovyy, *Pure $SU(2)$ gauge theory partition function and generalized Bessel kernel*, in *Proc. Symp. Pure Math.*, A.-K. Kashani-Poor, R. Minasian, N. Nekrasov and B. Pioline, eds., vol. 18, pp. 181–208, 2018 [1705.01869].

[150] H. Desiraju, *Fredholm determinant representation of the homogeneous painlevé ii τ-function*, *Nonlinearity* **34** (2020) 6507 .

[151] F. Del Monte, H. Desiraju and P. Gavrylenko, *Isomonodromic Tau Functions on a Torus as Fredholm Determinants, and Charged Partitions*, *Commun. Math. Phys.* **398** (2023) 1029 [2011.06292].

[152] A.B. Goncharov and R. Kenyon, *Dimers and cluster integrable systems*, *Annales scientifiques de l'École Normale Supérieure* **46** (2013) 747 [1107.5588].

[153] V.V. Fock and A. Marshakov, *Loop Groups, Clusters, Dimers and Integrable Systems*, in *Geometry and Quantization of Moduli Spaces*, L. Alvarez Consul, J.E. Andersen and I. Mundet i Riera, eds., Advanced Courses in Mathematics - CRM Barcelona, pp. 1–65, Birkhäuser (2016), DOI [1401.1606].

[154] S.N.M. Ruijsenaars and H. Schneider, *A New Class of Integrable Systems and Its Relation to Solitons*, *Annals Phys.* **170** (1986) 370.

[155] R.M. Kashaev and S.M. Sergeev, *Spectral equations for the modular oscillator*, *Rev. Math. Phys.* **30** (2018) 1840009 [1703.06016].

[156] R. Kashaev and S. Sergeev, *On the Spectrum of the Local $\mathbb{P}^2$ Mirror Curve*, *Annales Henri Poincare* **21** (2020) 3479 [1904.12315].

[157] M. Marino and S. Zakany, *Matrix Models from Operators and Topological Strings*, *Annales Henri Poincare* **17** (2016) 1075 [1502.02958].

[158] A. Grassi, *Spectral determinants and quantum theta functions*, *J. Phys. A* **49** (2016) 505401 [1604.06786].

[159] G. Bonelli, F. Globlek, N. Kubo, T. Nosaka and A. Tanzini, *M2-branes and* $\mathfrak{q}$*-Painlevé equations*, *Lett. Math. Phys.* **112** (2022) 109 [2202.10654].

[160] S. Moriyama and T. Nosaka, *40 bilinear relations of q-Painlevé VI from $\mathcal{N} = 4$ super Chern-Simons theory*, *JHEP* **08** (2023) 191 [2305.03978].

[161] G. Bonelli, F. Del Monte and A. Tanzini, *BPS Quivers of Five-Dimensional SCFTs, Topological Strings and q-Painlevé Equations*, *Annales Henri Poincaré* **22** (2021) 2721–2773 [2007.11596].

[162] T. Nosaka, *q-discrete Painleve VI equations from M2-branes*, *JHAP* **3** (2023) 57.

[163] T. Nosaka and T. Numasawa, *Chaos exponents of SYK traversable wormholes*, *JHEP* **02** (2021) 150 [2009.10759].

[164] F. Del Monte and P. Longhi, *The threefold way to quantum periods: WKB, TBA equations and q-Painlevé*, *SciPost Phys.* **15** (2023) 112 [2207.07135].

[165] G. Bonelli, P. Gavrylenko, I. Majtara and A. Tanzini, *Surface observables in gauge theories, modular Painlevé tau functions and non-perturbative topological strings*, *arXiv preprints: High Energy Physics - Theory* (2024) [2410.17868].

[166] A. Klemm and E. Zaslow, *Local Mirror Symmetry at Higher Genus*, in *Winter School on Mirror Symmetry and Vector Bundles*, C. Vafa and S.T. Yau, eds., vol. 23 of *Studies in Advanced Mathematics*, pp. 183–207, AMS/IP, 2001, DOI [hep-th/9906046].

[167] S.N.M. Ruijsenaars, *Relativistic Toda systems*, *Communications in Mathematical Physics* **133** (1990) 217 .

[168] S. Garoufalidis and R. Kashaev, *Evaluation of state integrals at rational points*, *Commun. Num. Theor. Phys.* **09** (2015) 549 [1411.6062].

[169] J. Gu and M. Marino, *Peacock patterns and new integer invariants in topological string theory*, *SciPost Phys.* **12** (2022) 058 [2104.07437].

[170] J. Ellegaard Andersen and R. Kashaev, *A TQFT from Quantum Teichmüller Theory*, *Commun. Math. Phys.* **330** (2014) 887 [1109.6295].

[171] S. Zakany, *Matrix models for topological strings: exact results in the planar limit*, *arXiv preprints: High Energy Physics - Theory* (2018) [1810.08608].

[172] P.D. Miller, *Applied Asymptotic Analysis*, vol. 75 of *Graduate Studies in Mathematics*, American Mathematical Society, Providence, Rhode Island (2006), 10.1090/gsm/075.

[173] F. Fucito, J.F. Morales and R. Poghossian, *Wilson loops and chiral correlators on squashed spheres*, *JHEP* **11** (2015) 064 [1507.05426].

[174] Y. Hatsuda, M. Marino, S. Moriyama and K. Okuyama, *Non-perturbative effects and the refined topological string*, *JHEP* **09** (2014) 168 [1306.1734].

[175] M. Mariño, *Spectral Theory and Mirror Symmetry*, in *Proceedings of Symposia in Pure Mathematics*, vol. 98, pp. 259–294, American Mathematical Society, 2018, DOI [1506.07757].

[176] M. Mariño, *Les Houches lectures on non-perturbative topological strings*, *arXiv preprints: High Energy Physics - Theory* (2024) [2411.16211].

[177] J. Gu, A. Klemm, M. Marino and J. Reuter, *Exact solutions to quantum spectral curves by topological string theory*, *JHEP* **10** (2015) 025 [1506.09176].

[178] Y. Hatsuda, "-." Unpublished notes.

[179] Y. Hatsuda, S. Moriyama and K. Okuyama, *Instanton Bound States in ABJM Theory*, *JHEP* **1305** (2013) 054 [1301.5184].

[180] N. Drukker, M. Marino and P. Putrov, *Nonperturbative aspects of ABJM theory*, *JHEP* **1111** (2011) 141 [1103.4844].

[181] Y. Hatsuda and K. Okuyama, *Resummations and Non-Perturbative Corrections*, *JHEP* **09** (2015) 051 [1505.07460].

[182] A. Grassi, M. Marino and S. Zakany, *Resumming the string perturbation series*, *JHEP* **05** (2015) 038 [1405.4214].

[183] M. Marino, *Les Houches lectures on matrix models and topological strings*, hep-th/0410165.

[184] M.-x. Huang and X.-f. Wang, *Topological Strings and Quantum Spectral Problems*, *JHEP* **09** (2014) 150 [1406.6178].

[185] Y. Hatsuda and M. Marino, *Exact quantization conditions for the relativistic Toda lattice*, *JHEP* **05** (2016) 133 [1511.02860].

[186] B.M. McCoy, *The Romance of the Ising Model*, in *Symmetries, Integrable Systems and Representations*, K. Iohara, S. Morier-Genoud and B. Rémy, eds., vol. 40 of *Springer Proceedings in Mathematics & Statistics*, (London), pp. 263–295, Springer, 2013, DOI [1111.7006].

[187] X. Wang, G. Zhang and M.-x. Huang, *New Exact Quantization Condition for Toric Calabi-Yau Geometries*, *Phys. Rev. Lett.* **115** (2015) 121601 [1505.05360].

[188] H. Nakajima and K. Yoshioka, *Lectures on instanton counting*, in *CRM Workshop on Algebraic Structures and Moduli Spaces Montreal, Canada, July 14-20, 2003*, 2003 [math/0311058].

[189] V.A. Fateev and A.V. Litvinov, *On AGT conjecture*, *JHEP* **02** (2010) 014 [0912.0504].

[190] D. Maulik and A. Okounkov, *Quantum Groups and Quantum Cohomology*, *arXiv preprints* (2012) [1211.1287].

[191] N. Iorgov, O. Lisovyy and Y. Tykhyy, *Painlevé VI connection problem and monodromy of $c = 1$ conformal blocks*, *JHEP* **12** (2013) 029 [1308.4092].

[192] H. Desiraju, P. Ghosal and A. Prokhorov, *Proof of Zamolodchikov conjecture for semi-classical conformal blocks on the torus*, *arXiv preprints: Mathematical Physics* (2024) [2407.05839].

[193] B.C. Hall, *Quantum Theory for Mathematicians*, vol. 267 of *Graduate Texts in Mathematics*, Springer New York (June, 2013), 10.1007/978-1-4614-7116-5.

[194] R. Couso-Santamaría, M. Marino and R. Schiappa, *Resurgence Matches Quantization*, *J. Phys. A* **50** (2017) 145402 [1610.06782].

[195] M. Alim, A. Saha, J. Teschner and I. Tulli, *Mathematical Structures of Non-perturbative Topological String Theory: From GW to DT Invariants*, *Commun. Math. Phys.* **399** (2023) 1039 [2109.06878].

[196] C. Rella, *Resurgence, Stokes constants, and arithmetic functions in topological string theory*, *Commun. Num. Theor. Phys.* **17** (2023) 709 [2212.10606].

[197] M. Alim, L. Hollands and I. Tulli, *Quantum Curves, Resurgence and Exact WKB*, *SIGMA* **19** (2023) 009 [2203.08249].

[198] A. Grassi, Q. Hao and A. Neitzke, *Exponential Networks, WKB and Topological String*, *SIGMA* **19** (2023) 064 [2201.11594].

[199] J. Gu and M. Marino, *On the resurgent structure of quantum periods*, *SciPost Phys.* **15** (2023) 035 [2211.03871].

[200] R.B. Dingle and G.J. Morgan, *Wkb methods for difference equations. i, ii*, *Applied Scientific Research* **18** (1967) 221.

[201] A.-K. Kashani-Poor, *Quantization condition from exact WKB for difference equations*, *JHEP* **06** (2016) 180 [1604.01690].

[202] F. Del Monte and P. Longhi, *Monodromies of Second Order q-difference Equations from the WKB Approximation*, 2406.00175.

[203] V. Fantini and C. Rella, *Strong-weak symmetry and quantum modularity of resurgent topological strings on local $\mathbb{P}^2$*, *Commun. Num. Theor. Phys.* **19** (2025) 1 [2404.10695].

[204] A. Turbiner and A. Ushveridze, *Spectral singularities and quasi-exactly solvable quantal problem*, *Physics Letters A* **126** (1987) 181.

[205] K. Ito, T. Kondo, K. Kuroda and H. Shu, *WKB periods for higher order ODE and TBA equations*, *JHEP* **10** (2021) 167 [2104.13680].

[206] A. Grassi and J. Gu, *Argyres-Douglas theories, Painlevé II and quantum mechanics*, *JHEP* **02** (2019) 060 [1803.02320].

[207] K. Ito and H. Shu, *ODE/IM correspondence and the Argyres-Douglas theory*, *JHEP* **08** (2017) 071 [1707.03596].

[208] K. Ito, S. Koizumi and T. Okubo, *Quantum Seiberg-Witten curve and Universality in Argyres-Douglas theories*, *Phys. Lett. B* **792** (2019) 29 [1903.00168].

[209] K. Ito, M. Mariño and H. Shu, *TBA equations and resurgent Quantum Mechanics*, *JHEP* **01** (2019) 228 [1811.04812].

[210] F. Fucito, A. Grassi, J.F. Morales and R. Savelli, *Partition functions of non-Lagrangian theories from the holomorphic anomaly*, *JHEP* **07** (2023) 195 [2306.05141].

[211] K. Ito and J. Yang, *TBA equations and quantum periods for D-type Argyres-Douglas theories*, *JHEP* **01** (2025) 047 [2408.01124].

[212] G. Bonelli, A. Shchechkin and A. Tanzini, *Refined Painlevé/gauge theory correspondence and quantum tau functions*, *arXiv preprints: High Energy Physics - Theory* (2025) [2502.01499].

[213] S. Chakrabarti and M. Raman, *Exploring T-Duality for Self-Dual Fields*, *Fortsch. Phys.* **72** (2024) 2400023 [2311.09153].

[214] F.A. Berezin and M.A. Shubin, *The One-dimensional Schrödinger Equation*, in *The Schrödinger Equation*, vol. 66 of *Mathematics and Its Applications*, (Dordrecht), pp. 50–149, Springer (1991), DOI.

[215] M.C. Gutzwiller, *The quantum mechanical Toda lattice*, *Ann. Phys.* **124** (1980) 347.

[216] M.C. Gutzwiller, *The quantum mechanical Toda lattice, II*, *Ann. Phys.* **133** (1981) 304.

[217] E.K. Sklyanin, *The quantum Toda chain*, in *Nonlinear Equations in Classical and Quantum Field Theory*, N. Sanchez, ed., vol. 226 of *Lecture Notes in Physics*, (Berlin, Heidelberg), pp. 196–233, Springer (1985), DOI.

[218] V. Pasquier and M. Gaudin, *The periodic Toda chain and a matrix generalization of the Bessel function recursion relations*, *J. Phys. A: Math. Gen.* **25** (1992) 5243.

[219] R. Yaris, J. Bendler, R.A. Lovett, C.M. Bender and P.A. Fedders, *Resonance calculations for arbitrary potentials*, *Phys. Rev. A* **18** (1978) 1816.

[220] E. Caliceti, S. Graffi and M. Maioli, *Perturbation theory of odd anharmonic oscillators*, *Communications in Mathematical Physics* **75** (1980) 51.

[221] E. Caliceti and M. Maioli, *Odd anharmonic oscillators and shape resonances*, *Annales de l'I.H.P. Physique théorique* **38** (1983) 175.

[222] M. Maioli, *Exponential perturbations of the harmonic oscillator*, *Journal of Mathematical Physics* **22** (1981) 1952.

[223] M. François, A. Grassi and T. Pedroni, "From deformed Schrödinger equations to the Toda lattice: degeneracy and integrability." Work in progress.

[224] K. Hori, S. Katz, A. Klemm, R. Pandharipande, R. Thomas, C. Vafa et al., *Mirror Symmetry*, vol. 1 of *Clay Mathematics Monographs*, American Mathematical Society, Providence, USA (2003).

[225] Q. Hao, *Exact WKB of solutions by Borel summation and open TBA*, *arXiv preprints: High Energy Physics - Theory* (2025) [2507.06922].

[226] J. Gu and M. Marino, *Thou shalt not tunnel: Complex instantons and tunneling suppression in deformed quantum mechanics*, *arXiv preprints* (2026) [2602.20576].

[227] A. Ilyin, A. Laptev, L. Schimmer and A. Zernova, *Eigenvalues of non-selfadjoint functional difference operators*, *arXiv preprints: Spectral Theory* (2025) [2504.06858].

[228] Y. Hatsuda, S. Moriyama and K. Okuyama, *Instanton Effects in ABJM Theory from Fermi Gas Approach*, *JHEP* **01** (2013) 158 [1211.1251].

[229] V.S. Adamchik, *Symbolic and numeric computations of the Barnes function*, *Computer Physics Communications* **157** (2004) 181 [math/0308086].

[230] Wolfram Research, "EllipticK." https://reference.wolfram.com/language/ref/EllipticK.html, 2022.

[231] Wolfram Research, "EllipticF." https://reference.wolfram.com/language/ref/EllipticF.html, 2022.

[232] Wolfram Research, "EllipticE." https://reference.wolfram.com/language/ref/EllipticE.html, 2022.

[233] Wolfram Research, "EllipticPi." https://reference.wolfram.com/language/ref/EllipticPi.html, 2022.

[234] S. Cheng and P. Sułkowski, *Refined open topological strings revisited*, *Phys. Rev. D* **104** (2021) 106012 [2104.00713].

[235] M. Aganagic, A. Klemm, M. Marino and C. Vafa, *The Topological vertex*, *Commun.Math.Phys.* **254** (2005) 425 [hep-th/0305132].

[236] A. Iqbal and A.-K. Kashani-Poor, *Instanton counting and Chern-Simons theory*, *Adv. Theor. Math. Phys.* **7** (2003) 457 [hep-th/0212279].

[237] A. Losev, N. Nekrasov and S.L. Shatashvili, *Testing Seiberg-Witten Solution*, in *Strings, Branes and Dualities*, L. Baulieu, P. Di Francesco, M. Douglas, V. Kazakov, M. Picco and P. Windey, eds., vol. 520 of *NATO ASI Series*, (Dordrecht), pp. 359–372, Springer (1999), DOI [hep-th/9801061].